Escola de Camins
Escola Tècnica Superior d'Enginyeria de Camins, Canals i Ports
UPC BARCELONATECH

TESI DE MÀSTER

Màster

ENGINYERIA DE CAMINS, CANALS I PORTS

Títol

LATERAL STABILITY ANALYSIS OF LONG PRECAST PRESTRESSED CONCRETE BEAMS

Autor

VÍCTOR HERRANDO GERMÁN

Tutor

ALBERT DE LA FUENTE ANTEQUERA
JESÚS MIGUEL BAIRÁN GARCÍA

Intensificació

ENGINYERIA D'ESTRUCTURES I CONSTRUCCIÓ

Data

Febrer de 2015

ACKNOWLEDGEMENTS

I would like to express my gratitude and my sincerest appreciation to those who helped me accomplish this study.

In particular, I would like to make special mention to Professor Albert de la Fuente and Professor Jesús Miguel Bairán for supervising my work and giving me guidance along an arduous process. As a student, it has been extremely positive to attend to the meetings we had and receive firsthand your comments and remarks.

In particular, I would like to thank Professor de la Fuente for his permanent dedication and trust, both from an academic and personal point of view.

To my family, special recognition for encouraging me in all my pursuits and supporting me emotionally and financially.

Lateral stability analysis of long precast prestressed concrete girders during lifting

Author: Herrando Germán, Víctor

Supervisors: de la Fuente Antequera, Albert; Bairán García, Jesús Miguel

ABSTRACT

Most structures are designed according to several factors but cost and utility are usually the two main factors which are considered. Structures are normally designed for a certain period of time and must meet specific safety standards during all their design life. Furthermore, due to economic reasons, optimizing the design is essential to reduce costs and produce highly competitive products. Sometimes, engineering solutions can seem permanent but as time goes by, these solutions develop thanks to technological advances and innovative engineering approaches.

Precast prestressed concrete girders are an example of this development. Since the construction of the world's first prestressed concrete bridge in Oued Al Fodda, Algeria, during the years 1936-1937, the utilization and variety of precast prestressed concrete girders in structures have steadily increase. Specially during the last two decades, an increased demand has been placed on the engineering community to extend the span ranges of precast prestressed girders. Increases in concrete strength, strand diameter and improved manufacturing processes have enabled lengthening of girders achieving lower construction time and cost savings.

A consequence of increasing the span has been increased weight, so that the longest girders are now limited mainly by transportation considerations. To maximize the span range, the weight of modern girders has been kept to a minimum reducing the width of the flanges, hence resulting much more slender when compared to former sections. Consequently, the likelihood of occurring a stability failure has increased and may become a significant design constraint. In recent years there have been a number of accidents of modern slender precast concrete girders which have led to increased concern about stability considerations. Many times, designers ignore the issue of lateral stability related to the construction and handling stages to the fabricators and contractors, only considering the stability of the finished structure. Nevertheless, accidents occurred in diverse construction stages: transportation, lifting and also once the girder was placed onto supports before a top slab is cast.

Currently used design codes lack sufficient guidance on the subject of stability of precast prestressed concrete girders. For the aforementioned reasons, this paper is intended to investigate the parameters governing the lateral stability of precast prestressed concrete girders. Special attention is drawn to the case of a girder lifted by two cables which is considered the worst case scenario against lateral buckling due to an absence of rotational restrain from the supports.

Análisis de la estabilidad lateral de vigas prefabricadas de hormigón pretensado

Autor: Herrando Germán, Víctor

Supervisores: de la Fuente Antequera, Albert; Bairán García, Jesús Miguel

RESUMEN

En el diseño de la mayoría de estructuras se busca la consonancia entre diversos factores donde destacan en peso, funcionalidad y precio, dando por sentada la seguridad de la misma. Cualquier tipo de construcción ha de ser capaz de garantizar un adecuado comportamiento durante el periodo para el que es diseñada, y a su vez, debido a la naturaleza competitiva de nuestra sociedad, interesa optimizar su diseño en aras de encontrar soluciones más económicas. En algunos casos, las soluciones pueden parecer definitivas pero, de manera general, evolucionan con el tiempo y de la mano de los avances tecnológicos.

Un ejemplo de ello se encuentra en las vigas prefabricadas de hormigón pretensado. Desde la construcción del primer puente de hormigón pretensado en Oued Al Fodda, Algeria, durante los años 1936-1937, el uso y la diversidad de vigas prefabricadas de hormigón en estructuras ha crecido incesantemente. Especialmente durante las dos últimas décadas, se ha hecho hincapié en la conveniencia de ampliar la longitud de dichas vigas. Aumentos en la resistencia del hormigón, el uso de cables de pretensado de mayor diámetro y mejoras en el proceso de fabricación de las vigas han permitido alcanzar mayores longitudes en las vigas, y por ende, reducir los tiempos de construcción y el coste ecónomico de las obras.

El aumento de luz en las vigas ha conllevado un importante incremento de su peso de manera que las vigas de mayor longitud se ven ahora limitadas por dificultades en el transporte. Para maximizar el rango de longitudes de las vigas modernas se ha procedido manteniendo su peso al mínimo, reduciendo el ancho de las alas y propiciando la aparición de vigas con secciones mucho más esbeltas que sus predecesoras. Consecuentemente, la probabilidad de que un fallo por inestabilidad lateral ocurra aumenta, pudiendo llegar a convertirse en un factor decisivo en el diseño de vigas prefabricadas de hormigón. Durante los últimos años se han producido diversos accidentes en vigas modernas que han conducido a una mayor preocupación sobre la estabilidad lateral de las mismas. Generalmente, la estabilidad lateral durante las diferentes fases de construcción de una estructura ha sido ignorada en la fase de diseño, únicamente considerándose la estabilidad de la estructura acabada. Sin embargo, varios accidentes han sucedido durante el transporte, el izado e incluso tras colocar la viga en sus apoyos, momentos antes de hormigonar la losa superior.

Cabe añadir que las normativas actuales no tratan en profundidad el tema de la estabilidad lateral de vigas prefabricas de hormigón. Por las razones hasta ahora mencionadas, este documento tiene como objetivo principal investigar la influencia de los numerosos parámetros que gobiernan la estabilidad lateral de vigas prefabricadas de hormigón pretensado. Especialmente se tratará el caso del izado por considerarse el escenario más propicio a inestabilidad por pandeo lateral debido a la ausencia de restricción de la rotación por parte de los apoyos.

LIST OF SYMBOLS AND ABBREVIATIONS

A	Cross-sectional area.
C_w	Warping constant.
E	Young's modulus.
G	Torsional shear modulus.
H	Height from center of gravity of the whole girder to roll axis.
H_g	Vertical distance from cross section center of gravity to bottom fiber.
I_y	Moment of inertia about y-axis.
I_z	Moment of inertia about the z-axis.
J	St. Venant's torsion constant.
K_0	Initial midspan curvature about weak-axis.
K_{ms}	Midspan curvature about weak-axis.
L	Length of girder.
L_B	Maximum length due to lateral buckling of the imperfect girder.
L_C	Maximum length due to cracking of the imperfect girder.
L_T	Maximum design length of the straight girder
M_p	Moment caused by the prestressing force.
M_x	Twisting moment.
M_y	Bending moment about the y-axis.
M_z	Bending moment about the z-axis.
N_x	Internal force parallel to x-axis.
N_y	Internal force parallel to y-axis.
N_z	Internal force parallel to z-axis.
P	Prestressing force.
P_{max}	Maximum prestressing force for a given cross section.
Q	Total girder self-weight.
R	Radius of curvature.
U	Longitudinal deflection.
V	Strong axis deflection.

W	Weak axis deflection.
W_{ms}	Weak axis deflection at midspan.
a	Distance to lift points from girder end.
b	Length between lift points.
e	Eccentricity of girder center of gravity with respect to roll axis.
e_p	Eccentricity of prestressing force.
d	Depth of girder.
d_1	Vertical distance from cross section center of gravity to top fiber.
f_{ck}	Characteristic resistance of the concrete.
f_{ctm}	Mean resistance of the concrete.
f_{ctd}	Design resistance of the concrete
h_l	Height of the lifting loops.
q	Self-weight of girder per unit length.
q_{bckl}	Buckling load per unit length.
x	Longitudinal axis tangential to girder curved axis.
y	Strong axis of the cross section.
z	Weak axis of the cross section.
α	Subtended angle of half girder measured from center of curvature.
β	Roll angle.
β_i	Initial roll angle due geometric imperfections.
γ	Subtended angle from midspan to lift point measured from center of curvature.
δ	Lateral sweep.
θ	Cylindrical coordinate. Zero at midspan.
ν	Poisson coefficient.
σ_{mP}	Stresses due to prestressing moment.
σ_P	Stresses due to prestressing axial force.
σ_{mz}	Stresses due to strong axis bending.
σ_{my}	Stresses due to weak axis bending.
σ_t	Total stresses.
ϕ	Angle of twist.
ψ	Inclination angle of lifting cables with respect to vertical.

TABLE OF CONTENTS

CHAPTER 1.

INTRODUCTION

1.1 Introduction

The utilization, diversity and availability of precast prestressed concrete girders in structures have steadily increased since the construction of the world's first prestressed concrete bridge in Oued Al Fodda, Algeria, during the years 1936-1937. The bridge had a span of 20 meters and was constructed by the French company Campenon Bernard. Two years later in Oelde, Germany, a prestressed concrete bridge 36 meters long was built by the contracting firm Wayss & Freytag Aktiengesellschaft., which was granted a license to use the prestressing system introduced by Freyssinet during that time. As World War II ended in 1945, the construction of both the 60 meter long Luzancy bridge in 1946 in France and the 54 meters Walnut Memorial Bridge in Philadelphia, United States, in 1948 marked a significant milestone because of their good structural perfomance and economy associated with this type of bridge technology. For nearly 50 years following the construction of the Walnut Lane Memorial Bridge, precast prestressed girders were limited to bridges in which the spans did not exceed its length.[1, 2]

Specially during the last two decades, an increased demand has been placed on the engineering community to extend the span ranges of precast prestressed girders. Increases in concrete strength, strand diameter and improved manufacturing processes have enabled lengthening of girders achieving lower construction time and cost savings. As the spans have increased, so has the depth of the girders leading to more slender girders, hence increasing the likelihood of occurring a stability failure. Stability failures would cause a detrimental impact due to the costs associated with delays, damage to construction equipment and, more importantly, could endanger the lives of construction personnel.

In recent years there have been a number of accidents of modern slender precast concrete girders which have led to increased concern about stability considerations. Many times, designers ignore the issue of lateral stability related to the construction and handling stages to the fabricators and contractors, only considering the stability of the finished structure. Nevertheless accidents have occurred in diverse construction stages: transportation, lifting and also once the girder was placed onto supports before a top slab is cast. Therefore many authors pointed out the convenience of pursuing further the study of lateral stability of precast prestressed concrete girders.

The collapse of a precast prestressed concrete girder due to lateral instability may be caused by two phenomenons: lateral-torsional buckling and rollover. Rollover failure would be the controlling stability phenomenon for cases where the girder is not laterally braced. It consists of the girder as a whole tipping over since there is no physical restraint to prevent this from occurring. For the cases where the girder is laterally braced and thus cannot fail due to rollover, lateral instability would occur due to lateral-torsional buckling.

1.2 Objectives

The **main objective** of this paper is to study the influence of the parameters which could lead to a lateral instability phenomenon of a precast prestressed concrete girder while is being lifted. Those parameters are: length of the girder, position and height of the lifting loops, characteristic resistance of the concrete at the time of lifting, magnitude of the prestressing force, cross-sectional properties of the girder, inclination angle of the lifting cables and, above all, lateral sweep.

The parametric analysis is intended to be representative of the most commonly used girder cross sections. This includes girders with I, T and channel shaped cross sections. Once the parametric analysis is done, a design criteria to ensure lateral stability of those girders will be proposed.

1.3 Methodology

First, a thorough review of the existent literature regarding lateral stability of precast concrete beams has been carried out. Different approaches to this problem from the late 50s until recent times have been analyzed pointing out its limitations and improvements over time. As a result, a validated analytical calculation method has been chosen to perform a parametric study of the several parameters involved in the stability of a hanging girder. Furthermore, currently used girder cross sections found in a commercial catalogue haven been implemented. Throughout an analysis of the obtained results a design criteria has been proposed. Lastly, the applicability of the proposed criteria has been verified in a real case example.

CHAPTER 2.

STATE OF THE ART

2.1 Introduction

Precast, prestressed concrete girders are widely used in construction projects where speed and ease of erection are of paramount importance. Bridges built using prestressed concrete girders have proven to be economical, exhibit good structural performance, and typically require minimal maintenance. Through the use of improved materials, the introduction of more efficient girder shapes, larger prestressing strands, and the development of other enhancements, the range of spans for which precast prestressed concrete girders are used has increased over the years[3]. Actually, it is believed that the record length for a precast concrete plant-cast girder ever manufactured, is the 65 meters long, 2.8 meters deep girder used for the Bow River Bridge near Calgary, Alberta, in Canada[4]. However, such girders are still used infrequently for spans in excess of 48 meters. This upper limit of practical use exists for several reasons, including material limitations, structural considerations, size and weight limitations on girder shipping and handling, and a general lack of information necessary to design and build longer spans[3].

Since their manufacture, precast concrete girders are handled in a variety of ways; must be transported from the precast yard to the construction site and may be lifted as many as four times between the casting bed and their final position within the bridge. The three important stages identified in the construction process are: transportation, lifting and placement in structure or temporary storage[5]. Those three stages are illustrated in figures 2.1, 2.2 and 2.3 respectively.

Figure 2. 1. Transport of precast concrete girder to construction site. [6]

Figure 2. 2. Lifting of precast concrete girder for placement onto supports. [6]

A consequence of increasing the span has been increased weight, so that the longest girders are now limited mainly by transportation considerations. To maximize the span range, the weight of modern beams has been kept to a minimum reducing the width of the flanges, resulting in a lower minor-axis and torsional stiffnesses compared to former sections. The increased weight means that only a single beam can be carried on a truck, whereas two or more have been carried in the past, which allowed them to be cross-braced to each other. It has also been the practice to pay little attention to buckling considerations, since concrete girders have always been considered to have a large reserve of minor-axis stiffness. Girders are now available which, although they are stable if built and handled properly, are in the region where an instability phenomena may occur, particularly due to its sensitivity to lateral imperfections. Any further increase in span (beyond 40 m) or slenderness will mean that stability will definitely become a significant design constraint.[5]

Figure 2. 3. Precast concrete girders placed on bearings. [7]

In recent years there have been a number of failures of modern slender girders, which have led to increased concern about stability considerations. Example of that is the accident which occurred in 2013 in Portland's Marquam Bridge, USA, as illustrated in figure 2.4. According to traffic investigators the driver attempted to brake on a sloping bend in the bridge and the combination of both stopping and camber of the road tipped the semi and trailer.[8]

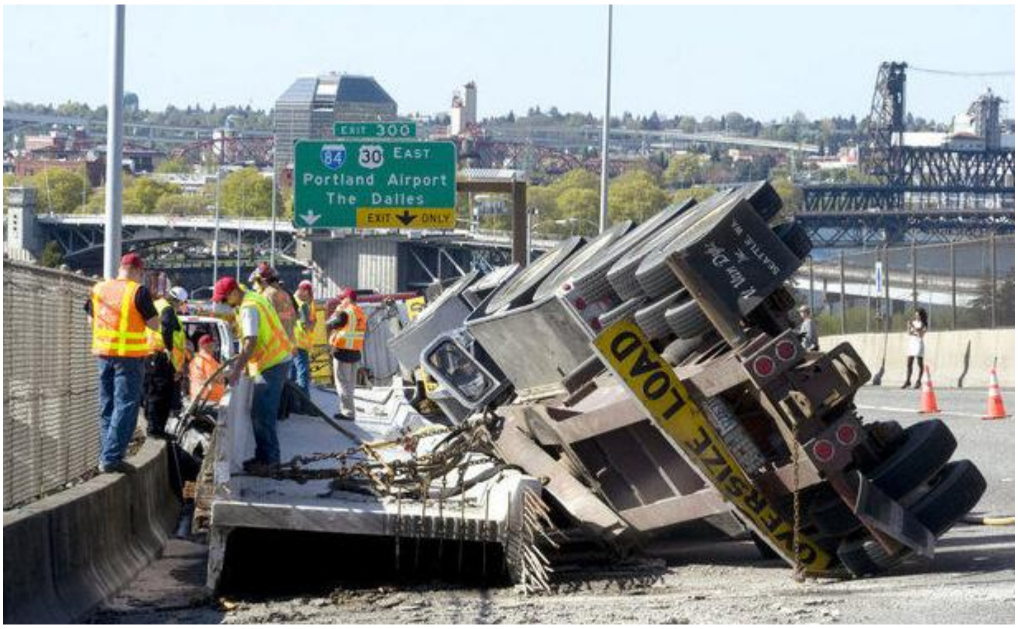

Figure 2. 4. Accident during transportation of a precast girder in Portland's Marquam Bridge, USA. [8]

Problems during lifting also arose during the construction of a viaduct near to a town called Olost, in Catalonia, Spain. Many of the precast prestressed concrete girders manufactured for the construction of the viaduct presented a small initial horizontal imperfection which shifted the center of gravity of the girder laterally. Due to this bowing, when the girder was lifted it slightly rolled. Thus a component of the self-weight load acted in the weak-axis direction, increasing its deflection. Some of the girders had an asymmetric cross section which amplified that mechanism.

Beyond a certain deflection one of the girders was lowered down for safety reasons. Cracks were observed all along the beam so it was eventually replaced[9]. Figure 2.4 shows one of the described girders during lifting. One can easily assess how the beam has rotated and deflected laterally.

Figure 2. 5. Precast concrete beam rolls and deflects laterally during erection due to an initial horizontal imperfection and the asymmetry of the cross section. [9]

The collapse of 45.7 meters long precast prestressed concrete bridge girders in Pennsylvania in 2004, depicted in figure 2.6, also resonated the need to understand the behaviour of such girders, particularly with respect to their stability. Mr. Brian Thompson, Pennsylvania Assistant State Bridge Engineer, suspected that additional sweep (lateral deformations) could have occurred due to the sun heating one side of the girder and causing the girder to bow. Additional sweep in the girders would have increased the possibility of a stability failure because eccentricity of the gravity load would apply torsion to these girders.[10]

Figure 2. 6. Stability failure of precast prestressed concrete girders I-80 in Pennsylvania. [10]

More recently in 2007, during the construction of the Red Mountain Freeway near Power Road in Mesa, Arizona, nine girders collapsed as shown in figure 2.7. The Arizona Department of Transportation hired the consultancy company CTL Group to investigate the collapse. It was concluded that the collapse probably was due to lateral instability of one girder which caused a progressive collapse of the adjacent eight girders. It was believed several factors caused the instability including bearing eccentricity, initial sweep, thermal sweep, creep sweep, and support slope in both the transverse and longitudinal directions. [10]

Figure 2. 7. Stability failure of AASHTO Type V bridge girders in Arizona. [10]

Investigating the effect of girder sweep and eccentricity is of utmost importance due to the potential for a decrease in lateral stability caused by the imperfections. There are several causes of accidental eccentricity in precast prestressed concrete girders such as: 1) imperfections during fabrication, 2) eccentricity of prestressing strands in the girder, 3) cracking and permanent deformations from handling and transportation of the girder and lastly, 4) the eccentricity caused by solar radiation heating the girder on one side, only. Additionally, bearing support conditions can also adversely affect the stability of bridge girders. Therefore, understanding the stability behaviour of precast prestressed bridge girders, including reasonable magnitudes of girder and support imperfections and their effect on stability behaviour, is paramount in ensuring safety during erection of such girders.[10]

There exist studies regarding stability of precast since the 1950s until recent times. First of them were based on the assumption that the beam was completely straight. The above specified imperfections were not taken into account in the formulations the authors developed. Therefore failure was due to lateral buckling of the perfectly straight girder. Muller[11] (1962) proposed an equation to compute the critical lateral buckling load for long precast concrete beams. Anderson[12] (1972) defined a factor of safety against lateral buckling which was slightly modified by Swann[13] (1972) and Laszlo and Imper[14] (1987). Some initial research was done on girder rollover by Laszlo and Imper, but this was expanded by Mast (1989-1994) for the case of a hanging girder[15], and for the case of a girder on elastic supports[16]. Mast was the first at considering lateral imperfections. He proposed a new factor of safety against lateral buckling and presented a method to compute the roll angle of an imperfect beam lifted by cables. He went further and also investigated the behaviour of the beam once it cracks. Mast (1994) includes the results of a lateral bending test to destruction on a long prestressed concrete beam[17].

Stratford and Burgoyne (1999-2000) carried out a finite element method analysis for three different support conditions: simply supported, transport-supported and hanging beam. It was concluded that the hanging beam support condition was the most critical against lateral buckling, among the three support conditions analyzed, due to the absence of any rotational restraint of the supports[5, 18]. The authors also proposed an analytical procedure to compute the roll angle of a beam lifted by two cables and the associated lateral deflection and additional stresses[19]. Their analysis remains always linear elastic since cracking is considered to greatly increase the possibility of buckling. Later on Stratford and Burgoyne (2001) also investigated the lateral stability of long-span prestressed concrete beams on flexible bearings[20]. Plaut and Moen (2012) presented a set of analytical formulas which allow an exhaustive computation of beams lifted by cables. Their formulation is valid both for curved concrete beams and metallic beams since, unlike the rest of authors, they do not neglect torsional effects[21, 22].

Hurff[10] (2012) carried out a set of experiments on six rectangular precast prestressed concrete beams designed to fail by lateral-torsional buckling. The results showed that the prestressing strands did not restrain the beams from buckling out-of-plane or destabilize the beam. The beams buckled after flexural cracking had occurred and did so at a load much less than what elastic lateral-torsional buckling theory predicted. Initial imperfections were shown to decrease the lateral-torsional buckling load. Figure 2.8 depicts one of the beams while being tested. The beam is end supported and a restrain system holds the beam from lateral deflections.

Figure 2. 8. Rectangular cross section concrete prestressed beam under midspan point load during a lateral-torsional buckling test. The beam is end supported and lateral deflection is restrained at the supports. [10]

Hurff and Kahn[23] (2012) performed a rollover stability test on a PCI BT-54 subjected to a midspan point load. Figure 2.9 shows the tested beam supported on elastomeric bearing pads. The torsional restraint was only provided by the couple created by the bottom flange and the elastomeric bearing pads. A rollover failure occurred well before an inelastic lateral-torsional buckling mode was anticipated. In fact, the girder never cracked during the testing. It was concluded that for prestressed concrete bridge girders, rollover will control over lateral-torsional buckling for cases where the ends are not laterally braced.

Figure 2. 9. Rollover stability test on a PCI BT-54 prestressed concrete beam supported on elastomeric bearing pads. [23]

Throughout the research undertaken it is apparent that the two phenomenons controlling lateral stability of long precast prestressed concrete girders are rollover and lateral-torsional buckling. Rollover is the controlling stability phenomenon for cases where the girder is not laterally braced[10]. This includes girders supported on elastomeric bearing pads which, even though they offer some rotational restraint, may not impede the beam from tipping over. For the cases where the girder is laterally braced and thus cannot fail due to rollover, lateral instability would occur due to lateral-torsional buckling. Buckling failure is unlikely once the girder is positioned in the structure, however, during lifting a beam is less stable[5]. Both buckling and tipping over would cause the collapse of the beam. Hence they are considered Ultimate Limit States (ULS) and both loads and materials mechanic properties shall be affected by partial safety factors.

Nevertheless special attention must be paid to hanging girders, which are supported from cables attached to lifting loops located above the girder. Contrary to girders supported from below, a girder lifted by two cables cannot collapse by tipping over liberating from its support connections. Since no restraint is provided against rigid-body rotation, the girder is free to roll until equilibrium is reached or it fails due to bending about the weak-axis. Consequently, the rotation of a hanging girder due to lateral sweep would be greater than in the other construction stages, making the girder susceptible to cracking while it is being lifted, hence increasing the possibility of rollover failure when placed onto supports.

With regard to current codes, they include very crude stability checks[5]. The *PCI Bridge Design Manual*[24, 25] and the Spanish concrete instruction *EHE-08*[26] specifically state a tolerance on initial sweep in a prestressed concrete girder. *Eurocode 2: Design of concrete structures*[27] gives simple checks against lateral buckling but states that a more detailed analysis may be advisable. Nevertheless, current codes do not define a criterion for the initial rotation of prestressed concrete girders when lifted or placed onto supports. For the aforementioned reasons it seems necessary to pursuing further the study of the parameters governing the rotation of girders at the different construction stages and define a new stability criterion with higher representativeness. Even though cracking is considered a Service Limit State (SLS), when occurs, it leads to an increased possibility of instability failure both for buckling of the hanging girder or rollover of the girder supported from below. This thesis refers specifically to the case of girders lifted by two cables and its aimed to propose a design criterion to ensure that cracking has not occurred before the beam is settled onto supports.

2.2 Problem definition

Understanding the stability problem of precast prestressed bridge girders would require the consideration of two different stability phenomenons: rollover and lateral-torsional buckling.

Rollover failure consists of the girder as a whole tipping over since there is no physical restraint to prevent this from occurring. When a girder is placed onto supports it is expected to stay in place simply by using its self-weight. However, if the girder's self-weight is off-center at all, an overturning moment would have been created that would try to tip the girder over if it became larger than resisting moment provided by the support. There could be several causes of overturning moment. Foremost among them are: [10, 18]

- The eccentricity effect from imperfections during fabrication.
- The eccentricity of prestressing strands in the girder.
- Difference in the forces of the prestressing strands.
- Variations of the elastic modulus within the concrete.
- Cracking and permanent deformation from handling and transportation of the girder.
- The eccentricity caused by solar radiations inconsistently heating the girder.

All the above mentioned reasons would cause the girder to laterally deflect as shown in plan view in figure 2.10.

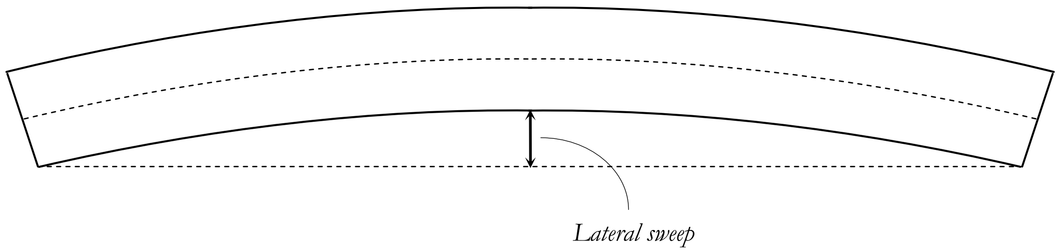

Figure 2. 10 Plan view of a beam accidentally laterally deflected.

If the girder has an initial lateral imperfection there would be an overturning moment M_0 that would be a function of the self-weight of the girder and the initial lateral deformation of the girder which could be generalized as in equation 2.1[10]. q is the girder self-weight as it varies along the girder length L, and e_i is the eccentricity of the girder center of gravity as it varies along the girder length.

$$M_o = \int_0^L q(x) \cdot e_i(x) dx \tag{2.1}$$

The effect of the eccentricity induced overturning moment in equation 2.1 would be amplified by considering that the girder is not rigid. The initial imperfections in the girder included rotation; therefore, a component of the self-weight load of the girder would act about the weak-axis of the girder causing the girder to both deform an rotate more. The additional deformation and rotation would add to the overturning moment which in turn would cause the girder to deform and rotate more, and so on. Mathematically it would become an iterative process until the system converged to equilibrium, or becomes unstable. Furthermore, many bridges use elastomeric bearing pads which have the capacity to deform under load. As the overturning moment increases, more of the load is transferred from one corner of the bottom of the girder into the bearing pad. This fact was reviewed in detail by Bairán and Cladera and applied to a real case[28].

Figure 2.11 illustrates the rollover phenomenon of a beam supported from below by elastomeric pads. The beam is supposed to have a lateral imperfection which shifts the center of gravity of the beam (see figure 2.10) and triggers the overturning mechanism. The elastic support deforms under load, slightly tipping the beam but countering the overturning moment. The beam may tip over if equilibrium of moments is not reached.

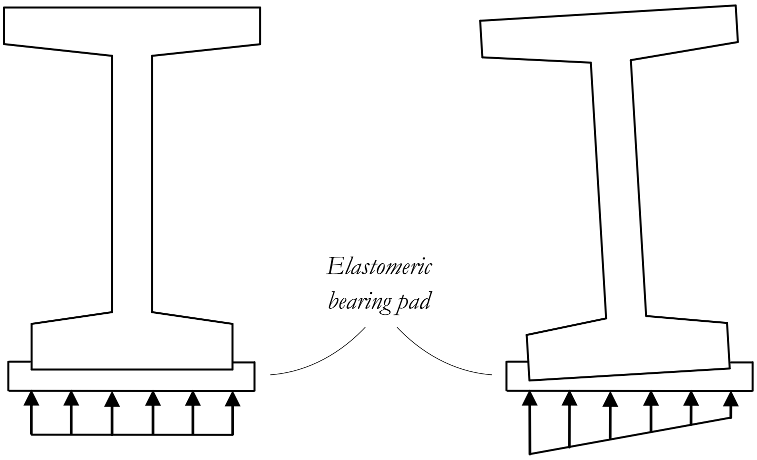

Figure 2. 11 Elastomeric bearing pad deformation and load condition for an imperfect beam.

Overturning moment could also be created due to the support conditions. The bearing pads on which the girders rest may not have provided a level surface. If the bearing pad has a lateral slope, the girder would have an initial rotation at the ends of the girder which would cause an overturning moment.

The second possible instability phenomenon that can cause collapse of precast concrete girders is lateral-torsional buckling. If a perfect beam is loaded with a uniformly distributed load, it will eventually buckle sideways at a load q_{cbckl}. When the beam is supported against rotation at its ends, there will also be a variation in twist along the length as shown in figure 2.12.

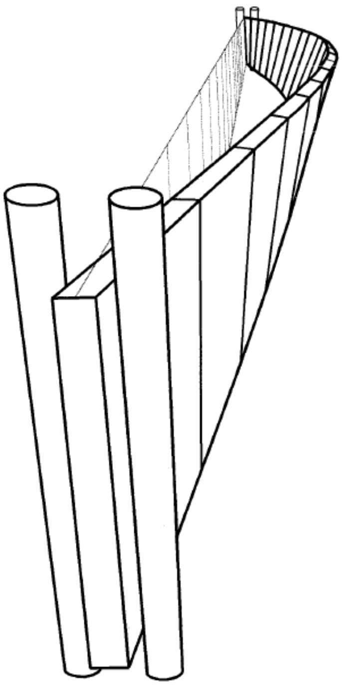

Figure 2. 12 Idealized view of lateral-torsional buckling load. [18]

If the lateral deflection is plotted against load it will follow the curve shown as the perfect case in figure 2.13. The beam will equally likely to buckle in either direction. However, no beam is perfect, so the beam will have some lateral deflection before being loaded. When such beam is loaded it does not buckle at a fixed load, but the minor-axis deflection tends to increase, eventually becoming asymptotic to the post-buckling response, but only at a large deflection (see fig. 2.13). Even if the beam is at a load below q_{bckl} the lateral deflection can give rise to problems caused by stresses generated by the minor-axis curvature. In cases where the beam is already highly stressed because of the prestress and the dead weight, these can lead to problems, either of overstressing in compression or of cracking of the beam in tension.[18]

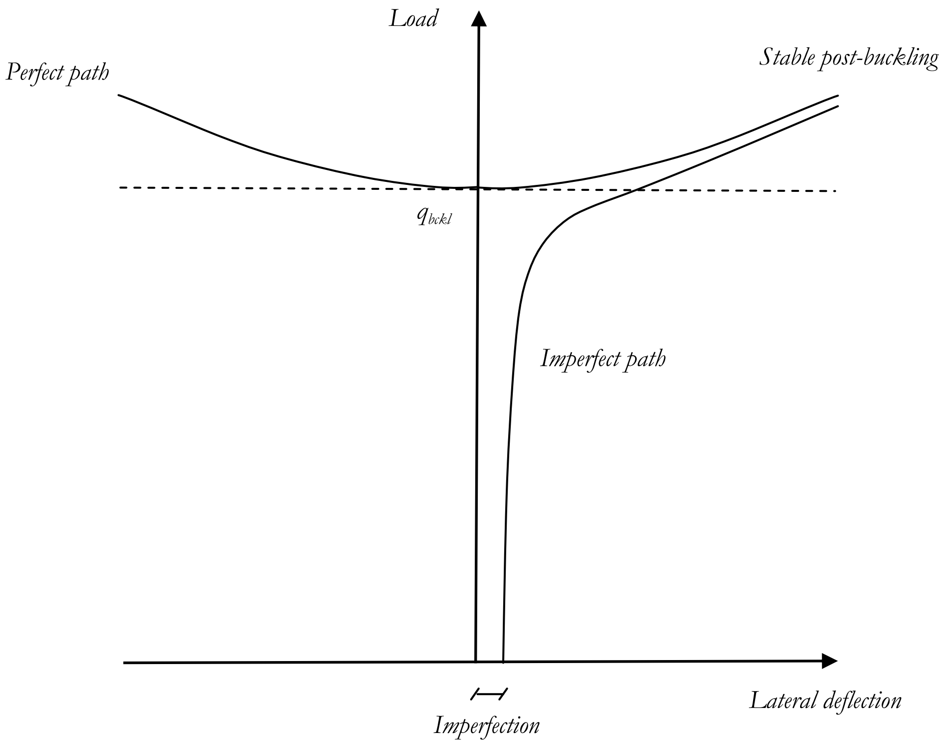

Figure 2. 13. Fundamental path of stable post-buckling behaviour, and behaviour of imperfect element. (Stratford et. al [18])

Both rollover and lateral-torsional buckling would cause the collapse of the beam. Nevertheless special attention must be paid to hanging beams, which are supported from lifting loops located above the beam. Contrary to beams on elastic supports, a beam lifted by two cables cannot collapse by tipping over liberating itself from the supports. Since no restraint is provided against rigid-body rotation the beam is free to roll around a line passing through the lifting loops, which corresponds to the roll axis. Eventually, equilibrium is reached or the beam fails due to bending about the minor-axis.

Note that when a beam is supported from below the overturning moment tends to destabilize the beam leading to a rollover failure unless such moment is countered by the supports. Figure 2.14a shows the cross section of a beam on an elastic support subjected to an overturning moment M_0 due to lateral sweep. Figure 2.14b shows the same cross section of the beam after having slightly tipped and deformed the elastic bearing pad. Due to the rotation a component of the self-weight would act about the weak-axis, causing the beam to both deform and rotate more. If the support restrain capacity is not enough, the beam will eventually tip over as shown in figure 2.14c.

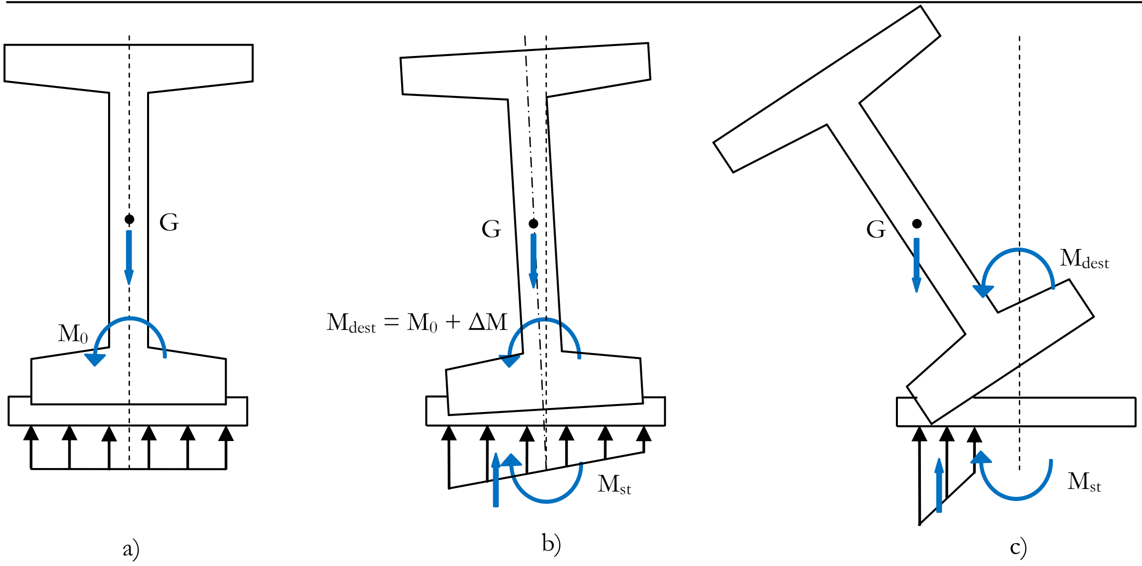

Figure 2. 14. Imperfect beam on elastomeric pad: a) initial configuration subjected to an overturning moment due to lateral sweep, b) rotated configuration, c) rollover failure.

However, the same moment applied on a hanging beam tends to stabilize the system. The rotation induced leads to a balanced configuration of the beam with no need of rotational restrain from the supports. In fact, the two cables the beam is hanging from do not restrain the beam from rotating. Thus, the rotation of a beam lifted by two cables is likely to be greater than in any other construction stage. Such rotation would cause the beam to bend about its minor-axis and may induce problems of overstressing in compression or tension at midspan.

Figure 2.15a shows the cross section of a beam hanging from a cable attached to a lifting loop and subjected to an overturning moment M_0 (eq. 2.1). Such moment causes the beam to rotate as shown in figure 2.15b. As in the previous examples, owing to the rotation the beam would both deform and rotate more. Lastly, the beam would reach an equilibrium configuration or fail due to minor-axis bending. Figure 2.15c shows the rotated cross section at midspan of a hanging beam whose top flange has cracked because of bending about its minor-axis.

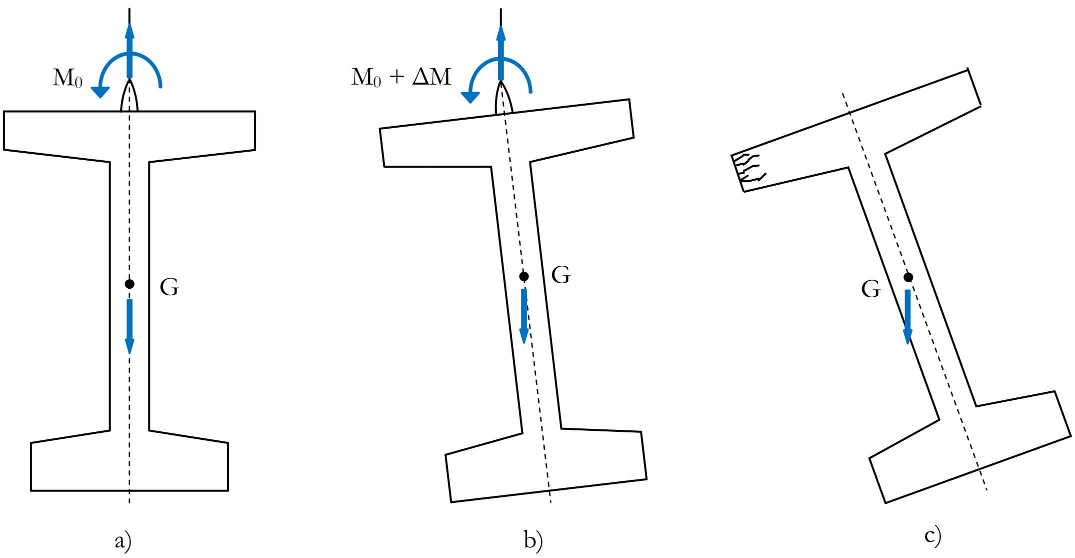

Figure 2. 15. Imperfect beam hanging from cables: a) cross section subjected to an overturning moment due to lateral sweep, b) rotated configuration, c) cracking of the top flange due to excessive bending about the weak-axis at midspan.

On account of what has been exposed so far the hanging beam situation is the most severe from a tensional point of view, making the beam susceptible to cracking during the construction process. Although crack width is considered a Service Limit State (SLS), if it occurs, the geometrical and mechanical properties of the concrete cross section would reduce, leading to a greater lateral sweep and so increased possibilities of stability failure. For that reason, this thesis is intended to provide a design criterion to assure that cracking does not occur when a beam is being lifted.

2.3 Literature review

2.3.1 Introduction

Several authors such as Magnel (1950), Billig (1953), and Leondhardt (1955) had come to the conclusion that a prestressed concrete beam where the strands were bonded to the concrete cannot buckle. The reasoning behind not needing to perform stability calculations was due to the member being in equilibrium from the lateral reaction of the strand[10]. Magnel used an example to analytically prove his theory. He considered a beam with a prestressing tendon running through a duct sufficiently larger than the tendon, where the tendon was rigidly attached only at the center by way of a cross-plate as depicted in figure 2.16.

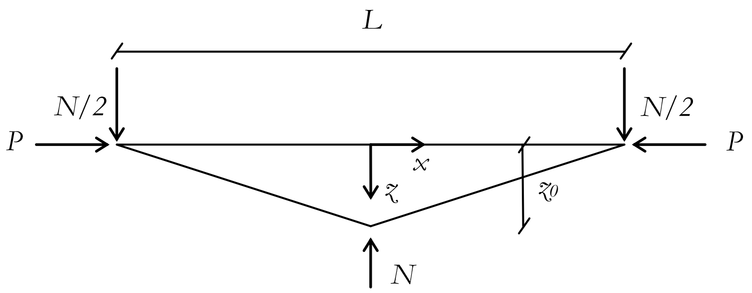

Figure 2. 16. System forces by Magnel. [10]

Equilibrium in figure 2.15 leads to a transverse load N which is given by expression 2.2.

$$N = \frac{4z_0}{L}P \tag{2.2}$$

The second-order differential equation was then determined to be:

$$EI_y\,\frac{d^2z}{dx^2} = -Pz + \frac{N}{2}\left(\frac{L}{2} - x\right) \tag{2.3}$$

Where P is the prestressing force, z the lateral coordinate axis perpendicular to the centroidal axis of the girder and N the lateral restoring force. Solving the differential equation by using the boundary conditions $z' = 0$ at $x = 0$ and $z = 0$ at $x = L/2$ gave the critical buckling load as:

$$P_{bckl} = \frac{4EI_y\pi^2}{L^2} \tag{2.4}$$

The critical buckling load was four times the Euler buckling load. Additional calculations would show that for n number of contact points between the tendon and the concrete would give n^2 times the Euler buckling load for the critical load. Therefore Magnel claimed that it was impossible to buckle a prestressed member if the tendon was continuously in contact with the concrete.[10]

Molke (1956) considered it was well established in literature that with straight or curved concrete columns, there was no concern with respect to stability failure as long as the prestressing strands were located at the centroid of the section. Any bending moment created by the prestressing force in the strands would then be countered by an equal opposite restoring force. Molke believed this had been often misconstrued to mean there was never any stability concern in prestressed concrete member. Any externally applied loads on the member could produce the same type of buckling failures as considered if the member had not been prestressed. Therefore Molke believed that proof of a minimum factor of safety for buckling in concrete structures should be calculated based on elastic theory and should be a code requirement.[10]

The concept that Molke discussed in which the effect of prestressing in the strands would not cause instability, but externally applied loads could potentially cause a buckling issue was repeated by Muller (1962).

2.3.2 Muller, J.

In the year 1962 Jean Muller[11] stated that stability had become a concern due to the long spans of the precast beams and referred to handling and placing as the critical conditions for stability failure. Based upon the results of an analytical study undertaken by Pierre Lebelle[29], who investigated the elastic stability of monosymmetric I-shaped sections, Muller presented a method for computing the lateral buckling load of slender symmetrical beams under uniform vertical load (eq. 2.5). Coefficient m is a variable dependent upon the end boundary conditions. For the case in which the girder is simply supported and subjected to a uniform vertical load m = 28.4; and the buckling load is thus given by equation 2.6.

$$q_{bckl} = m\frac{\sqrt{EI_yGJ}}{L^3} \tag{2.5}$$

$$q_{bckl} = 28.4\frac{\sqrt{EI_yGJ}}{L^3} \tag{2.6}$$

The preceding equations are valid for a rectangular section with small transverse dimensions in proportion to the span length; and the load is calculated as applied at the level of the centroid. Top and bottom flanges introduce additional restraint towards lateral deflections. The increase of the buckling load due to bending rigidity is given by affecting equation 2.5 with coefficient k_2 in equation 2.7. If the load is not applied at the centroid of the section, but a at a distance s from it, a rotation of the cross section results in an additional transverse load. Buckling load is thereby affected by the correcting factor k_1 (eq. 2.8). For unsymmetrical cross section, y_0 represents the distance of the point of application of the load to the center of torsion and not to the centroid.[11]

$$k_2 = \sqrt{1 + \frac{\pi^2}{4}\frac{2EI_y^f}{GJ}\frac{h_0^2}{L^2}} \tag{2.7}$$

$$k_1 = 1 - 0.72\frac{2y_0}{L}\sqrt{\frac{EI_y^f}{GJ}} \tag{2.8}$$

$$I_y^f = \frac{2}{\dfrac{1}{I_y^{f1}} + \dfrac{1}{I_y^{f2}}} \tag{2.9}$$

In which:

- y_0 : Distance of the point of load application to the shear center. It is negative if the load is applied below the shear center and positive otherwise.
- h_0 : Distance between the centroids of top and bottom flanges.
- I_y^{f1}: Moment of inertia about the axis of buckling of the top flange.
- I_y^{f2}: Moment of inertia about the axis of buckling of the bottom flange.

Muller also refers to the buckling capacity of beams lifted by cables. He points out the importance of reducing the distance between lift points since the presence of the cantilevered section contributes to increase the critical load very rapidly. According to Muller, pick up points located at $0.25L$ and $0.75L$ would give the beam its maximum capacity against lateral buckling. Nevertheless, such an arrangement may seldom be used for a prestressed concrete girder because of the internal stresses induced.

Figure 2.17a illustrates a precast prestressed concrete girder while being lifted. In this example the lifting loops A and B are located at both ends of the girder. The loads acting on the girder are its self-weight q per unit length and a prestressing force P. The prestressing force is assumed to act at a distance e_p from the centroid of the girder cross-section, thus inducing a bending moment $M_p = P \cdot e_p$. Figure 2.17b, 2.17c and 2.17d represent the bending moment diagram caused by the eccentricity of the prestressing force, the bending moment diagram due to the self-weight load, and the axial force diagram of the girder, respectively.

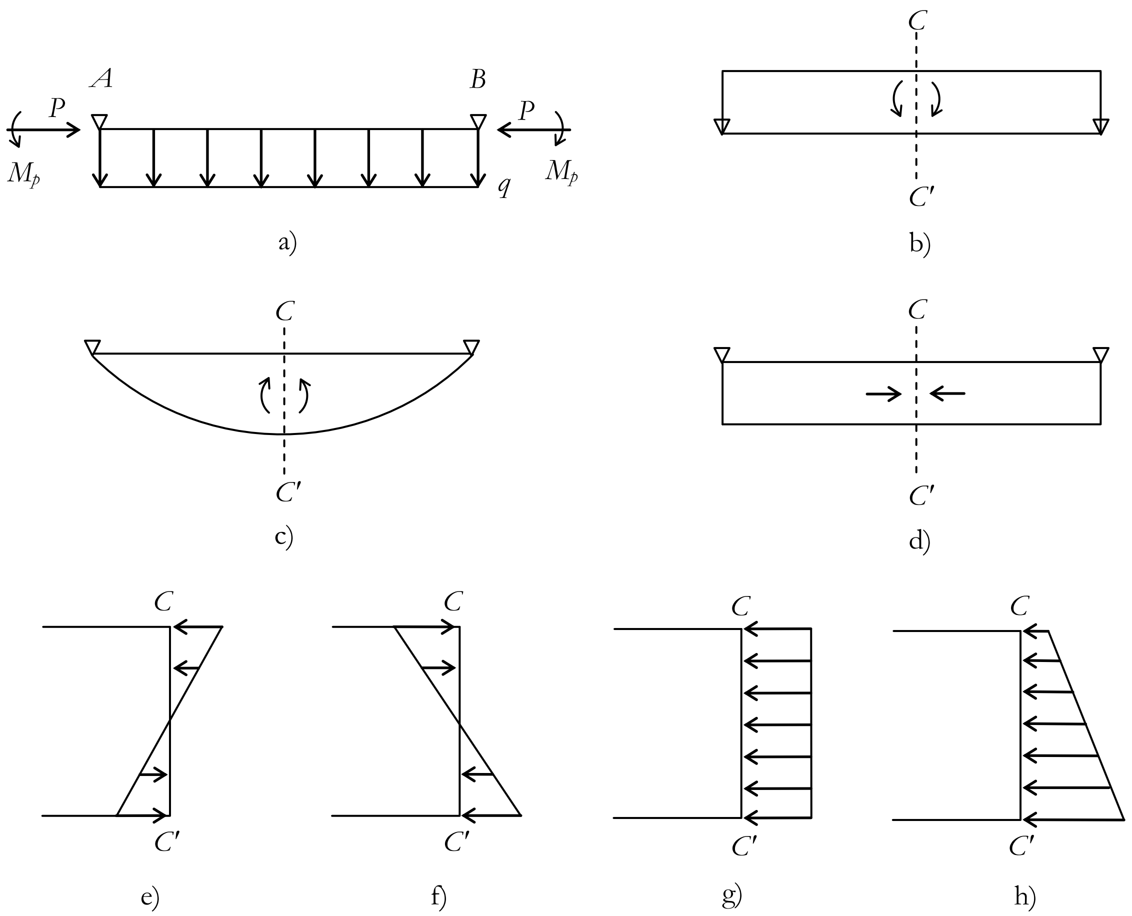

Figure 2. 17. End supported hanging girder: a) acting loads, b) prestressing moment diagram, c) self-weight bending diagram, d) axial force diagram, e) self-weight bending stresses, f) prestressing moment stresses, g) axial force stresses, h) final stress state.

Those internal forces would cause, individually, a stress state at midspan (*C-C'*) as shown in figure 2.17e for the bending moment due to self-weight, figure 2.17f for the prestressing moment and figure 2.17g for the prestressing compression force. When combined, the final stress state of the cross section at midspan is obtained (fig. 2.17h). As can be seen, the tensile stresses generated by the bending moment due to self-weight have been countered by the effect of the prestressing, thus all the cross section is under a compressive state.

The same girder is depicted in figure 2.18a although in that case pick up points *A* and *B* have been moved inwards. The presence of the overhangs would cause the bending moment diagram due to the self-weight load to be as shown in 2.18c. Both the prestressing moment diagram (2.18b) and axial force diagram (2.18d) would remain as in the previous case (fig. 2.17). Those internal forces would cause a stress state at the support *A* (*A-A'*) as shown in figure 2.17e for the bending moment due to self-weight, figure 2.18f for the prestressing moment and figure 2.18g for the prestressing compression force. Consequently, the final stress state of the cross section at the support would be as depicted in figure 2.18h. Note that in that case excessive tensile stresses may develop at the top fiber of the beam for which the beam has not been designed for (fig. 2.18h).

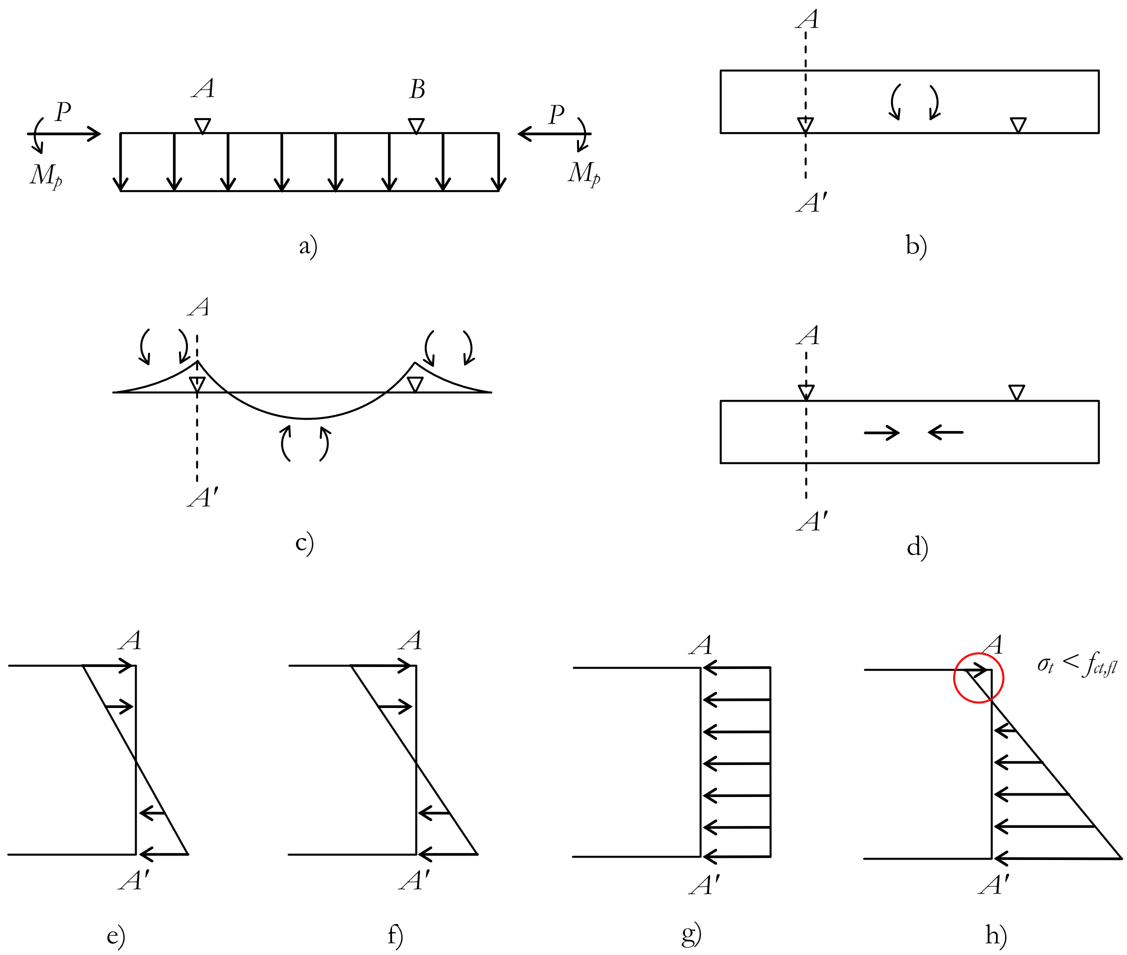

Figure 2. 18. Hanging girder with inner lift points: a) acting loads, b) prestressing moment diagram, c) self-weight bending diagram, d) axial force diagram, e) self-weight bending stresses, f) prestressing moment stresses, g) axial force stresses, h) final stress state.

2.3.3 Anderson, A. R. and Swann, W. G.

In 1971 Anderson highlighted the need to pay more attention to temporary stresses and lateral stability of precast prestressed concrete beams during transportation and erection. He experienced firsthand the problem of lateral instability during lifting of a 150 ft (45.72 m) long beam from the stressing bed. The beam started to tip and deflect laterally so it was immediately lowered back and restored to its initial straight condition. Anderson's factor of safety against lateral buckling for a beam that is lifted at the crane hooks is given by equation 2.10.[12]

$$F.S. = \frac{H_y}{W_{ms}} \tag{2.10}$$

where:

- H_y: Distance from the beam top face to the beam centroid.
- W_{ms}: Midspan deflection when the beam's self weight is applied in the weak-axis direction.

Both parameters are graphically defined in figure 2.19.

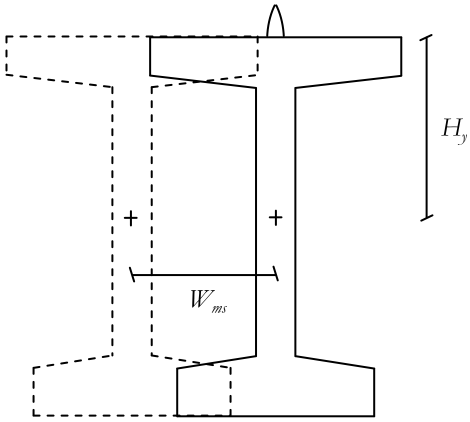

Figure 2. 19. Parameters involved in Anderson's F.S. Solid line, initial position of the cross section at support; dashed line, deflected position of the cross section at midspan after self-weight is applied laterally..

Note that W_{ms} is a fictitious quantity because most beams would fail if the full weight were applied laterally. In the case of an end supported prismatic beam with uniform weight and constant moment of inertia, the deflection W_{ms} may be calculated using equation 2.11.

$$W_{ms} = \frac{5}{384}\frac{qL^4}{EI_y} \tag{2.11}$$

Along with Anderson factor of safety, Swann identified the term in the denominator of equation 2.10 to be the shift of the center of gravity of the beam after deflecting laterally. Its value may be found by integrating the deflected shape of the beam as follows:[15]

$$W_G = \frac{\int_0^L W(x)dx}{L} \tag{2.12}$$

in which *W(x)* would be the deflected shape of an end supported beam:

$$W(x) = \frac{q}{24EI_y}(x^4 - 2Lx^3 + L^3x) \tag{2.13}$$

The deflection of the center of mass W_G of a simply supported beam is thus given by equation 2.14.

$$W_G = \frac{qL^4}{120EI_y} \tag{2.14}$$

Since $W_G = 0.64 \cdot W_{ms}$ Swann proposed a new equation for the factor of safety against buckling given by equation 2.15[13]. Swann also modified the vertical distance H_y defined by Anderson. It became the vertical distance between a line through the two lifting points and the center of gravity of the whole beam *(H)*, instead of the distance between the top face of the beam and the center of gravity *(H_y)*.

$$F.S. = \frac{H}{0.64\ W_{ms}} \tag{2.15}$$

Figure 2.20 shows the differences between the parameters used for computing Anderson's factor of safety (eq. 2.10) and Swann's factor of safety (eq. 2.15). *G* accounts for the position of the center of gravity of the beam. *G'* accounts for the position of the center of gravity of the whole beam after being laterally deflected.

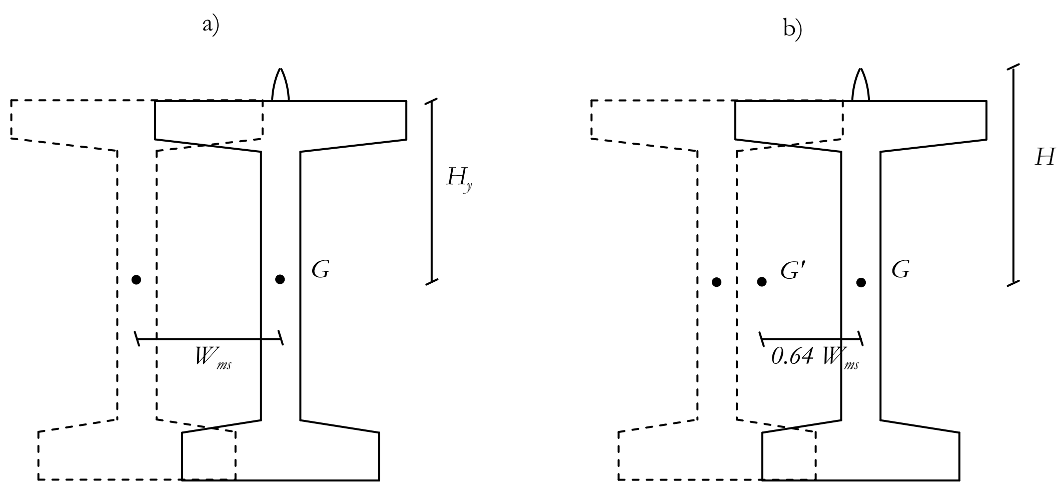

Figure 2. 20 Example of beam cross section. Solid line, initial position of the cross section; dashed line, deflected position of the cross section at midspan after self-weight is applied laterally. a) Parameters involved in Anderson's F.S. b) Parameters involved in Swann's F.S.

Furthermore, Swan noted the importance of considering geometric imperfections in stability calculations such as lateral sweep δ and lateral eccentricity of the fixation points with respect to the centroid of the cross section e_l. These two types of imperfection are shown in figure 2.21.

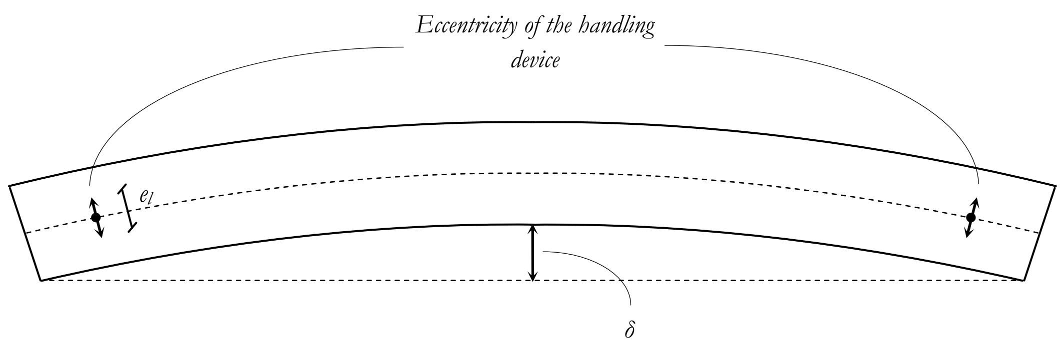

Figure 2. 21 Plan view of a beam. Lateral sweep imperfection and handling device eccentricity.

2.3.4 Laszlo, G. and Imper, R. R.

George Laszlo and Richard Imper published in 1987 *Handling and Shipping of long span bridge beams*[14]. In accordance with their investigation, lateral stability problem arises because of the imperfections during production: slight horizontal eccentricity in prestress from the vertical axis, the lifting loops not centered in the section or thermal gradient from one side of the beam to the other.

Such variations cause the beam to bow horizontally during handling, thus shifting the center of mass away from the original centroid of the beam. When the beam is lifted, the combination of the horizontal bow with the tilting action causes the beam to bend and deflect progressively in the weak axis. As soon as the moment of inertia of the weak axis becomes cracked, the phenomenon rapidly increases until the beam fails in compression or tension. For this reason, failure due to lateral instability is related to deflection along the weak axis.

Based on plant and field experience, Laszlo and Imper suggested new values for the factor of safety defined by Swann (eq. 2.15). Those were F.S. > 1.5 for plant handling and F.S. > 1.75 for field handling. Once the cross section and the prestress level are already established, the authors proposed three options available to the producer to reduce lateral deflection and their limitations. Those are:

- Shorten the handling and shipping span. Since beams are designed for in place conditions, it is impractical to move in the lifting points beyond a certain distance due to the tensile stresses induced. This was also stated by Muller (see section 2.3.1).
- Improve the modulus of elasticity of concrete. Considered an expensive solution. Especially for prestressed members for which an early transfer strength and handling from the casting bed is performed.
- Brace the member to increase the moment of inertia along the weak axis. Most common option used in the past years by stiffening the weak part of the beam (most often the top flange). Since every long beam has to be stiffened temporary bracing system can be very expensive.

Laszlo and Imper also pointed out the limitation of the king post truss system. The most commonly used bracing system for shipping long span bridge beams. They noted that beyond a certain horizontal deflection of the beam, the system was useless and could not prevent its collapse. On the other hand, this system could be effective for short durations such as when moving on superelevated roads because the beam deflection is not instantaneous. It is gradual and can be observed visually due to the plastic characteristic and creep of the concrete.

The effects of lateral instability were observed by one of the authors in a 40 m long, 2134 mm deep concrete I-beam. First, the beam was lifted from the truck trailer and had to be replaced because the crane could not handle the load. Upon being replaced, due to road superelevation and the beam offset on the truck, the beam had about 8.67 degrees tilt. Although the beam had five strands bracing it on each side of the king posts, it took about 20 minutes to reach the critical deflection about 305 mm, before the beam collapsed.

Finally, the authors also drew attention to the fact that only few codes of practice addressed allowable stresses and other parameters in handling and shipping of long prestressed concrete beams. Thus they presented a step by step analytical procedure for dealing with stability when handling and shipping long span prestressed concrete bridge beams[14]. The specified procedure was based on Anderson and Swann formulations explained in section 2.3.3 respectively, which consider an initially straight beam. However, Laszlo and Imper included the possibility of road superelevation during transportation.

With regard to their method, the critical points were located at the downward top flange under high tension and the upward bottom flange under high compression at the midspan of a bulb T or I beam (see fig. 2.22). To counter the tensile stresses, it was suggested using supplementary reinforcing bars or temporary post-tensioning near the outer edges of the top flange.

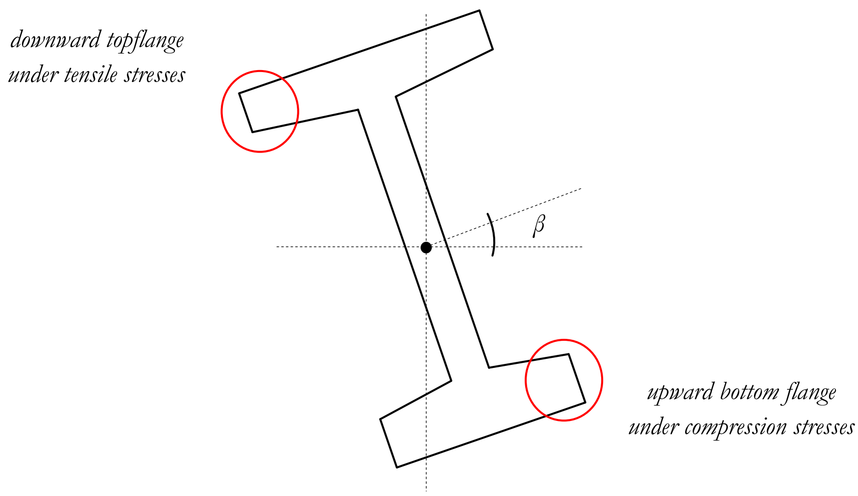

Figure 2. 22 Tilted beam showing the location of the maximum tensile and compressive stresses during lifting. β, angle of tilt.

2.3.5 Mast, R. F.

Lateral Stability of Long Prestressed Concrete Beams, Part 1[15], was written by Robert F. Mast in 1989. He believed the lateral buckling formulas in most textbooks were not adequate to deal with the special cases of a beam suspended on cables or a beam on "springy" supports. Hence, he provided the background and derivations of a new formulation to deal with these two special cases. *Part 1* deals with lateral bending stability of beams when suspended from loops. *Part 2*, from 1993, deals with the stability of beams when supported on elastic supports below the beam.

According to Mast, classic studies of lateral buckling of beams are based on the assumption that the beams are rigidly restrained from rotation at supports. Buckling is caused by the middle part of the span twisting relative to the support, creating sideways deflection. This type of buckling is important in steel I-beams, which have low torsional stiffness. Contrary to them, concrete I-beams, with relatively thick webs and flanges, are 100 to 1000 times stiffer in torsion. Also, concrete I-beams normally have much greater torsional stiffness than the roll stiffness of the supports when the beam is hanging. Such flexibility of the supports allows beams to roll sideways, producing lateral bending moment of the beam, which is the cause of most lateral stability problems of long concrete beams.[15]

As a result, he stated torsional rigidity for a concrete beam can be assumed. This allows to transform the problem from a buckling problem to a simple bending an equilibrium problem for the case of beams hanging from cables.

Mast, in accordance to basic theory of roll equilibrium, defines the rotation axis of a hanging beam as the line passing through the points where the support joins the rigid body, which are the lifting loops. If the beam were perfect, it would hang in a plumb position, with the center of gravity of the beam directly beneath the roll axis. But, sweep tolerances and lifting loop placement tolerances (fig. 2.21) always cause the center of gravity of the beam to be slightly to one side of the roll axis. This causes the beam to tip about the roll axis (fig. 2.23) by a small angle β_i which can be computed using equation 2.16.

$$\tan \beta_i = e/H \qquad (2.16)$$

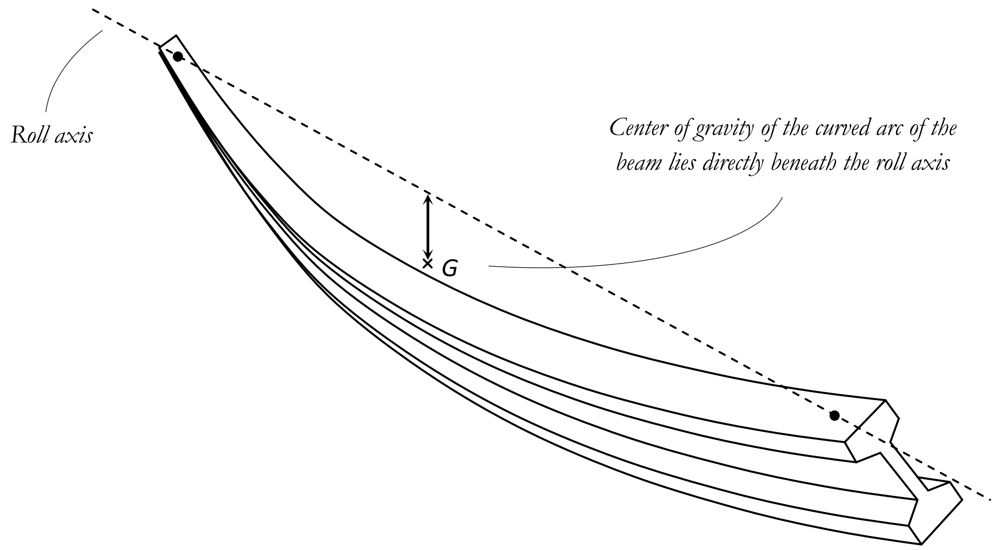

Figure 2. 23 Perspective of a beam free to roll and deflect laterally. [17]

The slight tipping of the beam causes a component of the beam weight q to be applied about the week axis of the beam. This component is $Q \cdot sin\beta_i$ and it causes a lateral deflection of a flexible beam, which further shifts the center of gravity of the mass of the beam. This causes an increase in the roll angle β, which causes further lateral load component and further deflection, etc. Depending on the lateral stiffness of the beam, it may reach equilibrium at a roll angle β slightly larger than β_i, or β may increase to the point where the lateral bending is sufficient to collapse the beam.

In accordance with Mast's theory, the final equilibrium position of the hanging beam is shown in figure 2.24. The beam is assumed to be uniformly tipped by an angle β. The component of the dead weight acting about the weak axis $Q \cdot sin\beta$ has caused and additional lateral deflection W of the center of gravity of the mass of the now curved beam. To find the equilibrium angle β, one must find W, but it is determined by the weight component $Q \cdot sin\beta$, which is itself dependent on β.

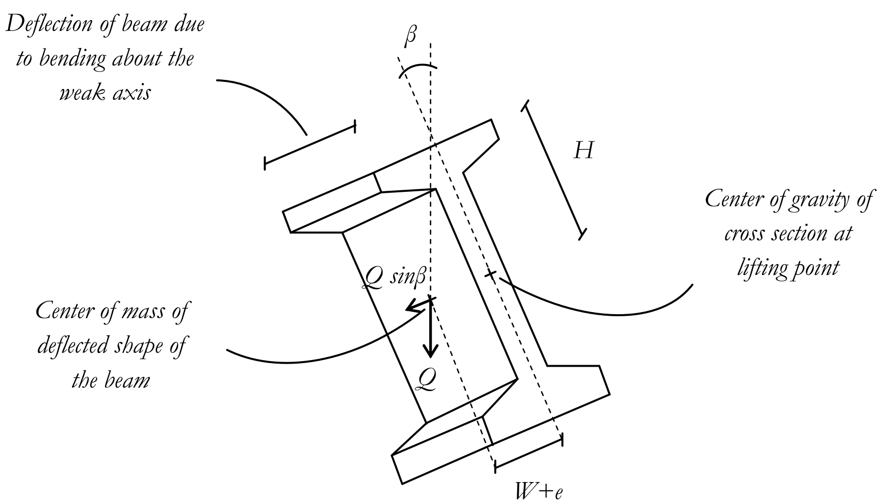

Figure 2. 24 Final equilibrium position of the hanging beam. [17]

That problem may be solved by first computing a theoretical deflection W_G of the center of gravity of the mass of the beam with the full weight Q applied about the weak axis. Then, because the weak axis component of the weight is $Q \cdot sin\beta$, W may be found applying equation 2.17. Expression 2.18

allows the computation of W_G. It considers the possibility of the lifting loops being moved in a distance a from the end of the beam. The overall equilibrium described above leads to equation 2.19, which permits the roll angle β to be obtained by successive approximations.

$$W = W_G \sin\beta \tag{2.17}$$

$$W_G = \frac{q}{12EI_yL}\left(\frac{1}{10}b^5 - a^2b^3 + 3a^2b + \frac{6}{5}a^5\right) \tag{2.18}$$

$$\tan\beta = \frac{W_G \sin\beta + e}{H} \tag{2.19}$$

In line with Mast theory, equation 2.15 may be thought of as the factor of safety against lateral buckling instability. It gives the gross factor of safety against total instability for a near perfect beam. Beams with initial imperfections may fail before total instability is reached, as there is a limit on the angle β that the lateral bending strength of the beam can tolerate. Mast proposed equation 2.20 and equation 2.21 as new factors of safety, being the lower value between them the true factor of safety. The difference between both expressions is whether the dominant effect is the lateral stiffness (eq. 2.20) or the initial lateral eccentricity (eq. 2.21). Note that for the case of a perfect beam with no sweep and eccentricity imperfections, β_i would be zero, hence coinciding expressions 2.4 and 2.20.

$$F.S. = \frac{y_r}{z_0}\left(1 - \frac{\beta_i}{\beta_{max}}\right) \tag{2.20}$$

$$F.S. = \frac{\beta_{max}}{\beta_i}\left(1 - \frac{z_0}{y_r}\right) \tag{2.21}$$

In *Part 2*[16], equation 2.22 is given to replace both equations 2.20 and 2.21. This new formula gives lower factors of safety, for it considers the combined effect of the two previous ratios varying simultaneously.

$$F.S. = \frac{1}{\frac{W_G}{H} + \frac{\beta_i}{\beta_{max}}} \tag{2.22}$$

Nevertheless, there is no explanation regarding how to mathematically define β_{max} since it is determined by the lateral bending strength of the beam, which is dependent on the amount of precompression in the top flange. In accordance with Mast, a conservative approach is to compute β_{max} based on the lateral moment, which, when combined with the vertical moment, produces a tension in the top corner equal to the modulus of rupture. In *Part 2* the author deepens further in the behaviour of the beam once it cracks.

Mast also refers to the effect of camber, which raises the centroid of the mass of the beam, and thus decreases the distance H between the roll axis and the centroid of the mass. According to him, it is sufficiently accurate to assume the centroid of the mass is shifted upward by 2/3 of the midspan camber. Therefore, camber would reduce the safety factor defined in equations 2.20, 2.21 and 2.22.

Options to increase beam stability are proposed. Most of them are the same explained by Laszlo and Imper (section 2.3.4) such as move the lifting points inward, increasing the modulus of elasticity of the concrete or bracing the member. Additionally, the possibility of raising the roll axis by providing a yoke attached to the beam at the lifting points or modifying the beam cross section are also considered.

In connection with the last mentioned idea, the author points out the importance of realizing that the bottom flange contributes just as much to lateral stability as the top flange. In fact, adding material to the bottom flange is more beneficial because it lowers the center of gravity and increases H as well as I_y. Furthermore, the bottom flange is under compression and not as subject to loss of stiffness through cracking as is the top flange. This fact is illustrated in figure 2.25.

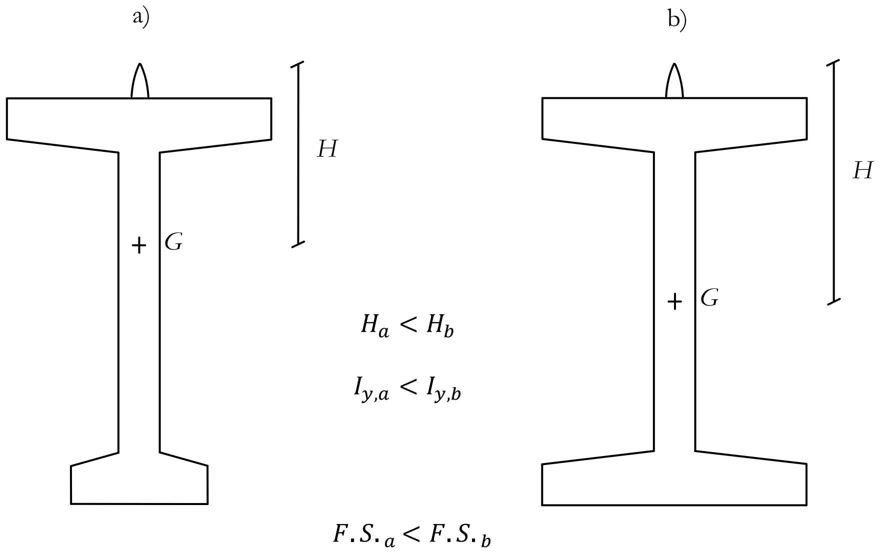

Figure 2. 25 Factor of safety against lateral instability comparison. a) original cross section of beam, b) modified cross section of beam adding material to bottom flange.

To emphasize the importance of this new approach, Mast includes a real case example in his paper[15]. In 1963, two prestressed I-girder normally used on bridge spans of about 30 m were stretched to 44.2 m long. Both beams were carefully checked by classical lateral buckling formulas and found to be satisfactory. The first beam to be lifted was 42 hours old and was handled without incident. The second, beam 18 hours old, tilted immediately on being lifted and bent sideways approximately 300 mm so it was set down on the plant floor. Fortunately, it righted itself instead of rolling over. Using the theory presented in *Part 1*[15] the factor of safety against lateral bending, computed after the fact, was almost exactly 1.0. The initial eccentricity although it was not known, it was believed to be quite small. Apparently, the slight difference in E of the two beams caused one beam to be stable and the other to buckle.

Mast also carried out a test on a 45.4 m prestressed concrete I-beam[17]. The beam was gradually tilted under control conditions and strains and deflections were measured at intervals during the tilting process. The test withstood a tilt of 32 degrees prior to failure and the following aspects were confirmed:

- Beams tolerated lateral loads considerably in excess of the theoretical cracking load, without any visible sign of damage once the lateral load was removed.
- The king-post brace system had only minimal effect on the behaviour of the beam when subjected to lateral loads.
- The assumption that twist may be neglected appeared reasonable.

2.3.6 Stratford, T. J. and Burgoyne, C. J.

In a study carried out in 1999 Stratford and Burgoyne investigated the lateral stability problem throughout finite element techniques[5]. The finite element models were constructed from two-noded, linear beam elements aligned with the beam centroid; these elements were able to allow the effects of warping and the position of the center of the shear to be taken into account. However, as it will be explained later, torsional effects were not found to be significant.

Three different types of buckling failure related to three different support conditions were analyzed: simply supported, transport-supported and hanging beam. For each case, the authors provided solutions to quantities that are important when investigating the stability of long precast concrete beams: the critical load of a perfect beam (buckling load), the load-deflection curve of the imperfect beam, the curvature associated with a given lateral deflection and the stresses which are additional to those due to the primary bending moment and the prestress.

It was found that the case of the beam hanging from cables was the most critical condition, when compared with simply supported and transport-supported cases, due to the absence of any rotational restraint. They also confirmed that the relatively high torsional stiffness of concrete beams meant that beams tend to rotate as a rigid body, with very little variation of twist along the length of the beam. Therefore, assuming torsional rigidity, the buckling mode of a hanging concrete beam can be regarded, to a large degree, as a lateral bending of the beam about its minor axis, combined with a rigid body rotation about the points of attachment to the supporting cables. Note that it coincides with Mast basic hypothesis described in section 2.3.5.

Figure 2.26 shows the variation in twist component of the buckling modes for an end-supported hanging beam, normalized by the largest twist. As can be seen the variation in twist along the beam is very small. The analyzed beam is an *SY*-6 40 m long, 2 m deep. Other beam properties are included in the specified figure.

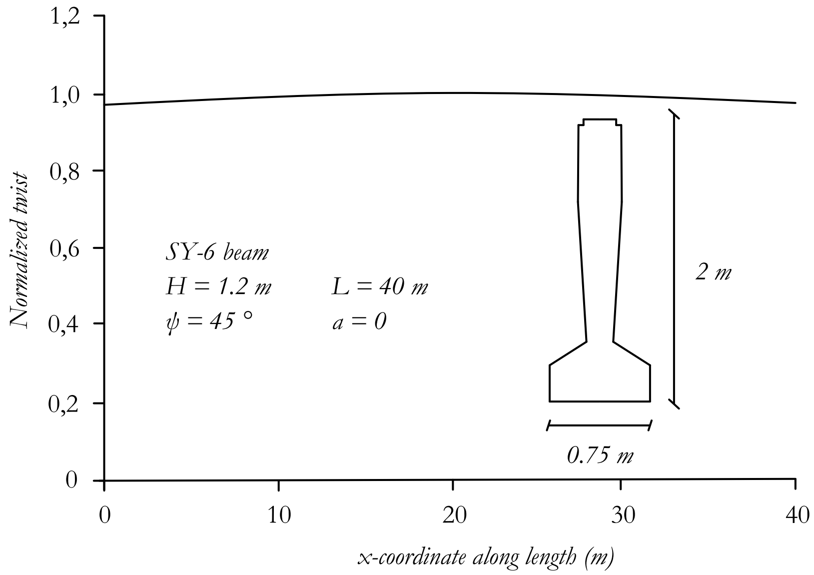

Figure 2. 26 Twist component of the buckling mode of a hanging beam. Beam type: SY-6, length of beam L = 40 m, length of overhang a = 0 m, height of the yoke to cable attachment point H = 1.2 m, cable inclination angle above the horizontal ψ = 45 º, yoke inclination angle above the horizontal β = 90 º. [18]

The background formulation Stratford and Burgoyne used to provide the equations for the hanging beam problem is found in *The toppling of hanging beams*[19]. In that paper, the geometry of the problem is defined as shown in figure 2.27.

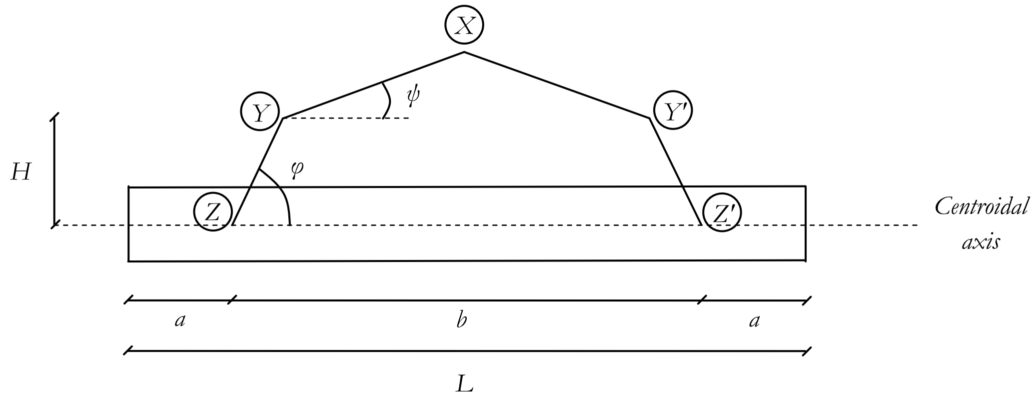

Figure 2. 27 Undeformed geometry of a beam hanging from inclined yokes and cables. [19]

A beam of length *L* is supported at a distance *a* from each end by two yokes *ZY* and *Z'Y'*, which are rigidly attached to the beam and are inclined at an angle *β* to the centroidal axis. The half-distance between the supports is *b*. The tops of the yokes are attached to cables which are inclined at an angle *ψ* and meet at *X*. In practice, *φ* will be either 90º if the yokes are prevented from rotating about the horizontal axis, or be equal to *ψ* if the yokes can align with the cables. The cables are attached to the yokes at a height of *H* above the centroidal axis.

With respect to the structural behaviour of the beam, it is important to underline some of the main assumptions made prior to the development of the formulation. Those are:

- The beam is considered to not deflect by bending about its major-axis or by torsion. However, it is free to bend about its minor-axis and to topple as a rigid-body.
- The yokes are assumed to be rigidly connected to the beam.
- The beam is acted on by a lateral load *t* per unit length, which is applied at a distance *r* below the yoke-cable attachment points. *t* is assumed to act parallel to the direction of the beam's major principal axis as the beam rotates.
- The beam has a small initial imperfection *δ(x)* which varies as a single sinusoidal half wave along the beam's length, but offset so that *δ* is *0* at the yoke attachment points.
- The minor-axis deflection *W* is assumed to be small by comparison with the length of the beam.
- The beam remains linear elastic at all times with fixed section properties. The analysis does not attempt to look at the behaviour of the beam after cracking takes place.

Figure 2.28 shows the deflected shape of the beam under the assumptions previously mentioned.

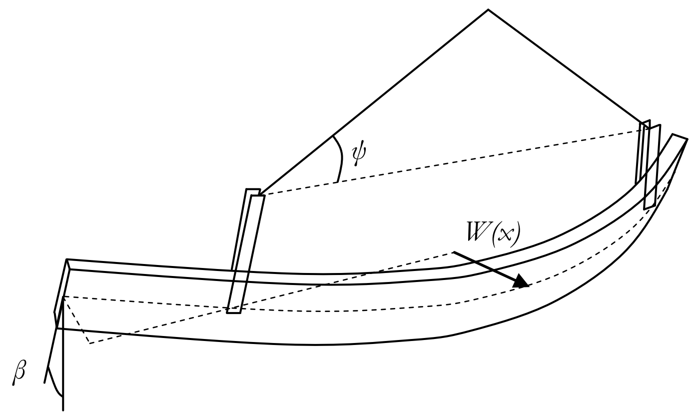

Figure 2. 28 Buckling mode of a typical beam hanging from inclined cables showing the parameters used to define its shape. [19]

The loads acting on the beam are the self-weight q per unit length, which acts at the centroid, and a load t per unit length which acts normal to the beam. The load t considers the effect of wind loads and dynamic factors combined, acting through a single point at a distance r below the top of the yokes Y and Y'. A scheme of the forces acting on the beam when hanging is presented in figure 2.29.

The cable tension F can be found by applying the cosine rule to the polygon shown in the inset in figure 2.12. Hence, F is given by equation 2.23.

$$F = \frac{L\sqrt{q^2 + t^2 + 2qt\sin\beta}}{2\sin\psi} \tag{2.23}$$

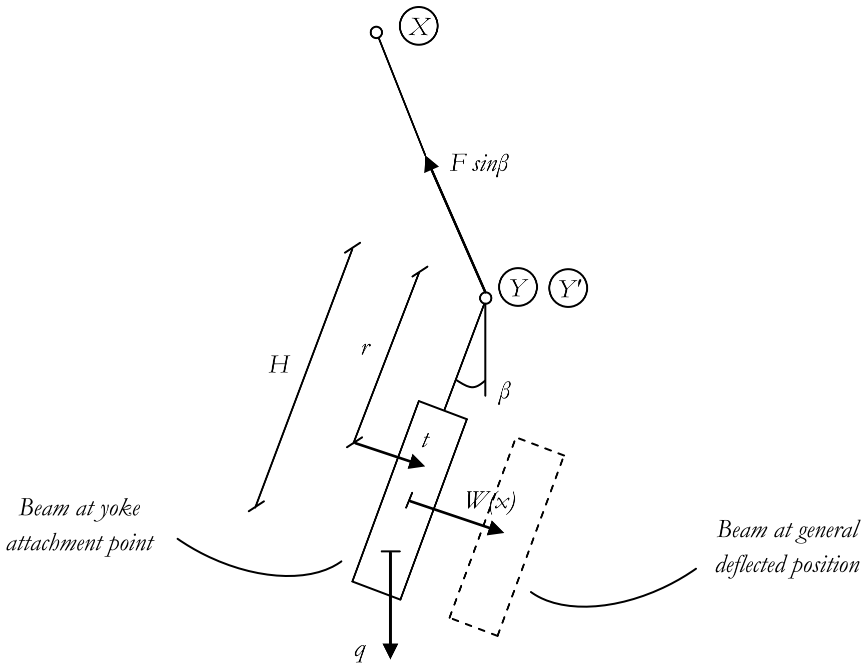

Figure 2. 29 Forces acting on deflected hanging beam. Section at one of the yoke attachment points. [19]

The entire formulation developed by Stratford and Burgoyne can be found in reference 17. Due to its complexity and extension the only equations included in this section are the ones needed to compute the roll angle of the whole beam β, the mid-span lateral deflection W_{ms} and the mid-span curvature K_{ms} for the case of a beam hanging from vertical cables. The equations are 2.24, 2.25 and 2.26 respectively. The value of parameters C and D involved in equation 2.24 are also specified below in equations 2.27 and 2.28 respectively.

$$\left(H\sin\beta + \frac{t}{q}r\right) = C\cos\beta\,(q\sin\beta + t) + D\cos\beta \tag{2.24}$$

$$W_{ms} = \frac{\psi}{384EI_y}(5L^2 - 20aL - 4a^2)(2a - L)^2 + \delta\left(1 - \sin\frac{\pi a}{L}\right) \tag{2.25}$$

$$K_0 + K_{ms} = \frac{\psi}{8EI_y}(L^2 - 4aL) + \frac{\delta\pi^2}{L^2} \tag{2.26}$$

$$C = \frac{1}{12EI_y}\left[\frac{L^4}{10} - aL^3 + 3a^2L^2 - 2a^3L - a^4\right] \tag{2.27}$$

$$D = 2\delta\left[\frac{1}{\pi} - \frac{1}{2}\sin\frac{\pi a}{L}\right] \tag{2.28}$$

In general, no analytical solution exists for equation 2.24 but it can be solved by a suitable numerical technique.

The results of the analysis performed by Stratford and Burgoyne were used in *Stability design of long precast concrete beams*[16] to give design guidance, with particular attention paid to the stresses induced by the pre-buckling deformations. Figure 2.30 shows the stresses to be combined when checking the limit stress state.

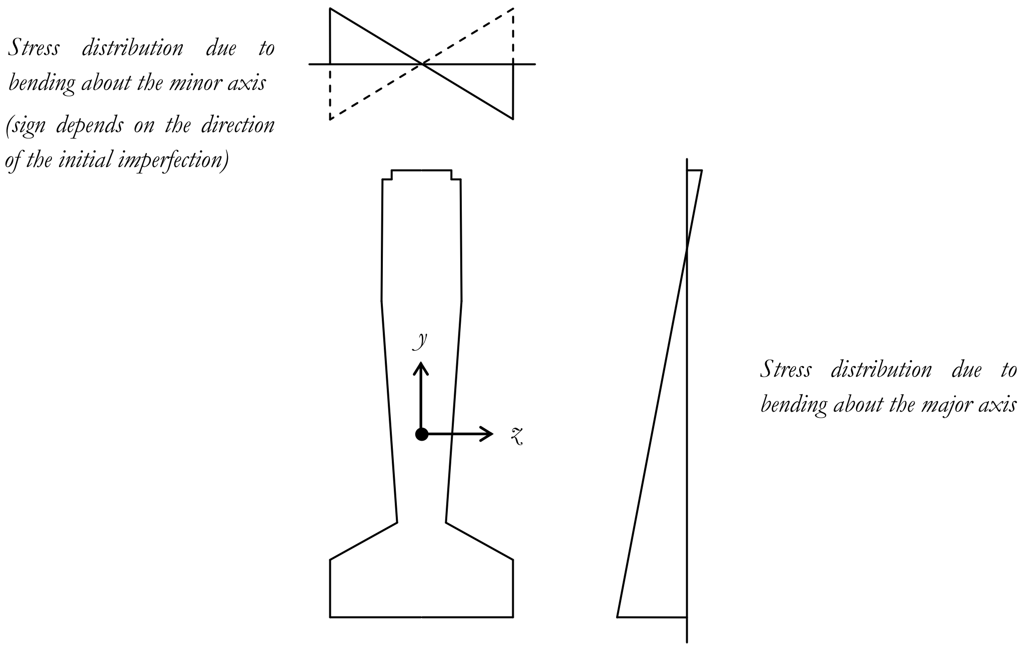

Figure 2. 30 Stresses to be combined when assessing a beam (note that minor-axis stresses can be in either sense). [18]

Stress distribution due to bending about the minor axis includes stresses due to lateral stability effects and initial imperfection. Stress distribution due to bending about the major axis includes the effect of self-weight bending moment in the major-axis direction, the stress distribution due to prestress and the additional force and bending moment resulting from the axial force if the beam is hanging from inclined cables. Nevertheless, the authors affirmed that no attempt was made to evaluate the stresses causing the initial imperfection (due to K_0) since they are heavily dependent on their original cause.

The change in stress due to lateral stability effects at midspan are given by equation 2.29. E corresponds to the Young modulus of the concrete, K_{ms} is the curvature at midspan (eq. 2.26) and y the vertical coordinate with respect to the cross section center of gravity.

$$\Delta\sigma = EK_{ms}y \tag{2.29}$$

2.3.7 Plaut, R. and Moen, C.

Raymond Plaut and Christopher Moen presented in 2011 *Theory and applications of the lifting of elastic, doubly symmetric, horizontally curved beams*[21]. The main objective of this paper was to obtain analytical solutions for displacements, forces, and moments in a basic curved beam during lifting by two cables.

The formulation was applied to examples of curved concrete and steel beams, and the effects of various parameters (e.g., weak-axis bending stiffness, inclination of the cables and overhangs length) were examined. For concrete beams, the initial curvature corresponds to a small lateral imperfection.

With regard to their formulation, the following assumptions are made:

- The cross-sectional dimensions are small compared to the radius of curvature.
- The cross section is uniform and doubly symmetric so its center of gravity coincides with its shear center.
- The material is assumed to be homogeneous and linearly elastic.
- Distortion of cross sections in their own plane is neglected and shear deformation of the middle surface of the beam is neglected.
- Camber, prestress, and residual stresses are not included.
- Deformations are assumed to be small.

The problem is defined as follows. A perspective with inclined cables is shown in figure 2.31, a top view in figures 2.32 and 2.33, a side view (from the center of curvature) in figure 2.34, and another perspective in figure 2.35. The radius of curvature of the unstrained beam is *R* and the beam length is *L*.

The subtended angle of the beam is 2α, and the cylindrical coordinate θ is zero at midspan as shown in figure 2.31a. The beam is suspended by two cables. The connections points *D* and *K* lie on the *y* axis at θ = -γ and γ, respectively, at a distance *a* from the near end of the beam and a height *H* above the shear center. The line passing through *D* and *K*, which is dashed in figure 2.31c, is the roll axis and the offset of the center of the beam from the chord through the ends is denoted δ. The inclination angle of the cables from the vertical is *ψ* toward midspan as indicated in figure 2.31d, and it is assumed that *ψ* is not altered by the deformations of the beam.

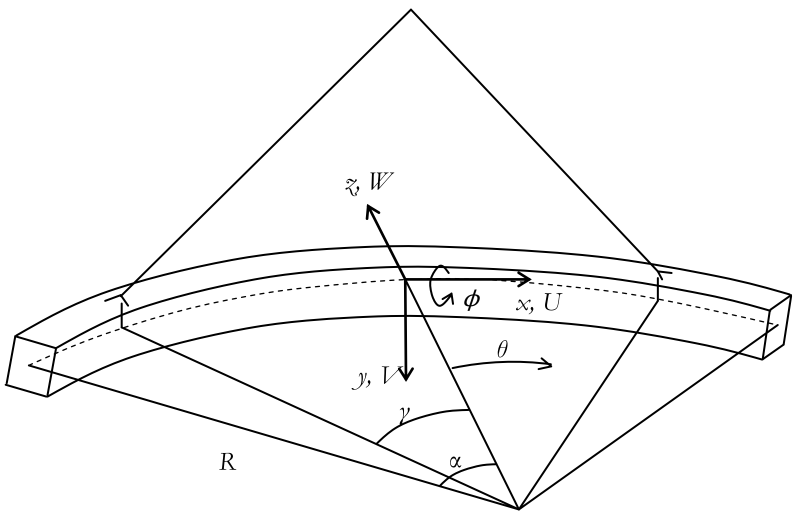

Figure 2. 31 Perspective of beam geometry. [22]

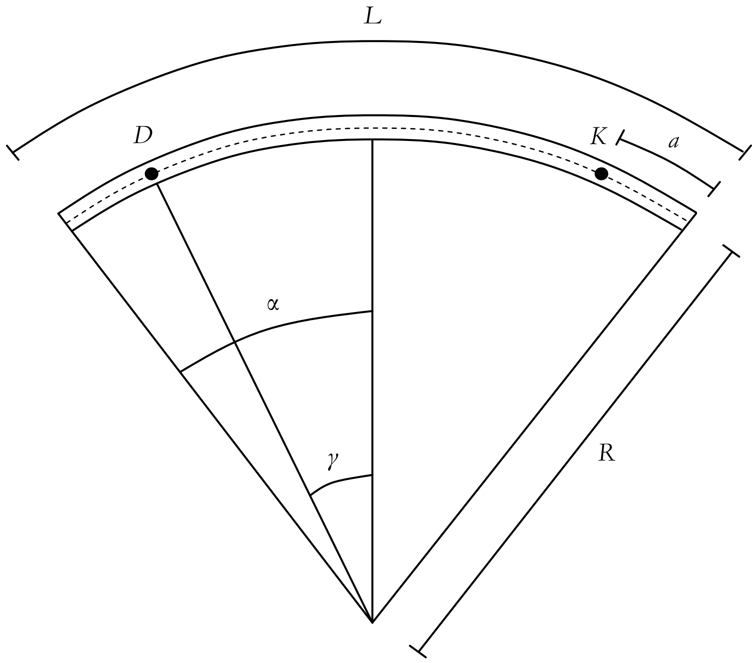

Figure 2. 32 Top view of beam geometry. [22]

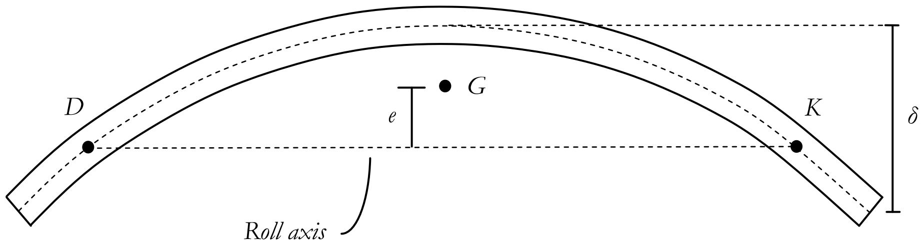

Figure 2. 33 Top view of beam geometry showing center of gravity eccentricity. [22]

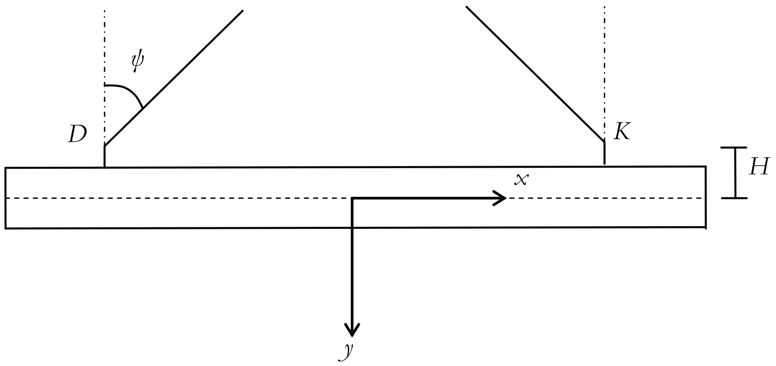

Figure 2. 34 Side view from center of curvature. [22]

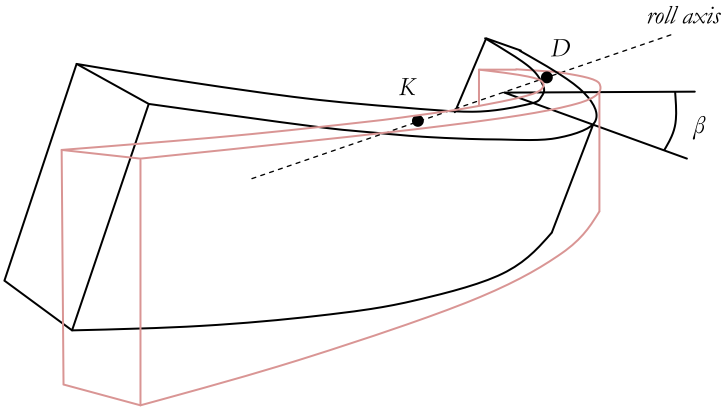

Figure 2. 35 Perspective showing roll angle. [22]

As shown in figure 2.36, the y and z axes are the principal axes of the cross section, and the longitudinal x axis is tangential to the curved axis of the member through the shear center. The origin is at midspan, so that $x = R\theta = L\theta/(2\alpha)$. The center of gravity of the beam lies along the central ray $\theta = 0$ and at a radial distance (eccentricity) e from the roll axis.

Weak-axis bending occurs in the x-z plane, and the corresponding moment of inertia is I_y, whereas strong-axis bending occurs in the x-y plane with moment of inertia I_z. The longitudinal deflection is U, the strong-axis deflection is V, the weak-axis deflection is W (positive if radially outward), and the angle of twist is ϕ. The internal forces parallel to the x-, y-, and z-axes, respectively, are N_x, N_y, and N_z, with corresponding twisting moment (torque) M_x and bending moments M_y and M_z (fig. 2.32).

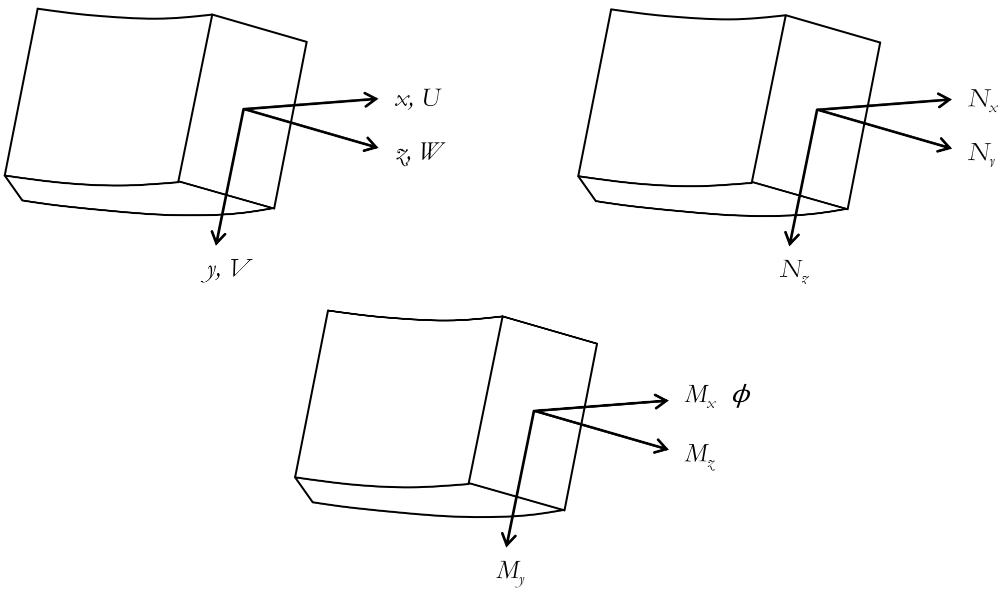

Figure 2. 36 a) Axes and deflections, b) Internal forces, c) Moments and twist angle. [22]

Their analysis was carried out for two main cases: uniform torsion and non uniform torsion. The difference between them is whether the effects of warping, which is the axial distortion of a section due to torsion, are included in the formulation or not. Warping should be considered for thin-walled sections such as steel I-beams since restraint of this deformation effectively increases the stiffness of a beam, and hence its buckling capacity. On the other hand, for a typical concrete beam section the effects of warping are negligible[21, 22] which simplifies the set of equations to be used.

The entire formulation developed by Plaut and Moen can be found in reference 22 and also, including some examples, in reference 21 where, warping is not included when analyzing concrete beams. For the reasons outlined before, the equations included in this section are just valid for the case of uniform torsion (no consideration of warping) which is characteristic of typical concrete beam cross sections.

The analysis is conducted in terms of the nondimensional quantities defined by expressions 2.20 to 2.30.

$$h = \frac{H}{L} \qquad (2.30) \qquad\qquad m_x = \frac{M_x}{qL^2} \qquad (2.31)$$

$$m_y = \frac{M_y}{qL^2} \qquad (2.32) \qquad\qquad m_z = \frac{M_z}{qL^2} \qquad (2.33)$$

$$u = \frac{U}{L} \qquad (2.34) \qquad\qquad v = \frac{V}{L} \qquad (2.35)$$

$$w = \frac{W}{L} \qquad (2.36) \qquad\qquad \lambda_x = \frac{GJ}{qL^3} \qquad (2.37)$$

$$\lambda_y = \frac{EI_y}{qL^3} \qquad (2.38) \qquad\qquad \lambda_z = \frac{EI_z}{qL^3} \qquad (2.39)$$

$$\lambda_A = \frac{EA}{qL} \qquad (2.40)$$

Roll angle β is given by equation 2.41 and it can be computed by successive approximations. The integral inside equation 2.41 is equivalent to expression 2.42. Coefficients c_9 and c_{10} are specified in references 19 and 20 along with subsequent parameters $c_1, c_2, \ldots, c_{29}$.

$$2h\alpha^2 \tan\beta = \sin\alpha - \alpha\cos\gamma + 2\alpha \int_0^{\alpha} w(\theta)cos(\theta)\, d\theta \qquad (2.41)$$

$$\int_0^{\alpha} w(\theta)cos(\theta)\, d\theta = c_9 \sin\beta + c_{10} \tan\psi \qquad (2.42)$$

where:

- h : dimensionless height from the center of gravity to roll axis (eq. 2.30).
- α : angle of the beam as shown in figure 2.31 and 2.32.
- γ : angle between the two lifting points as shown in figure 2.31 and 2.32.
- ψ : inclination angle of the cables from the vertical as shown in figure 2.35.

<u>Moments along the beam are obtained using the following equations:</u>

For the right half of the central portion of the beam ($0 \leq \theta < \gamma$), equations 2.33, 2.34 and 2.35.

$$m_x = \frac{1}{4\alpha^2}(c_1 \sin\theta - \theta\cos\beta) \tag{2.33}$$

$$m_y = \frac{1}{4\alpha^2}(\cos\alpha - \alpha\sin\gamma - \cos\theta - \theta\sin\theta)\sin\beta \tag{2.34}$$

$$m_z = \frac{1}{4\alpha^2}(\cos\beta - c_1\cos\theta) \tag{2.35}$$

For the overhang region ($\gamma < \theta \leq \alpha$) using equations 2.36, 2.37 and 2.38.

$$m_x = \frac{1}{4\alpha^2}[\alpha - \theta - \sin(\alpha - \theta)]\cos\beta \tag{2.36}$$

$$m_y = \frac{1}{4\alpha^2}[\cos\alpha - \cos\theta + (\alpha - \theta)\sin\theta]\sin\beta \tag{2.37}$$

$$m_z = \frac{1}{4\alpha^2}[1 - \cos(\alpha - \theta)]\cos\beta \tag{2.38}$$

<u>Displacements along the beam are obtained using the following equations:</u>

For $0 \leq \theta < \gamma$ using equations 2.39 and 2.40.

$$w = \frac{1}{64\alpha^4\lambda_y}\{[-4c_2 + 3\theta\sin\theta + (c_3 - \theta^2)\cos\theta]\sin\beta \\ + (4\alpha\cos\gamma - 2\alpha\theta\sin\theta + c_4\cos\theta)\tan\psi\} \tag{2.39}$$

$$v = \frac{1}{32\alpha^4\lambda_x\lambda_z}(c_{19} - \lambda_z\theta^2\cos\beta + c_{20}\cos\theta + c_{21}\theta\sin\theta) \tag{2.40}$$

For $\gamma < \theta \leq \alpha$ using equations 2.41 and 2.42.

$$w = \frac{1}{64\alpha^4\lambda_y}\{[4(\cos\theta\sec\gamma - 1)\cos\alpha \\ + (c_5 + 3\theta)\sin\theta + (\gamma - \theta)(c_6 + \theta)\cos\theta - c_7\cos\theta]\sin\beta \\ + c_8\sin(\gamma - \theta)\tan\psi\} \tag{2.41}$$

$$v = \frac{1}{64\alpha^4\lambda_x\lambda_z}(c_{22} + 2\alpha c_{23}\theta - c_{23}\theta^2 \\ + c_{24}\sin\theta + c_{25}\cos\theta + c_{26}\theta\sin\theta + c_{27}\theta\cos\theta) \tag{2.42}$$

<u>Twist angle along the beam is obtained using the following equations:</u>

For $0 \leq \theta < \gamma$ using equation 2.43.

$$\phi = \frac{\lambda_x + \lambda_z}{16\alpha^3\lambda_x\lambda_z}(-2\cos\beta + c_{13}\cos\theta + c_1\theta\sin\theta) \tag{2.43}$$

For $\gamma < \theta \leq \alpha$ using equation 2.44.

$$\phi = \frac{\lambda_x + \lambda_z}{64\alpha^3\lambda_x\lambda_z}(c_{14} + c_{15}\sin\theta + c_{16}\cos\theta + c_{17}\theta\sin\theta + c_{18}\theta\cos\theta) \tag{2.44}$$

As a conclusion, Plaut and Moen point out that the locations of the lift points are crucial in determining the roll angle and deformations of the beam. If the overhangs are approximately one-fifth of the length of the beam, the roll angle and twist angle will be very small. Nevertheless, for prestressed or reinforced concrete beams, having such a large overhang may not be possible because of excessive longitudinal tensile stresses at the top of the beam and its negative effect on cracking. Lateral wind loads were included in Stratford and Burgoyne (see section 2.2.6). However, lifting is usually performed when wind loads are not significant.

Razvan Cojocaru studied in 2012 the applicability of Plaut and Moen formulation to singly symmetric normally used prestressed concrete cross sections such as the PCI-BT-72 and the AASHTO Type IV beams[30]. Analytical results obtained under the assumption that the center of shear coincide with the center of gravity for these beams were compared with the results obtained by the finite element method computer program ABAQUS. It was concluded that Plaut and Moen formulation offered conservative results for weak-axis moment and displacement for beams with the center of twist below the centroid, and non-conservative results for beams with the center of twist above the centroid. However, the difference in results between the FE model and the Plaut and Moen method is small, not exceeding ± 5 percent.

2.4 Limitations of current literature

All the methods presented in chapter 2.3 are useful tools for investigating lateral stability during lifting of precast concrete beams. Nonetheless, they all are subject to limitations in their applicability.

For example, the methods presented by Muller (2.3.2), Anderson and Swann (2.3.3) and Laszlo and Imper (2.3.4) do not consider the effect of lateral sweep. The beam is assumed to be perfectly straight. Mast (2.3.5) is the first to introduce the effect of initial imperfections for the hanging beam case. Yet, the computation of its factor of safety requires the knowledge of the maximum roll angle the beam can sustain. According to him, a conservative approach of that maximum angle would be the one producing a tension in the top corner equal to the modulus of rupture of the concrete, although he states that precast prestressed concrete beams can tolerate loads considerably in excess of the theoretical cracking load. A lateral bending test on a long prestressed concrete beam confirmed that fact. Mast's theory allows to obtain the roll angle caused by horizontal imperfections and lateral deflection in a hanging beam. Its limitations are that torsional effects are neglected and simple equations to compute the internal forces, displacements and stresses are not explicitly defined. Lastly, Mast's procedure does not treat the case of inclined cables in detail.

Stratford and Burgoyne (2.3.6) provided useful and explicit equations for computing the roll angle, the critical buckling load, the lateral deflection due to lateral bending and also the stresses produced during lifting of a precast prestressed concrete beam. They included the possibility of inclined cables and lateral loads, such as wind. In the same way than Mast, the beam is assumed to be torsionally rigid. This hypothesis is confirmed to be reasonable throughout a comparison carried out using a finite element method computer program. Their analysis is linearly elastic with no attempt to look at the behaviour of the beam once it cracks.

Finally, Plaut and Moen (2.3.7) analytical formulas allow the computation of vertical and horizontal displacements, internal forces and moments in a curved beam during lifting. The possibility of inclined cables is also taken into account. Plaut and Moen formulation considers two different torsional approaches: uniform and non uniform torsion. This fact makes the method useful both for concrete beams and metallic beams. Regarding its limitations, the method is based on the assumption that the center of shear coincides with center of gravity of the cross section, which is true only for doubly symmetric cross sections. The analysis remains linearly elastic in every moment.

2.5 Lateral stability specifications in current regulations

In this chapter attention is drawn to how different regulations deal with lateral stability of precast beams. Special attention is paid to the Spanish concrete Instruction *EHE-08 Instrucción de Hormigón Estructural*[26]. Both the *Eurocode 2: Design of concrete structures*[27] and the *PCI Bridge Design Manual*[24, 25] have also been checked.

EHE-08 Instrucción de Hormigón Estructural:

"Artículo 16.2 Imperfecciones. En los casos en los que resulte significativo el efecto de las imperfecciones geométricas, éstas se tendrán en cuenta para la evaluación del efecto de las acciones sobre la estructura.

Artículo 60. Elementos estructurales para puentes. Deberá garantizarse la resistencia y estabilidad de la estructura en todas las fases intermedias de construcción, así como en el estado definitivo de la misma. En el caso de elementos pretensados, se realizarán las comprobaciones que correspondan tanto en la fase de transferencia del pretensado como el instante inicial de puesta en servicio y a largo plazo.

Artículo 70.4.2 Destesado de armaduras pretesas. Si el destesado se realiza elemento por elemento la operación deberá hacerse de acuerdo con un orden preestablecido con el fin de evitar asimetrías que puedan resultar perjudiciales en el esfuerzo de pretensado.

Artículo 76.2 Acopio en obra. Los elementos deberán acopiarse sobre apoyos horizontales que sean lo suficientemente rígidos en función de las características del suelo, de sus dimensiones y del peso. En el caso de viguetas y losas alveolares, se apilarán limpias sobre durmientes que coincidirán en la misma vertical, con vuelos, en su caso, no mayores de 0,50 m, ni alturas de pila superiores a 1,50 m, salvo que el fabricante indique otro mayor.

Artículo 76.3.2 Otros elementos prefabricados lineales. El proyecto deberá incluir, en su caso, un estudio del montaje de los elementos prefabricados que requieran arriostramientos provisionales para evitar posibles problemas de inestabilidad durante el montaje de la estructura

Anejo 11: Tolerancias. Artículo 5.4 Piezas prefabricadas, 5.4.1 Tolerancias de fabricación de elementos lineales. Flecha lateral respecto al plano vertical que contiene al eje de la pieza, no será superior a $L/750$. Además, en función de la luz L, deberán cumplir:

$L \leq 6\,m$	$\pm 6\,mm$
$6\,m < L \leq 12\,m$	$\pm 10\,mm$
$L > 12\,m$	$\pm 12\,mm$"

Eurocode 2: Design of concrete structures:

In section 4.3.5.7 it is pointed out that when the safety of beams against lateral buckling is in doubt, it shall be checked by an appropriate method. The safety against lateral buckling of reinforced and prestressed concrete beams may be assumed to be adequate if the requirements given by equations 2.45 and 2.46 are satisfied. Otherwise, a more detailed analysis should be carried out.

$$l_{ot} < |50|\, b_f \tag{2.45}$$

$$h < |2.5|\, b_f \tag{2.46}$$

where:

- b_f : Width of the compression flange.
- h : Total depth of the beam.
- l_{ot} : Length of the compression flange measured between lateral supports.

<u>PCI Bridge Design Manual:</u>

The *PCI Bridge Design Manual* addresses the lateral stability of prestressed concrete bridge girders for two cases: when the girder is hanging from a lifting device and when the girder is resting on flexible supports specifically referring to the case of the girder being transported. The *PCI Bridge Design Manual* provides an explicit procedure to determining the safety against instability for those two cases which were based on Mast paper from 1989[15] with respect to a hanging girder and Mast paper from 1993[16] with respect to a girder in transit.[10]

There are several construction tolerances specified by the Precast Prestressed Institute[25]. The *PCI Bridge Design Manual* specifies a sweep tolerance of $1/8$ in. (3.2 mm) per 10 ft. (3 m) of girder length. Section 8.10 of the PCI Bridge Design Manual suggests a value of 1.5 for the factor of safety against failure for hanging beams. Due to the possibility of a catastrophic failure, it is recommended that the factor of safety against failure to be conservatively taken as the factor of safety against cracking. However, the manual states that the necessary factors of safety cannot be determined scientifically, and that they must be determined from experience by employing sound engineering judgment.

It is apparent that the governing design codes lack sufficient guidance on the subject of stability of precast prestressed concrete girders during lifting.

CHAPTER 3.

GENERAL AND SPECIFIC DESIGN CRITERIA

3.1 General criteria

EHE-08[27] principles and requirements for the safety, serviceability and durability of structures have been followed. These are based on the theory of the limit states, situations in which the structure no longer satisfies the design performance requirements. Limit states are classified into: ultimate limit states (ULS) and serviceability limit states (SLS).

3.1.1 Ultimate limit state

Ultimate limit states are those associated with collapse, or with other forms of structural failure which may endanger the safety of people. States prior to structural collapse which, for simplicity, are considered in place of the collapse itself are also treated as ultimate limit states. May require consideration of ultimate limit state:

- Loss of equilibrium of the structure or any part of it, considered as a rigid body.
- Failure by excessive deformation, rupture, or loss of stability of the structure or any part of it, including supports and foundations.

3.1.2 Serviceability limit state

Serviceability limit states correspond to states beyond which specified service requirements are no longer met. Serviceability limit states which may require consideration include:

- Deformations or deflections which affect the appearance or effective use of the structure (including the malfunction of machines or services) or cause damage to the building or its contents, or which limits its functional effectiveness.
- Vibration which causes discomfort to people, damage to the building or its contents, or which limits its functional effectiveness.
- Cracking of the concrete which is likely to affect appearance, durability or water tightness adversely.
- Damaging of concrete in the presence of excessive compression which is likely to lead to loss of durability.

3.1.3 Verifications based on the safety factor format

The design value F_d of an action is expressed in general terms as indicated in equation 3.1 where γ_F is the partial safety factor for the actions considered taking account of, for example, the possibility of unfavorable deviations of the actions, the possibility of inaccurate modeling of the actions, uncertainties in the assessment of effects of actions, and uncertainties in the assessment of the limit state considered.

$$F_d = \gamma_F \cdot F_k \tag{3.1}$$

The design value X_d of a material property is given by equation 3.2 where γ_M is the partial safety factor for the material property which is assumed to take account of differences between the strength of test specimens of the structural material and their strength in situ.

$$X_d = \frac{X_k}{\gamma_M} \tag{3.2}$$

Partial safety factors for ultimate limit states and serviceability limit states in different design situations are given in table 3.1 and 3.2, respectively. Partial safety factors for material properties are given in table 3.3.

Effect	**Permanent actions (γ_G)**	**Variable actions (γ_Q)**	**Prestressing (γ_P)**
Favorable	1.0	0	1.0
Unfavorable	1.35	1.5	1.0

Figure 3.1 Partial safety factors for ultimate limit states.

Effect	**Permanent actions (γ_G)**	**Variable actions (γ_Q)**	**Prestressing pre-tensioned (γ_P)**	**Prestressing post-tensioned (γ_P)**
Favorable	1.0	0	0.95	0.90
Unfavorable	1.0	1.0	1.05	1.10

Figure 3.2 Partial safety factors for serviceability limit states.

Type of action	Concrete (γ_C)	Steel reinforcement or prestressing tendons (γ_S)
Permanent	1.5	1.15
Accidental	1.3	1.0

Figure 3.3. Partial safety factors for material properties

3.2 Specific criteria

3.2.1 Lifting analysis formulation

The analysis is carried out using Plaut and Moen formulation. A general description of the method is found in section 2.3.7. The formulation includes the following assumptions:

- The cross-sectional dimensions are small compared to the radius of curvature *R*. (see fig. 2.31 and 2.32)
- The cross section is uniform and doubly symmetric so its center of gravity coincides with its shear center.
- The material is assumed to be homogeneous and linearly elastic.
- Distortion of cross sections in their own plane is neglected and shear deformation of the middle surface of the beam is neglected.
- Camber, prestress, and residual stresses are not included.
- Deformations are assumed to be small.

Plaut and Moen model requires the following inputs:

- Material properties: modulus of elasticity E and modulus of rigidity G.
- Girder properties and dimensions: beam length L, cross-sectional area A, strong-axis and weak-axis moment of inertia I_z and I_y, torsion constant J, and self-weight per unit length q.
- Lifting device information: location of lifting device a from the ends of the girder, height of yoke to cable attachment points above the centroid of the beam H and the inclination angle of the cables ψ.
- Initial sweep imperfection δ.

Based on the received input, the following values at any location along the girder are computed:

- Roll angle.
- Twist angle.
- Internal forces (weak-axis shear, strong-axis shear, and longitudinal and axial force).
- Internal moments (twisting moment, weak-axis bending, and strong-axis bending).
- Deflections (weak-axis and strong-axis).

The cross section of the girders analyzed in this paper are not doubly symmetric. Nevertheless, the applicability of the method has been verified in singly symmetric normally used prestressed concrete cross sections such as the PCI-BT-72 and the AASHTO Type IV beams. The difference in results between the ABAQUS finite element model and the Plaut and Moen method is small, not exceeding ± 5 percent. It offers conservative results for weak-axis moment and displacement for beams with the center of twist below the centroid, and non-conservative results for beams with the center of twist above the centroid.[30]

Plaut and Moen formulation does not include the effect of the prestressing force when computing the roll angle, deflections and internal forces of a hanging girder. Therefore it will be added during a second phase after the rotation of the beam is obtained. This procedure is the same followed by Razvan Cojocaru[30].

Additionally, the equations derived by Plaut and Moen do not include the influence of camber. It was concluded that camber may not have a large influence on the roll angle and deformations of a curved beam during lifting[22].

3.2.2 Lateral buckling limit state

The lateral buckling of a prestressed concrete girder is regarded as a rigid body rotation about the points of attachment to the supporting cables combined with a lateral bending of the girder about its minor axis and cross-sectional twist. Excessive weak-axis bending may cause rupture or loss of stability. Therefore lateral buckling is considered a ultimate limit state (ULS) and the appropriate safety factors will be used.

Mast conducted a lateral bending test on a prestressed concrete I-girder to investigate the cracked section behaviour of girders subjected to lateral loads[17]. According to his findings the test girder tolerated lateral loads in excess of the theoretical cracking load, without any visible sign of damage once the lateral load was removed. Nevertheless if a cracked section is allowed during lifting there would be a reduction in the girder's stiffness, resulting in increased deflection and consequently increasing possibility of a self-propagating catastrophic stability failure. Therefore, as recommended by Stratford et al.[18], for safety considerations it is advised to not allow a cracked section during lifting. This consideration makes Plaut and Moen model valid since it assumes materials with linear elastic behaviour.

3.2.3 Cracking limit state

Stresses on the girder cross section are caused by the effect of the self-weight, the prestressing and, in the case of inclined cables, the additional normal stresses resulting from the axial force in the cables. For the precast prestressed concrete girders studied in this paper the maximum tensile stress typically occurs at midspan in the corner of the downward top flange of the rotated cross-section as shown in figure 3.1.

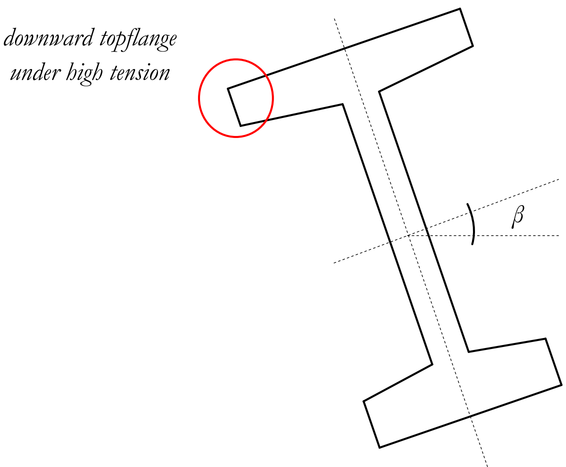

Figure 3.1. Tilted beam showing the location of the maximum tensile stresses during lifting. β, angle of tilt.

To ensure cracking does not occur tensile stresses are limited to the tensile strength of the concrete. *EHE-08* specifications state the mean tensile strength f_{ctm} of the concrete may be derived following equation 3.1. f_{ck} is the characteristic resistance of the concrete.

$$f_{ctm} = 0{,}30\, f_{ck}^{2/3} \tag{3.1}$$

3.2.4 Prestressing force

The number of prestressing cables in a precast prestressed concrete girder is established according to several factors although there exist an upper and lower limit for a given cross section. The lower limit responds to a minimum reinforcement requirement. The maximum number of cables is defined so that the girder does not fail at the moment the prestressing force is transferred.

Figure 3.2a shows a side view of a precast prestressed concrete girder under a prestressing force P which induces a prestressing moment $M_p = P \cdot e_p$. The stresses caused by the prestressing force and the prestressing moment are shown in figures 3.2b and 3.2c respectively. The bending moment due to self-weight would reduce the tensile stresses generated in the top fiber. Note that the girder is end supported and thus the bending moment due to self-weight is zero at the supports. The total stresses σ_t caused by the prestressing force and the prestressing moment must not reach the resistance to bending tension of the concrete f_{ct} as depicted in figure 3.2d.

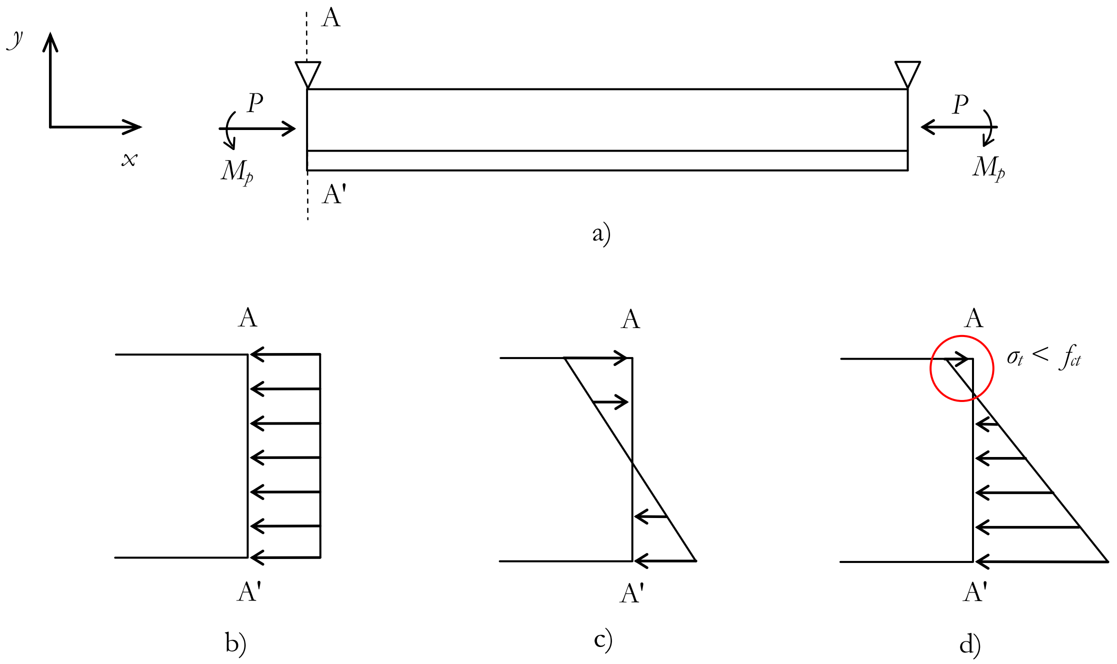

Figure 3.2. End supported hanging girder a) side view, b) axial force stresses, c) prestressing moment stresses d) final stress state.

In that sense, the maximum prestressing load P_{max} located at a distance e_p from the center of gravity is given by equation 3.2. d_1 is the vertical distance between the center of gravity and the top fiber of the cross section.

$$P_{max} = \frac{f_{ct}}{\left(\frac{1}{A} + \frac{e_p \cdot d_1}{I_z}\right)} \tag{3.2}$$

3.2.5 Graphical presentation of the results

Detailed results for each single case studied in this paper will be presented in appendix A. Nevertheless, to study greater generality of the results, these will be presented in chapter 4 using dimensionless parameters.

Figure 3.3 simulates the expected stress state σ_t that will be obtained at the downward top flange of an I girder (see fig. 3.1) for different spans L, given an initial lateral imperfection δ of the form $\delta = f(L)$. Note that an I shaped girder is used to resist vertical loads. Therefore it is much more stiffer in its vertical axis (strong-axis) than in the horizontal axis (weak-axis). As longer spans are evaluated girder's total weight increases hence compressive stresses are supposed to initially grow. Since lateral sweep has been defined as a function of L, the initial rotation of the girder β_i will also increase, causing a greater component of the self-weight to act in the weak-axis direction. At a certain length L_B, due to lateral sweep along with the lateral deflection induced by the self-weight component in the weak-axis direction, the total rotation β of the girder would be such that the tensile stresses will rapidly increase. Once the total stresses reach the tensile strength of the concrete f_{ct} at a length L_C cracks will develop.

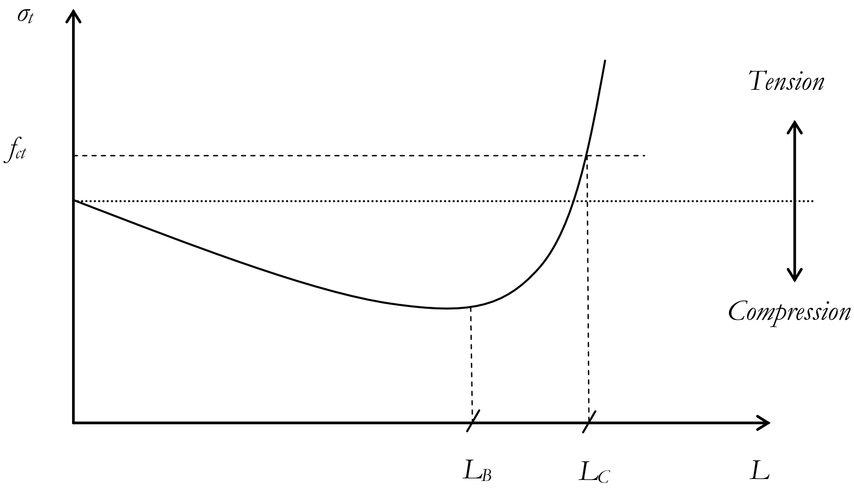

Figure 3.3. Expected stresses at the downward top flange of an I girder depending on its length.

3.2.6 Adopted safety factors

Safety verifications are based on the safety factor format as pointed out in 3.1.3. Lateral buckling will be treated as a ultimate limit state (ULS). Therefore the adopted value of the partial safety parameters is:

- Self-weight action partial safety factor $\gamma_G = 1.35$.
- Prestressing action partial safety factor $\gamma_P = 1.0$.
- Concrete resistance partial safety factor $\gamma_C = 1.50$.

As exposed in 3.2.5 from the span L_B which causes the instability tensile stresses will rapidly increase leading to cracking at a span L_C. For safety considerations, L_B will be assumed as the maximum length achievable with respect to lateral buckling.

CHAPTER 4.

PARAMETRIC STUDY OF A HANGING GIRDER

4.1 Introduction

The influence of several parameters which condition the lateral stability of a prestressed precast concrete girder while is being lifted is presented in this section. Lateral sweep, length of the girder, location of the lift points, the cross-sectional properties and the inclination angle of the lifting cables are some of the decisive factors analyzed below. In that sense, this section provides a thorough study of all of them under some specific assumptions and based on reasonable design criteria. Currently used girder cross sections have been studied in order to obtain more realistic results. Information regarding the geometry and other structural properties of those girders has been obtained from a commercial catalogue and its presented in Appendix A.

To facilitate the analysis it has been used an Excel calculation sheet. Obtaining the roll angle required an iterative calculation process so a root finding method has been programmed in Visual Basic. All the results obtained during the preparation of this paper are found in a detailed manner in Appendix B.

4.2 Scope of the study

a) Girder cross sections provided in the catalogue and analyzed in this paper:

- Girders I Series A. I60A100 to I130A100.
- Girders I Series B. I120B120 to I210B120.
- Girders I Series C base 100. I65C150 to I2135C150.
- Girders I Series D base 120. I75D200 to I245D200.
- Girders Artesa Series B. From A110B to A230B.

In figure 4.1 the cross-sectional geometry of the above mentioned girders is illustrated.

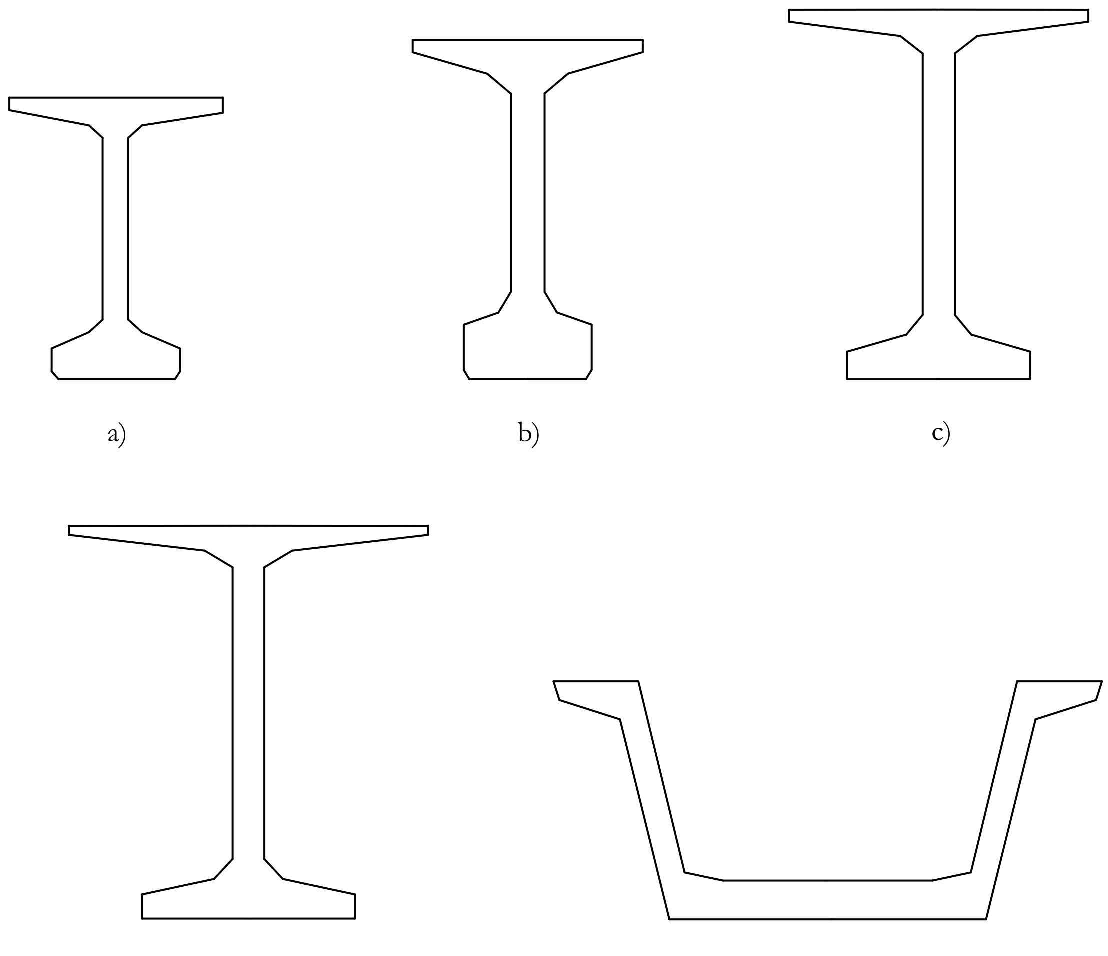

Figure 4.1. Girders cross-sectional geometry: a) I Series A, b) I Series B, c) I Series C, d) I Series D e) Artesa Series B.

b) Girder length *L*. From $L = 10$ m to $L = 60$ m.

c) Location of the lift points from the ends *a*. From $a = 0$ (end supported) to $a = 0.2$L (see fig. 4.2).

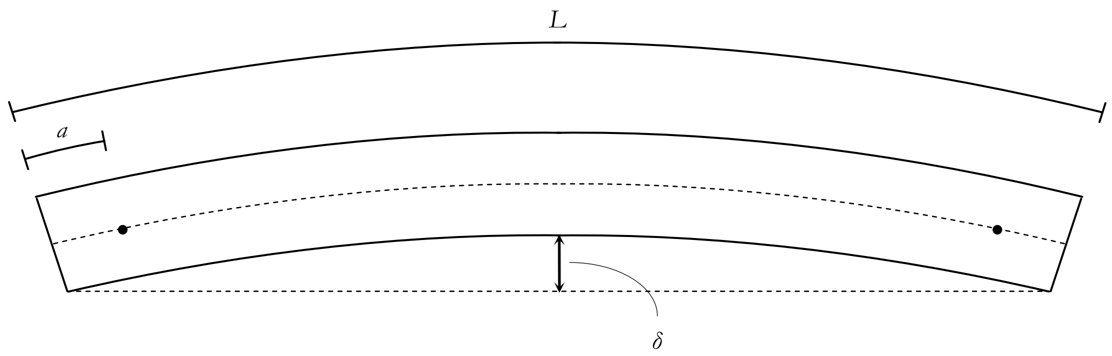

Figure 4.2. Plan view of a beam with a lateral sweep imperfection.

d) Lateral sweep δ. Values around EHE-08 maximum manufacturing tolerance $L/750$. Values from $L/500$ to L/2000 (see fig. 4.2).

e) Characteristic resistance of the concrete f_{ck}. Precast prestressed girders are usually lifted at a very young age. It is common practice to strip the forms and lift the beams from the casting bed within one day, before the characteristic resistance f_{ck} (typically defined at the age of 28 days) has been reached. The use of additives may contribute to rapidly increase concrete resistance. To represent different moments during the construction process f_{ck} will be analyzed from 20 MPa to 60 MPa.

f) Prestressing force P. From P = 0 to P_{max} given by equation 3.2 (see section 3.2.3). Prestressing force is assumed to act in the middle of the bottom flange.

e) Height of the lifting loops. From h_l = 20 cm to h_l = 140 cm (see fig. 4.3).

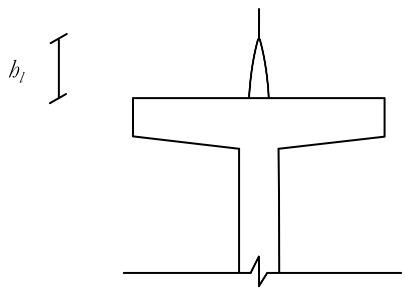

Figure 4.3 Girder cross section at a lift point.

f) Angle inclination of the cables ψ. From ψ = 0 (vertical cables) to 45° with respect to vertical (see fig. 4.4).

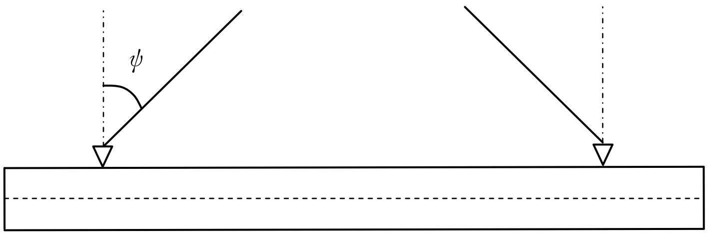

Figure 4.4. Side view of hanging girder with inclined cables.

4.3 Parametric study

4.3.1 Case 1: Variable length

As a start it has been chosen an I girder I245D200 from Series D which is the deeper in the commercial catalogue used in this thesis. Its cross-sectional properties are area A = 0.9198 m², depth d = 2.45 m and maximum width located at the top flange b_t = 2.00 m. Moments of inertia I_y = 8430800 cm⁴ and I_z = 79844400 cm⁴. Torsional constant J = 2587500 cm⁴. Height of the center of gravity H_g = 1.224 m. These values are indicated in table 4.1.

Girder	d (m)	A (m²)	H_g (m)	I_y (cm⁴)	I_z (cm⁴)	J (cm⁴)
I245D200	2.45	0.9198	1.224	8430800	79844400	2587500

Table 4. 1. Cross-sectional properties of I girder I245B200.

Lengths from L = 10 m to L_{max} = 60 meters have been analyzed while the other parameters adopted specific values. The beam is end-supported (a = 0) and the height of the lifting loops is h_l = 40 cm. Lateral sweep has been established as the maximum tolerance indicated in *EHE-08* δ =

$L/750$. It is been assumed that the girder is being lifted at a young age so the characteristic resistance of the concrete is f_{ck} = 20 MPa. The modulus of elasticity of the concrete is thus E = 20156 MPa and the shear modulus G is 8398 MPa. Poisson's ratio ν is 0.2. The prestressing force is P_{max} given by equation 3.2. The eccentricity of the prestressing force is e_p = 1.149 m. The girder is lifted by vertical cables (ψ = 0). All these values are presented in table 4.2.

L (m)	a (m)	δ (m)	h_l (cm)	f_{ck} (MPa)	P (KN)	ψ (°)
10 - 60	0	L/750	40	20	P_{max}	0

Table 4. 2. Parameters of case 1: variable length.

Results have been obtained for increments in length of 2 meters. Figure 4.5 shows the initial roll angle β_i of the imperfect girder due lateral sweep for different spans. β_i increases linearly since lateral imperfections were defined as $L/750$. β is the total rotation of the girder. It includes β_i as well as the rotation due to the deflection in the weak-axis. It can be seen the rotation increases almost linearly until $0.7L_{max}$ and do not go beyond 2.30°. This tendency changes suddenly for greater lengths. For instance, at $0.9L_{max}$ the girder suffers a rotation of 6.42° while at $0.96L_{max}$ the girder rotates 12.90°.

As it was explained in section 1 and section 2 of this paper, the rotation of the girder involves a solid rigid movement due to the initial lateral imperfection and also a rotation due to the deformation caused by the component of the self-weight acting in the weak-axis of the initially rotated girder. I girders are designed to resist vertical loads and for that reason their moment of about their horizontal axis I_z is much greater than about the vertical axis I_y (see table 4.1). Therefore, as the girder rotates, the deflection of the girder in the weak axis increases rapidly which, at the same time, induces a greater rotation.

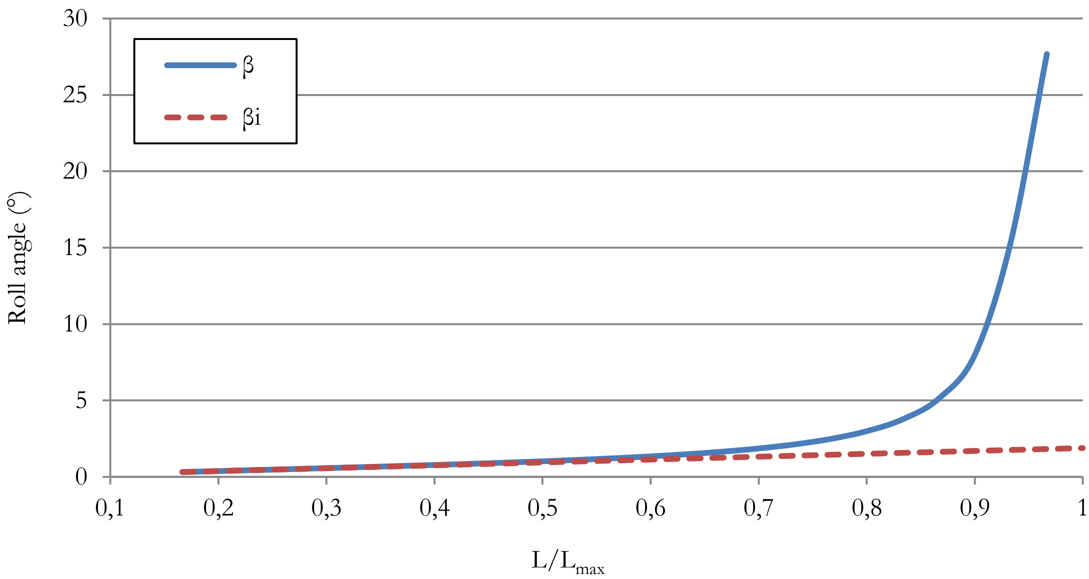

Figure 4. 5. Roll angle.

Figure 4.6 depicts both the deflection in the strong-axis V and weak-axis W. The deflection in the strong-axis does not include the contribution of the prestressing force P_{max}. The difference between the stiffnesses in both cross-sectional axis causes the beam to deflect much more in the weak-axis direction W. For lengths beyond $0.90L_{max}$ it can be seen as well a small increase of the major-axis deflection which is caused by a reduction of the self-weight component in the direction of the strong-axis of the cross section.

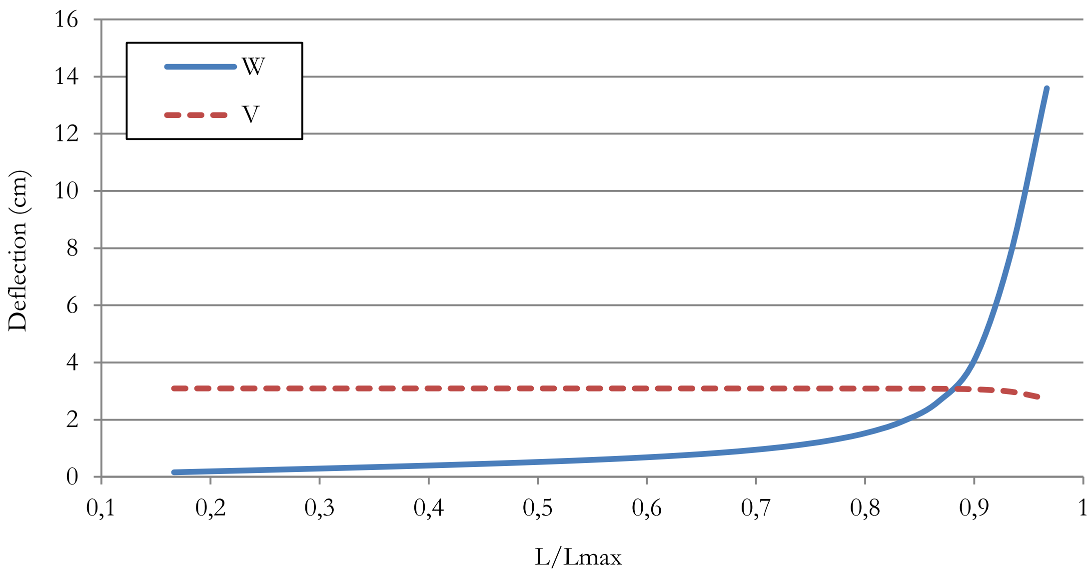

Figure 4.6. Strong-axis deflection V and weak-axis deflection W.

Figure 4.7 shows the total stresses σ_t at midspan in the downward top flange under the assumptions mentioned above. These results are tightly related with the rotation of the girder shown in figure 4.5. As longer spans are evaluated the compressive stresses slightly increase due to a greater self-weight until lengths around $0.8L_{max}$. However, at a certain rotation about β = 6.4° for $0.85L_{max}$ there is an abrupt variation of the stress state which rapidly leads to tension stresses ($\sigma_t < 0$).

An I girder weak-axis is not expected to resist part of the self-weight load, hence the rotation of the girder may induce cracks or even the collapse of the girder. For this case in which the characteristic resistance of the concrete is f_{ck} = 20 MPa, cracking would occur for stresses below f_{ctd} = -1.03 MPa (dotted line in fig. 4.7). Since Plaut and Moen formulation assumes the material to be linearly elastic the results obtained beyond $0.9L_{max}$ would thus not be valid.

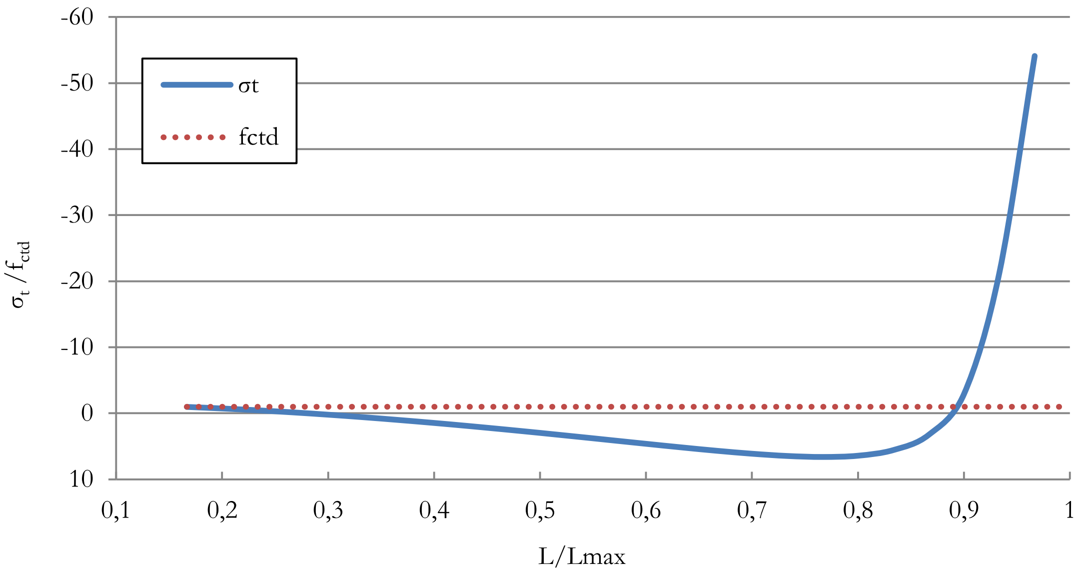

Figure 4.7. Stresses at the downward top flange.

The same process has been followed for the I girders from the Series A whose cross-sectional properties are indicated in table 4.3.

Girder	d (m)	A (m²)	H_g (m)	I_y (cm⁴)	I_z (cm⁴)	J (cm⁴)
I60A100	0.60	0.2267	0.312	841300	1090100	23500
I80A100	0.80	0.2507	0.411	844200	2263900	257700
I100A100	1.00	0.2747	0.51	847100	3938900	281900
I120A100	1.20	0.2987	0.609	849900	6163300	306100

Table 4. 3. Cross-sectional properties of I girders from Series A.

Figure 4.8 shows the total stresses at midspan in the downward top flange. It is apparent all the girders behave similarly to the above studied I245D200. However, since girders from Series A have much lower lateral stiffness cracking would occur for shorter spans, at $0.6L_{max}$. Deeper cross-sections are supposed to work properly for longer spans but there is almost no difference between the critical length of the I60A100 and the I120A100 since their lateral stiffnesses are quite similar.

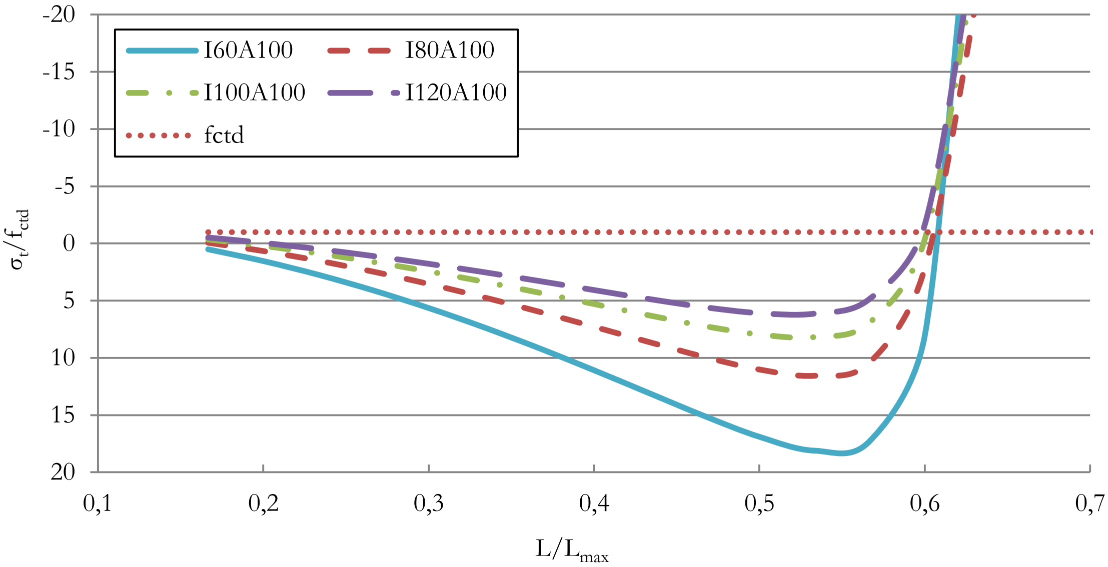

Figure 4.8. Stresses at the downward top flange of I girders from Series A.

The stresses due to bending in the strong-axis σ_{mz} and due to bending in the weak-axis σ_{my} for girders I60A100 and I120A100 are separately depicted in figure 4.9. Stresses due to prestress are not included. It can be seen how for lengths beyond $0.6L_{max}$ $\underline{\sigma_{my}}$ becomes a decisive factor which leads to a tension stress state. Stresses due to prestress are not included in figure 4.9.

The cross-sectional properties of five I girders from the Series B are listed in table 4.4.

Girder	d (m)	A (m²)	H_g (m)	I_y (cm⁴)	I_z (cm⁴)	J (cm⁴)
I120B120	1.20	0.4629	0.598	2004300	9100200	1255000
I140B120	1.40	0.4929	0.693	2009900	13414800	1301600
I160B120	1.60	0.5228	0.789	2015600	18713400	1348300
I180B120	1.80	0.5529	0.886	2021200	25056300	1394900
I200B120	2.00	0.5829	0.982	2026000	32503500	1441500

Table 4. 4. Cross-sectional properties of I girders from Series B.

The same phenomenon regarding the stress state of those girders at midspan is shown in figure 4.10 and the obtained results are alike. The critical length is in that case $0.67L_{max}$ since the lateral stiffness of the girders from Series B is greater that the lateral stiffness of the girders from Series A.

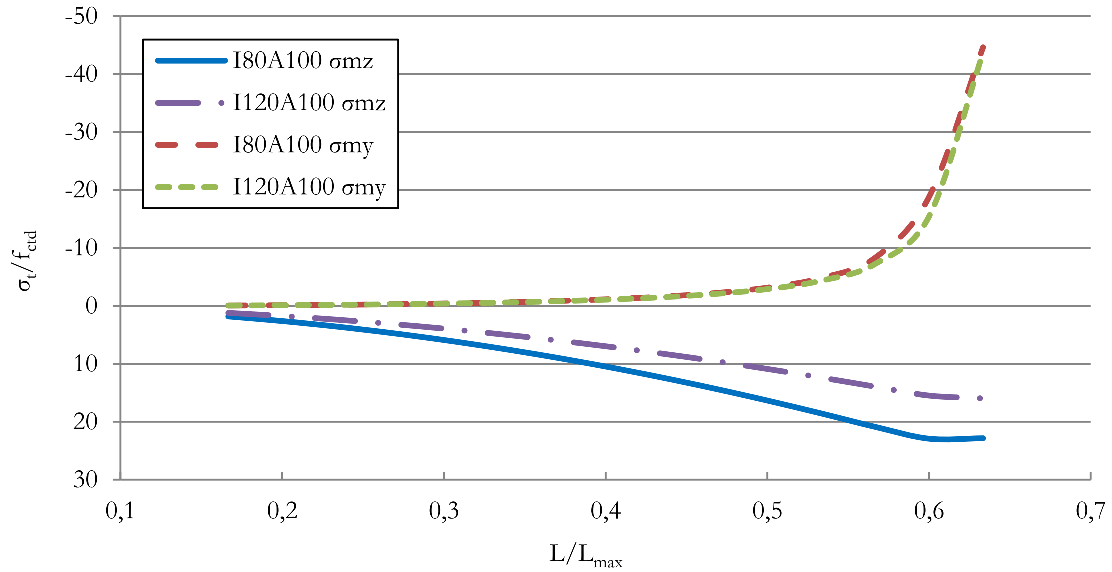

Figure 4.9. Stresses due to strong-axis bending and weak-axis bending I girders I60A100 and I120A100.

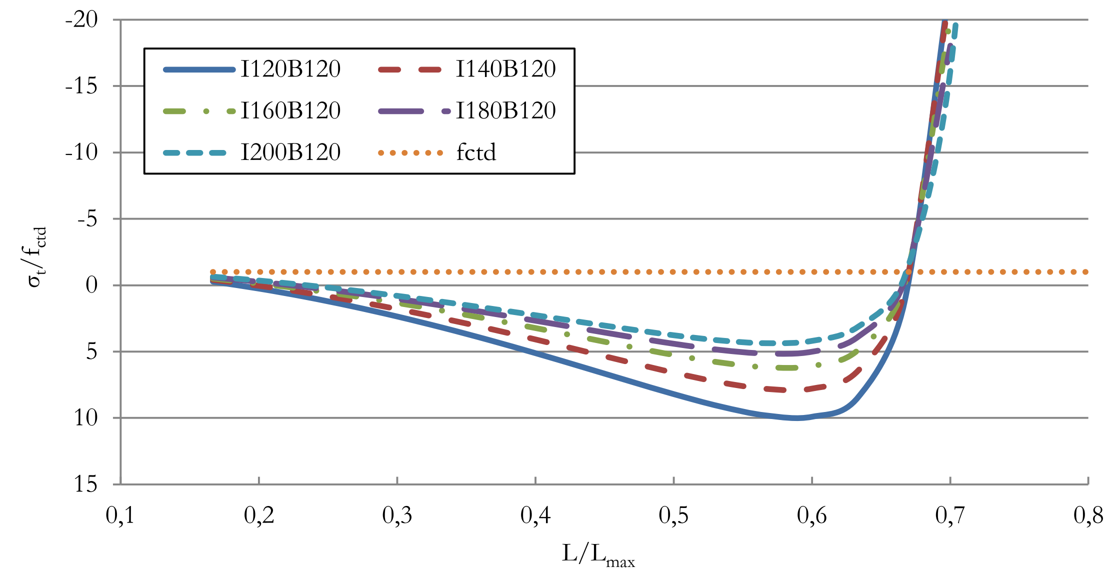

Figure 4.10. Stresses at the downward top flange of I girders from Series B.

The strong-axis moment of inertia I_z of the I girders studied in this paper is shown in figure 4.11. As can be seen, its value increases exponentially with the cross section depth in all the series. Since the width of the flanges remains constant for all the girders of the same series, the weak-axis moment of inertia I_y is almost constant as illustrated in figure 4.12. Due to that fact all the girders from the same family behave in similar manner when the weak-axis bending becomes critical. As a result, their response to initial lateral imperfections coincides and cracks would develop at approximately the same span. This fact was already presented in figures 4.8 and 4.10 for different I girders from Series A and B, respectively.

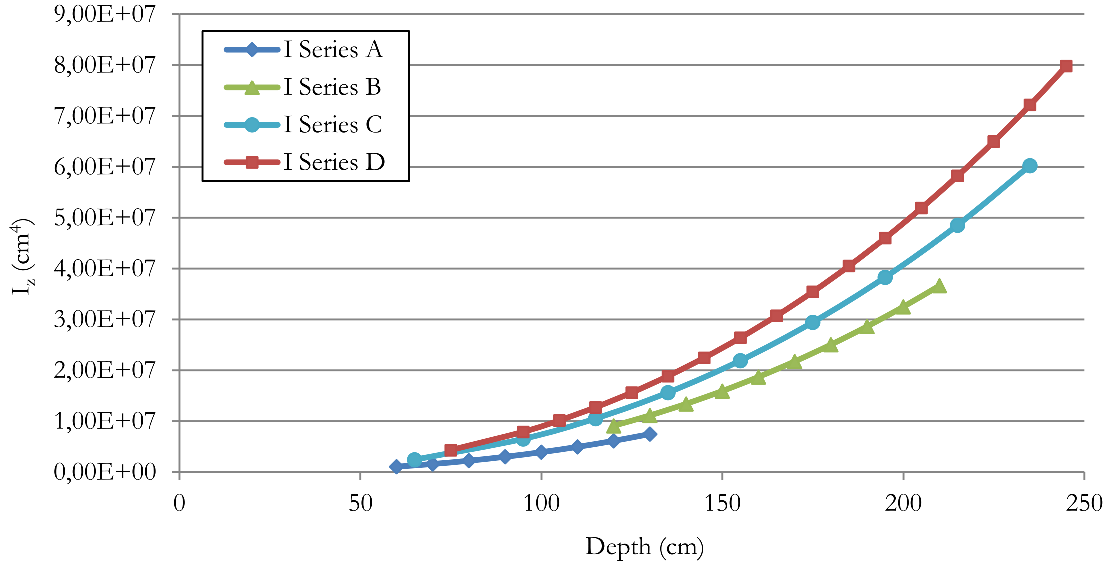

Figure 4.11. Strong-axis moment of inertia.

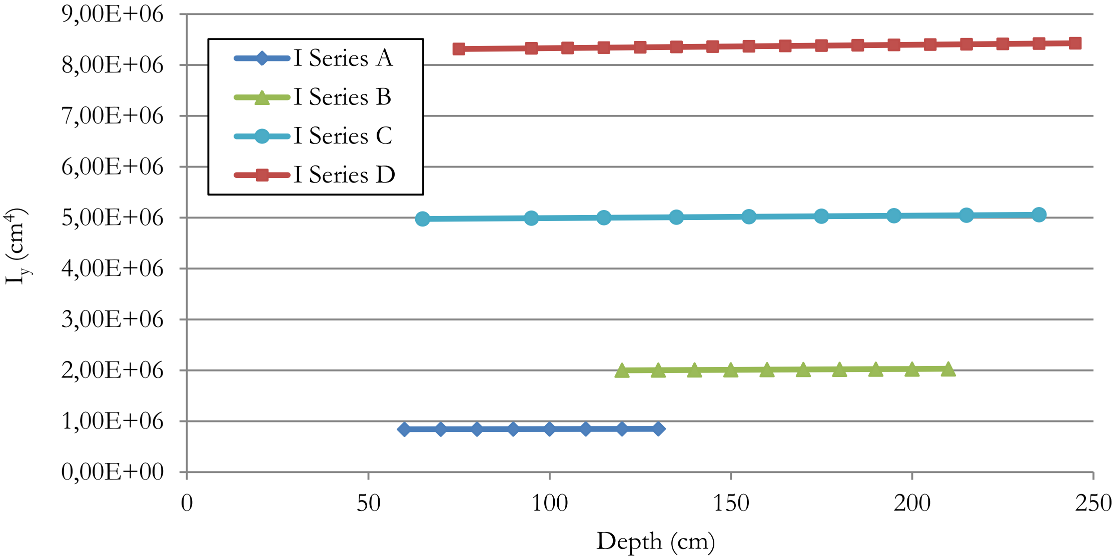

Figure 4.12. Weak-axis moment of inertia.

Figure 4.13 represents the behaviour of a single I girder from Series A, B, C, and D. Their cross-sectional properties are listed in table 4.5.

Girder	d (m)	A (m²)	H_g (m)	I_y (cm⁴)	I_z (cm⁴)	J (cm⁴)
I120A100	1.20	0.2987	0.609	849900	6163300	306100
I200B120	2.00	0.5829	0.982	2026000	32503500	1441500
I235C150	2.35	0.7680	1.198	5059800	60248800	2126900
I245D200	2.45	0.9198	1.224	8430800	79844400	2587500
A230B	2.45	0.9198	0.897	139661200	798367000	3593300

Table 4. 5. Cross-sectional properties of I girders from Series A, B, C, D and Artesa B.

As can be observed there is a different span range for each one of them. For instance, the girder I120A100 would crack for lengths beyond 0.6*L*. On the other hand, girder I245D200 could safely reach spans up to $0.9L_{max}$. The results of an Artesa A230B are also depicted in figure 4.13. Contrary to I girders, the Artesa Series is characterized for having a much greater lateral stiffness. As a result, its lateral deflection is very small thus tending to rotate less and showing no sign of lateral instability. Lateral stability of Artesa girders would not normally be of concern during design.

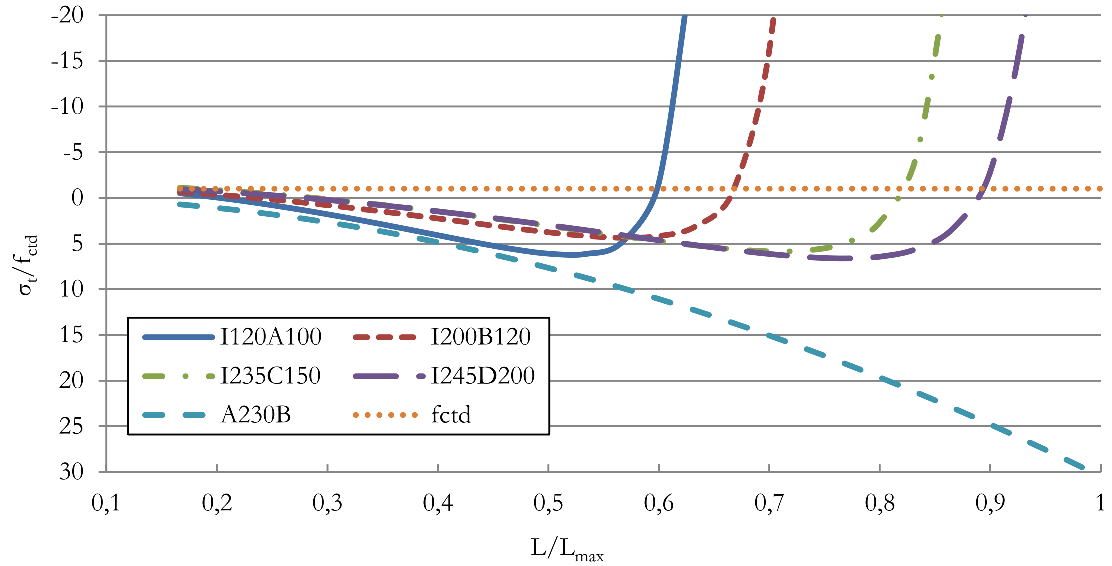

Figure 4.13 Stresses at the downward top flange. I girders from Series A, B, C, D and Artesa B.

The cross-sectional properties of the Artesa girders studied in this section are listed in table 4.6. The stresses obtained under the assumptions described at the beginning of this section are shown in figure 4.14.

Girder	d (m)	A (m²)	H_g (m)	I_y (cm⁴)	I_z (cm⁴)	J (cm⁴)
B A110B	1.10	0.2987	0.609	65429700	6163300	2925300
B A130B	1.40	0.5829	0.982	81303400	32503500	3092300
B A170B	1.70	0.7680	1.198	98893100	36619300	3259300
B A200B	2.00	0.9198	1.224	118147600	55444600	3426300
B A230B	2.30	0.9198	0.897	139661200	79844400	3593300

Table 4. 6. Cross-sectional properties of girders from Series Artesa B.

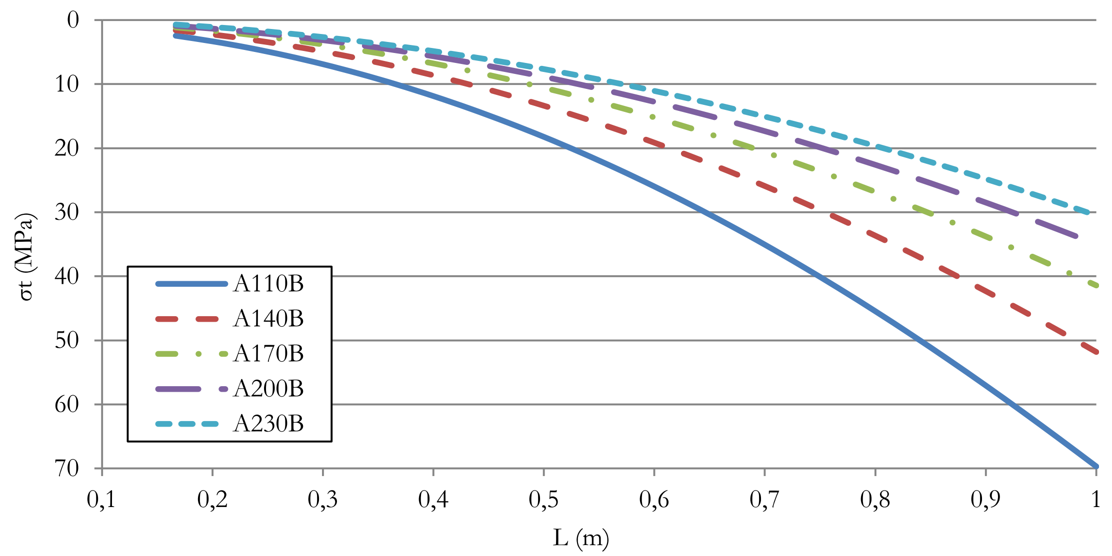

Figure 4.14. Stresses at the downward top flange of girders from Series Artesa B.

As already seen in figure 4.13 for the Artesa girder A230B, there is again no sign of lateral instability for the rest of the girders which indicates lateral buckling would not be a design constraint for spans up to L_{max}. Nevertheless those girders would generally be limited by other structural reasons which will be exposed in the next chapter.

4.3.2 Case 2: Variable location of the lift points

The results shown in the above section 4.3.1 respond for end-supported girders (a = 0). In this section the lifting loops are moved inwards up to a distance $a = 0.2L$. The parameters defining case 2 are indicated in table 4.7. The girder selected is an I245D200 whose cross-sectional properties are indicated in table 4.8.

L (m)	a (m)	δ (m)	h_l (cm)	f_{ck} (MPa)	P (KN)	ψ (°)
40	0 - 8	L/750	40	20	P_{max}	0

Table 4. 7. Parameters of case 2: variable location of lift points.

Girder	d (m)	A (m²)	H_g (m)	I_y (cm⁴)	I_z (cm⁴)	J (cm⁴)
I245D200	2.45	0.9198	1.224	8430800	79844400	2587500

Table 4. 8. Cross-sectional properties of I girder I245B200.

Figure 4.15 presented below shows the roll angle β depending on the distance a of the lifting loops to the end of the girder. It is apparent that moving the lift points inwards reduces the rotation of the girder. Note that the initial rotation due to lateral sweep β_i also decreases since the horizontal distance between the center of gravity of the whole girder and the lift points is also being reduced.

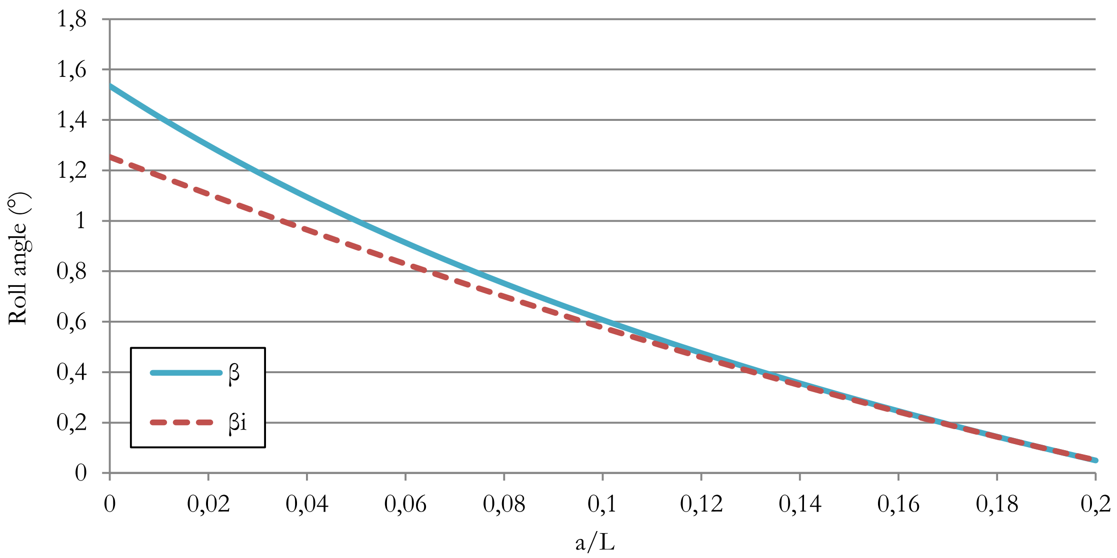

Figure 4.15. Roll angle.

Figure 4.16 shows the stresses generated at the downward top flange. Tensile stresses due to bending of the weak axis would decrease because they are related to the rotation of the girder shown in figure 4.15. The bending moment for both the weak-axis and strong-axis due to self-weight would also adopt smaller values at midspan since the distance between supports is shorter. However, the effect of the prestressing force which would be designed for in-place conditions (end-supported) is now more relevant. This fact explains why in figure 4.16 the total stress state tends to go from a compression state to a tensile state. According to the results cracking at midspan would not occur even for values of a = 0.2L. Nevertheless such disposition of the supports would certainly cause cracks at the top fiber of the supports cross-section if not its collapse.

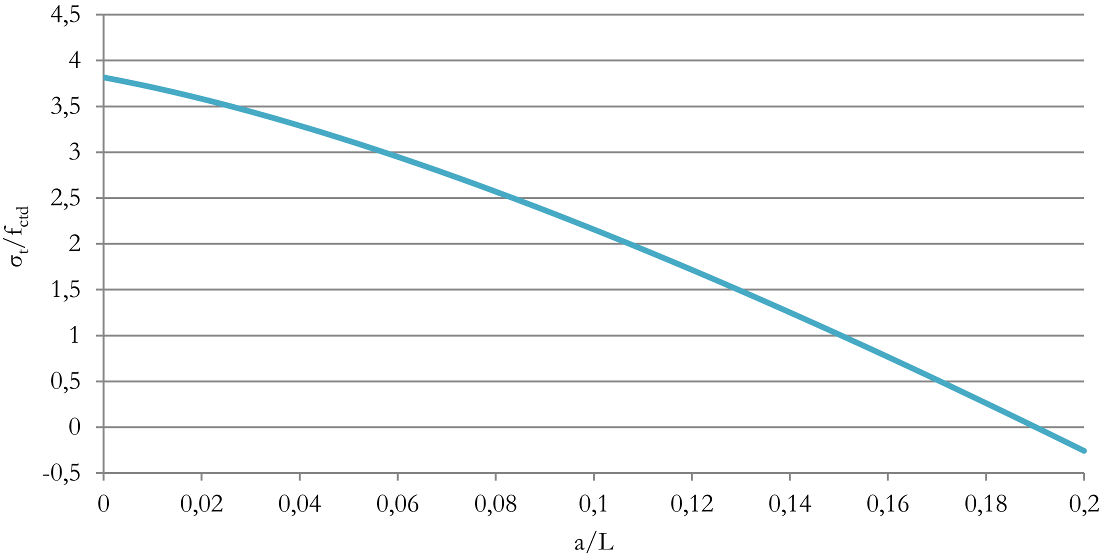

Figure 4.16. Stresses at the downward top flange.

Therefore moving in the lift points reduces the rotation of the girder β but also decreases the strong-axis bending moment due to self-weight which would counter the tensile stresses caused at the top flange by the prestressing moment. To conclude if such change of the supports location would allow to reach longer spans, figure 4.17 shows the results obtained in a I160B120 for different values of a and different spans. The cross sectional properties of the I160B120 are indicated in table 4.9.

Girder	d (m)	A (m²)	H_g (m)	I_y (cm⁴)	I_z (cm⁴)	J (cm⁴)
I160B120	1.60	0.5228	0.789	2015600	18713400	1348300

Table 4.9. Cross-sectional properties of I girder I160B120.

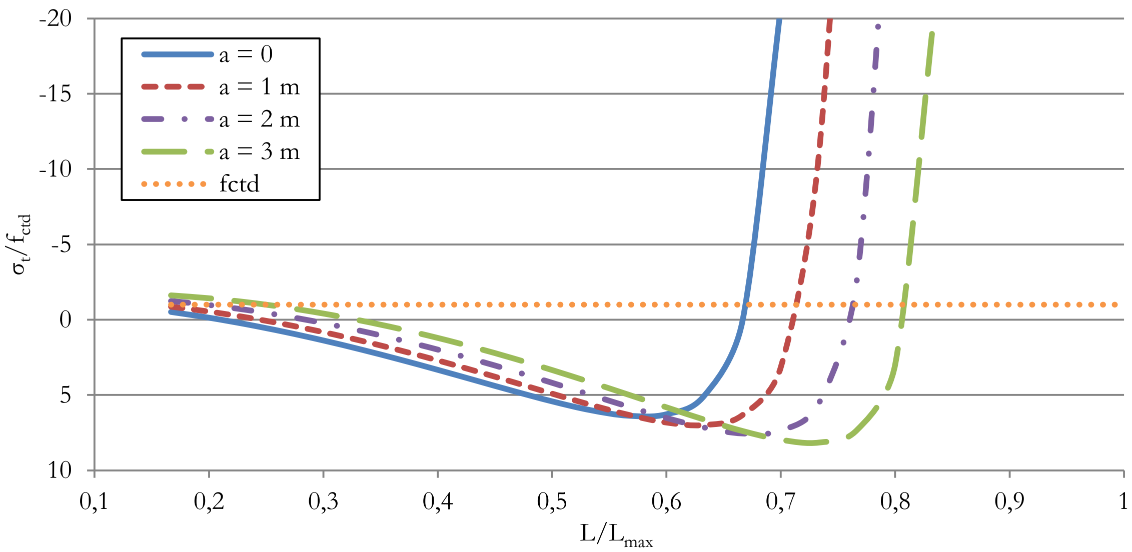

Figure 4.17. Stresses at the downward top flange of an I160B120.

In figure 4.17 can be seen that for the end-supported case the critical length inducing cracking at the downward top flange is $0.66L_{max}$. Nonetheless, moving in the lifting loops to a = 3 m would allow to reach spans up to $0.80L_{max}$.

4.3.3 Case 3: Variable resistance of the concrete

So far the characteristic resistance of the concrete f_{ck} has been fixed at 20 MPa simulating the girders are lifted at a young age. The use of additives in the concrete or lifting the girder in a later construction stage, such as in the field, would require the use of higher values of the concrete resistance. Consequently in this section different values of the characteristic resistance of the concrete from 20 to 60 MPa are analyzed. Varying f_{ck} imply different amounts for the concrete deformation modulus E and G which have been modified when needed. The parameters defining case 3 are listed in table 4.10.

L (m)	a (m)	δ (m)	h_l (cm)	f_{ck} (MPa)	P (KN)	ψ (°)
40	0	L/750	40	20-60	P_{max}	0

Table 4.10. Parameters of case 3: variable resistance of the concrete.

The roll angle of an end-supported 40 m long I girder I160B120 (cross-sectional properties in table 4.9) depending on the characteristic resistance of the concrete is shown in figure 4.18. Since lateral sweep is the same for all the cases, variations of the concrete resistance have no effect on the initial roll angle β_i. However, the total roll angle β decreases as the concrete resistance increases. A higher strength of the concrete reduces lateral deformations caused by the initial rotation which, eventually reduces the final rotation of the girder. Note that the differences in this case between the total roll angle are around 0.8° but beyond a concrete strength of $0.7f_{ck,max}$ there is almost no reduction in rotation.

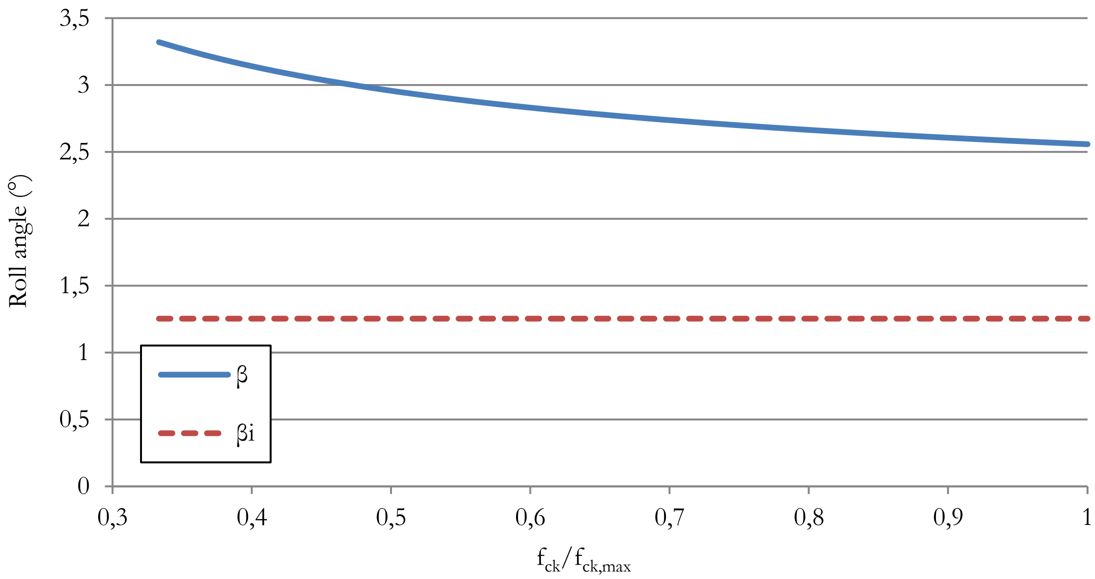

Figure 4.18. Roll angle.

Figure 4.19 shows the results obtained for an I160B120 with values of the characteristic resistance of the concrete 20, 40 and 60 MPa, and for spans up to L_{max}. As expected a higher strength of the concrete allows reaching longer spans. While for a characteristic strength of the concrete of f_{ck} = 20 MPa cracks would develop at $0.67L_{max}$, a more resistant concrete with f_{ck} = 60 MPa could reach spans until 0.73L_{max}. In connection to what is exposed regarding figure 4.18, it can be seen the improvement in the reachable spans is greater for the first increase of concrete characteristic resistance from 20 MPa to 60 MPa.

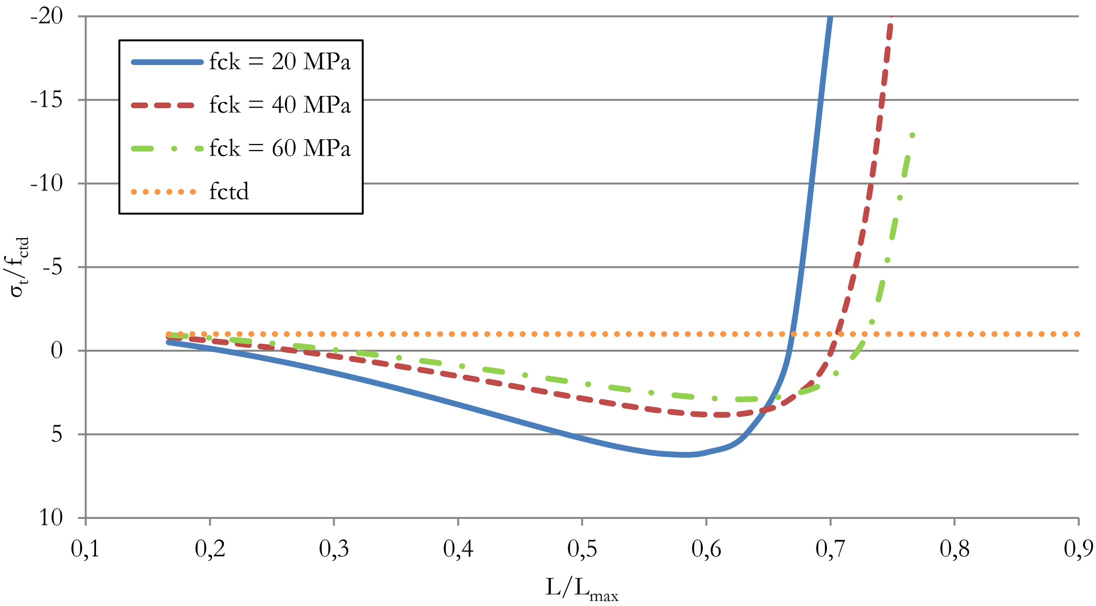

Figure 4.19. Stresses at the downward top flange of an I160B120.

4.3.4 Case 4: Variable lateral sweep

Up until now lateral sweep has been set at $\delta = L/750$ which is considered by the Spanish Instruction *EHE-08* the maximum allowed. In this section the influence of lateral sweep from a minimum value of $L/2000$ to a maximum value of $L/500$ is analyzed. The parameters established for this case of study are described in table 4.11.

L (m)	a (m)	δ (cm)	h_l (cm)	f_{ck} (MPa)	P (KN)	ψ (°)
40	0	2 - 8	40	20	P_{max}	0

Table 4.11. Parameters of case 4: variable lateral sweep.

An I girder I160B120 have been used in this section. Its cross-sectional properties are found in table 4.12.

Girder	d (m)	A (m²)	H_g (m)	I_y (cm⁴)	I_z (cm⁴)	J (cm⁴)
I160B120	1.60	0.5228	0.789	2015600	18713400	1348300

Table 4.12. Cross-sectional properties of I160B120.

In figure 4.20 is represented the girder rotation due to initial lateral imperfections β_i and the total roll angle β. It can be appreciated both values increase linearly as lateral sweep δ also increases, but with different slope. This fact shows that as the initial rotation increases, the rotation induced by the elastic deformation along the cross section weak-axis is more important. As a result the slope of the total roll angle β has a greater slope. Note that in this specific case small increases in lateral sweep δ have a significant impact on the girder roll angle.

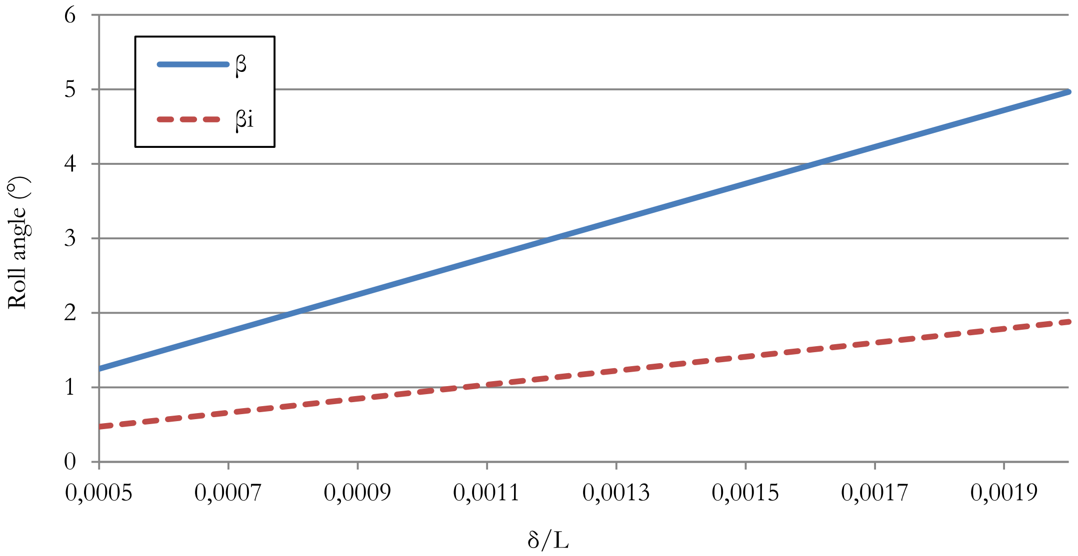

Figure 4.20. Roll angle.

Figure 4.21 shows the stresses obtained at the I160B120 downward top flange for different values of initial imperfection δ and spans up to L_{max}. Differences between the given values to lateral sweep do not exceed 6 cm. Nonetheless these small magnitudes are capable of reducing the maximum length the I160B120 can reach satisfying the cracking limit state. For example, for the case of $\delta = 8$ cm the tensile resistance of the concrete f_{ctd} would be reached at $0.65L_{max}$. Instead, reducing lateral sweep to $\delta = 2$ cm would allow spans up to $0.7L_{max}$.

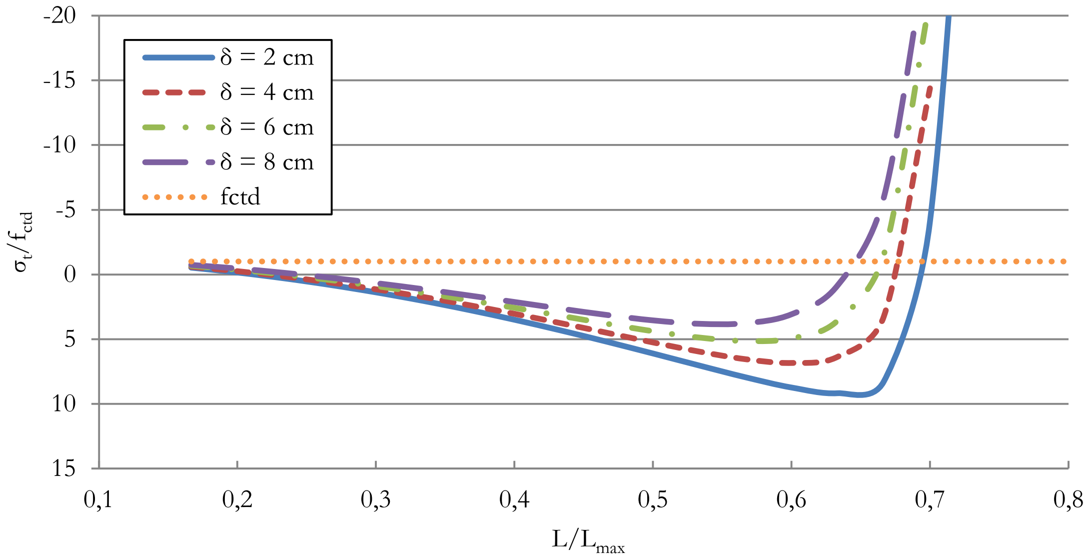

Figure 4.21. Stresses at the downward top flange of an I160B120.

4.3.5 Case 5: Variable prestressing force

In this section different values of the prestressing force P would be studied for a given reference girder. Previous results were obtained by considering a prestressing force P_{max} given by equation 3.2. Consequently, different values of the prestressing force in the interval between $P = 0$ and P_{max} are computed. This case is thus controlled by the parameters indicated in table 4.13.

L (m)	a (m)	δ (cm)	h_l (cm)	f_{ck} (MPa)	P (KN)	ψ (°)
40	0	L/750	40	20	0 - P_{max}	0

Table 4.13. Parameters of case 5: variable prestressing force.

The reference girder is an I235C150 whose cross-sectional properties are listed in table 4.14.

Girder	d (m)	A (m²)	H_g (m)	I_y (cm⁴)	I_z (cm⁴)	J (cm⁴)
I235C150	2.35	0.7680	1.198	5059800	60248800	2126900

Table 4.14. Cross-sectional properties of I235C150.

The effect of the prestressing force is included in a second phase once the rotation of the girder is calculated. As a result it has no effect on the girder rotation β. This assumption would not be completely true in cambered girders because its shifted center of gravity increases the initial rotation β_i and consequently as well β. Nevertheless Plaut and Moen state that camber may not have a large influence on the roll angle and deformations of a curved girder during lifting.

Figure 4.23 illustrates the stress state of the I235C150 for different spans and subjected to different values of prestressing force. It is apparent that all curves reach the tensile strength of the concrete f_{ctd} at the same length $0.83L_{max}$. Applying a higher prestressing force, would initially cause greater tensile stresses at the top flange which when combined with the weak-axis bending may lead faster to cracking than in other situation. However the influence of the stresses due to weak-axis bending is much more important. To confirm that fact a curve with a prestressing force $P = 0$ has been included in figure 4.23. Despite that would not be a feasible solution, in this case the top flange would be much more compressed than if any prestressing force is included. This can be observed in figure 4.23 since the curve representing $P = 0$ is clearly below the others under a more compressed stress state. However the cracks would develop the span around $0.83L_{max}$.

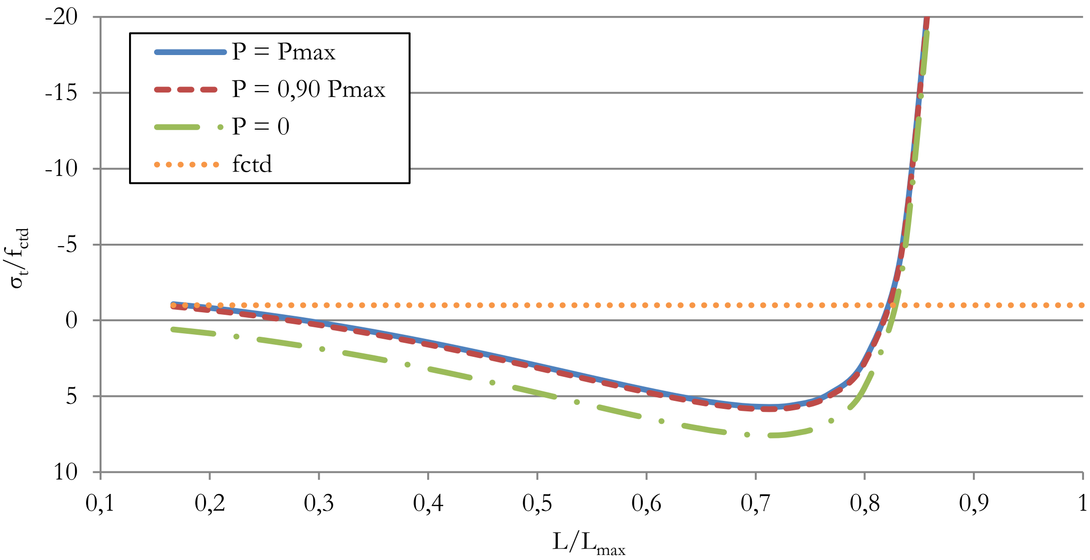

Figure 4.23. Stresses at the downward top flange of an I235C150.

4.3.6 Case 6: Variable height of the lifting loops

The height of the lifting loops has been so far fixed at h_l = 40 cm. To highlight its effect on the rotation of girders lifted by two cables, in this section it will be modified from 20 cm to 150 cm. The parameters governing the results in this section are indicated in table 4.15.

L (m)	a (m)	δ (m)	h_l (cm)	f_{ck} (MPa)	P (KN)	ψ (°)
40	0	L/750	20 - 150	20	P_{max}	0

Table 4.15. Parameters of case 6: variable height of the lifting loops.

The cross-sectional properties of the I235C150 analyzed are found in table 4.16.

Girder	d (m)	A (m²)	H_g (m)	I_y (cm⁴)	I_z (cm⁴)	J (cm⁴)
I235C150	2.35	0.7680	1.198	5059800	60248800	2126900

Table 4.16. Cross-sectional properties of I235C150.

Figure 4.24 represents the rotation of the I235C150 depending on the height of the lifting loops. As can be observed the initial rotation due to lateral sweep β_i decreases as the girder is supported from a higher location. As a result, the total roll angle β is also reduced since it depends both of the initial rotation and the elastic lateral deflection of the girder. The slope of both curves changes smoothly being higher the reduction of the rotation during the first half, from h_l/L_{max} = 0.005 to h_l/L_{max} = 0.02.

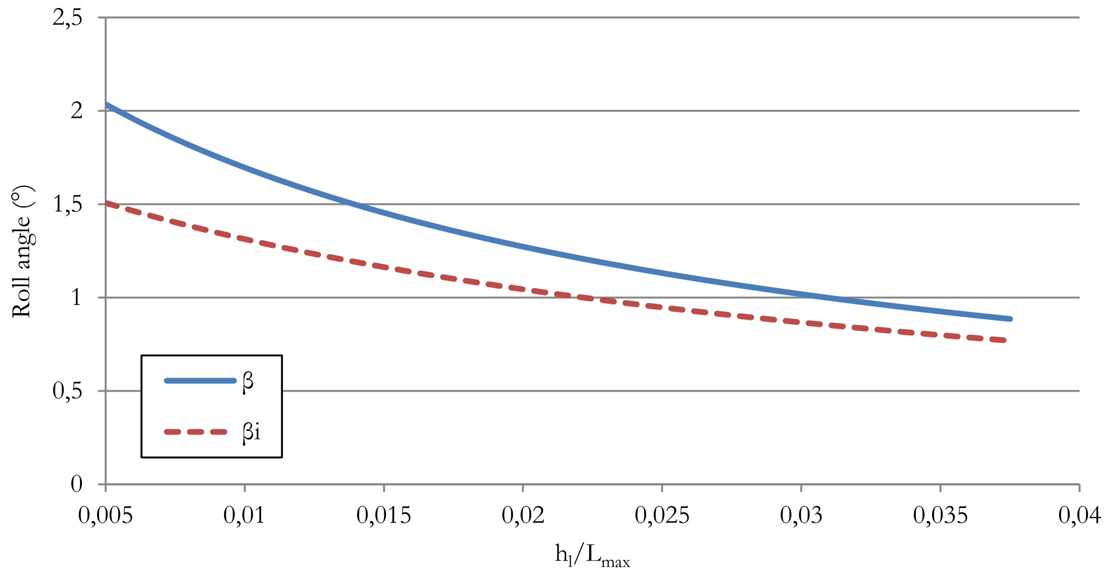

Figure 4.24. Roll angle.

In figure 4.25 are plotted the stresses at the downward top flange for different heights of the lifting loops and spans. The values given to the height of the lifting loops are equivalent to h_l = 20, 60, 100 and 140 cm.

The reduction of the girder rotation by supporting the girder from an above location allows reaching longer spans satisfying cracking considerations. For instance, if the girder is lifted with lifting loops whose height is h_l/L_{max} = 3.3E-03, cracking of the top flange would occur for spans close to 0.8L. If the girder is supported from and above location h_l/L_{max} = 1.6E-02 spans up to 0.9L_{max} could be reached with no sign of cracking. Although heights of the lifting loops such as h_l = 1.40 m are not normally used in these girders.

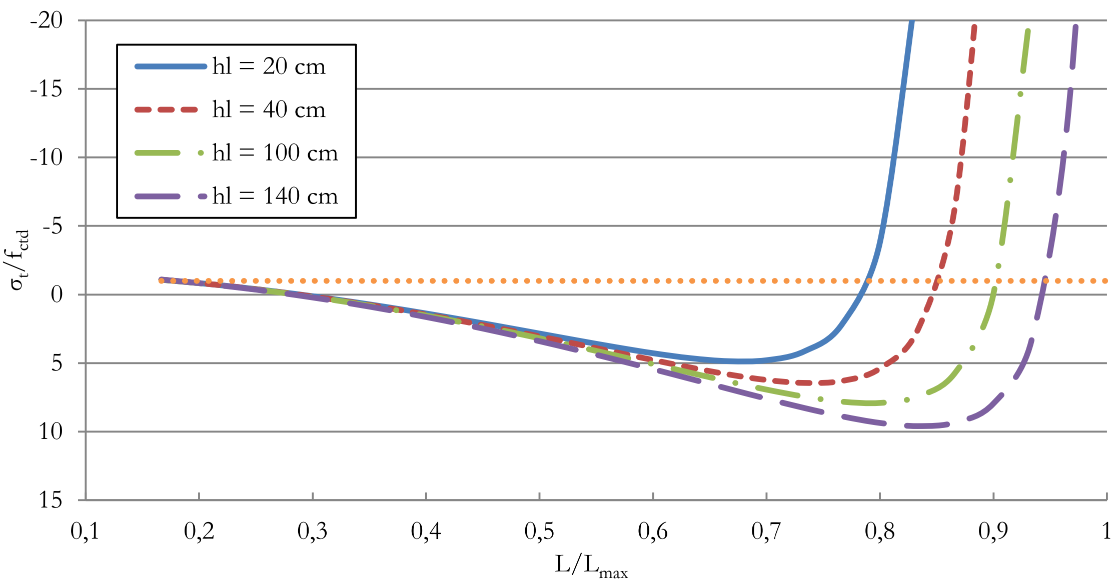

Figure 4.25. Stresses at the downward top flange of an I235C150.

4.3.7 Case 7: Variable inclination angle of the cables

When a girder is lifted on site, it typically hangs from two inclined cables on a single crane, while in the precasting factory it is invariably lifted using vertical cables supported from two cranes. In this section the inclination of the cables with respect to the vertical axis is analyzed. The adopted values go from ψ = 0° (vertical cables) and ψ = 45°. The parameters defining this section are found in table 4.17.

L (m)	a (m)	δ (cm)	h_l (cm)	f_{ck} (MPa)	P (KN)	ψ (°)
40	0	L/750	40	20	P_{max}	0 - 45

Table 4.17. Parameters of case 7: variable inclination angle of the cables.

A girder I235C150 with the cross-sectional properties shown in table 4.18 has been analyzed.

Girder	d (m)	A (m²)	H_g (m)	I_y (cm⁴)	I_z (cm⁴)	J (cm⁴)
I235C150	2.35	0.7680	1.198	5059800	60248800	2126900

Table 4.18. Cross-sectional properties of I235C150.

Figure 4.26 illustrates the rotation of the girder I235C150 for different inclination angles of the lifting cables ψ. As observed, different values of ψ do not affect the initial rotation due to lateral sweep β_i but slightly increase the total roll angle β. Inclined cables cause an axial force at the top of the lifting loops which induce a bending moment in the vertical plane. Since the girder has rotated due to the initial imperfection a component of this bending moment acts in the cross section weak-axis increasing the lateral deflection and thus the total roll angle β. However increasing from ψ = 0 to ψ_{max} = 45° has only meant a small increase of the total rotation passing from 1.7° to 1.8°.

Almost no difference are observed in figure 4.27 where the stresses at the downward top flange are plotted for different spans and inclination angles equivalent to 0, 15°, 30° and 45°. For all situations the tensile strength of the concrete would be reached at lengths $0.82L_{max}$.

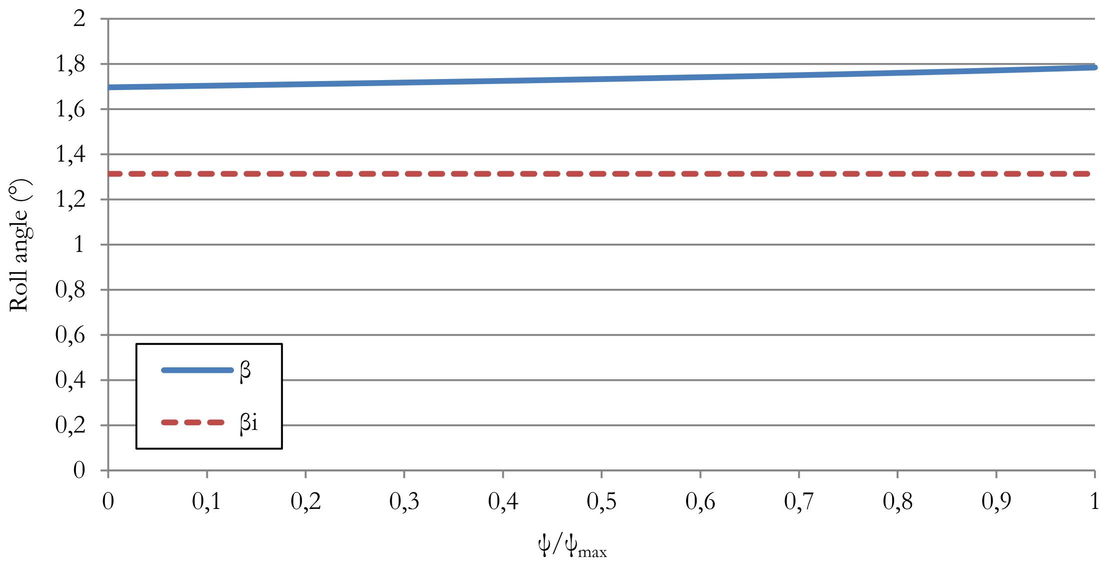

Figure 4.26. Roll angle.

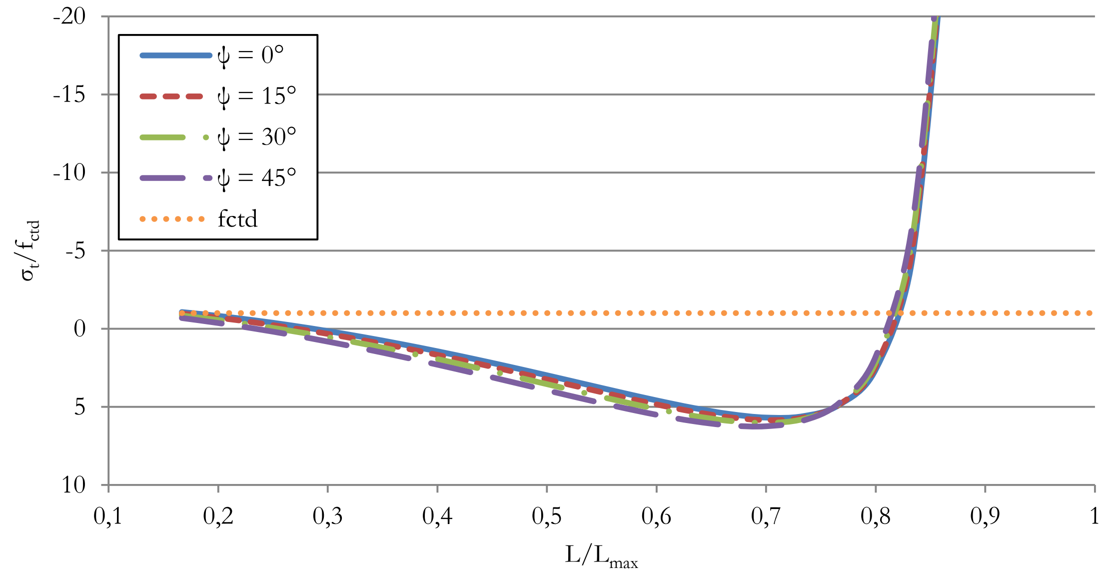

Figure 4.27. Stresses at the downward top flange of an I235C150.

CHAPTER 5.

ANALYSIS OF RESULTS

5.1 Introduction

Many times, designers ignore the issue of lateral stability related to the construction and handling stages to the fabricators and contractors, only considering the stability of the finished structure. In the previous chapter numerous girders were analyzed with respect to lateral buckling and were found to be limited to a certain span range depending, mainly, on lateral imperfections and their weak-axis stiffness. However, precast concrete girders are in the majority of cases not designed according to lateral buckling limitations.

In this chapter the achievable lengths according to traditional design methods are calculated. Those lengths are then compared with the span range were lateral buckling may occur. In this way it will be determined if lateral buckling should become in some cases a design constraint.

5.2 Straight girder and imperfect girder maximum spans

5.2.1 Straight girder maximum design span

During the design of most precast prestressed concrete girder is assumed that the girder will be completely straight and show no signs of accidental lateral imperfections. As a design criteria it is common to not allow tensile stresses higher than the concrete tensile strength f_{ct} and compressive stresses superior to $0.6{\cdot}f_{ck}$. This is applied both at the time of transferring the prestressing force (including the effect of self-weight) and during service (including self-weight and additional loads). As a result, there exist a maximum achievable span depending on the properties of the concrete, the cross section of a given girder and the specific additional loads of a certain structure.

Figure 5.1a shows and end-supported hanging girder of length L subjected to a prestressing force P, which induces a prestressing moment M_p, and its self-weight q. Those loads would cause, individually, a stress state at midspan as shown in figure 5.1b for the bending moment due to self-weight, figure 5.2c for the prestressing compression force and figure 5.2d for the prestressing moment. When combined, the final stress state of the cross section at midspan is obtained (fig. 5.1e). In accordance with what was mentioned above, the tensile stresses should be less than the tensile resistance of the concrete f_{ctm} (fig. 5.1e).

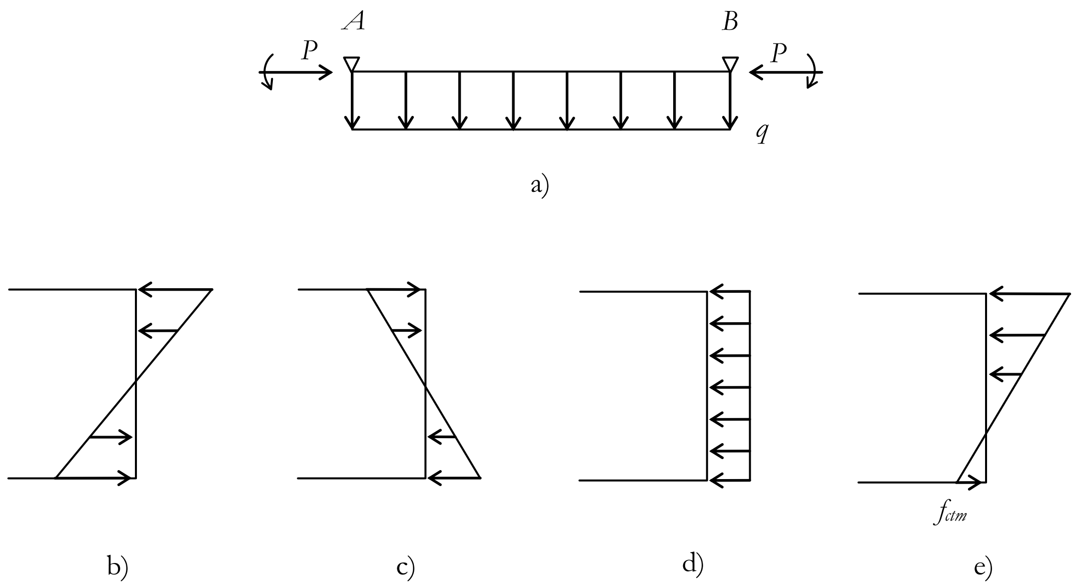

Figure 5.1. End supported girder: a) acting loads, b) self-weight bending stresses, c) prestressing moment stresses, d) axial force stresses, e) final stress state.

Note that in figure 5.1 additional loads which would vary depending on the project are not included. Accounting for that fact and in the interest of detecting if a given girder is susceptible to buckle in the span range in which they are designed for, a maximum length criteria is given by equation 5.1.

$$L_T = \sqrt{\frac{8 \cdot P_{max}\left(\frac{I_z}{A} + e_p \cdot H_g\right)}{q \cdot H_g}} \tag{5.1}$$

L_T corresponds to that length for which the maximum prestressing force P_{max} (eq. 3.2), that can be applied to a given cross section at an eccentricity e_p, counters the tensile stresses at midspan caused by the girder self-weight q. d_2 is the vertical distance between the center of gravity and the bottom fiber of the cross section. Equation 5.1 responds to a stress state as depicted in figure 5.2 under the effect of the girder self-weight and the prestressing.

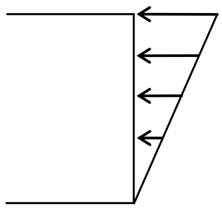

Figure 5.2. Stress state at midspan obtained using equation 5.1.

5.2.2 Imperfect girder maximum design span

If unexpected lateral deformations which may occur during the manufacturing and handling stages are considered, precast prestressed concrete girders maximum design length L_B may be limited by lateral buckling. As exposed in 3.2.5 and 3.2.6 from the span L_B which causes the instability tensile stresses rapidly increase leading to cracking at a span L_C. For safety considerations, L_B will be assumed as the maximum length achievable with respect to lateral buckling.

Furthermore, as observed in chapter 4 there are several parameters which can affect the maximum lateral buckling length L_B of a given girder. Also for safety considerations, their value will be taken on the safe side. In this regard, the girders are considered to be end-supported (a = 0), lateral sweep is the maximum allowed by the Spanish Instruction *EHE-08* $\delta = L/750$, the height of the lifting loops is h_l = 20 cm, and the prestressing force is P_{max}. Inclined lifting cables are not advisable since can easily lead to cracking due to excessive compression stresses. Therefore it will be assumed ψ = 0.

Since the maximum design length L_T (eq. 5.1) relies heavily upon the characteristic strength of the concrete f_{ck}, results will be compared for f_{ck} = 20, 40 and 60 MPa. The recently mentioned parameters are indicated in table 5.2.

L (m)	a (m)	δ (cm)	h_l (cm)	f_{ck} (MPa)	P (KN)	ψ (°)
0-60	0	L/750	20	20-60	P_{max}	0

Table 5.1. Fixed girder parameters.

5.3 Analysis of results

5.3.1 Series A, I girders

The cross-sectional properties of the I girders analyzed are shown in table 5.2.

Girder	d (m)	A (m²)	H_g (m)	I_y (cm⁴)	I_z (cm⁴)	J (cm⁴)
I60A100	0.60	0.2267	0.312	841300	1090100	23500
I80A100	0.80	0.2507	0.411	844200	2263900	257700
I100A100	1.00	0.2747	0.51	847100	3938900	281900
I120A100	1.20	0.2987	0.609	849900	6163300	306100

Table 5.2. Cross-sectional properties of I girders from Series A.

In accordance with equation 5.1 their maximum design spans L_T are shown in table 5.3. Note that these lengths are dependent on the characteristic strength of the concrete f_{ck} at the time of transferring the prestressing force.

f_{ck} (MPa)	L_T (m)			
	I60A100	I80A100	I100A100	I120A100
20	19.4	22.9	25.3	27.0
40	24.4	28.8	31.9	34.0
60	27.6	32.6	36.1	38.5

Table 5.3. Girders I Series A. Maximum design length.

Figure 5.3 shows the obtained stresses at midspan in the downward top flange for lengths up to L_{max} = 60 m and for the girders from the A Series indicated in table 5.2. This figure follows the same pattern used in chapter 4. Cracking would occur in all girders for spans about $L_C = 0.57L_{max}$. However for safety considerations the adopted maximum buckling length would correspond with $L_B = 0.49L_{max}$. Furthermore, in figure 5.3 is also plotted an arrowhead curve which indicates the dimensionless maximum design length (L_T/L_{max}) for all those girders, when their characteristic concrete strength is f_{ck} = 20 MPa. In this sense, using the cross section of the girder I120A100 would allow to achieve spans up to $L = 0.45L_{max}$. Lateral instability would become of concern for spans beyond $L_B = 0.49L_{max}$, therefore it would not be a design constraint for the I120A100. By extension, none of the girders from Series A when f_{ck} = 20 MPa would be limited by lateral buckling.

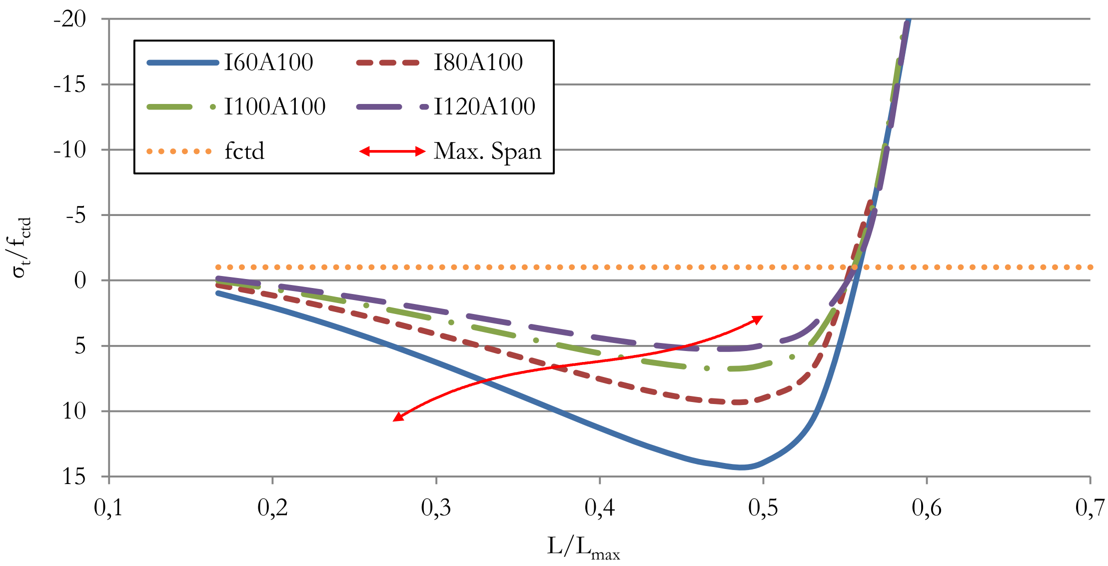

Figure 5.3. Stresses at the downward top flange of I girders from Series A. f_{ck} = 20 MPa.

The same process has been followed for f_{ck} = 40 MPa. The obtained results are shown in figure 5.4. Lateral buckling would become a concern for spans beyond $L_B = 0.53L_{max}$. As a result girders I100A100 and I120A100, which would be used in designs for spans until $0.53L_{max}$ and $0.57L_{max}$, respectively, are in the region where tensile stresses start to be significant hence an instability phenomenon may occur.

The results obtained for the girders from Series A and f_{ck} = 60 MPa are depicted in figure 5.5. Under this assumption, all these girders have a buckling length $L_B = 0.54L_{max}$. Girders I80A100, I100A100 and I120A100 could therefore show symptoms of lateral buckling for spans beyond L_B. The effects would be more sever for the I120A100 since it is used for spans up to $L_T = 0.64L_{max}$. Note that increasing f_{ck} from 20 MPa to 40 MPa varely increases the maximum buckling length L_B but it has a great influence on the maximum design length L_T.

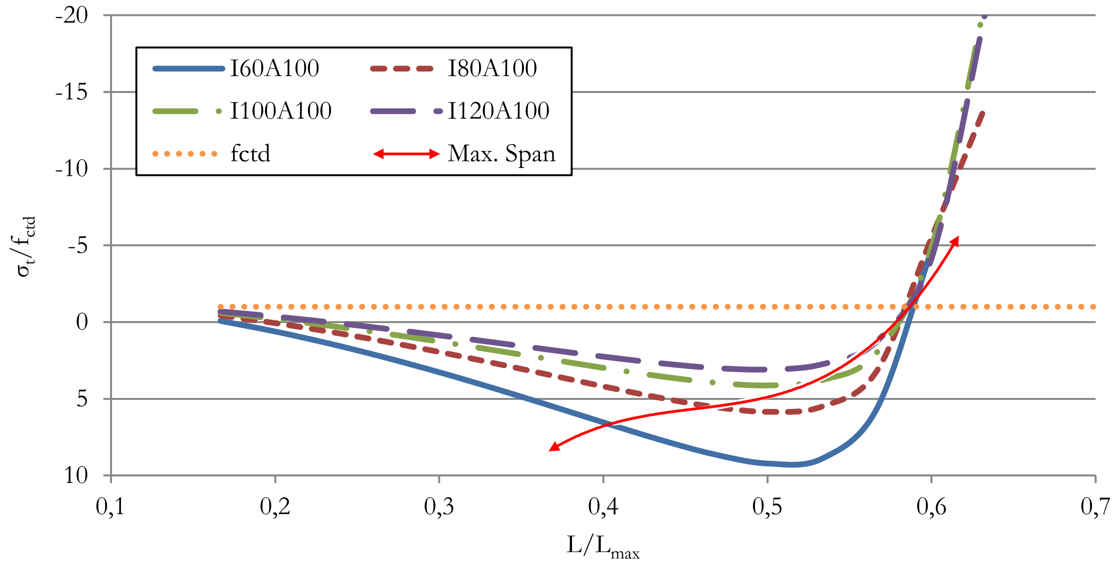

Figure 5.4. Stresses at the downward top flange of I girders from Series A. f_{ck} = 40 MPa.

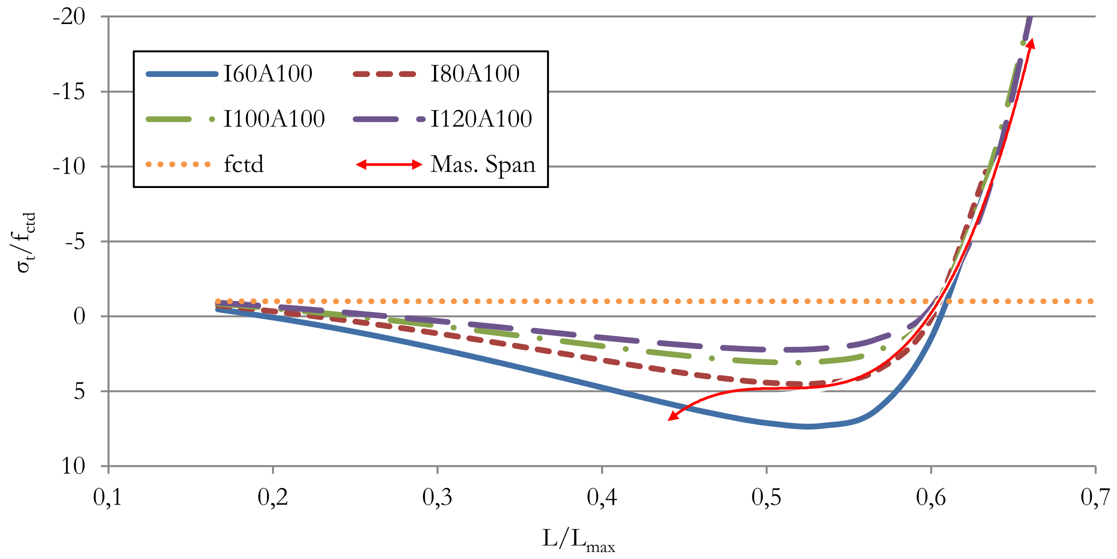

Figure 5.5. Stresses at the downward top flange of I girders from Series A. f_{ck} = 60 MPa.

5.3.2 Series B, I girders

The cross-sectional properties of the I girders from Series B analyzed are shown in table 5.4. Their maximum design spans L_T are shown in table 5.5.

Girder	d (m)	A (m²)	H_g (m)	I_y (cm⁴)	I_z (cm⁴)	J (cm⁴)
I120B120	1.20	0.4629	0.598	2004300	9100200	1255000
I140B120	1.40	0.4929	0.693	2009900	13414800	1301600
I180B120	1.80	0.5529	0.886	2021200	25056300	1394900
I200B120	2.00	0.5829	0.982	2026000	32503500	1441500

Table 5.4. Cross-sectional properties of I girders from Series B.

f_{ck} (MPa)	L_T (m)			
	I120B120	I140B120	I180B120	I200B120
20	27.9	29.9	32.7	33.8
40	35.1	37.6	41.3	42.6
60	39.7	42.6	46.7	48.2

Table 5.5. Girders I Series A. Maximum design length.

Figure 5.6 shows the obtained stresses at midspan in the downward top flange for lengths up to L_{max} = 60 m and for the girders belonging to Series B indicated in table 5.4. f_{ck} is 20 MPa. For those girders instability effects would start at $L_B = 0.55L_{max}$. Girder I200B120, which is the deeper shown in figure 5.6, has a maximum design span L_T which is near that value. Therefore, it would be advisable not pursuing longer spans maintaining its lateral stiffness.

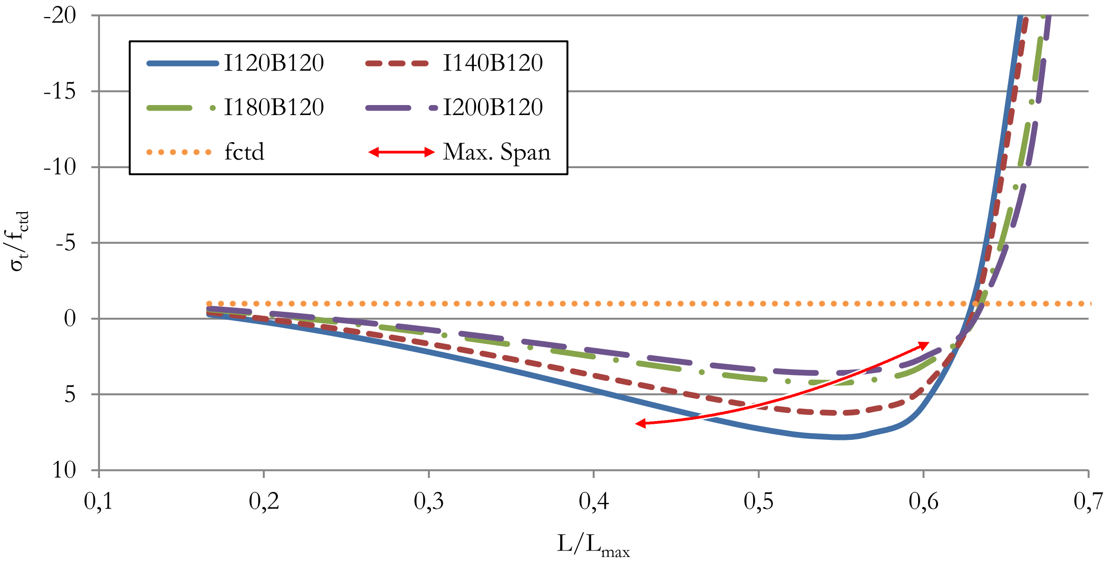

Figure 5.6. Stresses at the downward top flange of I girders from Series B. f_{ck} = 20 MPa.

The results obtained for the girders from Series B and f_{ck} = 40 MPa are depicted in figure 5.7. Under this assumption, all these girders would have a buckling length $L_B = 0.58L_{max}$.

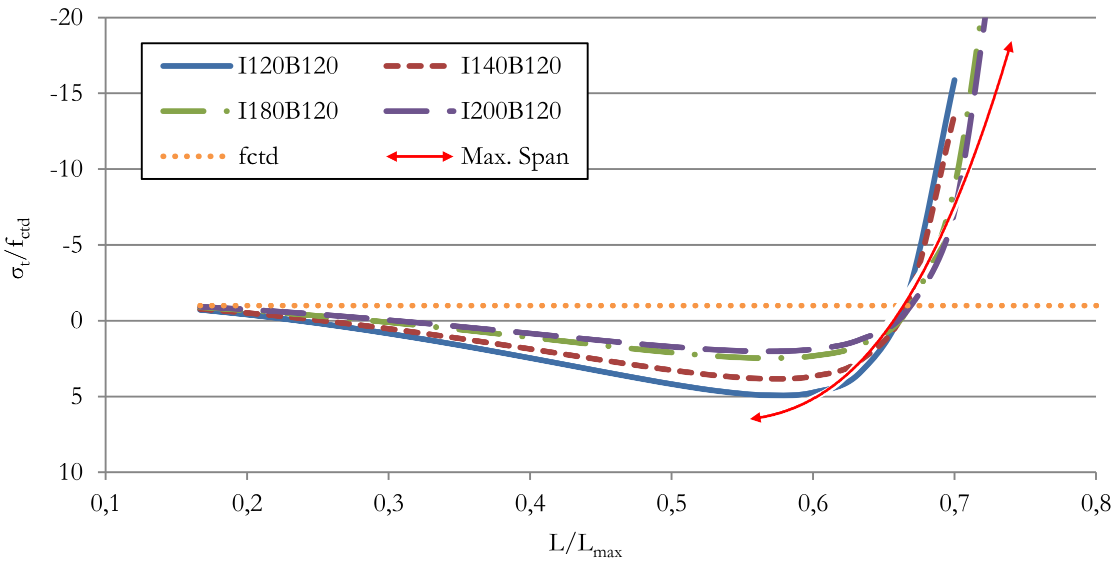

Figure 5.7. Stresses at the downward top flange of I girders from Series B. f_{ck} = 40 MPa.

As graphically shown in figure 5.7, the maximum design length L_T of all girders is longer than L_B. Due to that reason they all could show symptoms of lateral buckling for spans beyond L_B. The effects would be more sever for the deeper ones, I180B100 and I200B120, since they are used for spans up to $0.69L_{max}$ and $0.71L_{max}$.

If the characteristic strength of the concrete were 60 MPa there would be almost no variation in the buckling length L_B of girders from Series B. On the other hand, maximum design lengths L_T would greatly increase to at least $0.66L_{max}$ (for the girder I120B120). Consequently the likelihood of buckling for those girders would be much higher.

5.3.3 Series C, I girders

The cross-sectional properties of the I girders from Series C studied in this section are shown in table 5.6. Their maximum design spans L_T are shown in table 5.7.

Girder	d (m)	A (m²)	H_g (m)	I_y (cm⁴)	I_z (cm⁴)	J (cm⁴)
I95C150	0.95	0.5160	0.494	4991700	6533600	1498000
I135C150	1.35	0.5880	0.696	5011200	15641100	1677700
I175C150	1.75	0.6600	0.897	5030600	29452300	1857400
I215C150	2.15	0.7320	1.098	5050000	48543300	2037100

Table 5.6. Cross-sectional properties of I girders from Series C.

f_{ck} (MPa)	L_T (m)			
	I95C150	I135C150	I175C150	I215C150
20	25.0	29.9	33.0	35.05
40	31.5	37.7	41.5	44.2
60	35.6	42.7	47.0	50

Table 5.7. Girders I Series C. Maximum design length.

Figure 5.8 illustrates the obtained stresses at midspan in the downward top flange for lengths up to L_{max} = 60 m. The girders are from the C Series indicated in table 5.4 and the concrete characteristic resistance f_{ck} is 20MPa. For those girders instability effects would start at $L_B = 0.68L_{max}$.

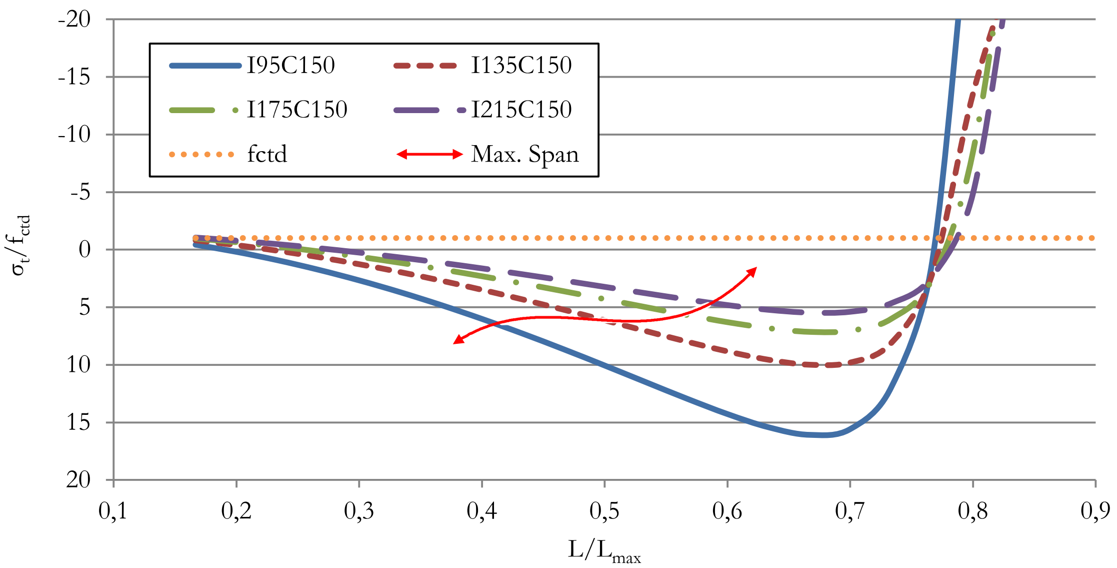

Figure 5.8. Stresses at the downward top flange of I girders from Series C. f_{ck} = 20 MPa.

Nevertheless their maximum design length L_T is far below that value. For instance, the deeper girder I215C150 would allow designs up to L_T = 0.59L_{max}. As a result, in that case lateral buckling would not be a design constraint for the I girders belonging to Series C.

For f_{ck} = 40 MPa, the results obtained are depicted in figure 5.9. In this situation L_B = 0.72L_{max}. Note that under this assumption girder I215C150 is at the limit were it could show symptoms of lateral instability since its maximum design length is L_T = 0.71L_{max}. Instead, girders I95C150, I135C150 and I175C150 could safely reach their respective maximum design lengths.

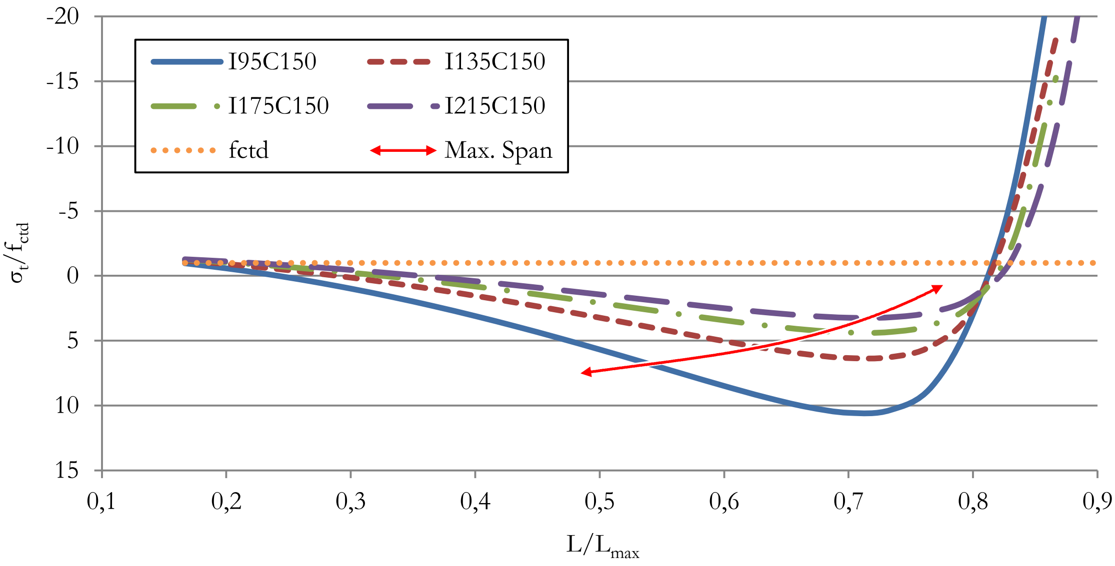

Figure 5.9. Stresses at the downward top flange of I girders from Series C. f_{ck} = 40 MPa.

The same process has been performed increasing f_{ck} to 60 MPa (fig. 5.10). In the same way than in Series A and B, the maximum buckling length remains almost the same adopting the value L_B = 0.74L_{max}.. However, maximum design lengths L_T of girders I175C150 and 215C150 are now 0.78L_{max} and 0.83L_{max}, respectively. Thus under the assumptions described at the beginning of this section girders I175C150 and 215C150 would be currently being used for spans in which their safety against lateral buckling is not ensured.

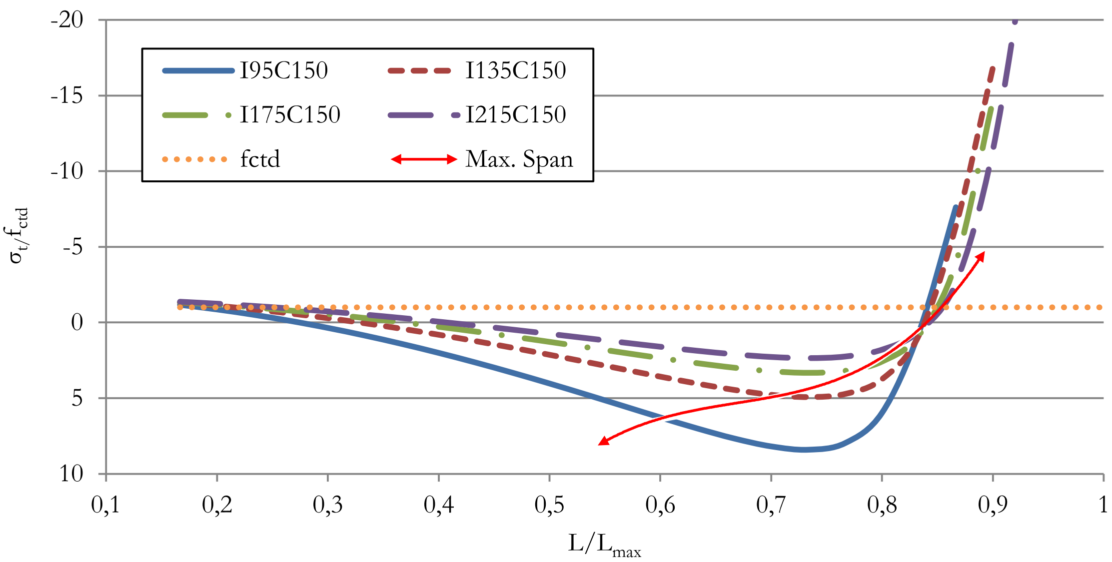

Figure 5.10. Stresses at the downward top flange of I girders from Series C. f_{ck} = 60 MPa.

5.3.4 Series D, I girders

The cross-sectional properties of the I girders belonging to Series D analyzed are indicated in table 5.8. Their corresponding maximum design lengths L_T depending on the concrete resistance are listed in table 5.9.

Girder	d (m)	A (m²)	H_g (m)	I_y (cm⁴)	I_z (cm⁴)	J (cm⁴)
I125D200	1.25	0.6798	0.632	8350800	15640500	1627500
I165D200	1.65	0.7598	0.829	8377500	30751500	1947500
I205D200	2.05	0.8396	1.026	8404200	51939400	2267500
I245D200	2.45	0.9198	1.149	8430800	79844400	2587500

Table 5.8. Cross-sectional properties of I girders from Series D.

f_{ck} (MPa)	L_T (m)			
	I125D200	I165D200	I205D200	I245D200
20	29.6	33.2	35.7	37.5
40	37.2	41.9	44.9	47.2
60	42.1	47.4	50.9	53.4

Table 5.9. Girders I Series D. Maximum design length.

Figure 5.11 shows the obtained stresses at midspan in the downward top flange for lengths up to L_{max} = 60 m and for the girders from the D Series indicated in table 5.4. f_{ck} is 20 MPa. For those girders instability effects would start at L_B = 0.74L_{max}. However, lateral buckling is unlikely to become a design constraint due to the fact that the maximum design length they can reach is, for the girder I245D200, L_T = 0.63L_{max}.

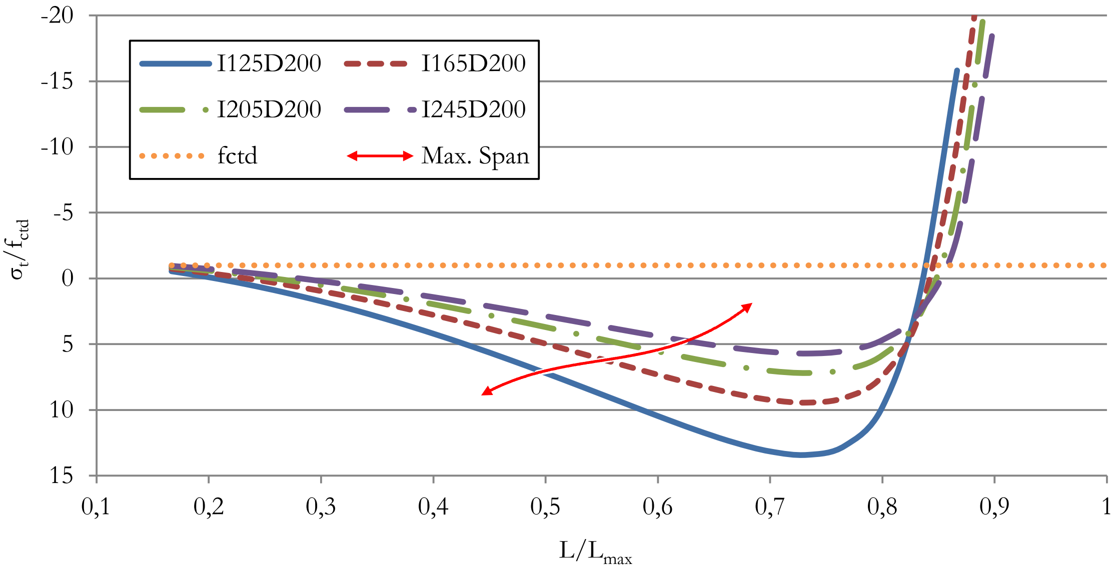

Figure 5.11. Stresses at the downward top flange of I girders from Series D. f_{ck} = 20 MPa.

Adopting f_{ck} =40 MPa allows reaching spans significantly longer as shown in figure 5.12. In this situation, lateral buckling would be of concern at lengths beyond L_B = 0.78L_{max}. According to the limitations in the maximum design span of girders from Series D, only the deeper cross section I245D200 has the possibility of being used up to that length. With regard to the other girders, lateral buckling would not be a design a limitation.

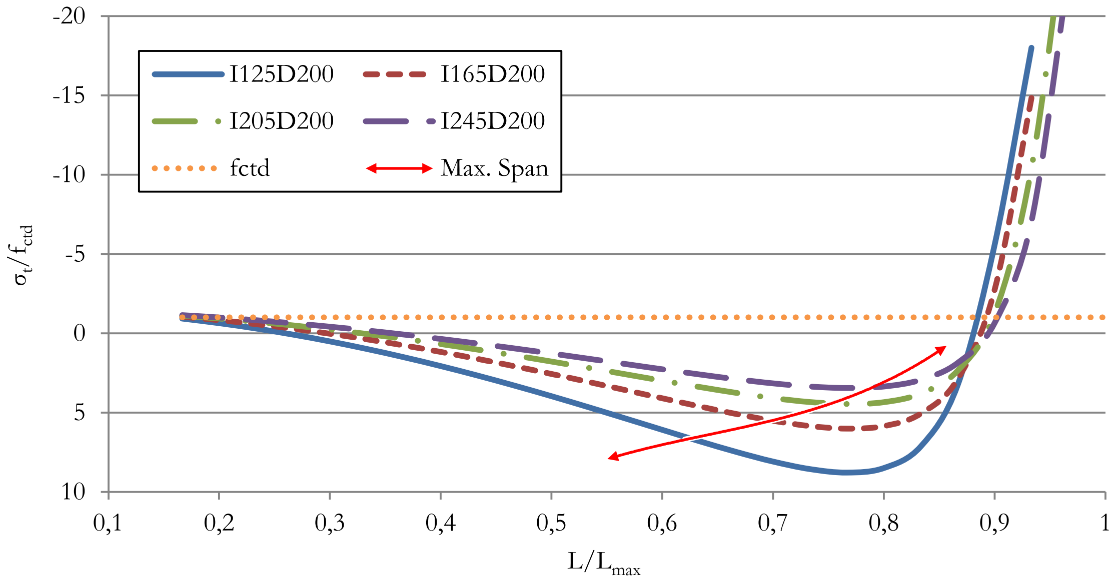

Figure 5.12. Stresses at the downward top flange of I girders from Series D. f_{ck} = 40 MPa.

The same process has been followed increasing f_{ck} to 60 MPa (fig. 13). Similarly to the other Series, the maximum buckling length slightly increases adopting the value L_B = 0.80L_{max}.. However, maximum design lengths L_T of girders I205D200 and 245D200 are now 0.84L_{max} and 0.89L_{max}, respectively. Thus under the assumptions described at the beginning of this section girders I205D200 and 245D200 could be currently being used for spans in which their safety against lateral buckling is not ensured.

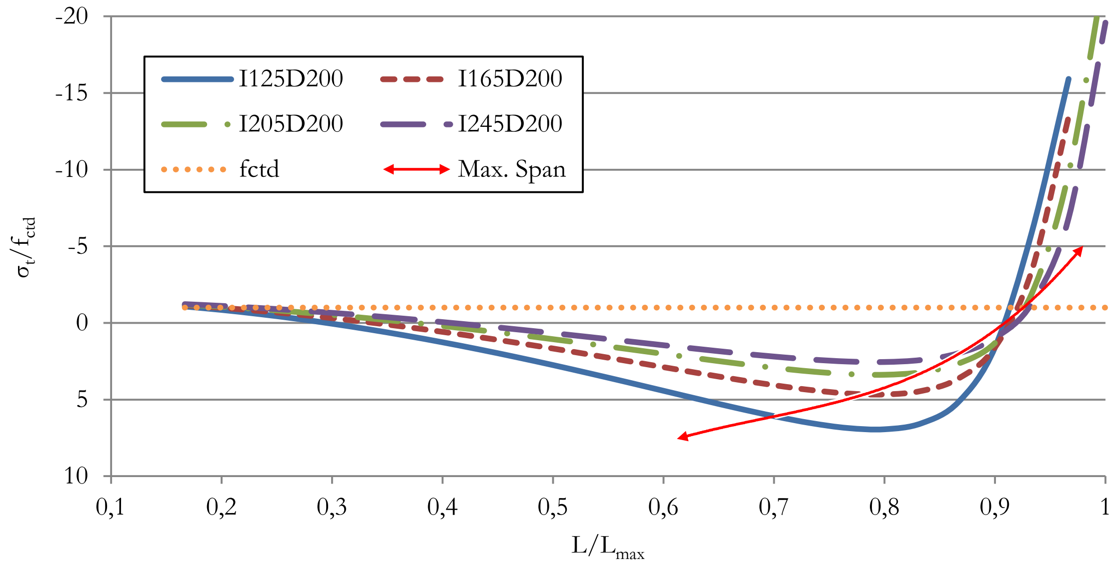

Figure 5.13. Stresses at the downward top flange of I girders from Series D. f_{ck} = 60 MPa.

5.4 Proposed design criteria

As exposed in 2.5 current codes give simple checks against lateral buckling but do not define a criterion for the rotation of precast prestressed girders during lifting.

Along this paper it has been shown the rotation of a hanging girder is influenced by several factors. The initial rotation β_i is basically dependant on lateral sweep δ and the vertical distance H between the center of gravity of the whole beam and the attachment points of the lifting cables to the lifting loops (roll axis). Current codes such as the Spanish concrete instruction *EHE-08*[27] specifically states a tolerance on lateral sweep which, if H were known, would allow to establish a limit on the initial rotation angle β_i.

During the design of precast prestressed concrete girders lateral imperfections are not usually taken into account. For that reason, reaching longer spans is just a matter of increasing the strong-axis stiffness by using deeper cross-sections. Meanwhile, weak-axis stiffness remains almost constant since the width of the flanges is not modified. In accordance with the results obtained both in chapters 4 and 5 it is apparent that all the I girders from the same Series have the same maximum buckling length L_B, which is due to the fact that their weak-axis stiffness EI_y are quite similar.

As a result, the total rotation of a hanging girder β for the I girders from Series A, B, C and D can be regarded, to a large degree, as a function of lateral sweep δ, the height between the center of gravity of the whole beam and the cable attachment points H and the weak-axis stiffness EI_y.

In this regard a safety factor is graphically presented in figure 5.14. It defines a minimum weak-axis moment of inertia I_y depending on the girders length L. It has been considered that the height of the lifting loops would be at least h_l = 20 cm and that the maximum allowed lateral sweep tolerance is $L/750$ as stated in *EHE-08*. Also, the lifting cables are vertical. As can be seen there are three different curves which account for the contribution of the characteristic resistance of the concrete f_{ck} at the time of lifting.

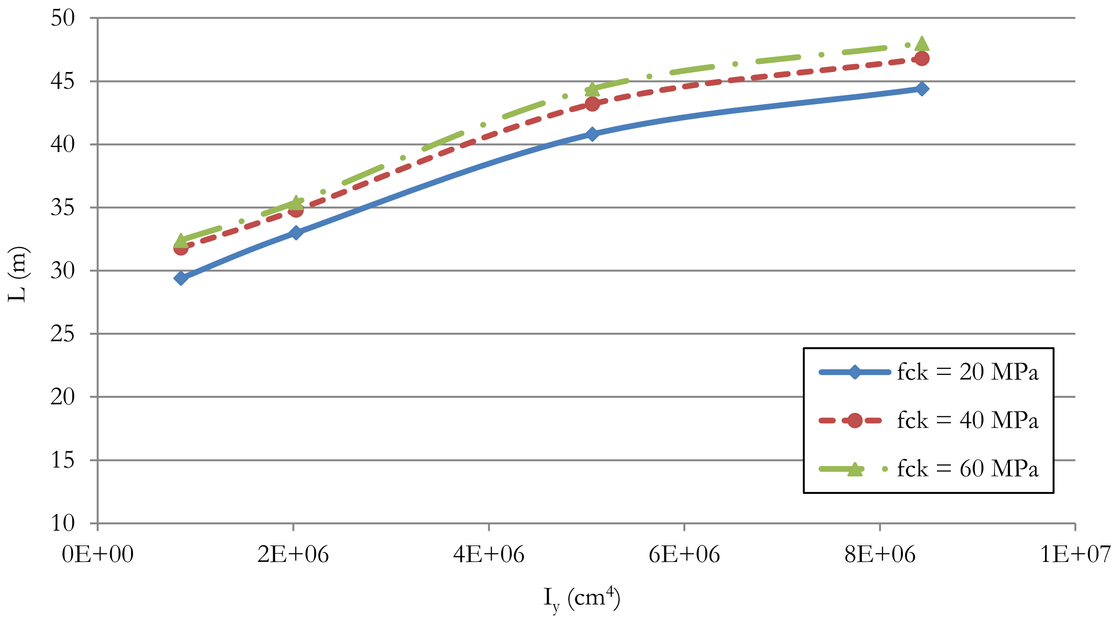

Figure 5.14. Minimum weak-axis stiffness requirement at the time of lifting.

CHAPTER 6.

REAL CASE STUDY

6.1 Introduction

Problems during lifting arose during the construction of a viaduct near to a town called Olost, in Catalonia, Spain. Some of the precast prestressed concrete girders manufactured for the construction of the viaduct presented a small initial horizontal imperfection which shifted the center of gravity of the girder laterally. Due to this bowing, when some of those girders were lifted they slightly rolled, and deflected in their weak-axis. Beyond a certain deflection one of the girders was lowered down for safety reasons. Cracks were observed all along the beam so it was eventually replaced.

In this chapter the lateral stability of those girders is analyzed throughout the analytical formulation used so far in this document. The information regarding this incident has been obtained from a report carried out by the Polytechnic University of Catalonia (UPC)[9].

6.2 Description of the case

The bridge presented a curved guideline when seen from above consisting of three spans of 20.45 m, 44.90 m and 45.57 m. The structure had four precast prestressed concrete girders on which a concrete slab had to be casted after the girders were placed onto its supports. The girders had an I cross section and were 2.0 m deep (code I200B120 in the commercial catalogue found in Appendix A).

According to the field technicians, the girders arrived to the construction site presenting some lateral deformation within a tolerance range of $\delta = L/500$. It is worth stressing that, contrary to the inner girders, the ones to be placed at the edges of the bridge included a mass concrete wall located at the end of the top flange. The original I200B120 is shown in figures 6.1 and 6.2 during the lifting stage. It can be appreciated the girder has slightly rolled and deflected in its weak-axis direction. The modified I200B120 edge girder including the mass concrete wall is illustrated in figure 6.3 in which it is also apparent its rotation.

Figure 6.1. Perspective of bridge girder I200B120 during lifting. [9]

Figure 6.2. Bridge girder I200B120 during lifting. [9]

Figure 6.3. Bridge girder I200B120 with modified top flange during lifting. [9]

The following information is referred to the second span of the bridge whose length is L = 44.90 m. The girders were prestressed by 54 strands type Y1860 whose area is A_S = 140 mm² each. 50 of these strands were located in the bottom flange and the other 4 in the top flange. Prestressing force is P_0 = 3276 KN applied at a distance from the center of gravity e_p = 0.502 m. At the time of lifting the prestressing force is considered to be $P = 0.9P_0$ = 2948 KN due to short time losses and part of the long time losses. The characteristic strength of the concrete is f_{ck} = 60 MPa. Nonetheless, at the time of transferring the prestressing force f_{ck} = 35 MPa. In accordance with figure 6.3 it will be considered h_l = 30 cm. The lift points are located at distance a = 1 m from the end. The inclination angle of the lifting cables is ψ = 0° (vertical cables).

During the design of the girders there was no account for possible lateral imperfections. The following section analyzes the likelihood of lateral buckling of both the inner girders and the edge girders.

6.3 Lateral buckling analysis of the girder I200B120

The cross sectional properties of the I200B120 are shown in table 6.2. The lifting conditions described in the previous section are included in table 6.3.

Girder	d (m)	A (m²)	H_g (m)	I_y (cm⁴)	I_z (cm⁴)	J (cm⁴)
I200B120	2.00	0.5829	0.982	2026000	32503500	1441500

Table 6.2. Cross-sectional properties of girder I200B120.

L (m)	a (m)	δ (cm)	h_l (cm)	f_{ck} (MPa)	P (KN)	ψ (°)
44.9	1	L/500	30	35	2948	0

Table 6.3. Girder characteristic during lifting.

Figure 6.4 shows the stresses at the downward top flange of an I200B120 under the assumptions indicated in table 6.3 and for lengths between 10 m and 50 m. The solid line corresponds to the results obtained using *ULS* safety factors. In this regard, the advisable maximum length with respect to lateral buckling would be L_B = 36 m. Spans beyond that length would rapidly lead to tensile stresses and the girder would clearly buckle for its span of 44.9 m. The dashed line indicates the stresses obtained if safety factors are not used. In that situation L_B = 39 m. Cracks would develop for spans beyond 46 m. Therefore, it is concluded the 44.9 m long girder I200B120 lifted according to the characteristics defined in table 6.3 is in the region for which an instability phenomenon may occur.

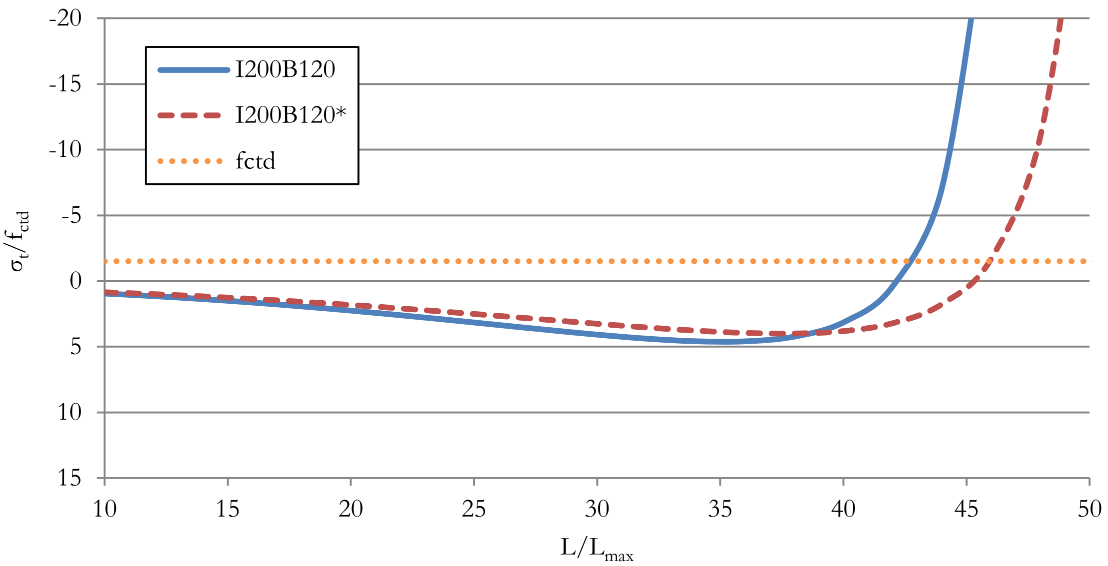

Figure 6.4. Stresses at the downward top flange of the girder I200B120.

CHAPTER 7.

CONCLUSIONS AND RECOMMENDATIONS

Conclusions and recommendations

By means of the results obtained in this paper and the reviewed literature, this chapter draws together the main findings arrived at with regard to the lateral stability of long precast prestressed concrete girders.

The stability of precast prestressed concrete girder requires consideration of two different phenomenons: rollover and lateral-torsional buckling. Rollover is the controlling stability phenomenon for cases where the girder is not laterally braced. Otherwise, instability failure would occur due to lateral-torsional buckling.

A girder lifted by two cables is considered the worst case scenario against lateral-torsional buckling due to the absence of rotational restraint per part of the supports. Lateral-torsional buckling of a hanging girder under its own self-weight is regarded as a rigid body rotation about the points of attachment to the supporting cables, triggered by accidental lateral deformations, combined with lateral bending of the girder about its minor axis and cross-sectional twist. Due to the lack of rotational restraint provided by the supports along with the great torsional stiffness of concrete girders, lateral-torsional buckling of a hanging girder is referred to as just lateral buckling.

Precast prestressed concrete girders are typically designed to not crack under self-weight and a complete straightness of the girders is assumed. Therefore, in most of precast concrete girder catalogs reaching longer spans has only meant a matter of increasing the strong-axis stiffness by using deeper cross-sections. Meanwhile, weak-axis stiffness remains almost constant for I shaped girders since the width of web and flanges is not modified. The presence of unexpected lateral deformations hence increases the likelihood of buckling failure in longer girders due to their increased weight, and lateral stability may become a design constraint.

This fact has been confirmed in this thesis for the I girders belonging to Series A, B, C and D of a commercial girders catalogue. Since all the girders from the same Series have similar weak-axis stiffnesses, lateral buckling would occur at the same spans. For example, in the case those girders are: lifted by vertical cables at a time in which their characteristic strength is 40 MPa, end-supported from 20 cm above their top flange and lateral sweep is $L/750$; lateral instability may become of concern for spans beyond 31.8 m, 34.8 m, 43.2 m and 46.8 m for the I girders from Series A, B, C and D, respectively. On the other hand, channel or box girders, like the Artesa girders defined in the catalogue, present greater lateral and torsional stiffnesses and lateral buckling is unlikely to become a design a constraint.

The parametric analysis shows the most efficient manners of increasing lateral stability are reducing the rigid body rotation and increasing the weak-axis stiffness of the girder. To this end, it is worth stressing the importance of moving the lift points inwards since not only the weak-axis deflection is greatly reduced but the weight in the overhangs is on the opposite side of the roll axis. Nevertheless there exist a practical limit when moving the lift points inwards due to the tensile stresses induced at the top fiber near supports location. Also, increasing the height of the lifting loops in order to raise the roll axis appears to be quite beneficial.

Weak-axis stiffness responds to the material properties and the cross-sectional geometry of the girder. Improving the material properties for lateral stability considerations maintaining the arrangement and force of the prestressing would imply a modification of the cracking design criteria used so far for the design of prestressed precast concrete girders. Furthermore, the girder would not be optimally prestressed. There also exists a practical-economical limit on the concrete properties, specially for prestressed members for which an early transfer strength and handling from the casting bed is performed. Consequently, it would seem more efficient to adapt the cross-sectional geometry, increasing the width of the flanges, and therefore increasing its lateral moment of inertia.

It is worth highlighting that the bottom flange contributes just as much to lateral stability as the top flange. In fact, adding material to the bottom flange is more beneficial because it lowers the center of gravity, which would slightly reduce the girder rigid body rotation as well as increase lateral stiffness. Moreover, it would probably also improve the factor of safety against rollover failure when the girder is supported from below. The implementation of a wider bottom flange allows for a wider elastomeric bearing pad to be used.

Current codes such as the Spanish concrete instruction *EHE-08* specifically state a tolerance on lateral sweep which, knowing the depth of the girder and height of the lifting loops, would allow to establish a limit on the rigid body initial rotation. However, there is no limit on the girder total rotation which would also rely upon the girder weak-axis stiffness. In this regard, this thesis suggests a conservative method to ensure that lateral buckling does not occur during the lifting stage, consisting on establishing a minimum weak-axis moment of inertia depending on the length of the girder.

BIBLIOGRAPHY

[1] Marrey, B. and Grote, J. *"The story of prestressed concrete from 1930 to 1945: A step towards the European Union"*. Proceedings of the First International Congress on Construction History. Madrid, January 2003.

[2] Hurff, J. et al. "*Stability of Precast Prestressed Concrete Bridge Girders Considering Sweep and Thermal Effects*". Georgia Institute of Technology, School of Civil & Environmental Engineering. Prepared for Georgia Department of Transportation, June 15 2009.

[3] Castrodale, R. W. and White, C. D. "*Extending Span Ranges of Precast Prestressed Concrete Girders*". National Cooperative Highway Research Program, Report 517. Washington D. C., 2004.

[4] Canadian Precast Prestressed Concrete Institute. "*Record-Breaking Precast Nu Girders Installed in Alberta*". April 2002. www.cpci.ca/en/about_us/project_month/april_2002/.

[5] Stratford, T.J. and Burgoyne, C. J. "*Lateral stability of long precast concrete beams*". Proc. Instn Civ. Engrs Structures & Bldgs, May-August 1999, pp. 169-180.

[6] Redacción 360° en Concreto. "*Construcción de Puentes con Elementos Prefabricados de Concreto*". Blog Argos. June 2014. www.blogargos.smdigitaltest.com/construccion-de-puentes-con-elementos-prefabricados-de-concreto-2/.

[7] TechSOFT Engineering Services. "*ASTRA Pro, Structural Engineering Analysis and Design Software*". www.techsoftglobal.com/astrapage.aspx.

[8] Rose, J. "*Marquam Bridge wreck likely caused by truck with massive beam braking for Portland traffic jam*". The Oregonian, April 2013. www.oregonlive.com/commuting/index.ssf/2013/04/crippling_marquam_bridge_wreck.html.

[9] De la Fuente Antequera, A. et al. "*Simulación del comportamiento estructural de la viga de borde en situación de izado*". Universitat Politècnica de Catalunya-UTE Variant d'Olost, April 2013.

[10] Hurff, J. "*Stability of Precast Prestressed Concrete Bridge Girders Considering Imperfections and Thermal Effects*". Georgia Institute of Technology, School of Civil and Environmental Engineering, August 2010.

[11] Muller, J. "*Lateral Stability of Precast Members During Handling and Placing*". PCI Journal, February 1962, pp. 20-31.

[12] Anderson, A. R. "*Lateral stability of long prestressed concrete beams*". PCI Journal, 16(3), 7-9. May-June 1971.

[13] Swann, R. A., Readers comment to "*Lateral Stability of Long Prestressed Concrete Beams*", PCI Journal, 16(6), November-December 1971.

[14] Laszlo, G. and Imper, R. R. "*Handling and Shipping of Long Span Bridge Beams*". PCI Journal, November-December 1987, pp. 86-101.

[15] Mast, R. F. "*Lateral Stability of Long Prestressed Concrete Beams. Part 1*". PCI Journal, January-February 1989, pp. 34-53.

[16] Mast, R. F. "*Lateral Stability of Long Prestressed Concrete Beams. Part 2*". PCI Journal, January-February 1993, pp. 70-78. Reader comments by Castrodale R. W., May H. R., Nagle J. W., Zendegui S. and Mast, R. F. PCI Journal, pp. 96-100.

[17] Mast, R. F. "*Lateral Bending Test to Destruction of a 149 ft Prestressed Concrete I-Beam*". PCI Journal, July-August 1994, pp. 54-62.

[18] Stratford, T.J., et al.. "*Stability design of long precast concrete beams*". Proc. Instn Civ. Engrs Structures & Bldgs, May-August 1999, pp. 159-168.

[19] Stratford, T.J. and Burgoyne, C. J. "*The toppling of hanging beams*". International Journal of Solids and Structures, 2000, pp. 3569-3589.

[20] Stratford, T.J. and Burgoyne, C. J. "*Lateral instability of long-span prestressed concrete beams on flexible bearings*". The Structural Engineer, Volume 79/No 6, March 2001.

[21] Plaut, R. H. and Moen, C.D. "*Theory and Applications of the Lifting of Elastic, Doubly symmetric, Horizontally Curved Beams*". Virginia Polytechnic Institute and State University, Department of Civil and Environmental Engineering, December 2011.

[22] Plaut, R. H. and Moen, C.D. "Analysis of Elastic, Doubly Symmetric, Horizontally Curved Beams during Lifting." *Journal of Structural Engineering*, January 2013, pp. 39-46. Proceedings of the Annual Stability Research Conference, Structural Stability Research Council, May 10-14 2011.

[23] Hurff, J. and Kahn, L. "*Rollover stability of precast, prestressed concrete bridge girders with flexible bearings*". PCI Journal, Fall 2012.

[24] PCI Bridge Design Manual. Prestressed Concrete Institute, Chicago, IL. 2nd ed, 2003.

[25] PCI Tolerance Manual for Precast and Prestressed Concrete Construction. Prestressed Concrete Institute, Chicago, IL. 1st ed, 2000.

[26] Instrucción de Hormigón Estructural EHE-08. Comisión Permanente del Hormigón. Ministerio de Fomentos. 3ª edición, 2009.

[27] Eurocode 2: Design of Concrete Structures. Technical Sector Board for Building and Civil Engineering, 1999.

[28] Bairán, J. M. and Cladera, A. *"Collapse of a precast concrete beam for a light roof. Importance of elastomeric bearing pads in the element's stability"*. Engineering failure analysis, February 2014.

[29] Lebelle, P. "*Stabilité élastique des poutres en betón précontraint à l'égard du déversement lateral*". Institute Technique du Bâtiment et des Travaux Publics, September 1959.

[30] Cojocaru, R. "*Lifting Analysis of Precast Prestressed Concrete Beams*". Virginia Polytechnic Institute and State University, Master of Science in Civil Engineering, April 27 2012.

[31] Consolazio, G. R. and Hamilton, H. R., "*Lateral Bracing of Long-Span Florida Bulb-Tee Girders*". University of Florida, Civil and Coastal Engineering, July 2007.

93

APPENDIX A.

GIRDERS CATALOGUE

I girders

Series A

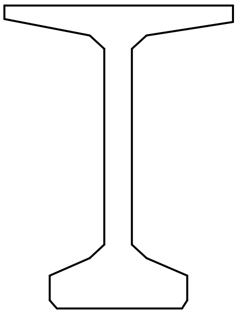

Figure A.1. Cross-sectional geometry girders I Series A.

Girder	d (m)	A (cm^2)	H_g (m)	I_y (cm^4)	I_z (cm^4)	J (cm^4)
I60A100	60	2267	0.312	0.252	841300	1090100
I70A100	70	2507	0.361	0.301	842700	1617300
I80A100	80	2747	0.411	0.351	844200	2263900
I90A100	90	2987	0.46	0.4	845600	3035700
I100A100	100	2747	0.51	0.45	847100	3938900
I110A100	110	2867	0.559	0.499	848500	4979500
I120A100	120	2987	0.609	0.549	849900	6163300
I130A100	130	3107	0.658	0.598	851400	7496600

Table A.1. Cross-sectional properties girders I Series A.

Series B

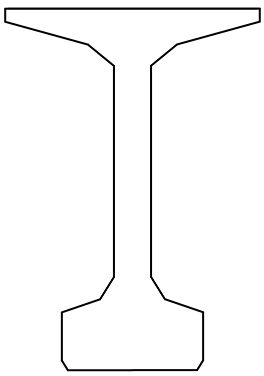

Figure A.2. Cross-sectional geometry girders I Series B.

Girder	d (m)	A (cm^2)	H_g (m)	I_y (cm^4)	I_z (cm^4)	J (cm^4)
I120B120	120	4629	0.598	0.488	2004300	9100200
I130B120	130	4779	0.645	0.535	2007100	11136300
I140B120	140	4929	0.693	0.583	2009900	13412800
I150B120	150	5079	0.741	0.631	2012300	15937400
I160B120	160	5228	0.789	0.679	2015600	18713400
I170B120	170	5379	0.837	0.727	2018400	21750600
I180B120	180	5529	0.886	0.776	2021200	25058300
I190B120	190	5678	0.934	0.824	2024000	28638100
I200B120	200	5829	0.982	0.872	2026000	32503500
I210B120	210	5979	1.031	0.921	2029600	36660100

Table A.2. Cross-sectional properties girders I Series B.

Series C

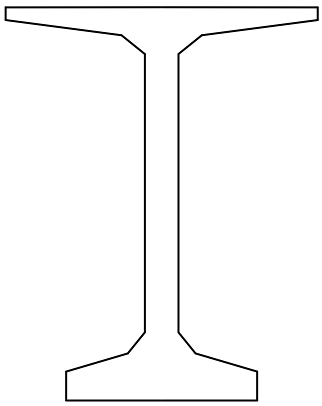

Figure A.3. Cross-sectional geometry girders I Series C.

Girder	d (m)	A (cm^2)	H_g (m)	I_y (cm^4)	I_z (cm^4)	J (cm^4)
I65C150	65	4620	0.342	0.267	4977155	2443200
I95C150	95	5160	0.494	0.419	4991735	6533600
I115C150	115	5526	0.595	0.52	5001455	10535400
I135C150	135	5880	0.696	0.621	5011175	15641100
I155C150	155	6240	0.796	0.721	5020895	21922700
I175C150	175	6600	0.897	0.822	5030615	29452300
I195C150	195	6960	0.997	0.922	5040335	38301800
I215C150	215	7329	1.098	1.023	5050055	48543300
I235C150	235	7680	1.198	1.123	5059775	60248800

Table A.3. Cross-sectional properties girders I Series C.

Series D

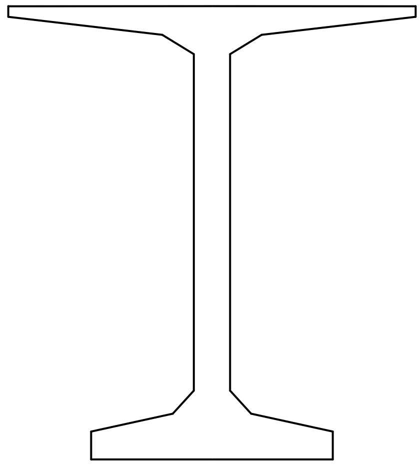

Figure A.4. Cross-sectional geometry girders I Series D.

Girder	d (m)	A (cm^2)	H_g (m)	I_y (cm^4)	I_z (cm^4)	J (cm^4)
I75D200	75	5798	0.388	0.313	8317500	4321400
I95D200	95	6198	0.466	0.391	8330800	7909800
I105D200	105	6398	0.534	0.459	8337500	10163600
I115D200	115	6598	0.583	0.508	8344200	12737200
I125D200	125	6798	0.632	0.557	8350800	15640500
I135D200	135	6998	0.682	0.607	8357500	18883600
I145D200	145	7198	0.731	0.656	8364200	22476400
I155D200	155	7398	0.78	0.705	8370800	26429100
I165D200	165	7598	0.829	0.754	8377500	30751500
I175D200	175	7789	0.878	0.803	8384200	35453800
I185D200	185	7998	0.928	0.853	8390800	40545800
I195D200	195	8198	0.977	0.902	8397500	46037700
I205D200	205	8396	1.026	0.951	8404200	51939400
I215D200	215	8598	1.075	1.000	8410800	58260900
I225D200	225	8798	1.125	1.050	8417500	65012200
I235D200	235	8998	1.175	1.100	8424200	72203400
I245D200	245	9198	1.224	1.149	8430800	79844400

Table A.4. Cross-sectional properties girders I Series C.

Artesa girders

Series B

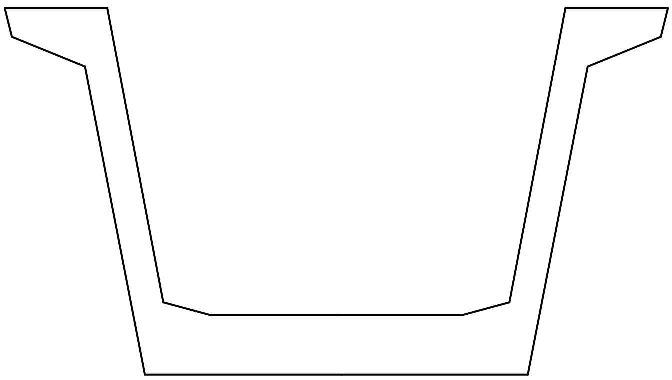

Figure A.5. Cross-sectional geometry girders Artesa Series D.

Girder	d (m)	A (cm²)	H_g (m)	I_y (cm⁴)	I_z (cm⁴)	J (cm⁴)
A110B	110	8236	0.41	0.2975	65429700	11586100
A140B	140	9389	0.537	0.4245	81303400	22145400
A170B	170	10956	0.663	0.5505	98893100	36619300
A200B	200	11256	0.78	0.6675	118147600	55444600
A230B	230	11632	0.897	0.7845	139661200	79367000

Table A.5. Cross-sectional properties girders Artesa Series B.

APPENDIX B.

DETAILED RESULTS

Cases analyzed

Chapter 4: Parametric study of a hanging girder

Case	L (m)	a (m)	δ (m)	h_l (cm)	f_{ck} (MPa)	P (KN)	ψ (°)
1	10 - 60	0	L/750	40	20	P_{max}	0
2	10 - 60	0 - 8	L/750	40	20	P_{max}	0
3	10 - 60	0	L/750	40	20-60	P_{max}	0
4	10 - 60	0	0,02 - 0,08	40	20	P_{max}	0
5	10 - 60	0	L/750	40	20	0 - P_{max}	0
6	10 - 60	0	L/750	20 - 150	20	P_{max}	0
7	10 - 60	0	L/750	40	20	P_{max}	0 - 45

Chapter 5: Analysis of results

Case	L (m)	a (m)	δ (m)	h_l (cm)	f_{ck} (MPa)	P (KN)	ψ (°)
8	10 - 60	0	L/750	20	20 - 60	P_{max}	0

Chapter 6: Real case study

Case	L (m)	a (m)	δ (m)	h_l (cm)	f_{ck} (MPa)	P (KN)	ψ (°)
9	44,9	1	L/500	30	35	2948	0

Case 1: I60A100

L (m)	β (°)	W (cm)	V (cm)	M_y (KNm)	M_z (KNm)	φ (°)	P_{max} (KN)	M_{Pmax} (KNm)	σ_{my} (Mpa)	σ_{mz} (Mpa)	σ_p (Mpa)	σ_{MP} (Mpa)	σ_t (Mpa)
10.00	0.72	0.91	55.79	1.20	-95.63	0.00	688.72	214.88	-0.07	2.53	3.04	-4.97	0.53
12.00	0.87	1.09	55.79	2.09	-137.70	0.00	688.72	214.88	-0.12	3.64	3.04	-4.97	1.58
14.00	1.02	1.29	55.79	3.34	-187.42	0.00	688.72	214.88	-0.20	4.95	3.04	-4.97	2.82
16.00	1.19	1.50	55.78	5.06	-244.78	0.00	688.72	214.88	-0.30	6.47	3.04	-4.97	4.24
18.00	1.36	1.72	55.78	7.37	-309.78	0.00	688.72	214.88	-0.44	8.18	3.04	-4.97	5.82
20.00	1.56	1.97	55.78	10.43	-382.41	0.00	688.72	214.88	-0.62	10.10	3.04	-4.97	7.55
22.00	1.80	2.26	55.77	14.50	-462.66	0.00	688.72	214.88	-0.86	12.22	3.04	-4.97	9.43
24.00	2.08	2.62	55.76	20.00	-550.51	0.00	688.72	214.88	-1.19	14.54	3.04	-4.97	11.43
26.00	2.45	3.09	55.75	27.63	-645.92	0.00	688.72	214.88	-1.64	17.07	3.04	-4.97	13.49
28.00	2.96	3.73	55.72	38.73	-748.80	0.00	688.72	214.88	-2.30	19.78	3.04	-4.97	15.55
30.00	3.74	4.71	55.68	56.13	-858.91	0.00	688.72	214.88	-3.34	22.69	3.04	-4.97	17.43
32.00	5.09	6.41	55.58	86.90	-975.47	0.00	688.72	214.88	-5.16	25.77	3.04	-4.97	18.68
34.00	8.02	10.09	55.25	154.29	-1094.76	0.00	688.72	214.88	-9.17	28.92	3.04	-4.97	17.82
36.00	16.66	20.72	53.45	355.29	-1187.46	0.00	688.72	214.88	-21.12	31.37	3.04	-4.97	8.33
38.00	181.29	-1.63	-55.78	-31.18	1380.67	0.00	688.72	214.88	1.85	-36.48	3.04	-4.97	-36.55
40.00	45.32	51.40	39.23	1088.05	-1075.97	0.00	688.72	214.88	-64.67	28.43	3.04	-4.97	-38.17
42.00	-4.70	-5.92	55.61	-138.24	-1681.39	0.00	688.72	214.88	8.22	44.42	3.04	-4.97	50.71
44.00	-3.22	-4.06	55.71	-104.02	-1848.63	-0.01	688.72	214.88	6.18	48.84	3.04	-4.97	53.09
46.00	-2.41	-3.04	55.75	-85.22	-2021.91	-0.01	688.72	214.88	5.07	53.42	3.04	-4.97	56.55
48.00	-1.90	-2.40	55.76	-73.24	-2202.29	-0.01	688.72	214.88	4.35	58.18	3.04	-4.97	60.61
50.00	-1.56	-1.96	55.77	-64.88	-2390.08	-0.01	688.72	214.88	3.86	63.14	3.04	-4.97	65.07
52.00	-1.30	-1.64	55.78	-58.68	-2585.40	-0.01	688.72	214.88	3.49	68.31	3.04	-4.97	69.86
54.00	-1.11	-1.40	55.79	-53.87	-2788.29	-0.01	688.72	214.88	3.20	73.67	3.04	-4.97	74.94
56.00	-0.96	-1.21	55.79	-50.00	-2998.80	-0.01	688.72	214.88	2.97	79.23	3.04	-4.97	80.27
58.00	-0.83	-1.05	55.79	-46.82	-3216.93	-0.01	688.72	214.88	2.78	84.99	3.04	-4.97	85.84
60.00	-0.73	-0.93	55.79	-44.13	-3442.70	-0.01	688.72	214.88	2.62	90.95	3.04	-4.97	91.65

Case 1: I80A100

L (m)	β (°)	W (cm)	V (cm)	M_y (KNm)	M_z (KNm)	φ (°)	P_{max} (KN)	M_{Pmax} (KNm)	σ_{my} (Mpa)	σ_{mz} (Mpa)	σ_p (Mpa)	σ_{MP} (Mpa)	σ_t (Mpa)
10.00	0.63	0.88	29.71	1.17	-105.76	0.00	757.62	311.38	-0.07	1.82	3.02	-4.83	-0.06
12.00	0.76	1.06	29.71	2.02	-152.29	0.00	757.62	311.38	-0.12	2.62	3.02	-4.83	0.69
14.00	0.90	1.25	29.71	3.24	-207.27	0.00	757.62	311.38	-0.19	3.56	3.02	-4.83	1.56
16.00	1.04	1.45	29.71	4.91	-270.71	0.00	757.62	311.38	-0.29	4.65	3.02	-4.83	2.55
18.00	1.19	1.66	29.71	7.14	-342.60	0.00	757.62	311.38	-0.42	5.89	3.02	-4.83	3.66
20.00	1.37	1.90	29.71	10.10	-422.93	0.00	757.62	311.38	-0.60	7.27	3.02	-4.83	4.86
22.00	1.57	2.18	29.70	14.02	-511.70	0.00	757.62	311.38	-0.83	8.79	3.02	-4.83	6.16
24.00	1.81	2.52	29.70	19.28	-608.89	0.00	757.62	311.38	-1.14	10.46	3.02	-4.83	7.51
26.00	2.13	2.96	29.69	26.56	-714.47	0.00	757.62	311.38	-1.57	12.28	3.02	-4.83	8.90
28.00	2.56	3.56	29.68	37.04	-828.36	0.00	757.62	311.38	-2.19	14.23	3.02	-4.83	10.23
30.00	3.21	4.46	29.67	53.26	-950.38	0.00	757.62	311.38	-3.15	16.33	3.02	-4.83	11.37
32.00	4.31	5.98	29.63	81.33	-1079.96	0.00	757.62	311.38	-4.82	18.56	3.02	-4.83	11.93
34.00	6.61	9.17	29.52	140.68	-1214.50	0.00	757.62	311.38	-8.33	20.87	3.02	-4.83	10.73
36.00	13.43	18.50	28.90	318.36	-1333.21	0.00	757.62	311.38	-18.86	22.91	3.02	-4.83	2.25
38.00	29.58	39.32	25.84	753.81	-1328.22	0.00	757.62	311.38	-44.65	22.82	3.02	-4.83	-23.63
40.00	-35.81	-46.62	24.10	-990.20	-1372.26	0.00	757.62	311.38	58.65	23.58	3.02	-4.83	80.42
42.00	-4.50	-6.25	29.62	-146.34	-1859.92	0.00	757.62	311.38	8.67	31.96	3.02	-4.83	38.82
44.00	-3.03	-4.20	29.67	-108.06	-2044.72	0.00	757.62	311.38	6.40	35.13	3.02	-4.83	39.73
46.00	-2.24	-3.12	29.69	-87.67	-2236.23	-0.01	757.62	311.38	5.19	38.42	3.02	-4.83	41.81
48.00	-1.76	-2.45	29.70	-74.88	-2435.64	-0.01	757.62	311.38	4.44	41.85	3.02	-4.83	44.48
50.00	-1.43	-1.99	29.70	-66.07	-2643.26	-0.01	757.62	311.38	3.91	45.42	3.02	-4.83	47.53
52.00	-1.19	-1.66	29.71	-59.58	-2859.22	-0.01	757.62	311.38	3.53	49.13	3.02	-4.83	50.85
54.00	-1.01	-1.41	29.71	-54.57	-3083.58	-0.01	757.62	311.38	3.23	52.98	3.02	-4.83	54.41
56.00	-0.87	-1.21	29.71	-50.58	-3316.35	-0.01	757.62	311.38	3.00	56.98	3.02	-4.83	58.17
58.00	-0.76	-1.06	29.71	-47.29	-3557.56	-0.01	757.62	311.38	2.80	61.13	3.02	-4.83	62.12
60.00	-0.67	-0.93	29.71	-44.54	-3807.22	-0.01	757.62	311.38	2.64	65.42	3.02	-4.83	66.25

Case 1: I100A100

L (m)	β (°)	W (cm)	V (cm)	M_y (KNm)	M_z (KNm)	φ (°)	P_{max} (KN)	M_{Pmax} (KNm)	σ_{my} (Mpa)	σ_{mz} (Mpa)	σ_p (Mpa)	σ_{MP} (Mpa)	σ_t (Mpa)
10.00	0.56	0.85	18.72	1.14	-115.88	0.00	790.37	403.09	-0.07	1.44	2.88	-4.61	-0.35
12.00	0.68	1.03	18.72	1.98	-166.87	0.00	790.37	403.09	-0.12	2.08	2.88	-4.61	0.23
14.00	0.80	1.21	18.71	3.17	-227.12	0.00	790.37	403.09	-0.19	2.83	2.88	-4.61	0.91
16.00	0.93	1.41	18.71	4.79	-296.64	0.00	790.37	403.09	-0.28	3.69	2.88	-4.61	1.68
18.00	1.06	1.61	18.71	6.96	-375.41	0.00	790.37	403.09	-0.41	4.67	2.88	-4.61	2.53
20.00	1.22	1.85	18.71	9.84	-463.45	0.00	790.37	403.09	-0.58	5.77	2.88	-4.61	3.46
22.00	1.39	2.12	18.71	13.64	-560.73	0.00	790.37	403.09	-0.81	6.98	2.88	-4.61	4.44
24.00	1.61	2.44	18.71	18.73	-667.25	0.00	790.37	403.09	-1.11	8.30	2.88	-4.61	5.47
26.00	1.88	2.86	18.70	25.73	-782.98	0.00	790.37	403.09	-1.52	9.74	2.88	-4.61	6.49
28.00	2.25	3.42	18.70	35.75	-907.86	0.00	790.37	403.09	-2.11	11.29	2.88	-4.61	7.46
30.00	2.81	4.26	18.69	51.08	-1041.74	0.00	790.37	403.09	-3.01	12.96	2.88	-4.61	8.22
32.00	3.73	5.66	18.68	77.17	-1184.18	0.00	790.37	403.09	-4.56	14.73	2.88	-4.61	8.45
34.00	5.60	8.49	18.63	130.76	-1333.27	0.00	790.37	403.09	-7.72	16.59	2.88	-4.61	7.14
36.00	11.04	16.66	18.37	287.63	-1474.11	0.00	790.37	403.09	-16.98	18.34	2.88	-4.61	-0.37
38.00	26.71	39.11	16.72	752.21	-1494.84	0.00	790.37	403.09	-44.40	18.60	2.88	-4.61	-27.53
40.00	-33.75	-48.34	15.56	-1030.18	-1541.70	0.00	790.37	403.09	60.81	19.18	2.88	-4.61	78.26
42.00	-4.32	-6.55	18.66	-154.02	-2038.46	0.00	790.37	403.09	9.09	25.36	2.88	-4.61	32.72
44.00	-2.86	-4.33	18.69	-111.79	-2240.81	0.00	790.37	403.09	6.60	27.88	2.88	-4.61	32.75
46.00	-2.10	-3.19	18.70	-89.88	-2450.55	-0.01	790.37	403.09	5.31	30.48	2.88	-4.61	34.06
48.00	-1.64	-2.49	18.71	-76.37	-2668.97	-0.01	790.37	403.09	4.51	33.20	2.88	-4.61	35.98
50.00	-1.33	-2.02	18.71	-67.13	-2896.43	-0.01	790.37	403.09	3.96	36.03	2.88	-4.61	38.27
52.00	-1.10	-1.68	18.71	-60.39	-3133.04	-0.01	790.37	403.09	3.56	38.98	2.88	-4.61	40.81
54.00	-0.94	-1.42	18.71	-55.21	-3378.85	-0.01	790.37	403.09	3.26	42.03	2.88	-4.61	43.56
56.00	-0.81	-1.22	18.72	-51.10	-3633.90	-0.01	790.37	403.09	3.02	45.21	2.88	-4.61	46.49
58.00	-0.70	-1.07	18.72	-47.73	-3898.19	-0.01	790.37	403.09	2.82	48.49	2.88	-4.61	49.58
60.00	-0.62	-0.94	18.72	-44.91	-4171.73	-0.01	790.37	403.09	2.65	51.90	2.88	-4.61	52.82

Case 1: I120A100

L (m)	β (°)	W (cm)	V (cm)	M_y (KNm)	M_z (KNm)	φ (°)	P_{max} (KN)	M_{Pmax} (KNm)	σ_{my} (Mpa)	σ_{mz} (Mpa)	σ_p (Mpa)	σ_{MP} (Mpa)	σ_t (Mpa)
10.00	0.51	0.83	13.01	1.12	-126.01	0.00	807.34	491.67	-0.07	1.21	2.70	-4.38	-0.53
12.00	0.61	1.01	13.01	1.94	-181.45	0.00	807.34	491.67	-0.11	1.74	2.70	-4.38	-0.05
14.00	0.72	1.18	13.01	3.10	-246.97	0.00	807.34	491.67	-0.18	2.37	2.70	-4.38	0.51
16.00	0.83	1.37	13.01	4.70	-322.56	0.00	807.34	491.67	-0.28	3.09	2.70	-4.38	1.14
18.00	0.96	1.58	13.01	6.82	-408.23	0.00	807.34	491.67	-0.40	3.91	2.70	-4.38	1.84
20.00	1.09	1.80	13.01	9.63	-503.96	0.00	807.34	491.67	-0.57	4.83	2.70	-4.38	2.59
22.00	1.25	2.06	13.01	13.34	-609.76	0.00	807.34	491.67	-0.78	5.85	2.70	-4.38	3.39
24.00	1.44	2.38	13.00	18.29	-725.61	0.00	807.34	491.67	-1.08	6.96	2.70	-4.38	4.21
26.00	1.69	2.77	13.00	25.07	-851.48	0.00	807.34	491.67	-1.47	8.16	2.70	-4.38	5.01
28.00	2.01	3.31	13.00	34.72	-987.33	0.00	807.34	491.67	-2.04	9.47	2.70	-4.38	5.75
30.00	2.49	4.10	13.00	49.36	-1133.04	0.00	807.34	491.67	-2.90	10.86	2.70	-4.38	6.28
32.00	3.28	5.40	12.99	73.93	-1288.26	0.00	807.34	491.67	-4.35	12.35	2.70	-4.38	6.33
34.00	4.85	7.97	12.96	123.22	-1451.49	0.00	807.34	491.67	-7.25	13.92	2.70	-4.38	4.99
36.00	9.27	15.18	12.84	263.04	-1611.81	0.00	807.34	491.67	-15.47	15.46	2.70	-4.38	-1.70
38.00	24.09	38.49	11.87	742.79	-1661.12	0.00	807.34	491.67	-43.70	15.93	2.70	-4.38	-29.45
40.00	-31.87	-49.77	11.05	-1064.42	-1712.34	0.00	807.34	491.67	62.62	16.42	2.70	-4.38	77.36
42.00	-4.16	-6.84	12.97	-161.36	-2217.01	0.00	807.34	491.67	9.49	21.26	2.70	-4.38	29.07
44.00	-2.71	-4.45	12.99	-115.25	-2436.89	0.00	807.34	491.67	6.78	23.37	2.70	-4.38	28.47
46.00	-1.98	-3.25	13.00	-91.92	-2664.85	-0.01	807.34	491.67	5.41	25.55	2.70	-4.38	29.28
48.00	-1.53	-2.52	13.00	-77.72	-2902.30	-0.01	807.34	491.67	4.57	27.83	2.70	-4.38	30.73
50.00	-1.24	-2.04	13.00	-68.11	-3149.59	-0.01	807.34	491.67	4.01	30.20	2.70	-4.38	32.53
52.00	-1.03	-1.69	13.01	-61.13	-3406.85	-0.01	807.34	491.67	3.60	32.67	2.70	-4.38	34.59
54.00	-0.87	-1.43	13.01	-55.80	-3674.12	-0.01	807.34	491.67	3.28	35.23	2.70	-4.38	36.84
56.00	-0.75	-1.23	13.01	-51.58	-3951.44	-0.01	807.34	491.67	3.03	37.89	2.70	-4.38	39.25
58.00	-0.65	-1.07	13.01	-48.13	-4238.81	-0.01	807.34	491.67	2.83	40.65	2.70	-4.38	41.80
60.00	-0.57	-0.94	13.01	-45.25	-4536.25	-0.01	807.34	491.67	2.66	43.50	2.70	-4.38	44.48

Case 1: I120B120

L (m)	β (°)	W (cm)	V (cm)	M_y (KNm)	M_z (KNm)	φ (°)	P_{max} (KN)	M_{Pmax} (KNm)	σ_{my} (Mpa)	σ_{mz} (Mpa)	σ_p (Mpa)	σ_{MP} (Mpa)	σ_t (Mpa)
10.00	0.51	0.55	13.65	1.74	-195.28	0.00	1448.85	866.41	-0.05	1.29	3.13	-4.65	-0.28
12.00	0.62	0.67	13.65	3.03	-281.19	0.00	1448.85	866.41	-0.09	1.86	3.13	-4.65	0.25
14.00	0.72	0.78	13.65	4.83	-382.73	0.00	1448.85	866.41	-0.14	2.53	3.13	-4.65	0.87
16.00	0.83	0.90	13.65	7.28	-499.88	0.00	1448.85	866.41	-0.22	3.31	3.13	-4.65	1.57
18.00	0.95	1.03	13.65	10.50	-632.63	0.00	1448.85	866.41	-0.31	4.19	3.13	-4.65	2.35
20.00	1.08	1.16	13.65	14.67	-781.00	0.00	1448.85	866.41	-0.44	5.17	3.13	-4.65	3.21
22.00	1.21	1.31	13.65	20.03	-944.96	0.00	1448.85	866.41	-0.60	6.25	3.13	-4.65	4.14
24.00	1.37	1.48	13.64	26.92	-1124.52	0.00	1448.85	866.41	-0.81	7.44	3.13	-4.65	5.12
26.00	1.56	1.68	13.64	35.85	-1319.64	0.00	1448.85	866.41	-1.07	8.73	3.13	-4.65	6.14
28.00	1.78	1.93	13.64	47.61	-1530.29	0.00	1448.85	866.41	-1.43	10.12	3.13	-4.65	7.18
30.00	2.07	2.24	13.64	63.54	-1756.41	0.00	1448.85	866.41	-1.90	11.62	3.13	-4.65	8.20
32.00	2.47	2.67	13.64	86.05	-1997.86	0.00	1448.85	866.41	-2.58	13.22	3.13	-4.65	9.12
34.00	3.05	3.29	13.63	119.96	-2254.30	0.00	1448.85	866.41	-3.59	14.91	3.13	-4.65	9.81
36.00	4.00	4.32	13.62	176.39	-2524.73	0.00	1448.85	866.41	-5.28	16.70	3.13	-4.65	9.91
38.00	5.85	6.32	13.58	287.54	-2805.21	0.00	1448.85	866.41	-8.61	18.56	3.13	-4.65	8.43
40.00	10.74	11.55	13.41	582.27	-3069.82	0.00	1448.85	866.41	-17.43	20.31	3.13	-4.65	1.36
42.00	24.18	25.37	12.45	1410.80	-3142.68	0.00	1448.85	866.41	-42.23	20.79	3.13	-4.65	-22.96
44.00	-27.23	-28.35	12.14	-1730.06	-3361.65	0.00	1448.85	866.41	51.79	22.24	3.13	-4.65	72.51
46.00	-5.32	-5.75	13.59	-383.48	-4114.39	0.00	1448.85	866.41	11.48	27.22	3.13	-4.65	37.18
48.00	-3.44	-3.72	13.62	-270.04	-4491.25	0.00	1448.85	866.41	8.08	29.71	3.13	-4.65	36.28
50.00	-2.51	-2.71	13.64	-213.73	-4877.43	0.00	1448.85	866.41	6.40	32.27	3.13	-4.65	37.15
52.00	-1.95	-2.11	13.64	-179.77	-5277.43	0.00	1448.85	866.41	5.38	34.91	3.13	-4.65	38.78
54.00	-1.58	-1.71	13.64	-156.92	-5692.33	0.00	1448.85	866.41	4.70	37.66	3.13	-4.65	40.84
56.00	-1.31	-1.42	13.64	-140.41	-6122.51	0.00	1448.85	866.41	4.20	40.50	3.13	-4.65	43.19
58.00	-1.12	-1.21	13.65	-127.87	-6568.13	0.00	1448.85	866.41	3.83	43.45	3.13	-4.65	45.76
60.00	-0.96	-1.04	13.65	-117.97	-7029.25	0.00	1448.85	866.41	3.53	46.50	3.13	-4.65	48.52

Case 1: I140B120

L (m)	β (°)	W (cm)	V (cm)	M_y (KNm)	M_z (KNm)	φ (°)	P_{max} (KN)	M_{Pmax} (KNm)	σ_{my} (Mpa)	σ_{mz} (Mpa)	σ_p (Mpa)	σ_{MP} (Mpa)	σ_t (Mpa)
10.00	0.47	0.54	9.86	1.70	-207.93	0.00	1481.75	1026.85	-0.05	1.10	3.01	-4.46	-0.41
12.00	0.56	0.65	9.86	2.94	-299.42	0.00	1481.75	1026.85	-0.09	1.58	3.01	-4.46	0.03
14.00	0.66	0.76	9.86	4.70	-407.54	0.00	1481.75	1026.85	-0.14	2.15	3.01	-4.46	0.55
16.00	0.76	0.87	9.86	7.07	-532.28	0.00	1481.75	1026.85	-0.21	2.81	3.01	-4.46	1.14
18.00	0.87	1.00	9.86	10.20	-673.65	0.00	1481.75	1026.85	-0.30	3.55	3.01	-4.46	1.79
20.00	0.98	1.13	9.86	14.24	-831.64	0.00	1481.75	1026.85	-0.43	4.38	3.01	-4.46	2.50
22.00	1.11	1.27	9.86	19.43	-1006.25	0.00	1481.75	1026.85	-0.58	5.30	3.01	-4.46	3.27
24.00	1.25	1.43	9.86	26.08	-1197.45	0.00	1481.75	1026.85	-0.78	6.31	3.01	-4.46	4.08
26.00	1.41	1.62	9.86	34.67	-1405.25	0.00	1481.75	1026.85	-1.04	7.41	3.01	-4.46	4.92
28.00	1.61	1.85	9.86	45.95	-1629.61	0.00	1481.75	1026.85	-1.37	8.59	3.01	-4.46	5.76
30.00	1.87	2.15	9.86	61.13	-1870.47	0.00	1481.75	1026.85	-1.82	9.86	3.01	-4.46	6.58
32.00	2.22	2.55	9.85	82.40	-2127.72	0.00	1481.75	1026.85	-2.46	11.22	3.01	-4.46	7.30
34.00	2.72	3.12	9.85	114.06	-2401.09	0.00	1481.75	1026.85	-3.40	12.66	3.01	-4.46	7.79
36.00	3.53	4.05	9.84	165.74	-2689.81	0.00	1481.75	1026.85	-4.95	14.18	3.01	-4.46	7.77
38.00	5.05	5.79	9.82	264.30	-2991.01	0.00	1481.75	1026.85	-7.89	15.77	3.01	-4.46	6.42
40.00	8.88	10.16	9.74	513.74	-3287.15	0.00	1481.75	1026.85	-15.34	17.33	3.01	-4.46	0.53
42.00	20.86	23.42	9.22	1306.00	-3427.70	0.00	1481.75	1026.85	-38.99	18.07	3.01	-4.46	-22.38
44.00	-179.06	-1.08	-9.86	-66.28	4025.19	0.00	1481.75	1026.85	1.98	-21.22	3.01	-4.46	-20.70
46.00	-5.40	-6.19	9.82	-414.29	-4380.48	0.00	1481.75	1026.85	12.37	23.09	3.01	-4.46	34.00
48.00	-3.39	-3.89	9.84	-283.29	-4782.57	0.00	1481.75	1026.85	8.46	25.21	3.01	-4.46	32.21
50.00	-2.44	-2.80	9.85	-221.16	-5193.81	0.00	1481.75	1026.85	6.60	27.38	3.01	-4.46	32.52
52.00	-1.88	-2.16	9.86	-184.53	-5619.69	0.00	1481.75	1026.85	5.51	29.62	3.01	-4.46	33.67
54.00	-1.51	-1.74	9.86	-160.24	-6061.43	0.00	1481.75	1026.85	4.78	31.95	3.01	-4.46	35.28
56.00	-1.26	-1.44	9.86	-142.87	-6519.46	0.00	1481.75	1026.85	4.26	34.36	3.01	-4.46	37.17
58.00	-1.06	-1.22	9.86	-129.76	-6993.92	0.00	1481.75	1026.85	3.87	36.87	3.01	-4.46	39.28
60.00	-0.91	-1.05	9.86	-119.48	-7484.91	0.00	1481.75	1026.85	3.57	39.45	3.01	-4.46	41.56

Case 1: I160B120

L (m)	β (°)	W (cm)	V (cm)	M_y (KNm)	M_z (KNm)	φ (°)	P_{max} (KN)	M_{Pmax} (KNm)	σ_{my} (Mpa)	σ_{mz} (Mpa)	σ_p (Mpa)	σ_{MP} (Mpa)	σ_t (Mpa)
10.00	0.43	0.52	7.50	1.65	-220.55	0.00	1502.42	1185.41	-0.05	0.96	2.87	-4.30	-0.52
12.00	0.52	0.63	7.50	2.87	-317.59	0.00	1502.42	1185.41	-0.09	1.38	2.87	-4.30	-0.14
14.00	0.61	0.74	7.50	4.58	-432.26	0.00	1502.42	1185.41	-0.14	1.87	2.87	-4.30	0.31
16.00	0.70	0.85	7.50	6.89	-564.58	0.00	1502.42	1185.41	-0.21	2.45	2.87	-4.30	0.81
18.00	0.80	0.97	7.50	9.93	-714.53	0.00	1502.42	1185.41	-0.30	3.10	2.87	-4.30	1.37
20.00	0.90	1.09	7.50	13.86	-882.11	0.00	1502.42	1185.41	-0.41	3.82	2.87	-4.30	1.98
22.00	1.01	1.23	7.50	18.90	-1067.32	0.00	1502.42	1185.41	-0.56	4.63	2.87	-4.30	2.64
24.00	1.14	1.39	7.50	25.35	-1270.14	0.00	1502.42	1185.41	-0.75	5.50	2.87	-4.30	3.32
26.00	1.29	1.57	7.50	33.65	-1490.57	0.00	1502.42	1185.41	-1.00	6.46	2.87	-4.30	4.03
28.00	1.47	1.79	7.50	44.51	-1728.58	0.00	1502.42	1185.41	-1.32	7.49	2.87	-4.30	4.74
30.00	1.70	2.07	7.49	59.05	-1984.11	0.00	1502.42	1185.41	-1.76	8.60	2.87	-4.30	5.41
32.00	2.01	2.44	7.49	79.29	-2257.09	0.00	1502.42	1185.41	-2.36	9.78	2.87	-4.30	5.99
34.00	2.45	2.98	7.49	109.08	-2547.28	0.00	1502.42	1185.41	-3.25	11.04	2.87	-4.30	6.36
36.00	3.15	3.82	7.49	156.92	-2854.08	0.00	1502.42	1185.41	-4.67	12.37	2.87	-4.30	6.27
38.00	4.42	5.37	7.48	245.68	-3175.32	0.00	1502.42	1185.41	-7.31	13.76	2.87	-4.30	5.02
40.00	7.49	9.07	7.43	460.13	-3498.75	0.00	1502.42	1185.41	-13.70	15.16	2.87	-4.30	0.04
42.00	17.77	21.24	7.14	1187.33	-3704.98	0.00	1502.42	1185.41	-35.34	16.06	2.87	-4.30	-20.72
44.00	540.88	-1.07	-7.50	-65.60	4269.43	0.00	1502.42	1185.41	1.95	-18.50	2.87	-4.30	-17.98
46.00	-5.51	-6.68	7.46	-447.91	-4645.39	0.00	1502.42	1185.41	13.33	20.13	2.87	-4.30	32.04
48.00	-3.35	-4.07	7.49	-296.90	-5072.90	0.00	1502.42	1185.41	8.84	21.98	2.87	-4.30	29.40
50.00	-2.38	-2.88	7.49	-228.59	-5509.13	0.00	1502.42	1185.41	6.80	23.88	2.87	-4.30	29.25
52.00	-1.82	-2.21	7.49	-189.23	-5960.80	0.00	1502.42	1185.41	5.63	25.83	2.87	-4.30	30.04
54.00	-1.46	-1.77	7.50	-163.49	-6429.30	0.00	1502.42	1185.41	4.87	27.86	2.87	-4.30	31.30
56.00	-1.20	-1.46	7.50	-145.26	-6915.07	0.00	1502.42	1185.41	4.32	29.97	2.87	-4.30	32.87
58.00	-1.02	-1.23	7.50	-131.60	-7418.29	0.00	1502.42	1185.41	3.92	32.15	2.87	-4.30	34.64
60.00	-0.87	-1.06	7.50	-120.94	-7939.05	0.00	1502.42	1185.41	3.60	34.41	2.87	-4.30	36.58

Case 1: I180B120

L (m)	β (°)	W (cm)	V (cm)	M_y (KNm)	M_z (KNm)	φ (°)	P_{max} (KN)	M_{Pmax} (KNm)	σ_{my} (Mpa)	σ_{mz} (Mpa)	σ_p (Mpa)	σ_{MP} (Mpa)	σ_t (Mpa)
10.00	0.40	0.51	5.92	1.62	-233.25	0.00	1514.27	1341.64	-0.05	0.85	2.74	-4.15	-0.61
12.00	0.48	0.61	5.92	2.80	-335.87	0.00	1514.27	1341.64	-0.08	1.23	2.74	-4.15	-0.27
14.00	0.56	0.72	5.92	4.47	-457.15	0.00	1514.27	1341.64	-0.13	1.67	2.74	-4.15	0.12
16.00	0.65	0.83	5.92	6.73	-597.09	0.00	1514.27	1341.64	-0.20	2.18	2.74	-4.15	0.56
18.00	0.74	0.94	5.92	9.70	-755.68	0.00	1514.27	1341.64	-0.29	2.76	2.74	-4.15	1.05
20.00	0.83	1.06	5.92	13.54	-932.91	0.00	1514.27	1341.64	-0.40	3.40	2.74	-4.15	1.58
22.00	0.94	1.20	5.92	18.45	-1128.79	0.00	1514.27	1341.64	-0.55	4.12	2.74	-4.15	2.15
24.00	1.05	1.35	5.92	24.72	-1343.31	0.00	1514.27	1341.64	-0.73	4.90	2.74	-4.15	2.75
26.00	1.19	1.53	5.92	32.78	-1576.45	0.00	1514.27	1341.64	-0.97	5.75	2.74	-4.15	3.36
28.00	1.36	1.74	5.92	43.28	-1828.19	0.00	1514.27	1341.64	-1.28	6.67	2.74	-4.15	3.97
30.00	1.56	2.00	5.92	57.28	-2098.50	0.00	1514.27	1341.64	-1.70	7.65	2.74	-4.15	4.54
32.00	1.84	2.35	5.92	76.65	-2387.28	0.00	1514.27	1341.64	-2.28	8.71	2.74	-4.15	5.02
34.00	2.23	2.85	5.92	104.89	-2694.36	0.00	1514.27	1341.64	-3.11	9.83	2.74	-4.15	5.30
36.00	2.84	3.63	5.91	149.64	-3019.25	0.00	1514.27	1341.64	-4.44	11.01	2.74	-4.15	5.15
38.00	3.93	5.03	5.91	230.72	-3360.26	0.00	1514.27	1341.64	-6.85	12.26	2.74	-4.15	3.99
40.00	6.44	8.23	5.88	418.60	-3708.50	0.00	1514.27	1341.64	-12.43	13.53	2.74	-4.15	-0.32
42.00	15.04	19.04	5.72	1067.77	-3973.62	0.00	1514.27	1341.64	-31.70	14.49	2.74	-4.15	-18.62
44.00	180.82	-1.06	-5.92	-65.01	4515.31	0.00	1514.27	1341.64	1.93	-16.47	2.74	-4.15	-15.96
46.00	-5.63	-7.20	5.89	-484.14	-4911.83	0.00	1514.27	1341.64	14.37	17.92	2.74	-4.15	30.87
48.00	-3.31	-4.24	5.91	-310.65	-5365.16	0.00	1514.27	1341.64	9.22	19.57	2.74	-4.15	27.38
50.00	-2.32	-2.97	5.92	-235.90	-5826.55	0.00	1514.27	1341.64	7.00	21.25	2.74	-4.15	26.84
52.00	-1.76	-2.25	5.92	-193.80	-6304.18	0.00	1514.27	1341.64	5.75	22.99	2.74	-4.15	27.33
54.00	-1.40	-1.80	5.92	-166.63	-6799.62	0.00	1514.27	1341.64	4.95	24.80	2.74	-4.15	28.33
56.00	-1.16	-1.48	5.92	-147.56	-7313.33	0.00	1514.27	1341.64	4.38	26.68	2.74	-4.15	29.64
58.00	-0.97	-1.25	5.92	-133.36	-7845.50	0.00	1514.27	1341.64	3.96	28.62	2.74	-4.15	31.16
60.00	-0.83	-1.07	5.92	-122.34	-8396.22	0.00	1514.27	1341.64	3.63	30.63	2.74	-4.15	32.84

Case 1: I200B120

L (m)	β (°)	W (cm)	V (cm)	M_y (KNm)	M_z (KNm)	φ (°)	P_{max} (KN)	M_{Pmax} (KNm)	σ_{my} (Mpa)	σ_{mz} (Mpa)	σ_p (Mpa)	σ_{MP} (Mpa)	σ_t (Mpa)
10.00	0.37	0.50	4.81	1.59	-245.90	0.00	1523.65	1496.22	-0.05	0.77	2.61	-4.01	-0.68
12.00	0.44	0.60	4.81	2.75	-354.10	0.00	1523.65	1496.22	-0.08	1.11	2.61	-4.01	-0.37
14.00	0.52	0.70	4.81	4.39	-481.96	0.00	1523.65	1496.22	-0.13	1.51	2.61	-4.01	-0.02
16.00	0.60	0.81	4.81	6.60	-629.49	0.00	1523.65	1496.22	-0.20	1.97	2.61	-4.01	0.38
18.00	0.68	0.92	4.81	9.51	-796.69	0.00	1523.65	1496.22	-0.28	2.50	2.61	-4.01	0.81
20.00	0.77	1.04	4.81	13.27	-983.55	0.00	1523.65	1496.22	-0.39	3.08	2.61	-4.01	1.29
22.00	0.87	1.17	4.81	18.07	-1190.06	0.00	1523.65	1496.22	-0.54	3.73	2.61	-4.01	1.79
24.00	0.98	1.32	4.81	24.19	-1416.23	0.00	1523.65	1496.22	-0.72	4.44	2.61	-4.01	2.32
26.00	1.10	1.49	4.81	32.05	-1662.04	0.00	1523.65	1496.22	-0.95	5.21	2.61	-4.01	2.86
28.00	1.26	1.69	4.81	42.26	-1927.46	0.00	1523.65	1496.22	-1.25	6.04	2.61	-4.01	3.39
30.00	1.45	1.95	4.81	55.82	-2212.48	0.00	1523.65	1496.22	-1.65	6.93	2.61	-4.01	3.88
32.00	1.70	2.28	4.81	74.48	-2517.01	0.00	1523.65	1496.22	-2.21	7.88	2.61	-4.01	4.28
34.00	2.05	2.76	4.81	101.51	-2840.90	0.00	1523.65	1496.22	-3.01	8.90	2.61	-4.01	4.49
36.00	2.59	3.48	4.81	143.82	-3183.74	0.00	1523.65	1496.22	-4.26	9.97	2.61	-4.01	4.31
38.00	3.54	4.76	4.80	219.07	-3544.16	0.00	1523.65	1496.22	-6.49	11.10	2.61	-4.01	3.21
40.00	5.65	7.60	4.79	387.53	-3915.42	0.00	1523.65	1496.22	-11.48	12.26	2.61	-4.01	-0.61
42.00	12.83	17.14	4.69	963.21	-4229.55	0.00	1523.65	1496.22	-28.53	13.25	2.61	-4.01	-16.68
44.00	29.30	37.77	4.20	2329.57	-4151.91	0.00	1523.65	1496.22	-68.99	13.00	2.61	-4.01	-57.39
46.00	5580.74	-0.99	-4.81	-66.91	5203.01	0.00	1523.65	1496.22	1.98	-16.30	2.61	-4.01	-15.71
48.00	-3.27	-4.41	4.81	-323.65	-5656.50	0.00	1523.65	1496.22	9.59	17.72	2.61	-4.01	25.90
50.00	-2.26	-3.05	4.81	-242.63	-6142.94	0.00	1523.65	1496.22	7.19	19.24	2.61	-4.01	25.03
52.00	-1.71	-2.30	4.81	-197.93	-6646.44	0.00	1523.65	1496.22	5.86	20.82	2.61	-4.01	25.28
54.00	-1.35	-1.82	4.81	-169.44	-7168.71	0.00	1523.65	1496.22	5.02	22.45	2.61	-4.01	26.07
56.00	-1.11	-1.50	4.81	-149.60	-7710.26	0.00	1523.65	1496.22	4.43	24.15	2.61	-4.01	27.18
58.00	-0.93	-1.26	4.81	-134.92	-8271.28	0.00	1523.65	1496.22	4.00	25.91	2.61	-4.01	28.50
60.00	-0.80	-1.08	4.81	-123.57	-8851.87	0.00	1523.65	1496.22	3.66	27.72	2.61	-4.01	29.98

Case 1: A110B

L (m)	β (°)	W (cm)	V (cm)	M_y (KNm)	M_z (KNm)	φ (°)	P_{max} (KN)	M_{Pmax} (KNm)	σ_{my} (Mpa)	σ_{mz} (Mpa)	σ_p (Mpa)	σ_{MP} (Mpa)	σ_t (Mpa)
10.00	0.63	0.04	19.07	3.81	-347.43	0.00	2775.15	1137.81	-0.01	2.07	3.37	-2.92	2.51
12.00	0.75	0.04	19.07	6.59	-500.29	0.00	2775.15	1137.81	-0.02	2.98	3.37	-2.92	3.41
14.00	0.88	0.05	19.07	10.47	-680.93	0.00	2775.15	1137.81	-0.03	4.06	3.37	-2.92	4.48
16.00	1.01	0.06	19.07	15.64	-889.34	0.00	2775.15	1137.81	-0.04	5.30	3.37	-2.92	5.71
18.00	1.13	0.07	19.07	22.28	-1125.53	0.00	2775.15	1137.81	-0.05	6.70	3.37	-2.92	7.10
20.00	1.26	0.07	19.07	30.60	-1389.48	0.00	2775.15	1137.81	-0.07	8.27	3.37	-2.92	8.65
22.00	1.39	0.08	19.07	40.80	-1681.18	0.00	2775.15	1137.81	-0.10	10.01	3.37	-2.92	10.36
24.00	1.52	0.09	19.06	53.07	-2000.63	0.00	2775.15	1137.81	-0.13	11.91	3.37	-2.92	12.24
26.00	1.65	0.10	19.06	67.66	-2347.81	0.00	2775.15	1137.81	-0.16	13.98	3.37	-2.92	14.27
28.00	1.78	0.11	19.06	84.79	-2722.72	0.00	2775.15	1137.81	-0.20	16.21	3.37	-2.92	16.46
30.00	1.92	0.11	19.06	104.73	-3125.33	0.00	2775.15	1137.81	-0.25	18.61	3.37	-2.92	18.81
32.00	2.06	0.12	19.06	127.76	-3555.63	0.00	2775.15	1137.81	-0.31	21.18	3.37	-2.92	21.32
34.00	2.20	0.13	19.06	154.22	-4013.60	0.00	2775.15	1137.81	-0.37	23.90	3.37	-2.92	23.98
36.00	2.35	0.14	19.06	184.46	-4499.22	0.00	2775.15	1137.81	-0.44	26.79	3.37	-2.92	26.80
38.00	2.50	0.15	19.05	218.91	-5012.45	0.00	2775.15	1137.81	-0.53	29.85	3.37	-2.92	29.77
40.00	2.66	0.16	19.05	258.08	-5553.27	0.00	2775.15	1137.81	-0.62	33.07	3.37	-2.92	32.90
42.00	2.83	0.17	19.05	302.54	-6121.61	0.00	2775.15	1137.81	-0.73	36.46	3.37	-2.92	36.18
44.00	3.01	0.18	19.05	353.00	-6717.44	0.00	2775.15	1137.81	-0.85	40.01	3.37	-2.92	39.61
46.00	3.20	0.19	19.04	410.33	-7340.66	0.00	2775.15	1137.81	-0.98	43.72	3.37	-2.92	43.18
48.00	3.41	0.20	19.04	475.58	-7991.20	0.00	2775.15	1137.81	-1.14	47.59	3.37	-2.92	46.90
50.00	3.63	0.21	19.03	550.06	-8668.91	0.00	2775.15	1137.81	-1.32	51.63	3.37	-2.92	50.76
52.00	3.88	0.23	19.03	635.41	-9373.64	0.00	2775.15	1137.81	-1.52	55.82	3.37	-2.92	54.75
54.00	4.15	0.24	19.02	733.76	-10105.15	0.00	2775.15	1137.81	-1.76	60.18	3.37	-2.92	58.87
56.00	4.46	0.26	19.01	847.84	-10863.11	0.00	2775.15	1137.81	-2.03	64.69	3.37	-2.92	63.11
58.00	4.82	0.28	19.00	981.27	-11647.08	0.00	2775.15	1137.81	-2.35	69.36	3.37	-2.92	67.46
60.00	5.22	0.31	18.99	1138.91	-12456.38	0.00	2775.15	1137.81	-2.73	74.18	3.37	-2.92	71.90

Case 1: A140B

L (m)	β (°)	W (cm)	V (cm)	M_y (KNm)	M_z (KNm)	φ (°)	P_{max} (KN)	M_{Pmax} (KNm)	σ_{my} (Mpa)	σ_{mz} (Mpa)	σ_p (Mpa)	σ_{MP} (Mpa)	σ_t (Mpa)
10.00	0.54	0.03	11.39	3.76	-396.50	0.00	2621.10	1407.53	-0.01	1.55	2.79	-2.70	1.63
12.00	0.65	0.04	11.39	6.50	-570.95	0.00	2621.10	1407.53	-0.01	2.22	2.79	-2.70	2.30
14.00	0.76	0.04	11.39	10.33	-777.11	0.00	2621.10	1407.53	-0.02	3.03	2.79	-2.70	3.10
16.00	0.87	0.05	11.39	15.42	-1014.97	0.00	2621.10	1407.53	-0.03	3.96	2.79	-2.70	4.01
18.00	0.98	0.05	11.39	21.97	-1284.53	0.00	2621.10	1407.53	-0.04	5.01	2.79	-2.70	5.05
20.00	1.09	0.06	11.39	30.17	-1585.78	0.00	2621.10	1407.53	-0.06	6.18	2.79	-2.70	6.21
22.00	1.20	0.06	11.39	40.21	-1918.72	0.00	2621.10	1407.53	-0.08	7.48	2.79	-2.70	7.49
24.00	1.31	0.07	11.39	52.28	-2283.34	0.00	2621.10	1407.53	-0.11	8.90	2.79	-2.70	8.88
26.00	1.42	0.08	11.38	66.62	-2679.63	0.00	2621.10	1407.53	-0.13	10.44	2.79	-2.70	10.40
28.00	1.54	0.08	11.38	83.43	-3107.58	0.00	2621.10	1407.53	-0.17	12.11	2.79	-2.70	12.03
30.00	1.65	0.09	11.38	102.96	-3567.17	0.00	2621.10	1407.53	-0.21	13.90	2.79	-2.70	13.78
32.00	1.77	0.10	11.38	125.46	-4058.40	0.00	2621.10	1407.53	-0.25	15.82	2.79	-2.70	15.65
34.00	1.89	0.10	11.38	151.24	-4581.25	0.00	2621.10	1407.53	-0.31	17.85	2.79	-2.70	17.64
36.00	2.01	0.11	11.38	180.61	-5135.69	0.00	2621.10	1407.53	-0.37	20.01	2.79	-2.70	19.74
38.00	2.14	0.12	11.38	213.93	-5721.71	0.00	2621.10	1407.53	-0.43	22.30	2.79	-2.70	21.96
40.00	2.27	0.12	11.38	251.63	-6339.29	0.00	2621.10	1407.53	-0.51	24.70	2.79	-2.70	24.29
42.00	2.41	0.13	11.38	294.19	-6988.38	0.00	2621.10	1407.53	-0.60	27.23	2.79	-2.70	26.73
44.00	2.55	0.14	11.38	342.16	-7668.95	0.00	2621.10	1407.53	-0.69	29.89	2.79	-2.70	29.28
46.00	2.71	0.15	11.38	396.24	-8380.95	0.00	2621.10	1407.53	-0.80	32.66	2.79	-2.70	31.95
48.00	2.87	0.16	11.37	457.21	-9124.32	0.00	2621.10	1407.53	-0.93	35.56	2.79	-2.70	34.72
50.00	3.04	0.16	11.37	526.06	-9898.97	0.00	2621.10	1407.53	-1.06	38.58	2.79	-2.70	37.60
52.00	3.23	0.17	11.37	603.97	-10704.81	0.00	2621.10	1407.53	-1.22	41.72	2.79	-2.70	40.58
54.00	3.43	0.19	11.37	692.43	-11541.70	0.00	2621.10	1407.53	-1.40	44.98	2.79	-2.70	43.67
56.00	3.66	0.20	11.36	793.28	-12409.46	0.00	2621.10	1407.53	-1.61	48.36	2.79	-2.70	46.84
58.00	3.91	0.21	11.36	908.88	-13307.85	0.00	2621.10	1407.53	-1.84	51.86	2.79	-2.70	50.11
60.00	4.19	0.23	11.36	1042.25	-14236.53	0.00	2621.10	1407.53	-2.11	55.48	2.79	-2.70	53.46

Case 1: A170B

L (m)	β (°)	W (cm)	V (cm)	M_y (KNm)	M_z (KNm)	φ (°)	P_{max} (KN)	M_{Pmax} (KNm)	σ_{my} (Mpa)	σ_{mz} (Mpa)	σ_p (Mpa)	σ_{MP} (Mpa)	σ_t (Mpa)
10.00	0.48	0.02	7.59	3.65	-436.88	0.00	2607.93	298.59	-0.01	1.24	2.52	-2.60	1.15
12.00	0.58	0.03	7.59	6.31	-629.09	0.00	2607.93	429.97	-0.01	1.78	2.52	-2.60	1.69
14.00	0.67	0.03	7.59	10.03	-856.25	0.00	2607.93	585.24	-0.02	2.42	2.52	-2.60	2.33
16.00	0.77	0.04	7.59	14.98	-1118.34	0.00	2607.93	764.39	-0.03	3.17	2.52	-2.60	3.06
18.00	0.86	0.04	7.59	21.33	-1415.36	0.00	2607.93	967.43	-0.04	4.01	2.52	-2.60	3.89
20.00	0.96	0.05	7.59	29.29	-1747.32	0.00	2607.93	1194.36	-0.05	4.95	2.52	-2.60	4.82
22.00	1.06	0.05	7.59	39.02	-2114.19	0.00	2607.93	1445.18	-0.07	5.99	2.52	-2.60	5.84
24.00	1.15	0.06	7.59	50.72	-2515.98	0.00	2607.93	1719.88	-0.09	7.12	2.52	-2.60	6.96
26.00	1.25	0.06	7.59	64.60	-2952.67	0.00	2607.93	2018.48	-0.11	8.36	2.52	-2.60	8.17
28.00	1.35	0.07	7.59	80.86	-3424.27	0.00	2607.93	2340.95	-0.14	9.70	2.52	-2.60	9.48
30.00	1.45	0.07	7.59	99.72	-3930.75	0.00	2607.93	2687.32	-0.17	11.13	2.52	-2.60	10.88
32.00	1.56	0.08	7.59	121.42	-4472.11	0.00	2607.93	3057.57	-0.21	12.66	2.52	-2.60	12.37
34.00	1.66	0.08	7.59	146.21	-5048.34	0.00	2607.93	3451.71	-0.25	14.30	2.52	-2.60	13.96
36.00	1.76	0.09	7.59	174.39	-5659.42	0.00	2607.93	3869.74	-0.30	16.03	2.52	-2.60	15.64
38.00	1.87	0.09	7.58	206.27	-6305.33	0.00	2607.93	4311.65	-0.36	17.86	2.52	-2.60	17.42
40.00	1.99	0.10	7.58	242.19	-6986.05	0.00	2607.93	4777.46	-0.42	19.78	2.52	-2.60	19.28
42.00	2.10	0.10	7.58	282.56	-7701.57	0.00	2607.93	5267.15	-0.49	21.81	2.52	-2.60	21.24
44.00	2.22	0.11	7.58	327.85	-8451.85	0.00	2607.93	5780.72	-0.57	23.93	2.52	-2.60	23.28
46.00	2.35	0.12	7.58	378.58	-9236.85	0.00	2607.93	6318.19	-0.66	26.16	2.52	-2.60	25.42
48.00	2.48	0.12	7.58	435.39	-10056.54	0.00	2607.93	6879.54	-0.76	28.48	2.52	-2.60	27.64
50.00	2.62	0.13	7.58	499.01	-10910.86	0.00	2607.93	7464.78	-0.87	30.90	2.52	-2.60	29.95
52.00	2.77	0.14	7.58	570.34	-11799.75	0.00	2607.93	8073.90	-0.99	33.41	2.52	-2.60	32.34
54.00	2.93	0.14	7.58	650.44	-12723.12	0.00	2607.93	8706.91	-1.13	36.03	2.52	-2.60	34.82
56.00	3.10	0.15	7.58	740.62	-13680.86	0.00	2607.93	9363.81	-1.29	38.74	2.52	-2.60	37.37
58.00	3.29	0.16	7.58	842.47	-14672.84	0.00	2607.93	10044.60	-1.47	41.55	2.52	-2.60	40.00
60.00	3.49	0.17	7.57	958.00	-15698.86	0.00	2607.93	10749.28	-1.67	44.46	2.52	-2.60	42.71

Case 1: A200B

L (m)	β (°)	W (cm)	V (cm)	M_y (KNm)	M_z (KNm)	φ (°)	P_{max} (KN)	M_{Pmax} (KNm)	σ_{my} (Mpa)	σ_{mz} (Mpa)	σ_p (Mpa)	σ_{MP} (Mpa)	σ_t (Mpa)
10.00	0.43	0.02	5.45	3.58	-474.85	0.00	2666.15	2079.59	-0.01	1.04	2.37	-2.50	0.90
12.00	0.52	0.02	5.45	6.18	-683.77	0.00	2666.15	2079.59	-0.01	1.50	2.37	-2.50	1.36
14.00	0.60	0.03	5.45	9.82	-930.67	0.00	2666.15	2079.59	-0.01	2.05	2.37	-2.50	1.90
16.00	0.69	0.03	5.45	14.66	-1215.55	0.00	2666.15	2079.59	-0.02	2.67	2.37	-2.50	2.52
18.00	0.78	0.03	5.45	20.88	-1538.40	0.00	2666.15	2079.59	-0.03	3.39	2.37	-2.50	3.22
20.00	0.86	0.04	5.45	28.67	-1899.22	0.00	2666.15	2079.59	-0.04	4.18	2.37	-2.50	4.00
22.00	0.95	0.04	5.45	38.18	-2298.00	0.00	2666.15	2079.59	-0.06	5.06	2.37	-2.50	4.86
24.00	1.04	0.05	5.45	49.63	-2734.74	0.00	2666.15	2079.59	-0.07	6.02	2.37	-2.50	5.81
26.00	1.13	0.05	5.45	63.18	-3209.43	0.00	2666.15	2079.59	-0.09	7.06	2.37	-2.50	6.83
28.00	1.22	0.05	5.45	79.05	-3722.06	0.00	2666.15	2079.59	-0.12	8.19	2.37	-2.50	7.94
30.00	1.31	0.06	5.45	97.45	-4272.62	0.00	2666.15	2079.59	-0.14	9.40	2.37	-2.50	9.12
32.00	1.40	0.06	5.45	118.58	-4861.11	0.00	2666.15	2079.59	-0.18	10.70	2.37	-2.50	10.39
34.00	1.49	0.07	5.45	142.69	-5487.52	0.00	2666.15	2079.59	-0.21	12.07	2.37	-2.50	11.73
36.00	1.58	0.07	5.45	170.05	-6151.82	0.00	2666.15	2079.59	-0.25	13.54	2.37	-2.50	13.15
38.00	1.68	0.07	5.45	200.92	-6854.02	0.00	2666.15	2079.59	-0.30	15.08	2.37	-2.50	14.65
40.00	1.78	0.08	5.45	235.62	-7594.09	0.00	2666.15	2079.59	-0.35	16.71	2.37	-2.50	16.23
42.00	1.88	0.08	5.45	274.49	-8372.02	0.00	2666.15	2079.59	-0.41	18.42	2.37	-2.50	17.88
44.00	1.98	0.09	5.45	317.95	-9187.77	0.00	2666.15	2079.59	-0.47	20.22	2.37	-2.50	19.61
46.00	2.09	0.09	5.44	366.42	-10041.34	0.00	2666.15	2079.59	-0.54	22.09	2.37	-2.50	21.42
48.00	2.20	0.10	5.44	420.43	-10932.67	0.00	2666.15	2079.59	-0.62	24.06	2.37	-2.50	23.30
50.00	2.32	0.10	5.44	480.58	-11861.75	0.00	2666.15	2079.59	-0.71	26.10	2.37	-2.50	25.25
52.00	2.44	0.11	5.44	547.57	-12828.51	0.00	2666.15	2079.59	-0.81	28.23	2.37	-2.50	27.28
54.00	2.58	0.11	5.44	622.24	-13832.90	0.00	2666.15	2079.59	-0.92	30.44	2.37	-2.50	29.38
56.00	2.72	0.12	5.44	705.57	-14874.86	0.00	2666.15	2079.59	-1.05	32.73	2.37	-2.50	31.55
58.00	2.87	0.13	5.44	798.77	-15954.28	0.00	2666.15	2079.59	-1.18	35.11	2.37	-2.50	33.79
60.00	3.03	0.14	5.44	903.27	-17071.05	0.00	2666.15	2079.59	-1.34	37.56	2.37	-2.50	36.09

Case 1: A230B

L (m)	β (°)	W (cm)	V (cm)	M_y (KNm)	M_z (KNm)	φ (°)	P_{max} (KN)	M_{Pmax} (KNm)	σ_{my} (Mpa)	σ_{mz} (Mpa)	σ_p (Mpa)	σ_{MP} (Mpa)	σ_t (Mpa)
10.00	0.39	0.02	4.14	3.54	-516.02	0.00	2718.07	2438.11	0.00	0.91	2.22	-2.41	0.72
12.00	0.47	0.02	4.14	6.11	-743.06	0.00	2718.07	2438.11	-0.01	1.31	2.22	-2.41	1.12
14.00	0.55	0.02	4.14	9.71	-1011.38	0.00	2718.07	2438.11	-0.01	1.79	2.22	-2.41	1.59
16.00	0.63	0.03	4.14	14.49	-1320.97	0.00	2718.07	2438.11	-0.02	2.34	2.22	-2.41	2.13
18.00	0.71	0.03	4.14	20.64	-1671.82	0.00	2718.07	2438.11	-0.03	2.96	2.22	-2.41	2.74
20.00	0.79	0.03	4.14	28.33	-2063.94	0.00	2718.07	2438.11	-0.04	3.65	2.22	-2.41	3.42
22.00	0.87	0.04	4.14	37.74	-2497.32	0.00	2718.07	2438.11	-0.05	4.41	2.22	-2.41	4.18
24.00	0.95	0.04	4.14	49.04	-2971.95	0.00	2718.07	2438.11	-0.07	5.25	2.22	-2.41	5.00
26.00	1.03	0.04	4.14	62.42	-3487.83	0.00	2718.07	2438.11	-0.08	6.17	2.22	-2.41	5.89
28.00	1.11	0.05	4.14	78.07	-4044.95	0.00	2718.07	2438.11	-0.10	7.15	2.22	-2.41	6.86
30.00	1.19	0.05	4.14	96.20	-4643.31	0.00	2718.07	2438.11	-0.13	8.21	2.22	-2.41	7.89
32.00	1.27	0.05	4.14	117.01	-5282.89	0.00	2718.07	2438.11	-0.16	9.34	2.22	-2.41	8.99
34.00	1.35	0.06	4.14	140.73	-5963.69	0.00	2718.07	2438.11	-0.19	10.54	2.22	-2.41	10.17
36.00	1.44	0.06	4.14	167.60	-6685.70	0.00	2718.07	2438.11	-0.22	11.82	2.22	-2.41	11.41
38.00	1.52	0.06	4.14	197.88	-7448.90	0.00	2718.07	2438.11	-0.26	13.17	2.22	-2.41	12.71
40.00	1.61	0.07	4.14	231.84	-8253.29	0.00	2718.07	2438.11	-0.31	14.59	2.22	-2.41	14.09
42.00	1.70	0.07	4.14	269.81	-9098.84	0.00	2718.07	2438.11	-0.36	16.08	2.22	-2.41	15.54
44.00	1.79	0.07	4.13	312.13	-9985.54	0.00	2718.07	2438.11	-0.42	17.65	2.22	-2.41	17.05
46.00	1.89	0.08	4.13	359.20	-10913.37	0.00	2718.07	2438.11	-0.48	19.29	2.22	-2.41	18.62
48.00	1.98	0.08	4.13	411.45	-11882.30	0.00	2718.07	2438.11	-0.55	21.00	2.22	-2.41	20.27
50.00	2.09	0.09	4.13	469.41	-12892.30	0.00	2718.07	2438.11	-0.63	22.79	2.22	-2.41	21.97
52.00	2.19	0.09	4.13	533.65	-13943.35	0.00	2718.07	2438.11	-0.71	24.65	2.22	-2.41	23.75
54.00	2.30	0.09	4.13	604.86	-15035.38	0.00	2718.07	2438.11	-0.81	26.58	2.22	-2.41	25.58
56.00	2.42	0.10	4.13	683.84	-16168.37	0.00	2718.07	2438.11	-0.92	28.58	2.22	-2.41	27.48
58.00	2.55	0.10	4.13	771.54	-17342.22	0.00	2718.07	2438.11	-1.03	30.66	2.22	-2.41	29.44
60.00	2.68	0.11	4.13	869.08	-18556.88	0.00	2718.07	2438.11	-1.16	32.80	2.22	-2.41	31.45

Case 1: I235C150

L (m)	β (°)	W (cm)	V (cm)	M_y (KNm)	M_z (KNm)	φ (°)	P_{max} (KN)	M_{Pmax} (KNm)	σ_{my} (Mpa)	σ_{mz} (Mpa)	σ_p (Mpa)	σ_{MP} (Mpa)	σ_t (Mpa)
10.00	0.32	0.23	3.42	1.80	-323.99	0.00	1830.74	2193.23	-0.03	0.62	2.38	-4.09	-1.11
12.00	0.38	0.27	3.42	3.12	-466.55	0.00	1830.74	2193.23	-0.05	0.89	2.38	-4.09	-0.86
14.00	0.45	0.32	3.42	4.97	-635.02	0.00	1830.74	2193.23	-0.07	1.21	2.38	-4.09	-0.56
16.00	0.51	0.37	3.42	7.45	-829.40	0.00	1830.74	2193.23	-0.11	1.59	2.38	-4.09	-0.23
18.00	0.58	0.41	3.42	10.66	-1049.70	0.00	1830.74	2193.23	-0.16	2.01	2.38	-4.09	0.14
20.00	0.65	0.46	3.42	14.73	-1295.91	0.00	1830.74	2193.23	-0.22	2.48	2.38	-4.09	0.56
22.00	0.72	0.51	3.42	19.80	-1568.02	0.00	1830.74	2193.23	-0.29	3.00	2.38	-4.09	1.00
24.00	0.80	0.57	3.42	26.06	-1866.04	0.00	1830.74	2193.23	-0.39	3.57	2.38	-4.09	1.48
26.00	0.88	0.63	3.42	33.71	-2189.96	0.00	1830.74	2193.23	-0.50	4.19	2.38	-4.09	1.98
28.00	0.97	0.69	3.42	43.06	-2539.78	0.00	1830.74	2193.23	-0.64	4.86	2.38	-4.09	2.51
30.00	1.07	0.76	3.42	54.50	-2915.47	0.00	1830.74	2193.23	-0.81	5.57	2.38	-4.09	3.06
32.00	1.18	0.84	3.42	68.57	-3317.03	0.00	1830.74	2193.23	-1.02	6.34	2.38	-4.09	3.62
34.00	1.32	0.94	3.42	86.05	-3744.42	0.00	1830.74	2193.23	-1.28	7.16	2.38	-4.09	4.18
36.00	1.48	1.05	3.42	108.12	-4197.62	0.00	1830.74	2193.23	-1.60	8.03	2.38	-4.09	4.72
38.00	1.67	1.19	3.42	136.58	-4676.53	0.00	1830.74	2193.23	-2.02	8.94	2.38	-4.09	5.21
40.00	1.93	1.37	3.42	174.43	-5181.03	0.00	1830.74	2193.23	-2.59	9.91	2.38	-4.09	5.62
42.00	2.28	1.62	3.42	226.94	-5710.81	0.00	1830.74	2193.23	-3.36	10.92	2.38	-4.09	5.85
44.00	2.78	1.98	3.42	304.36	-6265.21	0.00	1830.74	2193.23	-4.51	11.98	2.38	-4.09	5.76
46.00	3.59	2.55	3.42	429.40	-6842.33	0.00	1830.74	2193.23	-6.36	13.08	2.38	-4.09	5.01
48.00	5.10	3.62	3.41	663.50	-7435.36	0.00	1830.74	2193.23	-9.83	14.22	2.38	-4.09	2.68
50.00	8.73	6.18	3.38	1228.79	-8006.19	0.00	1830.74	2193.23	-18.21	15.31	2.38	-4.09	-4.61
52.00	19.03	13.28	3.24	2856.34	-8282.19	0.00	1830.74	2193.23	-42.34	15.84	2.38	-4.09	-28.21
54.00	180.81	-0.57	-3.42	-133.42	9446.83	0.00	1830.74	2193.23	1.98	-18.06	2.38	-4.09	-17.79
56.00	-1446.00	-4.26	3.40	-1062.25	-10104.89	0.00	1830.74	2193.23	15.75	19.32	2.38	-4.09	33.36
58.00	-3.72	-2.64	3.42	-706.41	-10876.37	0.00	1830.74	2193.23	10.47	20.80	2.38	-4.09	29.56
60.00	-2.67	-1.90	3.42	-543.21	-11651.26	0.00	1830.74	2193.23	8.05	22.28	2.38	-4.09	28.63

Case 1: I245D200

L (m)	β (°)	W (cm)	V (cm)	M_y (KNm)	M_z (KNm)	φ (°)	P_{max} (KN)	M_{Pmax} (KNm)	σ_{my} (Mpa)	σ_{mz} (Mpa)	σ_p (Mpa)	σ_{MP} (Mpa)	σ_t (Mpa)
10.00	0.31	0.16	3.09	2.13	-388.03	0.00	2285.24	2797.13	-0.03	0.60	2.48	-4.03	-0.97
12.00	0.38	0.19	3.09	3.68	-558.76	0.00	2285.24	2797.13	-0.04	0.86	2.48	-4.03	-0.73
14.00	0.44	0.23	3.09	5.85	-760.53	0.00	2285.24	2797.13	-0.07	1.17	2.48	-4.03	-0.44
16.00	0.50	0.26	3.09	8.75	-993.34	0.00	2285.24	2797.13	-0.10	1.53	2.48	-4.03	-0.12
18.00	0.57	0.29	3.09	12.51	-1257.18	0.00	2285.24	2797.13	-0.15	1.93	2.48	-4.03	0.24
20.00	0.64	0.33	3.09	17.25	-1552.06	0.00	2285.24	2797.13	-0.20	2.38	2.48	-4.03	0.64
22.00	0.71	0.36	3.09	23.12	-1877.96	0.00	2285.24	2797.13	-0.27	2.88	2.48	-4.03	1.07
24.00	0.78	0.40	3.09	30.30	-2234.89	0.00	2285.24	2797.13	-0.36	3.43	2.48	-4.03	1.53
26.00	0.85	0.44	3.09	39.00	-2622.85	0.00	2285.24	2797.13	-0.46	4.03	2.48	-4.03	2.02
28.00	0.93	0.48	3.09	49.47	-3041.81	0.00	2285.24	2797.13	-0.59	4.67	2.48	-4.03	2.54
30.00	1.02	0.52	3.09	62.05	-3491.79	0.00	2285.24	2797.13	-0.74	5.36	2.48	-4.03	3.08
32.00	1.11	0.57	3.09	77.17	-3972.76	0.00	2285.24	2797.13	-0.92	6.10	2.48	-4.03	3.64
34.00	1.22	0.62	3.09	95.41	-4484.70	0.00	2285.24	2797.13	-1.13	6.89	2.48	-4.03	4.21
36.00	1.34	0.68	3.09	117.57	-5027.60	0.00	2285.24	2797.13	-1.39	7.72	2.48	-4.03	4.78
38.00	1.48	0.76	3.09	144.80	-5601.40	0.00	2285.24	2797.13	-1.72	8.60	2.48	-4.03	5.34
40.00	1.65	0.84	3.09	178.75	-6206.03	0.00	2285.24	2797.13	-2.12	9.53	2.48	-4.03	5.87
42.00	1.86	0.95	3.09	221.99	-6841.39	0.00	2285.24	2797.13	-2.63	10.50	2.48	-4.03	6.33
44.00	2.13	1.09	3.09	278.63	-7507.24	0.00	2285.24	2797.13	-3.30	11.53	2.48	-4.03	6.68
46.00	2.48	1.27	3.09	355.69	-8203.17	0.00	2285.24	2797.13	-4.22	12.60	2.48	-4.03	6.84
48.00	2.99	1.53	3.09	466.28	-8928.22	0.00	2285.24	2797.13	-5.53	13.71	2.48	-4.03	6.64
50.00	3.77	1.92	3.09	637.76	-9679.96	0.00	2285.24	2797.13	-7.56	14.86	2.48	-4.03	5.76
52.00	5.13	2.61	3.08	937.31	-10450.59	0.00	2285.24	2797.13	-11.12	16.05	2.48	-4.03	3.39
54.00	7.99	4.07	3.06	1572.30	-11205.41	0.00	2285.24	2797.13	-18.65	17.21	2.48	-4.03	-2.98
56.00	15.41	7.78	2.98	3232.87	-11731.58	0.00	2285.24	2797.13	-38.35	18.01	2.48	-4.03	-21.87
58.00	27.67	13.59	2.74	6062.71	-11560.27	0.00	2285.24	2797.13	-71.91	17.75	2.48	-4.03	-55.70
60.00	-29.42	-14.38	2.69	-6861.50	-12168.11	0.00	2285.24	2797.13	81.39	18.68	2.48	-4.03	98.53

Case 2: I245D200, L = 40 m

a (m)	β (°)	W (cm)	V (cm)	M_y (KNm)	M_z (KNm)	φ (°)	P_{max} (KN)	M_{Pmax} (KNm)	σ_{my} (Mpa)	σ_{mz} (Mpa)	σ_p (Mpa)	σ_{MP} (Mpa)	σ_t (Mpa)
0.00	1.53	1.25	4.94	123.17	-4597.32	0.00	3264.63	3029.37	-1.46	7.06	2.69	-4.36	3.93
0.32	1.44	1.17	4.94	111.60	-4450.40	0.00	3264.63	3029.37	-1.32	6.83	2.69	-4.36	3.84
0.64	1.34	1.10	4.94	100.94	-4303.45	0.00	3264.63	3029.37	-1.20	6.61	2.69	-4.36	3.74
0.96	1.26	1.02	4.94	91.13	-4156.47	0.00	3264.63	3029.37	-1.08	6.38	2.69	-4.36	3.63
1.28	1.17	0.96	4.94	82.10	-4009.46	0.00	3264.63	3029.37	-0.97	6.16	2.69	-4.36	3.51
1.60	1.09	0.89	4.94	73.77	-3862.43	0.00	3264.63	3029.37	-0.88	5.93	2.69	-4.36	3.39
1.92	1.02	0.83	4.94	66.10	-3715.38	0.00	3264.63	3029.37	-0.78	5.70	2.69	-4.36	3.25
2.24	0.95	0.77	4.94	59.04	-3568.32	0.00	3264.63	3029.37	-0.70	5.48	2.69	-4.36	3.11
2.56	0.88	0.72	4.94	52.53	-3421.23	0.00	3264.63	3029.37	-0.62	5.25	2.69	-4.36	2.96
2.88	0.81	0.66	4.94	46.55	-3274.14	0.00	3264.63	3029.37	-0.55	5.03	2.69	-4.36	2.81
3.20	0.75	0.61	4.94	41.06	-3127.04	0.00	3264.63	3029.37	-0.49	4.80	2.69	-4.36	2.65
3.52	0.69	0.56	4.94	36.02	-2979.92	0.00	3264.63	3029.37	-0.43	4.58	2.69	-4.36	2.48
3.84	0.64	0.52	4.94	31.41	-2832.80	0.00	3264.63	3029.37	-0.37	4.35	2.69	-4.36	2.31
4.16	0.58	0.47	4.94	27.20	-2685.67	0.00	3264.63	3029.37	-0.32	4.12	2.69	-4.36	2.13
4.48	0.53	0.43	4.94	23.36	-2538.53	0.00	3264.63	3029.37	-0.28	3.90	2.69	-4.36	1.95
4.80	0.48	0.39	4.94	19.87	-2391.39	0.00	3264.63	3029.37	-0.24	3.67	2.69	-4.36	1.77
5.12	0.43	0.35	4.94	16.72	-2244.24	0.00	3264.63	3029.37	-0.20	3.45	2.69	-4.36	1.58
5.44	0.38	0.31	4.94	13.89	-2097.09	0.00	3264.63	3029.37	-0.16	3.22	2.69	-4.36	1.39
5.76	0.33	0.27	4.94	11.35	-1949.94	0.00	3264.63	3029.37	-0.13	2.99	2.69	-4.36	1.19
6.08	0.29	0.24	4.94	9.10	-1802.78	0.00	3264.63	3029.37	-0.11	2.77	2.69	-4.36	0.99
6.40	0.25	0.20	4.94	7.11	-1655.62	0.00	3264.63	3029.37	-0.08	2.54	2.69	-4.36	0.79
6.72	0.20	0.17	4.94	5.39	-1508.46	0.00	3264.63	3029.37	-0.06	2.32	2.69	-4.36	0.58
7.04	0.16	0.13	4.94	3.90	-1361.30	0.00	3264.63	3029.37	-0.05	2.09	2.69	-4.36	0.38
7.36	0.13	0.10	4.94	2.65	-1214.13	0.00	3264.63	3029.37	-0.03	1.86	2.69	-4.36	0.16
7.68	0.09	0.07	4.94	1.62	-1066.97	0.00	3264.63	3029.37	-0.02	1.64	2.69	-4.36	-0.05
8.00	0.05	0.04	4.94	0.81	-919.80	0.00	3264.63	3029.37	-0.01	1.41	2.69	-4.36	-0.27

Case 2: I215D200, L = 40 m

a (m)	β (°)	W (cm)	V (cm)	M_y (KNm)	M_z (KNm)	φ (°)	P_{max} (KN)	M_{Pmax} (KNm)	σ_{my} (Mpa)	σ_{mz} (Mpa)	σ_p (Mpa)	σ_{MP} (Mpa)	σ_t (Mpa)
0.00	1.71	1.30	6.32	127.96	-4297.06	0.00	3248.84	2838.30	-1.52	7.92	3.07	-4.87	4.60
0.32	1.60	1.22	6.32	115.86	-4159.79	0.00	3248.84	2838.30	-1.38	7.67	3.07	-4.87	4.49
0.64	1.49	1.14	6.32	104.73	-4022.47	0.00	3248.84	2838.30	-1.25	7.42	3.07	-4.87	4.37
0.96	1.39	1.06	6.32	94.50	-3885.12	0.00	3248.84	2838.30	-1.12	7.16	3.07	-4.87	4.23
1.28	1.30	0.99	6.32	85.08	-3747.74	0.00	3248.84	2838.30	-1.01	6.91	3.07	-4.87	4.09
1.60	1.21	0.93	6.32	76.41	-3610.33	0.00	3248.84	2838.30	-0.91	6.66	3.07	-4.87	3.94
1.92	1.13	0.86	6.32	68.44	-3472.90	0.00	3248.84	2838.30	-0.81	6.40	3.07	-4.87	3.78
2.24	1.05	0.80	6.32	61.10	-3335.45	0.00	3248.84	2838.30	-0.73	6.15	3.07	-4.87	3.62
2.56	0.97	0.74	6.32	54.35	-3197.98	0.00	3248.84	2838.30	-0.65	5.90	3.07	-4.87	3.45
2.88	0.90	0.69	6.32	48.14	-3060.49	0.00	3248.84	2838.30	-0.57	5.64	3.07	-4.87	3.27
3.20	0.83	0.64	6.32	42.45	-2923.00	0.00	3248.84	2838.30	-0.50	5.39	3.07	-4.87	3.08
3.52	0.77	0.59	6.32	37.23	-2785.49	0.00	3248.84	2838.30	-0.44	5.13	3.07	-4.87	2.89
3.84	0.70	0.54	6.32	32.45	-2647.97	0.00	3248.84	2838.30	-0.39	4.88	3.07	-4.87	2.69
4.16	0.64	0.49	6.32	28.09	-2510.45	0.00	3248.84	2838.30	-0.33	4.63	3.07	-4.87	2.49
4.48	0.58	0.44	6.32	24.12	-2372.92	0.00	3248.84	2838.30	-0.29	4.37	3.07	-4.87	2.28
4.80	0.53	0.40	6.32	20.52	-2235.38	0.00	3248.84	2838.30	-0.24	4.12	3.07	-4.87	2.07
5.12	0.47	0.36	6.32	17.26	-2097.83	0.00	3248.84	2838.30	-0.21	3.87	3.07	-4.87	1.86
5.44	0.42	0.32	6.32	14.33	-1960.29	0.00	3248.84	2838.30	-0.17	3.61	3.07	-4.87	1.64
5.76	0.37	0.28	6.32	11.71	-1822.73	0.00	3248.84	2838.30	-0.14	3.36	3.07	-4.87	1.42
6.08	0.32	0.24	6.32	9.39	-1685.18	0.00	3248.84	2838.30	-0.11	3.11	3.07	-4.87	1.19
6.40	0.27	0.21	6.32	7.34	-1547.62	0.00	3248.84	2838.30	-0.09	2.85	3.07	-4.87	0.96
6.72	0.23	0.17	6.32	5.56	-1410.06	0.00	3248.84	2838.30	-0.07	2.60	3.07	-4.87	0.73
7.04	0.18	0.14	6.32	4.02	-1272.50	0.00	3248.84	2838.30	-0.05	2.35	3.07	-4.87	0.49
7.36	0.14	0.11	6.32	2.73	-1134.93	0.00	3248.84	2838.30	-0.03	2.09	3.07	-4.87	0.26
7.68	0.10	0.07	6.32	1.67	-997.37	0.00	3248.84	2838.30	-0.02	1.84	3.07	-4.87	0.01
8.00	0.06	0.04	6.33	0.83	-859.80	0.00	3248.84	2838.30	-0.01	1.58	3.07	-4.87	-0.23

Case 2: I160B120, a = 3 m

L (m)	β (°)	W (cm)	V (cm)	M_y (KNm)	M_z (KNm)	φ (°)	P_{max} (KN)	M_{Pmax} (KNm)	σ_{my} (Mpa)	σ_{mz} (Mpa)	σ_p (Mpa)	σ_{MP} (Mpa)	σ_t (Mpa)
10.00	-0.11	-0.06	3.43	0.09	44.11	0.00	1502.42	1185.41	0.00	-0.19	2.87	-4.30	-1.62
12.00	-0.06	-0.04	3.43	0.00	0.00	0.00	1502.42	1185.41	0.00	0.00	2.87	-4.30	-1.43
14.00	-0.01	0.00	3.43	-0.01	-61.76	0.00	1502.42	1185.41	0.00	0.27	2.87	-4.30	-1.16
16.00	0.06	0.03	3.43	0.15	-141.16	0.00	1502.42	1185.41	0.00	0.61	2.87	-4.30	-0.82
18.00	0.13	0.07	3.43	0.54	-238.20	0.00	1502.42	1185.41	-0.02	1.03	2.87	-4.30	-0.41
20.00	0.20	0.11	3.43	1.25	-352.89	0.00	1502.42	1185.41	-0.04	1.53	2.87	-4.30	0.06
22.00	0.28	0.16	3.43	2.36	-485.22	0.00	1502.42	1185.41	-0.07	2.10	2.87	-4.30	0.61
24.00	0.36	0.20	3.43	3.99	-635.19	0.00	1502.42	1185.41	-0.12	2.75	2.87	-4.30	1.21
26.00	0.44	0.25	3.43	6.23	-802.80	0.00	1502.42	1185.41	-0.19	3.48	2.87	-4.30	1.87
28.00	0.54	0.30	3.43	9.24	-988.04	0.00	1502.42	1185.41	-0.28	4.28	2.87	-4.30	2.58
30.00	0.63	0.35	3.43	13.19	-1190.93	0.00	1502.42	1185.41	-0.39	5.16	2.87	-4.30	3.34
32.00	0.75	0.41	3.43	18.36	-1411.43	0.00	1502.42	1185.41	-0.55	6.12	2.87	-4.30	4.14
34.00	0.87	0.49	3.43	25.13	-1649.56	0.00	1502.42	1185.41	-0.75	7.15	2.87	-4.30	4.97
36.00	1.03	0.57	3.43	34.10	-1905.29	0.00	1502.42	1185.41	-1.02	8.26	2.87	-4.30	5.81
38.00	1.22	0.68	3.43	46.26	-2178.59	0.00	1502.42	1185.41	-1.38	9.44	2.87	-4.30	6.64
40.00	1.47	0.82	3.43	63.34	-2469.41	0.00	1502.42	1185.41	-1.89	10.70	2.87	-4.30	7.39
42.00	1.83	1.02	3.43	88.73	-2777.58	0.00	1502.42	1185.41	-2.64	12.04	2.87	-4.30	7.97
44.00	2.40	1.33	3.43	130.00	-3102.69	0.00	1502.42	1185.41	-3.87	13.45	2.87	-4.30	8.15
46.00	3.46	1.92	3.43	208.03	-3443.20	0.00	1502.42	1185.41	-6.19	14.92	2.87	-4.30	7.30
48.00	6.11	3.39	3.41	405.81	-3789.52	0.00	1502.42	1185.41	-12.08	16.42	2.87	-4.30	2.92
50.00	16.70	9.16	3.29	1204.48	-4013.71	0.00	1502.42	1185.41	-35.86	17.39	2.87	-4.30	-19.89
52.00	-383.31	-12.61	3.15	-1815.38	-4213.07	0.00	1502.42	1185.41	54.04	18.26	2.87	-4.30	70.87
54.00	-4.19	-2.33	3.42	-365.82	-4988.79	0.00	1502.42	1185.41	10.89	21.62	2.87	-4.30	31.08
56.00	-2.62	-1.46	3.43	-248.45	-5428.79	0.00	1502.42	1185.41	7.40	23.53	2.87	-4.30	29.50
58.00	-1.89	-1.05	3.43	-193.79	-5881.22	0.00	1502.42	1185.41	5.77	25.49	2.87	-4.30	29.83
60.00	-1.46	-0.81	3.43	-161.94	-6349.92	0.00	1502.42	1185.41	4.82	27.52	2.87	-4.30	30.91

Case 2: I160B120, a = 2 m

L (m)	β (°)	W (cm)	V (cm)	M_y (KNm)	M_z (KNm)	φ (°)	P_{max} (KN)	M_{Pmax} (KNm)	σ_{my} (Mpa)	σ_{mz} (Mpa)	σ_p (Mpa)	σ_{MP} (Mpa)	σ_t (Mpa)
10.00	0.02	0.01	4.59	0.01	-44.11	0.00	1502.42	1185.41	0.00	0.19	2.87	-4.30	-1.24
12.00	0.09	0.06	4.59	0.16	-105.87	0.00	1502.42	1185.41	0.00	0.46	2.87	-4.30	-0.97
14.00	0.16	0.12	4.59	0.52	-185.27	0.00	1502.42	1185.41	-0.02	0.80	2.87	-4.30	-0.64
16.00	0.24	0.18	4.59	1.16	-282.31	0.00	1502.42	1185.41	-0.03	1.22	2.87	-4.30	-0.24
18.00	0.32	0.24	4.59	2.19	-396.99	0.00	1502.42	1185.41	-0.07	1.72	2.87	-4.30	0.23
20.00	0.40	0.30	4.59	3.69	-529.32	0.00	1502.42	1185.41	-0.11	2.29	2.87	-4.30	0.76
22.00	0.49	0.36	4.59	5.77	-679.29	0.00	1502.42	1185.41	-0.17	2.94	2.87	-4.30	1.34
24.00	0.58	0.43	4.59	8.54	-846.89	0.00	1502.42	1185.41	-0.25	3.67	2.87	-4.30	1.99
26.00	0.68	0.50	4.59	12.19	-1032.13	0.00	1502.42	1185.41	-0.36	4.47	2.87	-4.30	2.68
28.00	0.79	0.58	4.59	16.93	-1234.99	0.00	1502.42	1185.41	-0.50	5.35	2.87	-4.30	3.42
30.00	0.91	0.67	4.59	23.08	-1455.48	0.00	1502.42	1185.41	-0.69	6.31	2.87	-4.30	4.19
32.00	1.05	0.78	4.59	31.11	-1693.58	0.00	1502.42	1185.41	-0.93	7.34	2.87	-4.30	4.99
34.00	1.23	0.91	4.58	41.78	-1949.26	0.00	1502.42	1185.41	-1.24	8.45	2.87	-4.30	5.78
36.00	1.45	1.08	4.58	56.35	-2222.48	0.00	1502.42	1185.41	-1.68	9.63	2.87	-4.30	6.53
38.00	1.76	1.31	4.58	77.14	-2513.14	0.00	1502.42	1185.41	-2.30	10.89	2.87	-4.30	7.17
40.00	2.21	1.64	4.58	108.83	-2821.01	0.00	1502.42	1185.41	-3.24	12.23	2.87	-4.30	7.56
42.00	2.96	2.20	4.58	162.55	-3145.33	0.00	1502.42	1185.41	-4.84	13.63	2.87	-4.30	7.37
44.00	4.47	3.32	4.57	272.27	-3482.97	0.00	1502.42	1185.41	-8.10	15.09	2.87	-4.30	5.56
46.00	8.90	6.58	4.53	596.44	-3808.88	0.00	1502.42	1185.41	-17.76	16.51	2.87	-4.30	-2.68
48.00	23.71	17.12	4.20	1703.10	-3877.08	0.00	1502.42	1185.41	-50.70	16.80	2.87	-4.30	-35.32
50.00	-31.72	-22.38	3.90	-2435.38	-3939.69	0.00	1502.42	1185.41	72.50	17.07	2.87	-4.30	88.14
52.00	-3.74	-2.78	4.58	-329.18	-5035.55	0.00	1502.42	1185.41	9.80	21.82	2.87	-4.30	30.19
54.00	-2.48	-1.84	4.58	-237.29	-5473.44	0.00	1502.42	1185.41	7.06	23.72	2.87	-4.30	29.36
56.00	-1.84	-1.36	4.58	-190.12	-5925.47	0.00	1502.42	1185.41	5.66	25.68	2.87	-4.30	29.91
58.00	-1.44	-1.07	4.58	-161.22	-6394.06	0.00	1502.42	1185.41	4.80	27.71	2.87	-4.30	31.08
60.00	-1.18	-0.88	4.58	-141.60	-6879.86	0.00	1502.42	1185.41	4.22	29.82	2.87	-4.30	32.60

Case 2: I160B120, a = 1 m

L (m)	β (°)	W (cm)	V (cm)	M_y (KNm)	M_z (KNm)	φ (°)	P_{max} (KN)	M_{Pmax} (KNm)	σ_{my} (Mpa)	σ_{mz} (Mpa)	σ_p (Mpa)	σ_{MP} (Mpa)	σ_t (Mpa)
10.00	0.20	0.19	5.94	0.46	-132.33	0.00	1502.42	1185.41	-0.01	0.57	2.87	-4.30	-0.87
12.00	0.28	0.27	5.94	1.03	-211.73	0.00	1502.42	1185.41	-0.03	0.92	2.87	-4.30	-0.54
14.00	0.36	0.35	5.94	1.96	-308.77	0.00	1502.42	1185.41	-0.06	1.34	2.87	-4.30	-0.15
16.00	0.45	0.43	5.94	3.32	-423.45	0.00	1502.42	1185.41	-0.10	1.84	2.87	-4.30	0.31
18.00	0.54	0.52	5.94	5.21	-555.77	0.00	1502.42	1185.41	-0.16	2.41	2.87	-4.30	0.83
20.00	0.63	0.61	5.94	7.76	-705.73	0.00	1502.42	1185.41	-0.23	3.06	2.87	-4.30	1.40
22.00	0.73	0.70	5.94	11.10	-873.33	0.00	1502.42	1185.41	-0.33	3.78	2.87	-4.30	2.03
24.00	0.84	0.80	5.94	15.43	-1058.55	0.00	1502.42	1185.41	-0.46	4.59	2.87	-4.30	2.70
26.00	0.95	0.92	5.94	21.00	-1261.40	0.00	1502.42	1185.41	-0.63	5.47	2.87	-4.30	3.41
28.00	1.09	1.05	5.94	28.20	-1481.86	0.00	1502.42	1185.41	-0.84	6.42	2.87	-4.30	4.16
30.00	1.25	1.20	5.93	37.60	-1719.92	0.00	1502.42	1185.41	-1.12	7.45	2.87	-4.30	4.91
32.00	1.45	1.40	5.93	50.13	-1975.54	0.00	1502.42	1185.41	-1.49	8.56	2.87	-4.30	5.64
34.00	1.72	1.65	5.93	67.41	-2248.65	0.00	1502.42	1185.41	-2.01	9.75	2.87	-4.30	6.31
36.00	2.09	2.00	5.93	92.45	-2539.11	0.00	1502.42	1185.41	-2.75	11.00	2.87	-4.30	6.82
38.00	2.65	2.55	5.93	131.63	-2846.53	0.00	1502.42	1185.41	-3.92	12.34	2.87	-4.30	6.99
40.00	3.63	3.49	5.92	201.10	-3169.62	0.00	1502.42	1185.41	-5.99	13.74	2.87	-4.30	6.32
42.00	5.80	5.56	5.91	355.42	-3502.07	0.00	1502.42	1185.41	-10.58	15.18	2.87	-4.30	3.17
44.00	12.96	12.36	5.78	870.67	-3782.86	0.00	1502.42	1185.41	-25.92	16.39	2.87	-4.30	-10.95
46.00	29.32	26.98	5.18	2086.82	-3715.15	0.00	1502.42	1185.41	-62.12	16.10	2.87	-4.30	-47.45
48.00	-179.22	-0.75	-5.94	-63.78	4657.68	0.00	1502.42	1185.41	1.90	-20.19	2.87	-4.30	-19.71
50.00	-3.48	-3.35	5.93	-308.32	-5063.38	0.00	1502.42	1185.41	9.18	21.94	2.87	-4.30	29.69
52.00	-2.41	-2.31	5.93	-231.12	-5500.19	0.00	1502.42	1185.41	6.88	23.84	2.87	-4.30	29.29
54.00	-1.82	-1.75	5.93	-188.74	-5951.99	0.00	1502.42	1185.41	5.62	25.79	2.87	-4.30	29.99
56.00	-1.44	-1.39	5.93	-161.79	-6420.52	0.00	1502.42	1185.41	4.82	27.83	2.87	-4.30	31.21
58.00	-1.19	-1.14	5.93	-143.05	-6906.29	0.00	1502.42	1185.41	4.26	29.93	2.87	-4.30	32.76
60.00	-1.00	-0.96	5.94	-129.20	-7409.51	0.00	1502.42	1185.41	3.85	32.11	2.87	-4.30	34.53

Case 2: I160B120, a = 0

L (m)	β (°)	W (cm)	V (cm)	M_y (KNm)	M_z (KNm)	φ (°)	P_{max} (KN)	M_{Pmax} (KNm)	σ_{my} (Mpa)	σ_{mz} (Mpa)	σ_p (Mpa)	σ_{MP} (Mpa)	σ_t (Mpa)
10.00	0.43	0.52	7.50	1.65	-220.55	0.00	1502.42	1185.41	-0.05	0.96	2.87	-4.30	-0.52
12.00	0.52	0.63	7.50	2.87	-317.59	0.00	1502.42	1185.41	-0.09	1.38	2.87	-4.30	-0.14
14.00	0.61	0.74	7.50	4.58	-432.26	0.00	1502.42	1185.41	-0.14	1.87	2.87	-4.30	0.31
16.00	0.70	0.85	7.50	6.89	-564.58	0.00	1502.42	1185.41	-0.21	2.45	2.87	-4.30	0.81
18.00	0.80	0.97	7.50	9.93	-714.53	0.00	1502.42	1185.41	-0.30	3.10	2.87	-4.30	1.37
20.00	0.90	1.09	7.50	13.86	-882.11	0.00	1502.42	1185.41	-0.41	3.82	2.87	-4.30	1.98
22.00	1.01	1.23	7.50	18.90	-1067.32	0.00	1502.42	1185.41	-0.56	4.63	2.87	-4.30	2.64
24.00	1.14	1.39	7.50	25.35	-1270.14	0.00	1502.42	1185.41	-0.75	5.50	2.87	-4.30	3.32
26.00	1.29	1.57	7.50	33.65	-1490.57	0.00	1502.42	1185.41	-1.00	6.46	2.87	-4.30	4.03
28.00	1.47	1.79	7.50	44.51	-1728.58	0.00	1502.42	1185.41	-1.32	7.49	2.87	-4.30	4.74
30.00	1.70	2.07	7.49	59.05	-1984.11	0.00	1502.42	1185.41	-1.76	8.60	2.87	-4.30	5.41
32.00	2.01	2.44	7.49	79.29	-2257.09	0.00	1502.42	1185.41	-2.36	9.78	2.87	-4.30	5.99
34.00	2.45	2.98	7.49	109.08	-2547.28	0.00	1502.42	1185.41	-3.25	11.04	2.87	-4.30	6.36
36.00	3.15	3.82	7.49	156.92	-2854.08	0.00	1502.42	1185.41	-4.67	12.37	2.87	-4.30	6.27
38.00	4.42	5.37	7.48	245.68	-3175.32	0.00	1502.42	1185.41	-7.31	13.76	2.87	-4.30	5.02
40.00	7.49	9.07	7.43	460.13	-3498.75	0.00	1502.42	1185.41	-13.70	15.16	2.87	-4.30	0.04
42.00	17.77	21.24	7.14	1187.33	-3704.98	0.00	1502.42	1185.41	-35.34	16.06	2.87	-4.30	-20.72
44.00	540.88	-1.07	-7.50	-65.60	4269.43	0.00	1502.42	1185.41	1.95	-18.50	2.87	-4.30	-17.98
46.00	-5.51	-6.68	7.46	-447.91	-4645.39	0.00	1502.42	1185.41	13.33	20.13	2.87	-4.30	32.04
48.00	-3.35	-4.07	7.49	-296.90	-5072.90	0.00	1502.42	1185.41	8.84	21.98	2.87	-4.30	29.40
50.00	-2.38	-2.88	7.49	-228.59	-5509.13	0.00	1502.42	1185.41	6.80	23.88	2.87	-4.30	29.25
52.00	-1.82	-2.21	7.49	-189.23	-5960.80	0.00	1502.42	1185.41	5.63	25.83	2.87	-4.30	30.04
54.00	-1.46	-1.77	7.50	-163.49	-6429.30	0.00	1502.42	1185.41	4.87	27.86	2.87	-4.30	31.30
56.00	-1.20	-1.46	7.50	-145.26	-6915.07	0.00	1502.42	1185.41	4.32	29.97	2.87	-4.30	32.87
58.00	-1.02	-1.23	7.50	-131.60	-7418.29	0.00	1502.42	1185.41	3.92	32.15	2.87	-4.30	34.64
60.00	-0.87	-1.06	7.50	-120.94	-7939.05	0.00	1502.42	1185.41	3.60	34.41	2.87	-4.30	36.58

Case 3: I160B120, L = 40 m

f_{ck} (MPa)	β (°)	W (cm)	V (cm)	M_y (KNm)	M_z (KNm)	φ (°)	P_{max} (KN)	M_{Pmax} (KNm)	σ_{my} (Mpa)	σ_{mz} (Mpa)	σ_p (Mpa)	σ_{MP} (Mpa)	σ_t (Mpa)
20.00	3.32	5.43	10.08	151.50	-2609.59	0.00	2146.31	1820.87	-4.51	11.31	4.41	-6.61	4.61
21.60	3.24	5.30	10.08	147.86	-2609.80	0.00	2146.31	1820.87	-4.40	11.31	4.41	-6.61	4.72
23.20	3.17	5.19	10.08	144.72	-2609.97	0.00	2146.31	1820.87	-4.31	11.31	4.41	-6.61	4.81
24.80	3.11	5.09	10.08	141.96	-2610.12	0.00	2146.31	1820.87	-4.23	11.31	4.41	-6.61	4.89
26.40	3.06	5.00	10.08	139.52	-2610.26	0.00	2146.31	1820.87	-4.15	11.31	4.41	-6.61	4.97
28.00	3.01	4.92	10.08	137.34	-2610.37	0.00	2146.31	1820.87	-4.09	11.31	4.41	-6.61	5.03
29.60	2.97	4.85	10.08	135.38	-2610.47	0.00	2146.31	1820.87	-4.03	11.31	4.41	-6.61	5.09
31.20	2.93	4.79	10.08	133.61	-2610.56	0.00	2146.31	1820.87	-3.98	11.31	4.41	-6.61	5.14
32.80	2.89	4.73	10.08	132.00	-2610.65	0.00	2146.31	1820.87	-3.93	11.31	4.41	-6.61	5.19
34.40	2.86	4.68	10.08	130.52	-2610.72	0.00	2146.31	1820.87	-3.89	11.31	4.41	-6.61	5.24
36.00	2.83	4.63	10.08	129.16	-2610.79	0.00	2146.31	1820.87	-3.84	11.31	4.41	-6.61	5.28
37.60	2.80	4.58	10.08	127.90	-2610.85	0.00	2146.31	1820.87	-3.81	11.31	4.41	-6.61	5.31
39.20	2.78	4.54	10.08	126.74	-2610.91	0.00	2146.31	1820.87	-3.77	11.32	4.41	-6.61	5.35
40.80	2.76	4.50	10.08	125.66	-2610.96	0.00	2146.31	1820.87	-3.74	11.32	4.41	-6.61	5.38
42.40	2.73	4.47	10.08	124.64	-2611.01	0.00	2146.31	1820.87	-3.71	11.32	4.41	-6.61	5.41
44.00	2.71	4.43	10.08	123.70	-2611.05	0.00	2146.31	1820.87	-3.68	11.32	4.41	-6.61	5.44
45.60	2.69	4.40	10.08	122.81	-2611.09	0.00	2146.31	1820.87	-3.66	11.32	4.41	-6.61	5.47
47.20	2.67	4.37	10.08	121.97	-2611.13	0.00	2146.31	1820.87	-3.63	11.32	4.41	-6.61	5.49
48.80	2.66	4.34	10.08	121.18	-2611.17	0.00	2146.31	1820.87	-3.61	11.32	4.41	-6.61	5.52
50.40	2.64	4.32	10.08	120.44	-2611.21	0.00	2146.31	1820.87	-3.59	11.32	4.41	-6.61	5.54
52.00	2.63	4.29	10.08	119.73	-2611.24	0.00	2146.31	1820.87	-3.56	11.32	4.41	-6.61	5.56
53.60	2.61	4.27	10.08	119.06	-2611.27	0.00	2146.31	1820.87	-3.54	11.32	4.41	-6.61	5.58
55.20	2.60	4.24	10.08	118.43	-2611.30	0.00	2146.31	1820.87	-3.53	11.32	4.41	-6.61	5.60
56.80	2.58	4.22	10.08	117.82	-2611.32	0.00	2146.31	1820.87	-3.51	11.32	4.41	-6.61	5.62
58.40	2.57	4.20	10.08	117.24	-2611.35	0.00	2146.31	1820.87	-3.49	11.32	4.41	-6.61	5.63
60.00	2.56	4.18	10.08	116.69	-2611.38	0.00	2146.31	1820.87	-3.47	11.32	4.41	-6.61	5.65

Case 3: I160B120, f_{ck} = 20 MPa

L (m)	β (°)	W (cm)	V (cm)	M_y (KNm)	M_z (KNm)	φ (°)	P_{max} (KN)	M_{Pmax} (KNm)	σ_{my} (Mpa)	σ_{mz} (Mpa)	σ_p (Mpa)	σ_{MP} (Mpa)	σ_t (Mpa)
10.00	0.43	0.52	7.50	1.65	-220.55	0.00	1502.42	1185.41	-0.05	0.96	2.87	-4.30	-0.52
12.00	0.52	0.63	7.50	2.87	-317.59	0.00	1502.42	1185.41	-0.09	1.38	2.87	-4.30	-0.14
14.00	0.61	0.74	7.50	4.58	-432.26	0.00	1502.42	1185.41	-0.14	1.87	2.87	-4.30	0.31
16.00	0.70	0.85	7.50	6.89	-564.58	0.00	1502.42	1185.41	-0.21	2.45	2.87	-4.30	0.81
18.00	0.80	0.97	7.50	9.93	-714.53	0.00	1502.42	1185.41	-0.30	3.10	2.87	-4.30	1.37
20.00	0.90	1.09	7.50	13.86	-882.11	0.00	1502.42	1185.41	-0.41	3.82	2.87	-4.30	1.98
22.00	1.01	1.23	7.50	18.90	-1067.32	0.00	1502.42	1185.41	-0.56	4.63	2.87	-4.30	2.64
24.00	1.14	1.39	7.50	25.35	-1270.14	0.00	1502.42	1185.41	-0.75	5.50	2.87	-4.30	3.32
26.00	1.29	1.57	7.50	33.65	-1490.57	0.00	1502.42	1185.41	-1.00	6.46	2.87	-4.30	4.03
28.00	1.47	1.79	7.50	44.51	-1728.58	0.00	1502.42	1185.41	-1.32	7.49	2.87	-4.30	4.74
30.00	1.70	2.07	7.49	59.05	-1984.11	0.00	1502.42	1185.41	-1.76	8.60	2.87	-4.30	5.41
32.00	2.01	2.44	7.49	79.29	-2257.09	0.00	1502.42	1185.41	-2.36	9.78	2.87	-4.30	5.99
34.00	2.45	2.98	7.49	109.08	-2547.28	0.00	1502.42	1185.41	-3.25	11.04	2.87	-4.30	6.36
36.00	3.15	3.82	7.49	156.92	-2854.08	0.00	1502.42	1185.41	-4.67	12.37	2.87	-4.30	6.27
38.00	4.42	5.37	7.48	245.68	-3175.32	0.00	1502.42	1185.41	-7.31	13.76	2.87	-4.30	5.02
40.00	7.49	9.07	7.43	460.13	-3498.75	0.00	1502.42	1185.41	-13.70	15.16	2.87	-4.30	0.04
42.00	17.77	21.24	7.14	1187.33	-3704.98	0.00	1502.42	1185.41	-35.34	16.06	2.87	-4.30	-20.72
44.00	540.88	-1.07	-7.50	-65.60	4269.43	0.00	1502.42	1185.41	1.95	-18.50	2.87	-4.30	-17.98
46.00	-5.51	-6.68	7.46	-447.91	-4645.39	0.00	1502.42	1185.41	13.33	20.13	2.87	-4.30	32.04
48.00	-3.35	-4.07	7.49	-296.90	-5072.90	0.00	1502.42	1185.41	8.84	21.98	2.87	-4.30	29.40
50.00	-2.38	-2.88	7.49	-228.59	-5509.13	0.00	1502.42	1185.41	6.80	23.88	2.87	-4.30	29.25
52.00	-1.82	-2.21	7.49	-189.23	-5960.80	0.00	1502.42	1185.41	5.63	25.83	2.87	-4.30	30.04
54.00	-1.46	-1.77	7.50	-163.49	-6429.30	0.00	1502.42	1185.41	4.87	27.86	2.87	-4.30	31.30
56.00	-1.20	-1.46	7.50	-145.26	-6915.07	0.00	1502.42	1185.41	4.32	29.97	2.87	-4.30	32.87
58.00	-1.02	-1.23	7.50	-131.60	-7418.29	0.00	1502.42	1185.41	3.92	32.15	2.87	-4.30	34.64
60.00	-0.87	-1.06	7.50	-120.94	-7939.05	0.00	1502.42	1185.41	3.60	34.41	2.87	-4.30	36.58

Case 3: I160B120, f_{ck} = 40 MPa

L (m)	β (°)	W (cm)	V (cm)	M_y (KNm)	M_z (KNm)	φ (°)	P_{max} (KN)	M_{Pmax} (KNm)	σ_{my} (Mpa)	σ_{mz} (Mpa)	σ_p (Mpa)	σ_{MP} (Mpa)	σ_t (Mpa)
10.00	0.43	0.41	5.95	1.65	-220.55	0.00	2384.94	1881.72	-0.05	0.96	4.56	-6.83	-1.36
12.00	0.52	0.50	5.95	2.86	-317.59	0.00	2384.94	1881.72	-0.09	1.38	4.56	-6.83	-0.97
14.00	0.61	0.58	5.95	4.57	-432.26	0.00	2384.94	1881.72	-0.14	1.87	4.56	-6.83	-0.53
16.00	0.70	0.67	5.95	6.86	-564.58	0.00	2384.94	1881.72	-0.20	2.45	4.56	-6.83	-0.02
18.00	0.79	0.76	5.95	9.87	-714.53	0.00	2384.94	1881.72	-0.29	3.10	4.56	-6.83	0.54
20.00	0.89	0.86	5.95	13.72	-882.11	0.00	2384.94	1881.72	-0.41	3.82	4.56	-6.83	1.15
22.00	1.00	0.96	5.95	18.61	-1067.32	0.00	2384.94	1881.72	-0.55	4.63	4.56	-6.83	1.81
24.00	1.12	1.08	5.95	24.77	-1270.15	0.00	2384.94	1881.72	-0.74	5.50	4.56	-6.83	2.50
26.00	1.25	1.21	5.95	32.57	-1490.59	0.00	2384.94	1881.72	-0.97	6.46	4.56	-6.83	3.22
28.00	1.41	1.36	5.95	42.49	-1728.63	0.00	2384.94	1881.72	-1.26	7.49	4.56	-6.83	3.96
30.00	1.60	1.54	5.95	55.32	-1984.22	0.00	2384.94	1881.72	-1.65	8.60	4.56	-6.83	4.69
32.00	1.83	1.77	5.95	72.31	-2257.32	0.00	2384.94	1881.72	-2.15	9.78	4.56	-6.83	5.36
34.00	2.15	2.07	5.95	95.61	-2547.82	0.00	2384.94	1881.72	-2.85	11.04	4.56	-6.83	5.93
36.00	2.59	2.50	5.94	129.24	-2855.47	0.00	2384.94	1881.72	-3.85	12.37	4.56	-6.83	6.26
38.00	3.27	3.15	5.94	181.73	-3179.62	0.00	2384.94	1881.72	-5.41	13.78	4.56	-6.83	6.10
40.00	4.46	4.29	5.93	274.43	-3518.19	0.00	2384.94	1881.72	-8.17	15.25	4.56	-6.83	4.81
42.00	7.05	6.78	5.91	477.53	-3861.17	0.00	2384.94	1881.72	-14.22	16.73	4.56	-6.83	0.25
44.00	14.80	14.11	5.75	1090.81	-4128.26	0.00	2384.94	1881.72	-32.47	17.89	4.56	-6.83	-16.85
46.00	29.70	27.36	5.17	2312.00	-4054.00	0.00	2384.94	1881.72	-68.82	17.57	4.56	-6.83	-53.52
48.00	-34.94	-31.63	4.88	-2910.32	-4165.63	0.00	2384.94	1881.72	86.64	18.05	4.56	-6.83	102.42
50.00	-4.23	-4.07	5.93	-406.28	-5498.88	0.00	2384.94	1881.72	12.09	23.83	4.56	-6.83	33.66
52.00	-2.91	-2.81	5.94	-302.97	-5956.10	0.00	2384.94	1881.72	9.02	25.81	4.56	-6.83	32.57
54.00	-2.20	-2.12	5.95	-246.42	-6426.65	0.00	2384.94	1881.72	7.34	27.85	4.56	-6.83	32.92
56.00	-1.74	-1.68	5.95	-210.50	-6913.39	0.00	2384.94	1881.72	6.27	29.96	4.56	-6.83	33.96
58.00	-1.43	-1.38	5.95	-185.55	-7417.14	0.00	2384.94	1881.72	5.52	32.14	4.56	-6.83	35.40
60.00	-1.21	-1.16	5.95	-167.13	-7938.21	0.00	2384.94	1881.72	4.98	34.40	4.56	-6.83	37.11

Case 3: I160B120, f_{ck} = 60 MPa

L (m)	β (°)	W (cm)	V (cm)	M_y (KNm)	M_z (KNm)	φ (°)	P_{max} (KN)	M_{Pmax} (KNm)	σ_{my} (Mpa)	σ_{mz} (Mpa)	σ_p (Mpa)	σ_{MP} (Mpa)	σ_t (Mpa)
10.00	0.43	0.36	5.20	1.65	-220.55	0.00	3053.66	2409.33	-0.05	0.96	5.84	-8.74	-1.99
12.00	0.52	0.43	5.20	2.86	-317.59	0.00	3053.66	2409.33	-0.09	1.38	5.84	-8.74	-1.61
14.00	0.60	0.51	5.20	4.56	-432.26	0.00	3053.66	2409.33	-0.14	1.87	5.84	-8.74	-1.16
16.00	0.69	0.59	5.20	6.85	-564.58	0.00	3053.66	2409.33	-0.20	2.45	5.84	-8.74	-0.66
18.00	0.79	0.66	5.20	9.83	-714.53	0.00	3053.66	2409.33	-0.29	3.10	5.84	-8.74	-0.10
20.00	0.89	0.75	5.20	13.65	-882.11	0.00	3053.66	2409.33	-0.41	3.82	5.84	-8.74	0.52
22.00	0.99	0.83	5.20	18.47	-1067.32	0.00	3053.66	2409.33	-0.55	4.63	5.84	-8.74	1.17
24.00	1.11	0.93	5.20	24.51	-1270.16	0.00	3053.66	2409.33	-0.73	5.50	5.84	-8.74	1.87
26.00	1.23	1.04	5.20	32.07	-1490.60	0.00	3053.66	2409.33	-0.95	6.46	5.84	-8.74	2.60
28.00	1.38	1.16	5.20	41.58	-1728.65	0.00	3053.66	2409.33	-1.24	7.49	5.84	-8.74	3.35
30.00	1.55	1.30	5.20	53.68	-1984.27	0.00	3053.66	2409.33	-1.60	8.60	5.84	-8.74	4.10
32.00	1.76	1.48	5.20	69.34	-2257.42	0.00	3053.66	2409.33	-2.06	9.78	5.84	-8.74	4.82
34.00	2.03	1.71	5.20	90.19	-2548.02	0.00	3053.66	2409.33	-2.68	11.04	5.84	-8.74	5.46
36.00	2.39	2.01	5.19	119.02	-2855.91	0.00	3053.66	2409.33	-3.54	12.38	5.84	-8.74	5.93
38.00	2.90	2.44	5.19	161.22	-3180.73	0.00	3053.66	2409.33	-4.80	13.78	5.84	-8.74	6.08
40.00	3.71	3.12	5.19	228.52	-3521.47	0.00	3053.66	2409.33	-6.80	15.26	5.84	-8.74	5.56
42.00	5.19	4.36	5.18	351.69	-3874.66	0.00	3053.66	2409.33	-10.47	16.79	5.84	-8.74	3.42
44.00	8.59	7.20	5.14	637.67	-4222.06	0.00	3053.66	2409.33	-18.98	18.30	5.84	-8.74	-3.59
46.00	18.41	15.23	4.93	1473.68	-4428.16	0.00	3053.66	2409.33	-43.87	19.19	5.84	-8.74	-27.58
48.00	180.97	-0.82	-5.20	-85.99	5080.85	0.00	3053.66	2409.33	2.56	-22.02	5.84	-8.74	-22.36
50.00	180.92	-0.78	-5.20	-88.87	5513.15	0.00	3053.66	2409.33	2.65	-23.89	5.84	-8.74	-24.15
52.00	-4.12	-3.47	5.18	-428.86	-5948.36	0.00	3053.66	2409.33	12.77	25.78	5.84	-8.74	35.64
54.00	-2.92	-2.45	5.19	-327.26	-6423.04	0.00	3053.66	2409.33	9.74	27.84	5.84	-8.74	34.68
56.00	-2.23	-1.88	5.19	-269.38	-6911.35	0.00	3053.66	2409.33	8.02	29.95	5.84	-8.74	35.07
58.00	-1.79	-1.51	5.20	-231.78	-7415.84	0.00	3053.66	2409.33	6.90	32.14	5.84	-8.74	36.14
60.00	-1.48	-1.25	5.20	-205.27	-7937.31	0.00	3053.66	2409.33	6.11	34.40	5.84	-8.74	37.61

Case 4: I160B120, L = 40 m

δ (m)	β (°)	W (cm)	V (cm)	M_y (KNm)	M_z (KNm)	φ (°)	P_{max} (KN)	M_{Pmax} (KNm)	σ_{my} (Mpa)	σ_{mz} (Mpa)	σ_p (Mpa)	σ_{MP} (Mpa)	σ_t (Mpa)
0.02	1.25	2.04	10.09	56.97	-2613.38	0.00	2146.31	1820.87	-1.70	11.33	4.41	-6.61	7.44
0.02	1.40	2.29	10.09	63.80	-2613.22	0.00	2146.31	1820.87	-1.90	11.33	4.41	-6.61	7.23
0.02	1.55	2.53	10.09	70.63	-2613.04	0.00	2146.31	1820.87	-2.10	11.32	4.41	-6.61	7.03
0.03	1.70	2.78	10.09	77.46	-2612.85	0.00	2146.31	1820.87	-2.31	11.32	4.41	-6.61	6.83
0.03	1.85	3.02	10.09	84.28	-2612.64	0.00	2146.31	1820.87	-2.51	11.32	4.41	-6.61	6.62
0.03	2.00	3.26	10.09	91.09	-2612.41	0.00	2146.31	1820.87	-2.71	11.32	4.41	-6.61	6.42
0.03	2.15	3.51	10.09	97.91	-2612.16	0.00	2146.31	1820.87	-2.91	11.32	4.41	-6.61	6.21
0.04	2.30	3.75	10.09	104.72	-2611.89	0.00	2146.31	1820.87	-3.12	11.32	4.41	-6.61	6.01
0.04	2.45	4.00	10.09	111.52	-2611.61	0.00	2146.31	1820.87	-3.32	11.32	4.41	-6.61	5.81
0.04	2.59	4.24	10.08	118.32	-2611.31	0.00	2146.31	1820.87	-3.52	11.32	4.41	-6.61	5.60
0.04	2.74	4.48	10.08	125.12	-2610.99	0.00	2146.31	1820.87	-3.72	11.32	4.41	-6.61	5.40
0.05	2.89	4.73	10.08	131.91	-2610.66	0.00	2146.31	1820.87	-3.93	11.31	4.41	-6.61	5.19
0.05	3.04	4.97	10.08	138.70	-2610.30	0.00	2146.31	1820.87	-4.13	11.31	4.41	-6.61	4.99
0.05	3.19	5.21	10.08	145.48	-2609.93	0.00	2146.31	1820.87	-4.33	11.31	4.41	-6.61	4.79
0.05	3.34	5.46	10.08	152.25	-2609.54	0.00	2146.31	1820.87	-4.53	11.31	4.41	-6.61	4.58
0.06	3.49	5.70	10.08	159.02	-2609.14	0.00	2146.31	1820.87	-4.73	11.31	4.41	-6.61	4.38
0.06	3.64	5.94	10.07	165.78	-2608.72	0.00	2146.31	1820.87	-4.94	11.31	4.41	-6.61	4.18
0.06	3.78	6.18	10.07	172.54	-2608.28	0.00	2146.31	1820.87	-5.14	11.30	4.41	-6.61	3.97
0.06	3.93	6.43	10.07	179.29	-2607.82	0.00	2146.31	1820.87	-5.34	11.30	4.41	-6.61	3.77
0.07	4.08	6.67	10.07	186.03	-2607.34	0.00	2146.31	1820.87	-5.54	11.30	4.41	-6.61	3.57
0.07	4.23	6.91	10.07	192.76	-2606.85	0.00	2146.31	1820.87	-5.74	11.30	4.41	-6.61	3.37
0.07	4.38	7.15	10.06	199.49	-2606.34	0.00	2146.31	1820.87	-5.94	11.30	4.41	-6.61	3.16
0.07	4.52	7.39	10.06	206.21	-2605.82	0.00	2146.31	1820.87	-6.14	11.29	4.41	-6.61	2.96
0.08	4.67	7.63	10.06	212.92	-2605.28	0.00	2146.31	1820.87	-6.34	11.29	4.41	-6.61	2.76
0.08	4.82	7.87	10.06	219.62	-2604.72	0.00	2146.31	1820.87	-6.54	11.29	4.41	-6.61	2.56
0.08	4.97	8.11	10.06	226.32	-2604.14	0.00	2146.31	1820.87	-6.74	11.29	4.41	-6.61	2.36

Case 4: I160B120, δ = 2 cm

L (m)	β (°)	W (cm)	V (cm)	M_y (KNm)	M_z (KNm)	φ (°)	P_{max} (KN)	M_{Pmax} (KNm)	σ_{my} (Mpa)	σ_{mz} (Mpa)	σ_p (Mpa)	σ_{MP} (Mpa)	σ_t (Mpa)
10.00	0.64	1.21	11.55	2.48	-220.54	0.00	1502.42	1185.41	-0.07	0.96	2.87	-4.30	-0.55
12.00	0.65	1.21	11.55	3.58	-317.58	0.00	1502.42	1185.41	-0.11	1.38	2.87	-4.30	-0.16
14.00	0.65	1.22	11.55	4.90	-432.26	0.00	1502.42	1185.41	-0.15	1.87	2.87	-4.30	0.30
16.00	0.66	1.23	11.55	6.46	-564.58	0.00	1502.42	1185.41	-0.19	2.45	2.87	-4.30	0.83
18.00	0.66	1.24	11.55	8.28	-714.55	0.00	1502.42	1185.41	-0.25	3.10	2.87	-4.30	1.42
20.00	0.68	1.26	11.55	10.40	-882.16	0.00	1502.42	1185.41	-0.31	3.82	2.87	-4.30	2.09
22.00	0.69	1.29	11.55	12.89	-1067.41	0.00	1502.42	1185.41	-0.38	4.63	2.87	-4.30	2.81
24.00	0.71	1.34	11.55	15.85	-1270.30	0.00	1502.42	1185.41	-0.47	5.51	2.87	-4.30	3.61
26.00	0.75	1.40	11.55	19.42	-1490.83	0.00	1502.42	1185.41	-0.58	6.46	2.87	-4.30	4.46
28.00	0.79	1.48	11.55	23.85	-1728.99	0.00	1502.42	1185.41	-0.71	7.49	2.87	-4.30	5.36
30.00	0.85	1.60	11.55	29.54	-1984.78	0.00	1502.42	1185.41	-0.88	8.60	2.87	-4.30	6.29
32.00	0.94	1.77	11.55	37.19	-2258.19	0.00	1502.42	1185.41	-1.11	9.79	2.87	-4.30	7.25
34.00	1.08	2.03	11.55	48.18	-2549.17	0.00	1502.42	1185.41	-1.43	11.05	2.87	-4.30	8.19
36.00	1.31	2.46	11.55	65.55	-2857.65	0.00	1502.42	1185.41	-1.95	12.38	2.87	-4.30	9.01
38.00	1.76	3.29	11.55	97.66	-3183.33	0.00	1502.42	1185.41	-2.91	13.80	2.87	-4.30	9.46
40.00	2.90	5.42	11.54	178.23	-3524.39	0.00	1502.42	1185.41	-5.31	15.27	2.87	-4.30	8.54
42.00	9.62	17.92	11.39	650.21	-3835.89	0.00	1502.42	1185.41	-19.36	16.62	2.87	-4.30	-4.16
44.00	390.69	54.74	9.94	2179.57	-3671.79	0.00	1502.42	1185.41	-64.88	15.91	2.87	-4.30	-50.40
46.00	-1.77	-3.32	11.55	-144.29	-4664.74	0.00	1502.42	1185.41	4.30	20.22	2.87	-4.30	23.08
48.00	-1.04	-1.95	11.55	-92.55	-5080.77	0.00	1502.42	1185.41	2.76	22.02	2.87	-4.30	23.35
50.00	-0.71	-1.33	11.55	-68.54	-5513.48	0.00	1502.42	1185.41	2.04	23.89	2.87	-4.30	24.51
52.00	-0.52	-0.98	11.55	-54.59	-5963.59	0.00	1502.42	1185.41	1.62	25.84	2.87	-4.30	26.04
54.00	-0.40	-0.76	11.56	-45.41	-6431.26	0.00	1502.42	1185.41	1.35	27.87	2.87	-4.30	27.80
56.00	-0.32	-0.60	11.56	-38.90	-6916.53	0.00	1502.42	1185.41	1.16	29.97	2.87	-4.30	29.71
58.00	-0.26	-0.49	11.55	-34.03	-7419.43	0.00	1502.42	1185.41	1.01	32.15	2.87	-4.30	31.74
60.00	-0.22	-0.41	11.56	-30.23	-7939.96	0.00	1502.42	1185.41	0.90	34.41	2.87	-4.30	33.88

Case 4: I160B120, δ = 4 cm

L (m)	β (°)	W (cm)	V (cm)	M_y (KNm)	M_z (KNm)	φ (°)	P_{max} (KN)	M_{Pmax} (KNm)	σ_{my} (Mpa)	σ_{mz} (Mpa)	σ_p (Mpa)	σ_{MP} (Mpa)	σ_t (Mpa)
10.00	1.29	2.41	11.55	4.96	-220.49	0.00	1502.42	1185.41	-0.15	0.96	2.87	-4.30	-0.62
12.00	1.29	2.42	11.55	7.17	-317.51	0.00	1502.42	1185.41	-0.21	1.38	2.87	-4.30	-0.26
14.00	1.30	2.43	11.55	9.81	-432.16	0.00	1502.42	1185.41	-0.29	1.87	2.87	-4.30	0.15
16.00	1.31	2.45	11.55	12.92	-564.46	0.00	1502.42	1185.41	-0.38	2.45	2.87	-4.30	0.63
18.00	1.33	2.48	11.55	16.55	-714.40	0.00	1502.42	1185.41	-0.49	3.10	2.87	-4.30	1.18
20.00	1.35	2.53	11.55	20.79	-881.97	0.00	1502.42	1185.41	-0.62	3.82	2.87	-4.30	1.78
22.00	1.38	2.59	11.55	25.77	-1067.17	0.00	1502.42	1185.41	-0.77	4.62	2.87	-4.30	2.43
24.00	1.43	2.67	11.55	31.68	-1269.99	0.00	1502.42	1185.41	-0.94	5.50	2.87	-4.30	3.13
26.00	1.49	2.79	11.55	38.83	-1490.44	0.00	1502.42	1185.41	-1.16	6.46	2.87	-4.30	3.88
28.00	1.58	2.96	11.55	47.68	-1728.49	0.00	1502.42	1185.41	-1.42	7.49	2.87	-4.30	4.64
30.00	1.70	3.19	11.55	59.05	-1984.11	0.00	1502.42	1185.41	-1.76	8.60	2.87	-4.30	5.41
32.00	1.89	3.53	11.55	74.34	-2257.26	0.00	1502.42	1185.41	-2.21	9.78	2.87	-4.30	6.14
34.00	2.16	4.05	11.55	96.28	-2547.80	0.00	1502.42	1185.41	-2.87	11.04	2.87	-4.30	6.75
36.00	2.62	4.91	11.54	130.89	-2855.40	0.00	1502.42	1185.41	-3.90	12.37	2.87	-4.30	7.05
38.00	3.50	6.55	11.53	194.55	-3178.87	0.00	1502.42	1185.41	-5.79	13.78	2.87	-4.30	6.56
40.00	5.70	10.66	11.50	350.66	-3511.42	0.00	1502.42	1185.41	-10.44	15.22	2.87	-4.30	3.35
42.00	14.87	27.51	11.17	998.15	-3760.38	0.00	1502.42	1185.41	-29.71	16.30	2.87	-4.30	-14.84
44.00	540.60	-1.12	-11.55	-44.73	4269.72	0.00	1502.42	1185.41	1.33	-18.50	2.87	-4.30	-18.60
46.00	-3.56	-6.66	11.53	-289.93	-4657.94	0.00	1502.42	1185.41	8.63	20.19	2.87	-4.30	27.39
48.00	-2.09	-3.91	11.55	-185.25	-5078.22	0.00	1502.42	1185.41	5.51	22.01	2.87	-4.30	26.10
50.00	-1.42	-2.67	11.55	-137.07	-5512.19	0.00	1502.42	1185.41	4.08	23.89	2.87	-4.30	26.54
52.00	-1.05	-1.96	11.55	-109.14	-5962.83	0.00	1502.42	1185.41	3.25	25.84	2.87	-4.30	27.66
54.00	-0.81	-1.51	11.55	-90.82	-6430.76	0.00	1502.42	1185.41	2.70	27.87	2.87	-4.30	29.15
56.00	-0.64	-1.21	11.55	-77.81	-6916.19	0.00	1502.42	1185.41	2.32	29.97	2.87	-4.30	30.86
58.00	-0.53	-0.98	11.55	-68.06	-7419.19	0.00	1502.42	1185.41	2.03	32.15	2.87	-4.30	32.75
60.00	-0.44	-0.82	11.55	-60.46	-7939.78	0.00	1502.42	1185.41	1.80	34.41	2.87	-4.30	34.78

Case 4: I160B120, δ = 6 cm

L (m)	β (°)	W (cm)	V (cm)	M_y (KNm)	M_z (KNm)	φ (°)	P_{max} (KN)	M_{Pmax} (KNm)	σ_{my} (Mpa)	σ_{mz} (Mpa)	σ_p (Mpa)	σ_{MP} (Mpa)	σ_t (Mpa)
10.00	1.93	3.62	11.55	7.44	-220.40	0.00	1502.42	1185.41	-0.22	0.96	2.87	-4.30	-0.69
12.00	1.94	3.63	11.55	10.74	-317.39	0.00	1502.42	1185.41	-0.32	1.38	2.87	-4.30	-0.37
14.00	1.95	3.65	11.55	14.70	-432.01	0.00	1502.42	1185.41	-0.44	1.87	2.87	-4.30	0.01
16.00	1.97	3.68	11.55	19.37	-564.26	0.00	1502.42	1185.41	-0.58	2.45	2.87	-4.30	0.44
18.00	1.99	3.72	11.55	24.82	-714.14	0.00	1502.42	1185.41	-0.74	3.09	2.87	-4.30	0.93
20.00	2.03	3.79	11.55	31.18	-881.64	0.00	1502.42	1185.41	-0.93	3.82	2.87	-4.30	1.47
22.00	2.07	3.88	11.55	38.64	-1066.76	0.00	1502.42	1185.41	-1.15	4.62	2.87	-4.30	2.05
24.00	2.14	4.01	11.55	47.50	-1269.48	0.00	1502.42	1185.41	-1.41	5.50	2.87	-4.30	2.66
26.00	2.24	4.19	11.55	58.21	-1489.79	0.00	1502.42	1185.41	-1.73	6.46	2.87	-4.30	3.30
28.00	2.37	4.43	11.54	71.48	-1727.65	0.00	1502.42	1185.41	-2.13	7.49	2.87	-4.30	3.93
30.00	2.56	4.78	11.54	88.51	-1983.00	0.00	1502.42	1185.41	-2.63	8.59	2.87	-4.30	4.53
32.00	2.83	5.29	11.54	111.40	-2255.72	0.00	1502.42	1185.41	-3.32	9.78	2.87	-4.30	5.03
34.00	3.24	6.07	11.54	144.20	-2545.52	0.00	1502.42	1185.41	-4.29	11.03	2.87	-4.30	5.31
36.00	3.93	7.35	11.53	195.82	-2851.66	0.00	1502.42	1185.41	-5.83	12.36	2.87	-4.30	5.10
38.00	5.22	9.77	11.51	290.00	-3171.57	0.00	1502.42	1185.41	-8.63	13.74	2.87	-4.30	3.68
40.00	8.36	15.59	11.43	512.90	-3491.40	0.00	1502.42	1185.41	-15.27	15.13	2.87	-4.30	-1.56
42.00	18.39	33.84	10.96	1227.58	-3691.84	0.00	1502.42	1185.41	-36.54	16.00	2.87	-4.30	-21.97
44.00	703.37	-30.69	11.07	-1221.88	-4091.38	0.00	1502.42	1185.41	36.37	17.73	2.87	-4.30	52.68
46.00	-5.38	-10.06	11.50	-437.92	-4646.35	0.00	1502.42	1185.41	13.04	20.14	2.87	-4.30	31.75
48.00	-3.14	-5.87	11.54	-278.24	-5073.96	0.00	1502.42	1185.41	8.28	21.99	2.87	-4.30	28.84
50.00	-2.14	-4.00	11.55	-205.69	-5510.04	0.00	1502.42	1185.41	6.12	23.88	2.87	-4.30	28.57
52.00	-1.57	-2.94	11.55	-163.74	-5961.56	0.00	1502.42	1185.41	4.87	25.84	2.87	-4.30	29.28
54.00	-1.21	-2.27	11.55	-136.24	-6429.95	0.00	1502.42	1185.41	4.06	27.87	2.87	-4.30	30.49
56.00	-0.97	-1.81	11.55	-116.72	-6915.63	0.00	1502.42	1185.41	3.47	29.97	2.87	-4.30	32.02
58.00	-0.79	-1.48	11.55	-102.10	-7418.78	0.00	1502.42	1185.41	3.04	32.15	2.87	-4.30	33.76
60.00	-0.65	-1.23	11.55	-90.70	-7939.48	0.00	1502.42	1185.41	2.70	34.41	2.87	-4.30	35.68

Case 4: I160B120, δ = 8 cm

L (m)	β (°)	W (cm)	V (cm)	M_y (KNm)	M_z (KNm)	φ (°)	P_{max} (KN)	M_{Pmax} (KNm)	σ_{my} (Mpa)	σ_{mz} (Mpa)	σ_p (Mpa)	σ_{MP} (Mpa)	σ_t (Mpa)
10.00	2.58	4.82	11.54	9.91	-220.28	0.00	1502.42	1185.41	-0.29	0.95	2.87	-4.30	-0.77
12.00	2.58	4.84	11.54	14.32	-317.22	0.00	1502.42	1185.41	-0.43	1.37	2.87	-4.30	-0.48
14.00	2.60	4.86	11.54	19.60	-431.79	0.00	1502.42	1185.41	-0.58	1.87	2.87	-4.30	-0.14
16.00	2.62	4.90	11.54	25.81	-563.98	0.00	1502.42	1185.41	-0.77	2.44	2.87	-4.30	0.25
18.00	2.65	4.96	11.54	33.07	-713.78	0.00	1502.42	1185.41	-0.98	3.09	2.87	-4.30	0.68
20.00	2.70	5.05	11.54	41.55	-881.19	0.00	1502.42	1185.41	-1.24	3.82	2.87	-4.30	1.15
22.00	2.76	5.17	11.54	51.49	-1066.19	0.00	1502.42	1185.41	-1.53	4.62	2.87	-4.30	1.66
24.00	2.86	5.34	11.54	63.29	-1268.77	0.00	1502.42	1185.41	-1.88	5.50	2.87	-4.30	2.19
26.00	2.98	5.58	11.54	77.56	-1488.89	0.00	1502.42	1185.41	-2.31	6.45	2.87	-4.30	2.72
28.00	3.16	5.91	11.54	95.23	-1726.48	0.00	1502.42	1185.41	-2.83	7.48	2.87	-4.30	3.22
30.00	3.41	6.37	11.54	117.90	-1981.45	0.00	1502.42	1185.41	-3.51	8.59	2.87	-4.30	3.65
32.00	3.77	7.04	11.53	148.33	-2253.56	0.00	1502.42	1185.41	-4.42	9.77	2.87	-4.30	3.92
34.00	4.32	8.07	11.52	191.86	-2542.34	0.00	1502.42	1185.41	-5.71	11.02	2.87	-4.30	3.88
36.00	5.22	9.76	11.51	260.13	-2846.49	0.00	1502.42	1185.41	-7.74	12.34	2.87	-4.30	3.17
38.00	6.91	12.91	11.47	383.40	-3161.61	0.00	1502.42	1185.41	-11.41	13.70	2.87	-4.30	0.86
40.00	10.82	20.14	11.35	662.73	-3466.05	0.00	1502.42	1185.41	-19.73	15.02	2.87	-4.30	-6.13
42.00	21.10	38.60	10.78	1400.32	-3629.81	0.00	1502.42	1185.41	-41.69	15.73	2.87	-4.30	-27.38
44.00	754.90	61.36	9.48	2443.18	-3501.86	0.00	1502.42	1185.41	-72.73	15.18	2.87	-4.30	-58.98
46.00	-7.26	-13.56	11.46	-589.90	-4629.48	0.00	1502.42	1185.41	17.56	20.06	2.87	-4.30	36.20
48.00	-4.19	-7.84	11.52	-371.71	-5067.95	0.00	1502.42	1185.41	11.07	21.96	2.87	-4.30	31.60
50.00	-2.85	-5.34	11.54	-274.42	-5507.02	0.00	1502.42	1185.41	8.17	23.87	2.87	-4.30	30.61
52.00	-2.10	-3.93	11.55	-218.37	-5959.79	0.00	1502.42	1185.41	6.50	25.83	2.87	-4.30	30.90
54.00	-1.62	-3.03	11.55	-181.67	-6428.80	0.00	1502.42	1185.41	5.41	27.86	2.87	-4.30	31.84
56.00	-1.29	-2.41	11.55	-155.64	-6914.84	0.00	1502.42	1185.41	4.63	29.97	2.87	-4.30	33.17
58.00	-1.05	-1.97	11.55	-136.14	-7418.21	0.00	1502.42	1185.41	4.05	32.15	2.87	-4.30	34.77
60.00	-0.87	-1.63	11.55	-120.94	-7939.05	0.00	1502.42	1185.41	3.60	34.41	2.87	-4.30	36.58

Case 5: I235C150, L = 40 m

P (KN)	β (°)	W (cm)	V (cm)	M_y (KNm)	M_z (KNm)	φ (°)	P_{max} (KN)	M_{Pmax} (KNm)	σ_{my} (Mpa)	σ_{mz} (Mpa)	σ_p (Mpa)	σ_{MP} (Mpa)	σ_t (Mpa)
2159.93	1.70	1.62	4.61	113.60	-3838.29	0.00	2615.35	2587.60	-1.68	7.34	2.81	-4.82	3.64
2178.17	1.70	1.62	4.61	113.60	-3838.29	0.00	2615.35	2609.45	-1.68	7.34	2.81	-4.82	3.64
2196.41	1.70	1.62	4.61	113.60	-3838.29	0.00	2615.35	2631.30	-1.68	7.34	2.81	-4.82	3.64
2214.65	1.70	1.62	4.61	113.60	-3838.29	0.00	2615.35	2653.15	-1.68	7.34	2.81	-4.82	3.64
2232.89	1.70	1.62	4.61	113.60	-3838.29	0.00	2615.35	2675.01	-1.68	7.34	2.81	-4.82	3.64
2251.13	1.70	1.62	4.61	113.60	-3838.29	0.00	2615.35	2696.86	-1.68	7.34	2.81	-4.82	3.64
2269.37	1.70	1.62	4.61	113.60	-3838.29	0.00	2615.35	2718.71	-1.68	7.34	2.81	-4.82	3.64
2287.61	1.70	1.62	4.61	113.60	-3838.29	0.00	2615.35	2740.56	-1.68	7.34	2.81	-4.82	3.64
2305.85	1.70	1.62	4.61	113.60	-3838.29	0.00	2615.35	2762.41	-1.68	7.34	2.81	-4.82	3.64
2324.09	1.70	1.62	4.61	113.60	-3838.29	0.00	2615.35	2784.26	-1.68	7.34	2.81	-4.82	3.64
2342.33	1.70	1.62	4.61	113.60	-3838.29	0.00	2615.35	2806.12	-1.68	7.34	2.81	-4.82	3.64
2360.57	1.70	1.62	4.61	113.60	-3838.29	0.00	2615.35	2827.97	-1.68	7.34	2.81	-4.82	3.64
2378.81	1.70	1.62	4.61	113.60	-3838.29	0.00	2615.35	2849.82	-1.68	7.34	2.81	-4.82	3.64
2397.05	1.70	1.62	4.61	113.60	-3838.29	0.00	2615.35	2871.67	-1.68	7.34	2.81	-4.82	3.64
2415.29	1.70	1.62	4.61	113.60	-3838.29	0.00	2615.35	2893.52	-1.68	7.34	2.81	-4.82	3.64
2433.53	1.70	1.62	4.61	113.60	-3838.29	0.00	2615.35	2915.37	-1.68	7.34	2.81	-4.82	3.64
2451.77	1.70	1.62	4.61	113.60	-3838.29	0.00	2615.35	2937.22	-1.68	7.34	2.81	-4.82	3.64
2470.01	1.70	1.62	4.61	113.60	-3838.29	0.00	2615.35	2959.08	-1.68	7.34	2.81	-4.82	3.64
2488.25	1.70	1.62	4.61	113.60	-3838.29	0.00	2615.35	2980.93	-1.68	7.34	2.81	-4.82	3.64
2506.49	1.70	1.62	4.61	113.60	-3838.29	0.00	2615.35	3002.78	-1.68	7.34	2.81	-4.82	3.64
2524.73	1.70	1.62	4.61	113.60	-3838.29	0.00	2615.35	3024.63	-1.68	7.34	2.81	-4.82	3.64
2542.97	1.70	1.62	4.61	113.60	-3838.29	0.00	2615.35	3046.48	-1.68	7.34	2.81	-4.82	3.64
2561.21	1.70	1.62	4.61	113.60	-3838.29	0.00	2615.35	3068.33	-1.68	7.34	2.81	-4.82	3.64
2579.45	1.70	1.62	4.61	113.60	-3838.29	0.00	2615.35	3090.19	-1.68	7.34	2.81	-4.82	3.64
2597.69	1.70	1.62	4.61	113.60	-3838.29	0.00	2615.35	3112.04	-1.68	7.34	2.81	-4.82	3.64
2615.93	1.70	1.62	4.61	113.60	-3838.29	0.00	2615.35	3133.89	-1.68	7.34	2.81	-4.82	3.64

Case 5: I235C150, P = 0,90P_{max}

L (m)	β (°)	W (cm)	V (cm)	M_y (KNm)	M_z (KNm)	φ (°)	P_{max} (KN)	M_{Pmax} (KNm)	σ_{my} (Mpa)	σ_{mz} (Mpa)	σ_p (Mpa)	σ_{MP} (Mpa)	σ_t (Mpa)
10.00	0.32	0.35	5.28	1.80	-323.99	0.00	1647.67	1973.91	-0.03	0.62	2.15	-3.68	-0.94
12.00	0.38	0.42	5.27	3.12	-466.55	0.00	1647.67	1973.91	-0.05	0.89	2.15	-3.68	-0.69
14.00	0.45	0.49	5.27	4.97	-635.02	0.00	1647.67	1973.91	-0.07	1.21	2.15	-3.68	-0.39
16.00	0.51	0.56	5.27	7.45	-829.40	0.00	1647.67	1973.91	-0.11	1.59	2.15	-3.68	-0.06
18.00	0.58	0.64	5.27	10.66	-1049.70	0.00	1647.67	1973.91	-0.16	2.01	2.15	-3.68	0.32
20.00	0.65	0.71	5.27	14.73	-1295.91	0.00	1647.67	1973.91	-0.22	2.48	2.15	-3.68	0.73
22.00	0.72	0.79	5.27	19.80	-1568.02	0.00	1647.67	1973.91	-0.29	3.00	2.15	-3.68	1.17
24.00	0.80	0.88	5.27	26.06	-1866.04	0.00	1647.67	1973.91	-0.39	3.57	2.15	-3.68	1.65
26.00	0.88	0.97	5.27	33.71	-2189.96	0.00	1647.67	1973.91	-0.50	4.19	2.15	-3.68	2.15
28.00	0.97	1.06	5.27	43.06	-2539.78	0.00	1647.67	1973.91	-0.64	4.86	2.15	-3.68	2.68
30.00	1.07	1.17	5.27	54.50	-2915.47	0.00	1647.67	1973.91	-0.81	5.57	2.15	-3.68	3.23
32.00	1.18	1.30	5.27	68.57	-3317.03	0.00	1647.67	1973.91	-1.02	6.34	2.15	-3.68	3.79
34.00	1.32	1.44	5.27	86.05	-3744.42	0.00	1647.67	1973.91	-1.28	7.16	2.15	-3.68	4.35
36.00	1.48	1.62	5.27	108.12	-4197.62	0.00	1647.67	1973.91	-1.60	8.03	2.15	-3.68	4.89
38.00	1.67	1.83	5.27	136.58	-4676.53	0.00	1647.67	1973.91	-2.02	8.94	2.15	-3.68	5.38
40.00	1.93	2.11	5.27	174.43	-5181.03	0.00	1647.67	1973.91	-2.59	9.91	2.15	-3.68	5.79
42.00	2.28	2.49	5.27	226.94	-5710.81	0.00	1647.67	1973.91	-3.36	10.92	2.15	-3.68	6.02
44.00	2.78	3.05	5.27	304.36	-6265.21	0.00	1647.67	1973.91	-4.51	11.98	2.15	-3.68	5.93
46.00	3.59	3.93	5.27	429.40	-6842.33	0.00	1647.67	1973.91	-6.36	13.08	2.15	-3.68	5.18
48.00	5.10	5.58	5.25	663.50	-7435.36	0.00	1647.67	1973.91	-9.83	14.22	2.15	-3.68	2.85
50.00	8.73	9.52	5.21	1228.79	-8006.19	0.00	1647.67	1973.91	-18.21	15.31	2.15	-3.68	-4.44
52.00	19.03	20.46	4.99	2856.34	-8282.19	0.00	1647.67	1973.91	-42.34	15.84	2.15	-3.68	-28.04
54.00	180.81	-0.89	-5.27	-133.42	9446.83	0.00	1647.67	1973.91	1.98	-18.06	2.15	-3.68	-17.62
56.00	-1446.00	-6.56	5.25	-1062.25	-10104.89	0.00	1647.67	1973.91	15.75	19.32	2.15	-3.68	33.53
58.00	-3.72	-4.07	5.26	-706.41	-10876.37	0.00	1647.67	1973.91	10.47	20.80	2.15	-3.68	29.73
60.00	-2.67	-2.92	5.27	-543.21	-11651.26	0.00	1647.67	1973.91	8.05	22.28	2.15	-3.68	28.80

Case 5: I235C150, P = P_{max}

L (m)	β (°)	W (cm)	V (cm)	M_y (KNm)	M_z (KNm)	φ (°)	P_{max} (KN)	M_{Pmax} (KNm)	σ_{my} (Mpa)	σ_{mz} (Mpa)	σ_p (Mpa)	σ_{MP} (Mpa)	σ_t (Mpa)
10.00	0.32	0.35	5.28	1.80	-323.99	0.00	1830.74	2193.23	-0.03	0.62	2.38	-4.09	-1.11
12.00	0.38	0.42	5.27	3.12	-466.55	0.00	1830.74	2193.23	-0.05	0.89	2.38	-4.09	-0.86
14.00	0.45	0.49	5.27	4.97	-635.02	0.00	1830.74	2193.23	-0.07	1.21	2.38	-4.09	-0.56
16.00	0.51	0.56	5.27	7.45	-829.40	0.00	1830.74	2193.23	-0.11	1.59	2.38	-4.09	-0.23
18.00	0.58	0.64	5.27	10.66	-1049.70	0.00	1830.74	2193.23	-0.16	2.01	2.38	-4.09	0.14
20.00	0.65	0.71	5.27	14.73	-1295.91	0.00	1830.74	2193.23	-0.22	2.48	2.38	-4.09	0.56
22.00	0.72	0.79	5.27	19.80	-1568.02	0.00	1830.74	2193.23	-0.29	3.00	2.38	-4.09	1.00
24.00	0.80	0.88	5.27	26.06	-1866.04	0.00	1830.74	2193.23	-0.39	3.57	2.38	-4.09	1.48
26.00	0.88	0.97	5.27	33.71	-2189.96	0.00	1830.74	2193.23	-0.50	4.19	2.38	-4.09	1.98
28.00	0.97	1.06	5.27	43.06	-2539.78	0.00	1830.74	2193.23	-0.64	4.86	2.38	-4.09	2.51
30.00	1.07	1.17	5.27	54.50	-2915.47	0.00	1830.74	2193.23	-0.81	5.57	2.38	-4.09	3.06
32.00	1.18	1.30	5.27	68.57	-3317.03	0.00	1830.74	2193.23	-1.02	6.34	2.38	-4.09	3.62
34.00	1.32	1.44	5.27	86.05	-3744.42	0.00	1830.74	2193.23	-1.28	7.16	2.38	-4.09	4.18
36.00	1.48	1.62	5.27	108.12	-4197.62	0.00	1830.74	2193.23	-1.60	8.03	2.38	-4.09	4.72
38.00	1.67	1.83	5.27	136.58	-4676.53	0.00	1830.74	2193.23	-2.02	8.94	2.38	-4.09	5.21
40.00	1.93	2.11	5.27	174.43	-5181.03	0.00	1830.74	2193.23	-2.59	9.91	2.38	-4.09	5.62
42.00	2.28	2.49	5.27	226.94	-5710.81	0.00	1830.74	2193.23	-3.36	10.92	2.38	-4.09	5.85
44.00	2.78	3.05	5.27	304.36	-6265.21	0.00	1830.74	2193.23	-4.51	11.98	2.38	-4.09	5.76
46.00	3.59	3.93	5.27	429.40	-6842.33	0.00	1830.74	2193.23	-6.36	13.08	2.38	-4.09	5.01
48.00	5.10	5.58	5.25	663.50	-7435.36	0.00	1830.74	2193.23	-9.83	14.22	2.38	-4.09	2.68
50.00	8.73	9.52	5.21	1228.79	-8006.19	0.00	1830.74	2193.23	-18.21	15.31	2.38	-4.09	-4.61
52.00	19.03	20.46	4.99	2856.34	-8282.19	0.00	1830.74	2193.23	-42.34	15.84	2.38	-4.09	-28.21
54.00	180.81	-0.89	-5.27	-133.42	9446.83	0.00	1830.74	2193.23	1.98	-18.06	2.38	-4.09	-17.79
56.00	-1446.00	-6.56	5.25	-1062.25	-10104.89	0.00	1830.74	2193.23	15.75	19.32	2.38	-4.09	33.36
58.00	-3.72	-4.07	5.26	-706.41	-10876.37	0.00	1830.74	2193.23	10.47	20.80	2.38	-4.09	29.56
60.00	-2.67	-2.92	5.27	-543.21	-11651.26	0.00	1830.74	2193.23	8.05	22.28	2.38	-4.09	28.63

Case 5: I235C150, P = 0

L (m)	β (°)	W (cm)	V (cm)	M_y (KNm)	M_z (KNm)	φ (°)	P_{max} (KN)	M_{Pmax} (KNm)	σ_{my} (Mpa)	σ_{mz} (Mpa)	σ_p (Mpa)	σ_{MP} (Mpa)	σ_t (Mpa)
10.00	0.32	0.35	5.28	1.80	-323.99	0.00	0.00	0.00	-0.03	0.62	0.00	0.00	0.59
12.00	0.38	0.42	5.27	3.12	-466.55	0.00	0.00	0.00	-0.05	0.89	0.00	0.00	0.85
14.00	0.45	0.49	5.27	4.97	-635.02	0.00	0.00	0.00	-0.07	1.21	0.00	0.00	1.14
16.00	0.51	0.56	5.27	7.45	-829.40	0.00	0.00	0.00	-0.11	1.59	0.00	0.00	1.48
18.00	0.58	0.64	5.27	10.66	-1049.70	0.00	0.00	0.00	-0.16	2.01	0.00	0.00	1.85
20.00	0.65	0.71	5.27	14.73	-1295.91	0.00	0.00	0.00	-0.22	2.48	0.00	0.00	2.26
22.00	0.72	0.79	5.27	19.80	-1568.02	0.00	0.00	0.00	-0.29	3.00	0.00	0.00	2.70
24.00	0.80	0.88	5.27	26.06	-1866.04	0.00	0.00	0.00	-0.39	3.57	0.00	0.00	3.18
26.00	0.88	0.97	5.27	33.71	-2189.96	0.00	0.00	0.00	-0.50	4.19	0.00	0.00	3.69
28.00	0.97	1.06	5.27	43.06	-2539.78	0.00	0.00	0.00	-0.64	4.86	0.00	0.00	4.22
30.00	1.07	1.17	5.27	54.50	-2915.47	0.00	0.00	0.00	-0.81	5.57	0.00	0.00	4.77
32.00	1.18	1.30	5.27	68.57	-3317.03	0.00	0.00	0.00	-1.02	6.34	0.00	0.00	5.33
34.00	1.32	1.44	5.27	86.05	-3744.42	0.00	0.00	0.00	-1.28	7.16	0.00	0.00	5.88
36.00	1.48	1.62	5.27	108.12	-4197.62	0.00	0.00	0.00	-1.60	8.03	0.00	0.00	6.42
38.00	1.67	1.83	5.27	136.58	-4676.53	0.00	0.00	0.00	-2.02	8.94	0.00	0.00	6.92
40.00	1.93	2.11	5.27	174.43	-5181.03	0.00	0.00	0.00	-2.59	9.91	0.00	0.00	7.32
42.00	2.28	2.49	5.27	226.94	-5710.81	0.00	0.00	0.00	-3.36	10.92	0.00	0.00	7.56
44.00	2.78	3.05	5.27	304.36	-6265.21	0.00	0.00	0.00	-4.51	11.98	0.00	0.00	7.47
46.00	3.59	3.93	5.27	429.40	-6842.33	0.00	0.00	0.00	-6.36	13.08	0.00	0.00	6.72
48.00	5.10	5.58	5.25	663.50	-7435.36	0.00	0.00	0.00	-9.83	14.22	0.00	0.00	4.38
50.00	8.73	9.52	5.21	1228.79	-8006.19	0.00	0.00	0.00	-18.21	15.31	0.00	0.00	-2.91
52.00	19.03	20.46	4.99	2856.34	-8282.19	0.00	0.00	0.00	-42.34	15.84	0.00	0.00	-26.50
54.00	180.81	-0.89	-5.27	-133.42	9446.83	0.00	0.00	0.00	1.98	-18.06	0.00	0.00	-16.09
56.00	-1446.00	-6.56	5.25	-1062.25	-10104.89	0.00	0.00	0.00	15.75	19.32	0.00	0.00	35.07
58.00	-3.72	-4.07	5.26	-706.41	-10876.37	0.00	0.00	0.00	10.47	20.80	0.00	0.00	31.27
60.00	-2.67	-2.92	5.27	-543.21	-11651.26	0.00	0.00	0.00	8.05	22.28	0.00	0.00	30.33

Case 6: I235C150, L = 40 m

h_l (m)	β (°)	W (cm)	V (cm)	M_y (KNm)	M_z (KNm)	φ (°)	P_{max} (KN)	M_{Pmax} (KNm)	σ_{my} (Mpa)	σ_{mz} (Mpa)	σ_p (Mpa)	σ_{MP} (Mpa)	σ_t (Mpa)
0.20	2.03	1.95	4.60	136.26	-3837.55	0.00	2615.35	2587.60	-2.02	7.34	2.81	-4.82	3.31
0.25	1.93	1.85	4.61	129.54	-3837.79	0.00	2615.35	2587.60	-1.92	7.34	2.81	-4.82	3.41
0.30	1.84	1.76	4.61	123.46	-3837.99	0.00	2615.35	2587.60	-1.83	7.34	2.81	-4.82	3.50
0.36	1.76	1.68	4.61	117.92	-3838.16	0.00	2615.35	2587.60	-1.75	7.34	2.81	-4.82	3.58
0.41	1.68	1.61	4.61	112.85	-3838.31	0.00	2615.35	2587.60	-1.67	7.34	2.81	-4.82	3.66
0.46	1.61	1.54	4.61	108.21	-3838.45	0.00	2615.35	2587.60	-1.60	7.34	2.81	-4.82	3.72
0.51	1.55	1.48	4.61	103.93	-3838.57	0.00	2615.35	2587.60	-1.54	7.34	2.81	-4.82	3.79
0.56	1.49	1.43	4.61	99.97	-3838.67	0.00	2615.35	2587.60	-1.48	7.34	2.81	-4.82	3.85
0.62	1.44	1.37	4.61	96.31	-3838.76	0.00	2615.35	2587.60	-1.43	7.34	2.81	-4.82	3.90
0.67	1.39	1.33	4.61	92.90	-3838.85	0.00	2615.35	2587.60	-1.38	7.34	2.81	-4.82	3.95
0.72	1.34	1.28	4.61	89.73	-3838.92	0.00	2615.35	2587.60	-1.33	7.34	2.81	-4.82	4.00
0.77	1.29	1.24	4.61	86.76	-3838.99	0.00	2615.35	2587.60	-1.29	7.34	2.81	-4.82	4.04
0.82	1.25	1.20	4.61	83.99	-3839.05	0.00	2615.35	2587.60	-1.24	7.34	2.81	-4.82	4.08
0.88	1.21	1.16	4.61	81.39	-3839.11	0.00	2615.35	2587.60	-1.21	7.34	2.81	-4.82	4.12
0.93	1.18	1.13	4.61	78.94	-3839.16	0.00	2615.35	2587.60	-1.17	7.34	2.81	-4.82	4.16
0.98	1.14	1.09	4.61	76.64	-3839.21	0.00	2615.35	2587.60	-1.14	7.34	2.81	-4.82	4.19
1.03	1.11	1.06	4.61	74.46	-3839.25	0.00	2615.35	2587.60	-1.10	7.34	2.81	-4.82	4.23
1.08	1.08	1.03	4.61	72.41	-3839.29	0.00	2615.35	2587.60	-1.07	7.34	2.81	-4.82	4.26
1.14	1.05	1.01	4.61	70.47	-3839.33	0.00	2615.35	2587.60	-1.04	7.34	2.81	-4.82	4.29
1.19	1.02	0.98	4.61	68.63	-3839.36	0.00	2615.35	2587.60	-1.02	7.34	2.81	-4.82	4.31
1.24	1.00	0.95	4.61	66.88	-3839.39	0.00	2615.35	2587.60	-0.99	7.34	2.81	-4.82	4.34
1.29	0.97	0.93	4.61	65.22	-3839.42	0.00	2615.35	2587.60	-0.97	7.34	2.81	-4.82	4.36
1.34	0.95	0.91	4.61	63.64	-3839.45	0.00	2615.35	2587.60	-0.94	7.34	2.81	-4.82	4.39
1.40	0.93	0.89	4.61	62.13	-3839.47	0.00	2615.35	2587.60	-0.92	7.34	2.81	-4.82	4.41
1.45	0.91	0.87	4.61	60.70	-3839.49	0.00	2615.35	2587.60	-0.90	7.34	2.81	-4.82	4.43
1.50	0.89	0.85	4.61	59.32	-3839.51	0.00	2615.35	2587.60	-0.88	7.34	2.81	-4.82	4.45

Case 6: I235C150, h_l = 20 cm

L (m)	β (°)	W (cm)	V (cm)	M_y (KNm)	M_z (KNm)	φ (°)	P_{max} (KN)	M_{Pmax} (KNm)	σ_{my} (Mpa)	σ_{mz} (Mpa)	σ_p (Mpa)	σ_{MP} (Mpa)	σ_t (Mpa)
10.00	0.36	0.40	5.27	2.06	-323.99	0.00	1830.74	2193.23	-0.03	0.62	2.38	-4.09	-1.12
12.00	0.44	0.48	5.27	3.57	-466.54	0.00	1830.74	2193.23	-0.05	0.89	2.38	-4.09	-0.87
14.00	0.51	0.56	5.27	5.69	-635.01	0.00	1830.74	2193.23	-0.08	1.21	2.38	-4.09	-0.57
16.00	0.59	0.64	5.27	8.52	-829.39	0.00	1830.74	2193.23	-0.13	1.59	2.38	-4.09	-0.24
18.00	0.67	0.73	5.27	12.21	-1049.68	0.00	1830.74	2193.23	-0.18	2.01	2.38	-4.09	0.12
20.00	0.75	0.82	5.27	16.89	-1295.88	0.00	1830.74	2193.23	-0.25	2.48	2.38	-4.09	0.52
22.00	0.83	0.91	5.27	22.74	-1567.98	0.00	1830.74	2193.23	-0.34	3.00	2.38	-4.09	0.96
24.00	0.92	1.01	5.27	29.98	-1865.99	0.00	1830.74	2193.23	-0.44	3.57	2.38	-4.09	1.42
26.00	1.02	1.11	5.27	38.89	-2189.88	0.00	1830.74	2193.23	-0.58	4.19	2.38	-4.09	1.91
28.00	1.12	1.23	5.27	49.86	-2539.65	0.00	1830.74	2193.23	-0.74	4.86	2.38	-4.09	2.41
30.00	1.25	1.36	5.27	63.39	-2915.29	0.00	1830.74	2193.23	-0.94	5.57	2.38	-4.09	2.93
32.00	1.39	1.52	5.27	80.23	-3316.77	0.00	1830.74	2193.23	-1.19	6.34	2.38	-4.09	3.45
34.00	1.55	1.70	5.27	101.48	-3744.04	0.00	1830.74	2193.23	-1.50	7.16	2.38	-4.09	3.95
36.00	1.76	1.93	5.27	128.84	-4197.03	0.00	1830.74	2193.23	-1.91	8.03	2.38	-4.09	4.41
38.00	2.02	2.21	5.27	165.09	-4675.61	0.00	1830.74	2193.23	-2.45	8.94	2.38	-4.09	4.79
40.00	2.38	2.60	5.27	215.07	-5179.50	0.00	1830.74	2193.23	-3.19	9.90	2.38	-4.09	5.01
42.00	2.89	3.16	5.27	288.06	-5708.06	0.00	1830.74	2193.23	-4.27	10.91	2.38	-4.09	4.94
44.00	3.69	4.04	5.26	404.12	-6259.56	0.00	1830.74	2193.23	-5.99	11.97	2.38	-4.09	4.27
46.00	5.15	5.64	5.25	615.62	-6828.09	0.00	1830.74	2193.23	-9.13	13.06	2.38	-4.09	2.23
48.00	8.49	9.26	5.22	1101.49	-7383.19	0.00	1830.74	2193.23	-16.33	14.12	2.38	-4.09	-3.91
50.00	17.85	19.24	5.02	2483.15	-7709.93	0.00	1830.74	2193.23	-36.81	14.74	2.38	-4.09	-23.77
52.00	180.90	-0.98	-5.27	-137.42	8759.82	0.00	1830.74	2193.23	2.04	-16.75	2.38	-4.09	-16.42
54.00	-35.56	-36.49	4.29	-5493.82	-7686.25	0.00	1830.74	2193.23	81.43	14.70	2.38	-4.09	94.43
56.00	-4.19	-4.59	5.26	-742.48	-10133.40	0.00	1830.74	2193.23	11.01	19.38	2.38	-4.09	28.68
58.00	-2.96	-3.25	5.27	-563.64	-10884.70	0.00	1830.74	2193.23	8.35	20.81	2.38	-4.09	27.46
60.00	-2.27	-2.49	5.27	-462.23	-11654.75	0.00	1830.74	2193.23	6.85	22.28	2.38	-4.09	27.43

Case 6: I235C150, h_l = 60 cm

L (m)	β (°)	W (cm)	V (cm)	M_y (KNm)	M_z (KNm)	φ (°)	P_{max} (KN)	M_{Pmax} (KNm)	σ_{my} (Mpa)	σ_{mz} (Mpa)	σ_p (Mpa)	σ_{MP} (Mpa)	σ_t (Mpa)
10.00	0.28	0.31	5.27	1.60	-323.99	0.00	1830.74	2193.23	-0.02	0.62	2.38	-4.09	-1.11
12.00	0.34	0.37	5.27	2.77	-466.55	0.00	1830.74	2193.23	-0.04	0.89	2.38	-4.09	-0.85
14.00	0.40	0.44	5.27	4.42	-635.02	0.00	1830.74	2193.23	-0.07	1.21	2.38	-4.09	-0.56
16.00	0.46	0.50	5.27	6.61	-829.41	0.00	1830.74	2193.23	-0.10	1.59	2.38	-4.09	-0.22
18.00	0.52	0.57	5.27	9.46	-1049.71	0.00	1830.74	2193.23	-0.14	2.01	2.38	-4.09	0.16
20.00	0.58	0.63	5.27	13.06	-1295.92	0.00	1830.74	2193.23	-0.19	2.48	2.38	-4.09	0.58
22.00	0.64	0.70	5.27	17.54	-1568.05	0.00	1830.74	2193.23	-0.26	3.00	2.38	-4.09	1.03
24.00	0.71	0.77	5.27	23.04	-1866.08	0.00	1830.74	2193.23	-0.34	3.57	2.38	-4.09	1.52
26.00	0.78	0.85	5.27	29.75	-2190.02	0.00	1830.74	2193.23	-0.44	4.19	2.38	-4.09	2.04
28.00	0.85	0.94	5.27	37.90	-2539.86	0.00	1830.74	2193.23	-0.56	4.86	2.38	-4.09	2.59
30.00	0.94	1.03	5.27	47.80	-2915.59	0.00	1830.74	2193.23	-0.71	5.57	2.38	-4.09	3.16
32.00	1.03	1.13	5.27	59.87	-3317.20	0.00	1830.74	2193.23	-0.89	6.34	2.38	-4.09	3.75
34.00	1.14	1.25	5.27	74.70	-3744.67	0.00	1830.74	2193.23	-1.11	7.16	2.38	-4.09	4.35
36.00	1.27	1.39	5.27	93.14	-4197.98	0.00	1830.74	2193.23	-1.38	8.03	2.38	-4.09	4.94
38.00	1.43	1.56	5.27	116.46	-4677.08	0.00	1830.74	2193.23	-1.73	8.94	2.38	-4.09	5.51
40.00	1.62	1.78	5.27	146.69	-5181.89	0.00	1830.74	2193.23	-2.17	9.91	2.38	-4.09	6.03
42.00	1.88	2.06	5.27	187.18	-5712.25	0.00	1830.74	2193.23	-2.77	10.92	2.38	-4.09	6.44
44.00	2.23	2.44	5.27	243.98	-6267.85	0.00	1830.74	2193.23	-3.62	11.98	2.38	-4.09	6.66
46.00	2.75	3.01	5.27	329.11	-6847.89	0.00	1830.74	2193.23	-4.88	13.09	2.38	-4.09	6.51
48.00	3.61	3.95	5.26	470.28	-7450.08	0.00	1830.74	2193.23	-6.97	14.25	2.38	-4.09	5.57
50.00	5.29	5.79	5.25	746.96	-8065.43	0.00	1830.74	2193.23	-11.07	15.42	2.38	-4.09	2.65
52.00	9.67	10.54	5.20	1470.94	-8636.53	0.00	1830.74	2193.23	-21.80	16.51	2.38	-4.09	-6.99
54.00	21.47	22.97	4.91	3458.12	-8792.15	0.00	1830.74	2193.23	-51.26	16.81	2.38	-4.09	-36.15
56.00	-325.89	35.20	4.37	5698.41	-8412.21	0.00	1830.74	2193.23	-84.47	16.08	2.38	-4.09	-70.09
58.00	-5.00	-5.47	5.25	-949.25	-10857.87	0.00	1830.74	2193.23	14.07	20.76	2.38	-4.09	33.13
60.00	-3.24	-3.55	5.27	-658.95	-11645.29	0.00	1830.74	2193.23	9.77	22.27	2.38	-4.09	30.33

Case 6: I235C150, h_l = 100 cm

L (m)	β (°)	W (cm)	V (cm)	M_y (KNm)	M_z (KNm)	φ (°)	P_{max} (KN)	M_{Pmax} (KNm)	σ_{my} (Mpa)	σ_{mz} (Mpa)	σ_p (Mpa)	σ_{MP} (Mpa)	σ_t (Mpa)
10.00	0.23	0.25	5.28	1.31	-324.00	0.00	1830.74	2193.23	-0.02	0.62	2.38	-4.09	-1.10
12.00	0.28	0.31	5.27	2.27	-466.55	0.00	1830.74	2193.23	-0.03	0.89	2.38	-4.09	-0.85
14.00	0.33	0.36	5.27	3.61	-635.03	0.00	1830.74	2193.23	-0.05	1.21	2.38	-4.09	-0.54
16.00	0.37	0.41	5.27	5.40	-829.42	0.00	1830.74	2193.23	-0.08	1.59	2.38	-4.09	-0.20
18.00	0.42	0.46	5.27	7.72	-1049.72	0.00	1830.74	2193.23	-0.11	2.01	2.38	-4.09	0.19
20.00	0.47	0.52	5.27	10.65	-1295.95	0.00	1830.74	2193.23	-0.16	2.48	2.38	-4.09	0.62
22.00	0.52	0.57	5.27	14.27	-1568.08	0.00	1830.74	2193.23	-0.21	3.00	2.38	-4.09	1.08
24.00	0.57	0.63	5.28	18.71	-1866.13	0.00	1830.74	2193.23	-0.28	3.57	2.38	-4.09	1.59
26.00	0.63	0.69	5.27	24.09	-2190.09	0.00	1830.74	2193.23	-0.36	4.19	2.38	-4.09	2.13
28.00	0.69	0.76	5.27	30.57	-2539.96	0.00	1830.74	2193.23	-0.45	4.86	2.38	-4.09	2.70
30.00	0.75	0.83	5.27	38.37	-2915.73	0.00	1830.74	2193.23	-0.57	5.58	2.38	-4.09	3.30
32.00	0.82	0.90	5.27	47.76	-3317.39	0.00	1830.74	2193.23	-0.71	6.34	2.38	-4.09	3.93
34.00	0.90	0.99	5.27	59.10	-3744.95	0.00	1830.74	2193.23	-0.88	7.16	2.38	-4.09	4.58
36.00	1.00	1.09	5.27	72.92	-4198.38	0.00	1830.74	2193.23	-1.08	8.03	2.38	-4.09	5.24
38.00	1.10	1.21	5.27	89.95	-4677.66	0.00	1830.74	2193.23	-1.33	8.94	2.38	-4.09	5.91
40.00	1.23	1.35	5.27	111.28	-5182.77	0.00	1830.74	2193.23	-1.65	9.91	2.38	-4.09	6.56
42.00	1.39	1.52	5.27	138.59	-5713.64	0.00	1830.74	2193.23	-2.05	10.92	2.38	-4.09	7.17
44.00	1.60	1.75	5.27	174.61	-6270.16	0.00	1830.74	2193.23	-2.59	11.99	2.38	-4.09	7.70
46.00	1.87	2.05	5.27	224.11	-6852.13	0.00	1830.74	2193.23	-3.32	13.10	2.38	-4.09	8.08
48.00	2.27	2.49	5.27	296.17	-7459.03	0.00	1830.74	2193.23	-4.39	14.26	2.38	-4.09	8.17
50.00	2.90	3.18	5.27	410.45	-8089.54	0.00	1830.74	2193.23	-6.08	15.47	2.38	-4.09	7.68
52.00	4.05	4.43	5.26	618.33	-8739.05	0.00	1830.74	2193.23	-9.17	16.71	2.38	-4.09	5.84
54.00	6.69	7.31	5.24	1100.38	-9383.47	0.00	1830.74	2193.23	-16.31	17.94	2.38	-4.09	-0.07
56.00	14.99	16.23	5.09	2627.70	-9814.90	0.00	1830.74	2193.23	-38.95	18.77	2.38	-4.09	-21.89
58.00	28.64	30.08	4.63	5223.85	-9565.86	0.00	1830.74	2193.23	-77.43	18.29	2.38	-4.09	-60.85
60.00	-33.94	-35.04	4.38	-6512.21	-9676.68	0.00	1830.74	2193.23	96.53	18.50	2.38	-4.09	113.33

Case 6: I235C150, h_l = 140 cm

L (m)	β (°)	W (cm)	V (cm)	M_y (KNm)	M_z (KNm)	φ (°)	P_{max} (KN)	M_{Pmax} (KNm)	σ_{my} (Mpa)	σ_{mz} (Mpa)	σ_p (Mpa)	σ_{MP} (Mpa)	σ_t (Mpa)
10.00	0.20	0.21	5.28	1.11	-324.00	0.00	1830.74	2193.23	-0.02	0.62	2.38	-4.09	-1.10
12.00	0.24	0.26	5.28	1.92	-466.55	0.00	1830.74	2193.23	-0.03	0.89	2.38	-4.09	-0.84
14.00	0.28	0.30	5.27	3.05	-635.03	0.00	1830.74	2193.23	-0.05	1.21	2.38	-4.09	-0.54
16.00	0.32	0.35	5.27	4.56	-829.42	0.00	1830.74	2193.23	-0.07	1.59	2.38	-4.09	-0.19
18.00	0.36	0.39	5.27	6.52	-1049.73	0.00	1830.74	2193.23	-0.10	2.01	2.38	-4.09	0.21
20.00	0.40	0.44	5.28	8.99	-1295.96	0.00	1830.74	2193.23	-0.13	2.48	2.38	-4.09	0.64
22.00	0.44	0.48	5.28	12.03	-1568.10	0.00	1830.74	2193.23	-0.18	3.00	2.38	-4.09	1.12
24.00	0.48	0.53	5.28	15.75	-1866.16	0.00	1830.74	2193.23	-0.23	3.57	2.38	-4.09	1.63
26.00	0.53	0.58	5.27	20.24	-2190.13	0.00	1830.74	2193.23	-0.30	4.19	2.38	-4.09	2.18
28.00	0.58	0.63	5.28	25.62	-2540.01	0.00	1830.74	2193.23	-0.38	4.86	2.38	-4.09	2.77
30.00	0.63	0.69	5.27	32.04	-2915.80	0.00	1830.74	2193.23	-0.47	5.58	2.38	-4.09	3.40
32.00	0.69	0.75	5.27	39.72	-3317.50	0.00	1830.74	2193.23	-0.59	6.34	2.38	-4.09	4.05
34.00	0.75	0.82	5.27	48.89	-3745.09	0.00	1830.74	2193.23	-0.72	7.16	2.38	-4.09	4.73
36.00	0.82	0.90	5.27	59.92	-4198.58	0.00	1830.74	2193.23	-0.89	8.03	2.38	-4.09	5.44
38.00	0.90	0.98	5.27	73.27	-4677.95	0.00	1830.74	2193.23	-1.09	8.94	2.38	-4.09	6.15
40.00	0.99	1.09	5.27	89.64	-5183.19	0.00	1830.74	2193.23	-1.33	9.91	2.38	-4.09	6.88
42.00	1.10	1.21	5.27	110.02	-5714.26	0.00	1830.74	2193.23	-1.63	10.93	2.38	-4.09	7.59
44.00	1.24	1.36	5.27	135.93	-6271.12	0.00	1830.74	2193.23	-2.01	11.99	2.38	-4.09	8.27
46.00	1.42	1.55	5.27	169.84	-6853.69	0.00	1830.74	2193.23	-2.52	13.10	2.38	-4.09	8.88
48.00	1.66	1.82	5.27	215.97	-7461.78	0.00	1830.74	2193.23	-3.20	14.27	2.38	-4.09	9.36
50.00	2.00	2.19	5.27	282.17	-8095.03	0.00	1830.74	2193.23	-4.18	15.48	2.38	-4.09	9.59
52.00	2.52	2.76	5.27	384.96	-8752.44	0.00	1830.74	2193.23	-5.71	16.74	2.38	-4.09	9.32
54.00	3.43	3.76	5.27	565.64	-9430.83	0.00	1830.74	2193.23	-8.38	18.03	2.38	-4.09	7.94
56.00	5.42	5.93	5.25	960.18	-10115.10	0.00	1830.74	2193.23	-14.23	19.34	2.38	-4.09	3.40
58.00	11.63	12.65	5.17	2197.83	-10675.39	0.00	1830.74	2193.23	-32.58	20.41	2.38	-4.09	-13.87
60.00	25.16	26.68	4.77	4959.12	-10557.18	0.00	1830.74	2193.23	-73.51	20.19	2.38	-4.09	-55.03

Case 7: I235C150, L = 40 m

ψ (°)	β (°)	W (cm)	V (cm)	M_y (KNm)	M_z (KNm)	φ (°)	P_{max} (KN)	M_{Pmax} (KNm)	σ_{my} (Mpa)	σ_{mz} (Mpa)	σ_p (Mpa)	σ_{MP} (Mpa)
0.00	1.70	1.68	4.74	113.60	-3838.29	0.00	2587.60	-1.35	7.34	2.81	-4.82	3.98
1.80	1.70	1.68	4.74	113.79	-3852.76	0.00	2587.60	-1.35	7.37	2.81	-4.82	4.01
3.60	1.70	1.69	4.74	113.98	-3867.21	0.00	2587.60	-1.35	7.39	2.81	-4.82	4.03
5.40	1.70	1.69	4.74	114.17	-3881.66	0.00	2587.60	-1.35	7.42	2.81	-4.82	4.06
7.20	1.71	1.69	4.74	114.36	-3896.16	0.00	2587.60	-1.36	7.45	2.81	-4.82	4.08
9.00	1.71	1.69	4.74	114.55	-3910.72	0.00	2587.60	-1.36	7.48	2.81	-4.82	4.11
10.80	1.71	1.70	4.74	114.74	-3925.38	0.00	2587.60	-1.36	7.51	2.81	-4.82	4.13
12.60	1.72	1.70	4.74	114.94	-3940.17	0.00	2587.60	-1.36	7.53	2.81	-4.82	4.16
14.40	1.72	1.70	4.74	115.14	-3955.11	0.00	2587.60	-1.37	7.56	2.81	-4.82	4.19
16.20	1.72	1.71	4.74	115.34	-3970.24	0.00	2587.60	-1.37	7.59	2.81	-4.82	4.21
18.00	1.72	1.71	4.74	115.54	-3985.60	0.00	2587.60	-1.37	7.62	2.81	-4.82	4.24
19.80	1.73	1.71	4.74	115.75	-4001.22	0.00	2587.60	-1.37	7.65	2.81	-4.82	4.27
21.60	1.73	1.71	4.74	115.97	-4017.13	0.00	2587.60	-1.38	7.68	2.81	-4.82	4.30
23.40	1.73	1.72	4.74	116.19	-4033.39	0.00	2587.60	-1.38	7.71	2.81	-4.82	4.32
25.20	1.74	1.72	4.74	116.41	-4050.03	0.00	2587.60	-1.38	7.74	2.81	-4.82	4.35
27.00	1.74	1.72	4.74	116.65	-4067.11	0.00	2587.60	-1.38	7.78	2.81	-4.82	4.38
28.80	1.74	1.73	4.74	116.89	-4084.66	0.00	2587.60	-1.39	7.81	2.81	-4.82	4.41
30.60	1.75	1.73	4.74	117.14	-4102.76	0.00	2587.60	-1.39	7.84	2.81	-4.82	4.45
32.40	1.75	1.74	4.74	117.39	-4121.47	0.00	2587.60	-1.39	7.88	2.81	-4.82	4.48
34.20	1.76	1.74	4.74	117.66	-4140.84	0.00	2587.60	-1.40	7.92	2.81	-4.82	4.51
36.00	1.76	1.74	4.74	117.94	-4160.97	0.00	2587.60	-1.40	7.96	2.81	-4.82	4.55
37.80	1.76	1.75	4.73	118.24	-4181.94	0.00	2587.60	-1.40	8.00	2.81	-4.82	4.58
39.60	1.77	1.75	4.73	118.54	-4203.84	0.00	2587.60	-1.41	8.04	2.81	-4.82	4.62
41.40	1.77	1.76	4.73	118.87	-4226.79	0.00	2587.60	-1.41	8.08	2.81	-4.82	4.66
43.20	1.78	1.76	4.73	119.21	-4250.91	0.00	2587.60	-1.41	8.13	2.81	-4.82	4.70
45.00	1.78	1.77	4.73	119.58	-4276.35	0.00	2587.60	-1.42	8.18	2.81	-4.82	4.75

Case 7: I235C150, $\psi = 0$

L (m)	β (°)	W (cm)	V (cm)	M_y (KNm)	M_z (KNm)	φ (°)	P_{max} (KN)	M_{Pmax} (KNm)	σ_{my} (Mpa)	σ_{mz} (Mpa)	σ_p (Mpa)	σ_{MP} (Mpa)	σ_t (Mpa)
10.00	0.32	0.35	5.28	1.80	-323.99	0.00	1830.74	2193.23	-0.03	0.62	2.38	-4.09	-1.11
12.00	0.38	0.42	5.27	3.12	-466.55	0.00	1830.74	2193.23	-0.05	0.89	2.38	-4.09	-0.86
14.00	0.45	0.49	5.27	4.97	-635.02	0.00	1830.74	2193.23	-0.07	1.21	2.38	-4.09	-0.56
16.00	0.51	0.56	5.27	7.45	-829.40	0.00	1830.74	2193.23	-0.11	1.59	2.38	-4.09	-0.23
18.00	0.58	0.64	5.27	10.66	-1049.70	0.00	1830.74	2193.23	-0.16	2.01	2.38	-4.09	0.14
20.00	0.65	0.71	5.27	14.73	-1295.91	0.00	1830.74	2193.23	-0.22	2.48	2.38	-4.09	0.56
22.00	0.72	0.79	5.27	19.80	-1568.02	0.00	1830.74	2193.23	-0.29	3.00	2.38	-4.09	1.00
24.00	0.80	0.88	5.27	26.06	-1866.04	0.00	1830.74	2193.23	-0.39	3.57	2.38	-4.09	1.48
26.00	0.88	0.97	5.27	33.71	-2189.96	0.00	1830.74	2193.23	-0.50	4.19	2.38	-4.09	1.98
28.00	0.97	1.06	5.27	43.06	-2539.78	0.00	1830.74	2193.23	-0.64	4.86	2.38	-4.09	2.51
30.00	1.07	1.17	5.27	54.50	-2915.47	0.00	1830.74	2193.23	-0.81	5.57	2.38	-4.09	3.06
32.00	1.18	1.30	5.27	68.57	-3317.03	0.00	1830.74	2193.23	-1.02	6.34	2.38	-4.09	3.62
34.00	1.32	1.44	5.27	86.05	-3744.42	0.00	1830.74	2193.23	-1.28	7.16	2.38	-4.09	4.18
36.00	1.48	1.62	5.27	108.12	-4197.62	0.00	1830.74	2193.23	-1.60	8.03	2.38	-4.09	4.72
38.00	1.67	1.83	5.27	136.58	-4676.53	0.00	1830.74	2193.23	-2.02	8.94	2.38	-4.09	5.21
40.00	1.93	2.11	5.27	174.43	-5181.03	0.00	1830.74	2193.23	-2.59	9.91	2.38	-4.09	5.62
42.00	2.28	2.49	5.27	226.94	-5710.81	0.00	1830.74	2193.23	-3.36	10.92	2.38	-4.09	5.85
44.00	2.78	3.05	5.27	304.36	-6265.21	0.00	1830.74	2193.23	-4.51	11.98	2.38	-4.09	5.76
46.00	3.59	3.93	5.27	429.40	-6842.33	0.00	1830.74	2193.23	-6.36	13.08	2.38	-4.09	5.01
48.00	5.10	5.58	5.25	663.50	-7435.36	0.00	1830.74	2193.23	-9.83	14.22	2.38	-4.09	2.68
50.00	8.73	9.52	5.21	1228.79	-8006.19	0.00	1830.74	2193.23	-18.21	15.31	2.38	-4.09	-4.61
52.00	19.03	20.46	4.99	2856.34	-8282.19	0.00	1830.74	2193.23	-42.34	15.84	2.38	-4.09	-28.21
54.00	180.81	-0.89	-5.27	-133.42	9446.83	0.00	1830.74	2193.23	1.98	-18.06	2.38	-4.09	-17.79
56.00	-1446.00	-6.56	5.25	-1062.25	-10104.89	0.00	1830.74	2193.23	15.75	19.32	2.38	-4.09	33.36
58.00	-3.72	-4.07	5.26	-706.41	-10876.37	0.00	1830.74	2193.23	10.47	20.80	2.38	-4.09	29.56
60.00	-2.67	-2.92	5.27	-543.21	-11651.26	0.00	1830.74	2193.23	8.05	22.28	2.38	-4.09	28.63

Case 7: I235C150, ψ = 15°

L (m)	β (°)	W (cm)	V (cm)	M_y (KNm)	M_z (KNm)	φ (°)	P_{max} (KN)	M_{Pmax} (KNm)	σ_{my} (Mpa)	σ_{mz} (Mpa)	σ_p (Mpa)	σ_{MP} (Mpa)	σ_t (Mpa)
10.00	0.32	0.44	6.36	1.81	-379.39	0.00	1830.74	2193.23	-0.03	0.73	2.38	-4.09	-1.01
12.00	0.38	0.51	6.17	3.12	-532.92	0.00	1830.74	2193.23	-0.05	1.02	2.38	-4.09	-0.73
14.00	0.45	0.58	6.04	4.98	-712.24	0.00	1830.74	2193.23	-0.07	1.36	2.38	-4.09	-0.42
16.00	0.52	0.65	5.95	7.46	-917.29	0.00	1830.74	2193.23	-0.11	1.75	2.38	-4.09	-0.06
18.00	0.58	0.73	5.87	10.68	-1148.00	0.00	1830.74	2193.23	-0.16	2.20	2.38	-4.09	0.33
20.00	0.65	0.80	5.80	14.77	-1404.24	0.00	1830.74	2193.23	-0.22	2.69	2.38	-4.09	0.76
22.00	0.73	0.89	5.75	19.88	-1685.89	0.00	1830.74	2193.23	-0.29	3.22	2.38	-4.09	1.22
24.00	0.80	0.97	5.70	26.18	-1992.77	0.00	1830.74	2193.23	-0.39	3.81	2.38	-4.09	1.72
26.00	0.89	1.06	5.66	33.92	-2324.70	0.00	1830.74	2193.23	-0.50	4.44	2.38	-4.09	2.24
28.00	0.98	1.16	5.63	43.39	-2681.44	0.00	1830.74	2193.23	-0.64	5.13	2.38	-4.09	2.78
30.00	1.08	1.27	5.59	55.00	-3062.71	0.00	1830.74	2193.23	-0.82	5.86	2.38	-4.09	3.34
32.00	1.20	1.40	5.56	69.34	-3468.23	0.00	1830.74	2193.23	-1.03	6.63	2.38	-4.09	3.90
34.00	1.33	1.55	5.53	87.21	-3897.61	0.00	1830.74	2193.23	-1.29	7.45	2.38	-4.09	4.46
36.00	1.50	1.73	5.50	109.83	-4350.46	0.00	1830.74	2193.23	-1.63	8.32	2.38	-4.09	4.99
38.00	1.70	1.96	5.47	139.13	-4826.28	0.00	1830.74	2193.23	-2.06	9.23	2.38	-4.09	5.46
40.00	1.97	2.25	5.45	178.22	-5324.47	0.00	1830.74	2193.23	-2.64	10.18	2.38	-4.09	5.83
42.00	2.33	2.64	5.42	232.65	-5844.24	0.00	1830.74	2193.23	-3.45	11.17	2.38	-4.09	6.02
44.00	2.86	3.22	5.39	313.15	-6384.33	0.00	1830.74	2193.23	-4.64	12.21	2.38	-4.09	5.86
46.00	3.71	4.15	5.36	443.49	-6942.19	0.00	1830.74	2193.23	-6.57	13.27	2.38	-4.09	5.00
48.00	5.29	5.87	5.32	687.80	-7510.01	0.00	1830.74	2193.23	-10.20	14.36	2.38	-4.09	2.46
50.00	9.05	9.97	5.25	1274.77	-8047.42	0.00	1830.74	2193.23	-18.90	15.39	2.38	-4.09	-5.21
52.00	19.41	20.95	4.99	2911.82	-8286.53	0.00	1830.74	2193.23	-43.16	15.84	2.38	-4.09	-29.02
54.00	180.85	-0.84	-4.87	-140.57	8841.82	0.00	1830.74	2193.23	2.08	-16.91	2.38	-4.09	-16.53
56.00	-179.18	-0.81	-4.85	-145.61	9484.13	0.00	1830.74	2193.23	2.16	-18.13	2.38	-4.09	-17.68
58.00	-3.97	-4.25	5.17	-753.79	-10723.40	0.00	1830.74	2193.23	11.17	20.50	2.38	-4.09	29.97
60.00	-2.87	-3.05	5.15	-583.30	-11427.39	0.00	1830.74	2193.23	8.65	21.85	2.38	-4.09	28.79

Case 7: I235C150, ψ = 30°

L (m)	β (°)	W (cm)	V (cm)	M_y (KNm)	M_z (KNm)	φ (°)	P_{max} (KN)	M_{Pmax} (KNm)	σ_{my} (Mpa)	σ_{mz} (Mpa)	σ_p (Mpa)	σ_{MP} (Mpa)	σ_t (Mpa)
10.00	0.32	0.54	7.60	1.81	-443.32	0.00	1830.74	2193.23	-0.03	0.85	2.38	-4.09	-0.88
12.00	0.38	0.61	7.21	3.13	-609.45	0.00	1830.74	2193.23	-0.05	1.17	2.38	-4.09	-0.59
14.00	0.45	0.69	6.93	4.98	-801.23	0.00	1830.74	2193.23	-0.07	1.53	2.38	-4.09	-0.25
16.00	0.52	0.76	6.72	7.47	-1018.48	0.00	1830.74	2193.23	-0.11	1.95	2.38	-4.09	0.13
18.00	0.58	0.83	6.55	10.70	-1261.02	0.00	1830.74	2193.23	-0.16	2.41	2.38	-4.09	0.55
20.00	0.66	0.91	6.41	14.82	-1528.61	0.00	1830.74	2193.23	-0.22	2.92	2.38	-4.09	1.00
22.00	0.73	0.99	6.29	19.96	-1820.93	0.00	1830.74	2193.23	-0.30	3.48	2.38	-4.09	1.48
24.00	0.81	1.08	6.19	26.32	-2137.64	0.00	1830.74	2193.23	-0.39	4.09	2.38	-4.09	1.99
26.00	0.89	1.17	6.11	34.15	-2478.29	0.00	1830.74	2193.23	-0.51	4.74	2.38	-4.09	2.53
28.00	0.99	1.27	6.03	43.76	-2842.42	0.00	1830.74	2193.23	-0.65	5.43	2.38	-4.09	3.08
30.00	1.09	1.39	5.96	55.58	-3229.44	0.00	1830.74	2193.23	-0.82	6.17	2.38	-4.09	3.65
32.00	1.21	1.52	5.89	70.22	-3638.72	0.00	1830.74	2193.23	-1.04	6.96	2.38	-4.09	4.21
34.00	1.35	1.68	5.82	88.53	-4069.54	0.00	1830.74	2193.23	-1.31	7.78	2.38	-4.09	4.76
36.00	1.53	1.86	5.76	111.82	-4521.10	0.00	1830.74	2193.23	-1.66	8.64	2.38	-4.09	5.28
38.00	1.74	2.10	5.70	142.07	-4992.49	0.00	1830.74	2193.23	-2.11	9.55	2.38	-4.09	5.74
40.00	2.02	2.40	5.64	182.60	-5482.67	0.00	1830.74	2193.23	-2.71	10.48	2.38	-4.09	6.07
42.00	2.40	2.82	5.58	239.24	-5990.35	0.00	1830.74	2193.23	-3.55	11.45	2.38	-4.09	6.20
44.00	2.95	3.43	5.52	323.29	-6513.76	0.00	1830.74	2193.23	-4.79	12.45	2.38	-4.09	5.96
46.00	3.85	4.40	5.46	459.75	-7049.75	0.00	1830.74	2193.23	-6.81	13.48	2.38	-4.09	4.96
48.00	5.50	6.21	5.39	715.78	-7589.59	0.00	1830.74	2193.23	-10.61	14.51	2.38	-4.09	2.20
50.00	9.43	10.48	5.28	1327.09	-8090.60	0.00	1830.74	2193.23	-19.67	15.47	2.38	-4.09	-5.91
52.00	19.84	21.49	5.00	2973.37	-8290.74	0.00	1830.74	2193.23	-44.07	15.85	2.38	-4.09	-29.93
54.00	180.90	-0.80	-4.45	-148.83	8215.56	0.00	1830.74	2193.23	2.21	-15.71	2.38	-4.09	-15.21
56.00	-36.52	-37.16	4.22	-6047.08	-8137.01	0.00	1830.74	2193.23	89.63	15.56	2.38	-4.09	103.49
58.00	-4.25	-4.46	5.09	-808.60	-10568.49	0.00	1830.74	2193.23	11.99	20.21	2.38	-4.09	30.49
60.00	-3.09	-3.19	5.03	-629.63	-11204.00	0.00	1830.74	2193.23	9.33	21.42	2.38	-4.09	29.05

Case 7: I235C150, ψ = 45°

L (m)	β (°)	W (cm)	V (cm)	M_y (KNm)	M_z (KNm)	φ (°)	P_{max} (KN)	M_{Pmax} (KNm)	σ_{my} (Mpa)	σ_{mz} (Mpa)	σ_p (Mpa)	σ_{MP} (Mpa)	σ_t (Mpa)
10.00	0.32	0.68	9.31	1.81	-530.56	0.00	1830.74	2193.23	-0.03	1.01	2.38	-4.09	-0.72
12.00	0.38	0.76	8.63	3.13	-713.84	0.00	1830.74	2193.23	-0.05	1.36	2.38	-4.09	-0.39
14.00	0.45	0.83	8.14	4.99	-922.48	0.00	1830.74	2193.23	-0.07	1.76	2.38	-4.09	-0.01
16.00	0.52	0.90	7.77	7.49	-1156.18	0.00	1830.74	2193.23	-0.11	2.21	2.38	-4.09	0.40
18.00	0.59	0.98	7.48	10.74	-1414.59	0.00	1830.74	2193.23	-0.16	2.70	2.38	-4.09	0.84
20.00	0.66	1.06	7.23	14.88	-1697.24	0.00	1830.74	2193.23	-0.22	3.25	2.38	-4.09	1.32
22.00	0.73	1.14	7.03	20.07	-2003.60	0.00	1830.74	2193.23	-0.30	3.83	2.38	-4.09	1.83
24.00	0.81	1.23	6.86	26.52	-2333.02	0.00	1830.74	2193.23	-0.39	4.46	2.38	-4.09	2.36
26.00	0.90	1.32	6.70	34.47	-2684.75	0.00	1830.74	2193.23	-0.51	5.13	2.38	-4.09	2.92
28.00	1.00	1.43	6.56	44.27	-3057.95	0.00	1830.74	2193.23	-0.66	5.85	2.38	-4.09	3.49
30.00	1.11	1.55	6.44	56.37	-3451.65	0.00	1830.74	2193.23	-0.84	6.60	2.38	-4.09	4.06
32.00	1.23	1.69	6.32	71.43	-3864.79	0.00	1830.74	2193.23	-1.06	7.39	2.38	-4.09	4.63
34.00	1.38	1.85	6.20	90.35	-4296.22	0.00	1830.74	2193.23	-1.34	8.21	2.38	-4.09	5.17
36.00	1.56	2.05	6.10	114.52	-4744.65	0.00	1830.74	2193.23	-1.70	9.07	2.38	-4.09	5.67
38.00	1.79	2.29	5.99	146.09	-5208.71	0.00	1830.74	2193.23	-2.17	9.96	2.38	-4.09	6.09
40.00	2.08	2.62	5.89	188.59	-5686.86	0.00	1830.74	2193.23	-2.80	10.87	2.38	-4.09	6.37
42.00	2.49	3.06	5.79	248.24	-6177.34	0.00	1830.74	2193.23	-3.68	11.81	2.38	-4.09	6.43
44.00	3.08	3.71	5.69	337.13	-6677.89	0.00	1830.74	2193.23	-5.00	12.77	2.38	-4.09	6.07
46.00	4.03	4.75	5.58	481.92	-7184.76	0.00	1830.74	2193.23	-7.14	13.74	2.38	-4.09	4.89
48.00	5.80	6.67	5.47	753.83	-7688.24	0.00	1830.74	2193.23	-11.17	14.70	2.38	-4.09	1.82
50.00	9.93	11.16	5.32	1397.24	-8142.97	0.00	1830.74	2193.23	-20.71	15.57	2.38	-4.09	-6.85
52.00	20.40	22.21	5.00	3053.50	-8295.31	0.00	1830.74	2193.23	-45.26	15.86	2.38	-4.09	-31.10
54.00	180.97	-0.73	-3.95	-160.11	7464.48	0.00	1830.74	2193.23	2.37	-14.27	2.38	-4.09	-13.60
56.00	-36.18	-36.71	4.23	-5998.20	-8151.75	0.00	1830.74	2193.23	88.91	15.59	2.38	-4.09	102.79
58.00	-4.65	-4.75	4.98	-883.69	-10387.00	0.00	1830.74	2193.23	13.10	19.86	2.38	-4.09	31.26
60.00	-3.41	-3.39	4.89	-692.98	-10946.51	0.00	1830.74	2193.23	10.27	20.93	2.38	-4.09	29.50

Case 8: I120A100, f_{ck} = 20 MPa

L (m)	β (°)	W (cm)	V (cm)	M_y (KNm)	M_z (KNm)	φ (°)	P_{max} (KN)	M_{Pmax} (KNm)	σ_{my} (Mpa)	σ_{mz} (Mpa)	σ_p (Mpa)	σ_{MP} (Mpa)	σ_t (Mpa)
10.00	0.64	2.39	27.76	1.40	-166.42	0.00	807.34	491.67	-0.08	1.60	2.70	-4.38	-0.16
12.00	0.77	2.72	26.42	2.44	-229.52	0.00	807.34	491.67	-0.14	2.20	2.70	-4.38	0.38
14.00	0.91	3.08	25.43	3.92	-302.27	0.00	807.34	491.67	-0.23	2.90	2.70	-4.38	0.99
16.00	1.06	3.47	24.66	5.98	-384.45	0.00	807.34	491.67	-0.35	3.69	2.70	-4.38	1.66
18.00	1.23	3.90	24.03	8.77	-475.76	0.00	807.34	491.67	-0.52	4.56	2.70	-4.38	2.37
20.00	1.43	4.39	23.48	12.55	-575.85	0.00	807.34	491.67	-0.74	5.52	2.70	-4.38	3.11
22.00	1.66	4.99	22.98	17.71	-684.29	0.00	807.34	491.67	-1.04	6.56	2.70	-4.38	3.84
24.00	1.97	5.76	22.53	24.92	-800.55	0.00	807.34	491.67	-1.47	7.68	2.70	-4.38	4.53
26.00	2.38	6.81	22.09	35.36	-924.02	0.00	807.34	491.67	-2.08	8.86	2.70	-4.38	5.10
28.00	2.99	8.34	21.66	51.46	-1053.95	0.00	807.34	491.67	-3.03	10.11	2.70	-4.38	5.40
30.00	3.99	10.88	21.23	78.90	-1189.19	0.00	807.34	491.67	-4.64	11.40	2.70	-4.38	5.08
32.00	5.98	15.92	20.75	134.49	-1327.13	0.00	807.34	491.67	-7.91	12.73	2.70	-4.38	3.14
34.00	11.44	29.58	20.07	288.82	-1453.40	0.00	807.34	491.67	-16.99	13.94	2.70	-4.38	-4.73
36.00	26.62	65.87	18.10	731.69	-1471.64	0.00	807.34	491.67	-43.04	14.11	2.70	-4.38	-30.61
38.00	-31.33	-74.77	16.98	-946.10	-1543.70	0.00	807.34	491.67	55.66	14.80	2.70	-4.38	68.78
40.00	-5.48	-13.09	19.07	-192.43	-1932.24	0.00	807.34	491.67	11.32	18.53	2.70	-4.38	28.17
42.00	-3.64	-8.46	18.66	-141.30	-2094.30	0.00	807.34	491.67	8.31	20.08	2.70	-4.38	26.72
44.00	-2.73	-6.14	18.23	-116.07	-2254.74	0.00	807.34	491.67	6.83	21.62	2.70	-4.38	26.77
46.00	-2.17	-4.74	17.78	-101.18	-2414.86	0.00	807.34	491.67	5.95	23.16	2.70	-4.38	27.43
48.00	-1.81	-3.81	17.33	-91.53	-2574.61	-0.01	807.34	491.67	5.38	24.69	2.70	-4.38	28.40
50.00	-1.54	-3.14	16.87	-84.90	-2733.71	-0.01	807.34	491.67	4.99	26.21	2.70	-4.38	29.53
52.00	-1.35	-2.64	16.41	-80.20	-2891.85	-0.01	807.34	491.67	4.72	27.73	2.70	-4.38	30.77
54.00	-1.20	-2.26	15.95	-76.80	-3048.77	-0.01	807.34	491.67	4.52	29.23	2.70	-4.38	32.08
56.00	-1.08	-1.96	15.50	-74.34	-3204.25	-0.01	807.34	491.67	4.37	30.73	2.70	-4.38	33.42
58.00	-0.98	-1.71	15.05	-72.57	-3358.17	-0.01	807.34	491.67	4.27	32.20	2.70	-4.38	34.79
60.00	-0.90	-1.51	14.61	-71.35	-3510.45	-0.01	807.34	491.67	4.20	33.66	2.70	-4.38	36.18

Case 8: I100A100, f_{ck} = 20 MPa

L (m)	β (°)	W (cm)	V (cm)	M_y (KNm)	M_z (KNm)	φ (°)	P_{max} (KN)	M_{Pmax} (KNm)	σ_{my} (Mpa)	σ_{mz} (Mpa)	σ_p (Mpa)	σ_{MP} (Mpa)	σ_t (Mpa)
10.00	0.72	2.41	38.58	1.46	-148.49	0.00	790.37	403.09	-0.09	1.85	2.88	-4.61	0.03
12.00	0.88	2.77	36.89	2.55	-205.65	0.00	790.37	403.09	-0.15	2.56	2.88	-4.61	0.68
14.00	1.04	3.14	35.64	4.11	-271.72	0.00	790.37	403.09	-0.24	3.38	2.88	-4.61	1.41
16.00	1.21	3.55	34.66	6.27	-346.51	0.00	790.37	403.09	-0.37	4.31	2.88	-4.61	2.21
18.00	1.41	4.00	33.85	9.21	-429.78	0.00	790.37	403.09	-0.54	5.35	2.88	-4.61	3.08
20.00	1.63	4.53	33.15	13.20	-521.22	0.00	790.37	403.09	-0.78	6.48	2.88	-4.61	3.98
22.00	1.91	5.18	32.52	18.67	-620.46	0.00	790.37	403.09	-1.10	7.72	2.88	-4.61	4.89
24.00	2.26	6.01	31.94	26.36	-727.04	0.00	790.37	403.09	-1.56	9.04	2.88	-4.61	5.76
26.00	2.75	7.16	31.37	37.64	-840.41	0.00	790.37	403.09	-2.22	10.45	2.88	-4.61	6.51
28.00	3.49	8.88	30.81	55.32	-959.84	0.00	790.37	403.09	-3.27	11.94	2.88	-4.61	6.95
30.00	4.75	11.81	30.23	86.30	-1084.08	0.00	790.37	403.09	-5.09	13.49	2.88	-4.61	6.66
32.00	7.37	17.92	29.56	152.26	-1209.50	0.00	790.37	403.09	-8.99	15.05	2.88	-4.61	4.33
34.00	14.91	35.21	28.34	344.66	-1312.47	0.00	790.37	403.09	-20.34	16.33	2.88	-4.61	-5.75
36.00	31.16	70.10	24.89	777.22	-1294.00	0.00	790.37	403.09	-45.88	16.10	2.88	-4.61	-31.51
38.00	-35.99	-78.08	23.17	-983.46	-1345.75	0.00	790.37	403.09	58.05	16.74	2.88	-4.61	73.07
40.00	-5.38	-11.85	27.41	-173.77	-1776.01	0.00	790.37	403.09	10.26	22.09	2.88	-4.61	30.62
42.00	-3.69	-7.92	26.88	-131.59	-1927.35	0.00	790.37	403.09	7.77	23.98	2.88	-4.61	30.02
44.00	-2.80	-5.84	26.30	-109.66	-2077.90	0.00	790.37	403.09	6.47	25.85	2.88	-4.61	30.59
46.00	-2.25	-4.55	25.69	-96.35	-2228.58	0.00	790.37	403.09	5.69	27.72	2.88	-4.61	31.68
48.00	-1.88	-3.68	25.08	-87.56	-2379.28	-0.01	790.37	403.09	5.17	29.60	2.88	-4.61	33.04
50.00	-1.61	-3.05	24.46	-81.43	-2529.69	-0.01	790.37	403.09	4.81	31.47	2.88	-4.61	34.55
52.00	-1.41	-2.58	23.83	-77.02	-2679.51	-0.01	790.37	403.09	4.55	33.33	2.88	-4.61	36.15
54.00	-1.25	-2.21	23.20	-73.80	-2828.43	-0.01	790.37	403.09	4.36	35.19	2.88	-4.61	37.81
56.00	-1.13	-1.92	22.58	-71.43	-2976.24	-0.01	790.37	403.09	4.22	37.02	2.88	-4.61	39.51
58.00	-1.02	-1.68	21.96	-69.71	-3122.75	-0.01	790.37	403.09	4.11	38.85	2.88	-4.61	41.23
60.00	-0.94	-1.49	21.34	-68.48	-3267.85	-0.01	790.37	403.09	4.04	40.65	2.88	-4.61	42.97

Case 8: I80A100, f_{ck} = 20 MPa

L (m)	β (°)	W (cm)	V (cm)	M_y (KNm)	M_z (KNm)	φ (°)	P_{max} (KN)	M_{Pmax} (KNm)	σ_{my} (Mpa)	σ_{mz} (Mpa)	σ_p (Mpa)	σ_{MP} (Mpa)	σ_t (Mpa)
10.00	0.84	2.46	59.10	1.55	-131.36	0.00	757.62	311.38	-0.09	2.26	3.02	-4.83	0.36
12.00	1.02	2.84	56.78	2.71	-182.73	0.00	757.62	311.38	-0.16	3.14	3.02	-4.83	1.17
14.00	1.21	3.24	55.06	4.36	-242.26	0.00	757.62	311.38	-0.26	4.16	3.02	-4.83	2.10
16.00	1.41	3.68	53.72	6.66	-309.79	0.00	757.62	311.38	-0.39	5.32	3.02	-4.83	3.12
18.00	1.64	4.17	52.61	9.80	-385.13	0.00	757.62	311.38	-0.58	6.62	3.02	-4.83	4.23
20.00	1.91	4.74	51.64	14.07	-468.01	0.00	757.62	311.38	-0.83	8.04	3.02	-4.83	5.40
22.00	2.24	5.45	50.76	19.98	-558.11	0.00	757.62	311.38	-1.18	9.59	3.02	-4.83	6.60
24.00	2.67	6.37	49.94	28.35	-655.03	0.00	757.62	311.38	-1.68	11.26	3.02	-4.83	7.77
26.00	3.27	7.66	49.14	40.81	-758.26	0.00	757.62	311.38	-2.42	13.03	3.02	-4.83	8.81
28.00	4.21	9.66	48.33	60.80	-867.05	0.00	757.62	311.38	-3.60	14.90	3.02	-4.83	9.49
30.00	5.86	13.20	47.46	97.24	-979.85	0.00	757.62	311.38	-5.76	16.84	3.02	-4.83	9.27
32.00	9.57	21.06	46.32	180.00	-1090.80	0.00	757.62	311.38	-10.66	18.74	3.02	-4.83	6.28
34.00	20.06	42.78	43.55	419.44	-1160.33	0.00	757.62	311.38	-24.84	19.94	3.02	-4.83	-6.71
36.00	-2160.65	-0.74	28.65	-15.62	-943.09	0.00	757.62	311.38	0.93	16.20	3.02	-4.83	15.32
38.00	-9.00	-18.55	44.00	-238.83	-1474.14	0.00	757.62	311.38	14.15	25.33	3.02	-4.83	37.67
40.00	-5.29	-10.66	43.49	-155.94	-1620.00	0.00	757.62	311.38	9.24	27.84	3.02	-4.83	35.27
42.00	-3.74	-7.36	42.71	-121.80	-1760.30	0.00	757.62	311.38	7.21	30.25	3.02	-4.83	35.66
44.00	-2.89	-5.53	41.86	-103.08	-1900.55	0.00	757.62	311.38	6.11	32.66	3.02	-4.83	36.96
46.00	-2.34	-4.36	40.98	-91.37	-2041.34	0.00	757.62	311.38	5.41	35.08	3.02	-4.83	38.68
48.00	-1.96	-3.55	40.07	-83.45	-2182.51	-0.01	757.62	311.38	4.94	37.50	3.02	-4.83	40.64
50.00	-1.69	-2.96	39.14	-77.85	-2323.76	-0.01	757.62	311.38	4.61	39.93	3.02	-4.83	42.73
52.00	-1.48	-2.51	38.20	-73.76	-2464.76	-0.01	757.62	311.38	4.37	42.35	3.02	-4.83	44.91
54.00	-1.31	-2.16	37.27	-70.73	-2605.22	-0.01	757.62	311.38	4.19	44.76	3.02	-4.83	47.15
56.00	-1.18	-1.88	36.32	-68.47	-2744.88	-0.01	757.62	311.38	4.06	47.16	3.02	-4.83	49.41
58.00	-1.08	-1.65	35.38	-66.79	-2883.54	-0.01	757.62	311.38	3.96	49.55	3.02	-4.83	51.70
60.00	-0.99	-1.46	34.44	-65.58	-3021.04	-0.01	757.62	311.38	3.88	51.91	3.02	-4.83	53.99

Case 8: I60A100, f_{ck} = 20 MPa

L (m)	β (°)	W (cm)	V (cm)	M_y (KNm)	M_z (KNm)	φ (°)	P_{max} (KN)	M_{Pmax} (KNm)	σ_{my} (Mpa)	σ_{mz} (Mpa)	σ_p (Mpa)	σ_{MP} (Mpa)	σ_t (Mpa)
10.00	1.00	2.55	106.91	1.68	-115.02	0.00	688.72	214.88	-0.10	3.04	3.04	-4.97	1.01
12.00	1.22	2.96	103.25	2.92	-160.74	0.00	688.72	214.88	-0.17	4.25	3.04	-4.97	2.14
14.00	1.44	3.40	100.54	4.72	-213.88	0.00	688.72	214.88	-0.28	5.65	3.04	-4.97	3.44
16.00	1.69	3.87	98.41	7.21	-274.29	0.00	688.72	214.88	-0.43	7.25	3.04	-4.97	4.89
18.00	1.96	4.41	96.64	10.62	-341.80	0.00	688.72	214.88	-0.63	9.03	3.04	-4.97	6.47
20.00	2.29	5.05	95.09	15.31	-416.21	0.00	688.72	214.88	-0.91	11.00	3.04	-4.97	8.16
22.00	2.70	5.85	93.67	21.84	-497.22	0.00	688.72	214.88	-1.30	13.14	3.04	-4.97	9.91
24.00	3.25	6.91	92.32	31.23	-584.49	0.00	688.72	214.88	-1.86	15.44	3.04	-4.97	11.66
26.00	4.04	8.43	90.98	45.50	-677.50	0.00	688.72	214.88	-2.70	17.90	3.04	-4.97	13.27
28.00	5.29	10.87	89.59	69.19	-775.37	0.00	688.72	214.88	-4.11	20.49	3.04	-4.97	14.44
30.00	7.67	15.46	87.95	114.84	-875.78	0.00	688.72	214.88	-6.83	23.14	3.04	-4.97	14.38
32.00	13.38	26.37	85.20	226.62	-967.40	0.00	688.72	214.88	-13.47	25.56	3.04	-4.97	10.16
34.00	27.04	51.25	77.31	502.64	-992.42	0.00	688.72	214.88	-29.87	26.22	3.04	-4.97	-5.58
36.00	-178.23	-2.85	-74.09	-38.33	1096.43	0.00	688.72	214.88	2.28	-28.97	3.04	-4.97	-28.62
38.00	-8.18	-15.26	82.56	-196.51	-1332.81	0.00	688.72	214.88	11.68	35.21	3.04	-4.97	44.96
40.00	-5.21	-9.51	81.61	-138.84	-1464.18	0.00	688.72	214.88	8.25	38.68	3.04	-4.97	45.01
42.00	-3.80	-6.80	80.28	-111.91	-1593.11	0.00	688.72	214.88	6.65	42.09	3.04	-4.97	46.81
44.00	-2.98	-5.20	78.83	-96.29	-1722.63	0.00	688.72	214.88	5.72	45.51	3.04	-4.97	49.30
46.00	-2.44	-4.15	77.31	-86.17	-1853.05	-0.01	688.72	214.88	5.12	48.96	3.04	-4.97	52.15
48.00	-2.06	-3.41	75.73	-79.18	-1984.18	-0.01	688.72	214.88	4.71	52.42	3.04	-4.97	55.20
50.00	-1.78	-2.86	74.12	-74.13	-2115.74	-0.01	688.72	214.88	4.41	55.90	3.04	-4.97	58.37
52.00	-1.56	-2.44	72.49	-70.38	-2247.39	-0.01	688.72	214.88	4.18	59.38	3.04	-4.97	61.63
54.00	-1.39	-2.10	70.83	-67.56	-2378.83	-0.01	688.72	214.88	4.02	62.85	3.04	-4.97	64.93
56.00	-1.25	-1.84	69.16	-65.43	-2509.81	-0.01	688.72	214.88	3.89	66.31	3.04	-4.97	68.27
58.00	-1.14	-1.62	67.48	-63.82	-2640.09	-0.01	688.72	214.88	3.79	69.75	3.04	-4.97	71.61
60.00	-1.04	-1.43	65.81	-62.62	-2769.50	-0.01	688.72	214.88	3.72	73.17	3.04	-4.97	74.96

Case 8: I120A100, f_{ck} = 40 MPa

L (m)	β (°)	W (cm)	V (cm)	M_y (KNm)	M_z (KNm)	φ (°)	P_{max} (KN)	M_{Pmax} (KNm)	σ_{my} (Mpa)	σ_{mz} (Mpa)	σ_p (Mpa)	σ_{MP} (Mpa)	σ_t (Mpa)
10.00	0.63	1.89	22.05	1.40	-166.49	0.00	1281.57	780.48	-0.08	1.60	4.29	-6.95	-1.15
12.00	0.77	2.16	20.99	2.43	-229.69	0.00	1281.57	780.48	-0.14	2.20	4.29	-6.95	-0.60
14.00	0.90	2.43	20.22	3.90	-302.63	0.00	1281.57	780.48	-0.23	2.90	4.29	-6.95	0.01
16.00	1.05	2.73	19.61	5.91	-385.13	0.00	1281.57	780.48	-0.35	3.69	4.29	-6.95	0.68
18.00	1.21	3.05	19.12	8.62	-476.95	0.00	1281.57	780.48	-0.51	4.57	4.29	-6.95	1.40
20.00	1.39	3.41	18.71	12.22	-577.80	0.00	1281.57	780.48	-0.72	5.54	4.29	-6.95	2.16
22.00	1.60	3.83	18.34	17.02	-687.34	0.00	1281.57	780.48	-1.00	6.59	4.29	-6.95	2.93
24.00	1.86	4.35	18.00	23.50	-805.14	0.00	1281.57	780.48	-1.38	7.72	4.29	-6.95	3.68
26.00	2.18	5.01	17.68	32.44	-930.70	0.00	1281.57	780.48	-1.91	8.92	4.29	-6.95	4.35
28.00	2.63	5.90	17.37	45.30	-1063.43	0.00	1281.57	780.48	-2.67	10.20	4.29	-6.95	4.87
30.00	3.28	7.22	17.07	64.94	-1202.56	0.00	1281.57	780.48	-3.82	11.53	4.29	-6.95	5.05
32.00	4.36	9.37	16.76	98.00	-1346.89	0.00	1281.57	780.48	-5.76	12.92	4.29	-6.95	4.49
34.00	6.44	13.56	16.41	163.49	-1493.37	0.00	1281.57	780.48	-9.62	14.32	4.29	-6.95	2.04
36.00	11.85	24.29	15.90	335.27	-1626.03	0.00	1281.57	780.48	-19.72	15.59	4.29	-6.95	-6.79
38.00	25.85	50.90	14.46	793.48	-1650.86	0.00	1281.57	780.48	-46.68	15.83	4.29	-6.95	-33.51
40.00	-26.68	-51.16	14.08	-905.25	-1787.30	0.00	1281.57	780.48	53.25	17.14	4.29	-6.95	67.73
42.00	-6.33	-12.10	15.20	-245.09	-2138.07	0.00	1281.57	780.48	14.42	20.50	4.29	-6.95	32.26
44.00	-4.15	-7.73	14.94	-176.61	-2313.71	0.00	1281.57	780.48	10.39	22.19	4.29	-6.95	29.91
46.00	-3.08	-5.59	14.63	-143.49	-2486.65	0.00	1281.57	780.48	8.44	23.84	4.29	-6.95	29.62
48.00	-2.45	-4.31	14.31	-124.06	-2659.32	0.00	1281.57	780.48	7.30	25.50	4.29	-6.95	30.14
50.00	-2.03	-3.46	13.98	-111.44	-2831.91	0.00	1281.57	780.48	6.56	27.16	4.29	-6.95	31.05
52.00	-1.73	-2.86	13.66	-102.73	-3004.20	-0.01	1281.57	780.48	6.04	28.81	4.29	-6.95	32.19
54.00	-1.50	-2.41	13.32	-96.48	-3175.86	-0.01	1281.57	780.48	5.68	30.45	4.29	-6.95	33.47
56.00	-1.33	-2.07	12.99	-91.89	-3346.62	-0.01	1281.57	780.48	5.41	32.09	4.29	-6.95	34.83
58.00	-1.20	-1.79	12.66	-88.48	-3516.20	-0.01	1281.57	780.48	5.21	33.72	4.29	-6.95	36.26
60.00	-1.09	-1.57	12.33	-85.94	-3684.42	-0.01	1281.57	780.48	5.06	35.33	4.29	-6.95	37.72

Case 8: I100A100, f_{ck} = 40 MPa

L (m)	β (°)	W (cm)	V (cm)	M_y (KNm)	M_z (KNm)	φ (°)	P_{max} (KN)	M_{Pmax} (KNm)	σ_{my} (Mpa)	σ_{mz} (Mpa)	σ_p (Mpa)	σ_{MP} (Mpa)	σ_t (Mpa)
10.00	0.72	1.91	30.64	1.46	-148.55	0.00	1254.64	639.87	-0.09	1.85	4.57	-7.31	-0.98
12.00	0.87	2.19	29.30	2.54	-205.80	0.00	1254.64	639.87	-0.15	2.56	4.57	-7.31	-0.33
14.00	1.03	2.48	28.32	4.08	-272.02	0.00	1254.64	639.87	-0.24	3.38	4.57	-7.31	0.40
16.00	1.20	2.79	27.56	6.20	-347.08	0.00	1254.64	639.87	-0.37	4.32	4.57	-7.31	1.21
18.00	1.38	3.13	26.94	9.05	-430.77	0.00	1254.64	639.87	-0.53	5.36	4.57	-7.31	2.08
20.00	1.59	3.52	26.41	12.84	-522.85	0.00	1254.64	639.87	-0.76	6.50	4.57	-7.31	3.00
22.00	1.83	3.97	25.94	17.92	-623.01	0.00	1254.64	639.87	-1.06	7.75	4.57	-7.31	3.95
24.00	2.13	4.52	25.51	24.80	-730.90	0.00	1254.64	639.87	-1.46	9.09	4.57	-7.31	4.89
26.00	2.52	5.24	25.10	34.38	-846.06	0.00	1254.64	639.87	-2.03	10.52	4.57	-7.31	5.75
28.00	3.05	6.23	24.70	48.31	-967.95	0.00	1254.64	639.87	-2.85	12.04	4.57	-7.31	6.45
30.00	3.85	7.71	24.29	69.96	-1095.81	0.00	1254.64	639.87	-4.13	13.63	4.57	-7.31	6.76
32.00	5.20	10.20	23.88	107.46	-1228.23	0.00	1254.64	639.87	-6.34	15.28	4.57	-7.31	6.19
34.00	7.95	15.29	23.37	185.36	-1360.88	0.00	1254.64	639.87	-10.94	16.93	4.57	-7.31	3.24
36.00	15.35	28.74	22.43	397.66	-1467.76	0.00	1254.64	639.87	-23.47	18.26	4.57	-7.31	-7.96
38.00	30.44	54.48	19.91	847.72	-1452.95	0.00	1254.64	639.87	-50.04	18.07	4.57	-7.31	-34.71
40.00	-32.82	-57.11	19.09	-1004.86	-1548.10	0.00	1254.64	639.87	59.31	19.26	4.57	-7.31	75.83
42.00	-6.16	-10.85	21.86	-219.34	-1965.12	0.00	1254.64	639.87	12.95	24.45	4.57	-7.31	34.65
44.00	-4.19	-7.20	21.50	-163.74	-2128.60	0.00	1254.64	639.87	9.66	26.48	4.57	-7.31	33.40
46.00	-3.16	-5.30	21.09	-135.22	-2290.58	0.00	1254.64	639.87	7.98	28.49	4.57	-7.31	33.73
48.00	-2.53	-4.13	20.66	-117.96	-2452.78	0.00	1254.64	639.87	6.96	30.51	4.57	-7.31	34.73
50.00	-2.11	-3.35	20.22	-106.53	-2615.28	0.00	1254.64	639.87	6.29	32.53	4.57	-7.31	36.08
52.00	-1.80	-2.78	19.78	-98.52	-2777.84	-0.01	1254.64	639.87	5.82	34.56	4.57	-7.31	37.63
54.00	-1.57	-2.35	19.33	-92.69	-2940.15	-0.01	1254.64	639.87	5.47	36.58	4.57	-7.31	39.30
56.00	-1.39	-2.02	18.87	-88.36	-3101.89	-0.01	1254.64	639.87	5.22	38.59	4.57	-7.31	41.06
58.00	-1.25	-1.76	18.42	-85.11	-3262.80	-0.01	1254.64	639.87	5.02	40.59	4.57	-7.31	42.87
60.00	-1.14	-1.54	17.96	-82.66	-3422.65	-0.01	1254.64	639.87	4.88	42.58	4.57	-7.31	44.71

Case 8: I80A100, f_{ck} = 40 MPa

L (m)	β (°)	W (cm)	V (cm)	M_y (KNm)	M_z (KNm)	φ (°)	P_{max} (KN)	M_{Pmax} (KNm)	σ_{my} (Mpa)	σ_{mz} (Mpa)	σ_p (Mpa)	σ_{MP} (Mpa)	σ_t (Mpa)
10.00	0.84	1.95	46.93	1.55	-131.41	0.00	1202.65	494.29	-0.09	2.26	4.80	-7.66	-0.70
12.00	1.01	2.25	45.10	2.70	-182.84	0.00	1202.65	494.29	-0.16	3.14	4.80	-7.66	0.12
14.00	1.20	2.56	43.76	4.33	-242.50	0.00	1202.65	494.29	-0.26	4.17	4.80	-7.66	1.04
16.00	1.39	2.89	42.71	6.58	-310.25	0.00	1202.65	494.29	-0.39	5.33	4.80	-7.66	2.07
18.00	1.61	3.25	41.86	9.62	-385.94	0.00	1202.65	494.29	-0.57	6.63	4.80	-7.66	3.20
20.00	1.85	3.67	41.12	13.67	-469.34	0.00	1202.65	494.29	-0.81	8.06	4.80	-7.66	4.39
22.00	2.14	4.16	40.47	19.13	-560.22	0.00	1202.65	494.29	-1.13	9.63	4.80	-7.66	5.63
24.00	2.50	4.77	39.86	26.57	-658.23	0.00	1202.65	494.29	-1.57	11.31	4.80	-7.66	6.87
26.00	2.97	5.57	39.29	37.04	-763.00	0.00	1202.65	494.29	-2.19	13.11	4.80	-7.66	8.05
28.00	3.63	6.69	38.72	52.51	-873.98	0.00	1202.65	494.29	-3.11	15.02	4.80	-7.66	9.04
30.00	4.65	8.42	38.14	77.14	-990.37	0.00	1202.65	494.29	-4.57	17.02	4.80	-7.66	9.58
32.00	6.44	11.45	37.49	121.48	-1110.30	0.00	1202.65	494.29	-7.19	19.08	4.80	-7.66	9.02
34.00	10.33	18.00	36.61	219.32	-1226.63	0.00	1202.65	494.29	-12.99	21.08	4.80	-7.66	5.22
36.00	20.49	34.63	34.46	479.82	-1297.01	0.00	1202.65	494.29	-28.42	22.29	4.80	-7.66	-9.00
38.00	181.65	-2.29	-30.96	-44.08	1338.52	0.00	1202.65	494.29	2.61	-23.00	4.80	-7.66	-23.26
40.00	181.58	-2.17	-30.71	-46.63	1473.31	0.00	1202.65	494.29	2.76	-25.32	4.80	-7.66	-25.42
42.00	-6.00	-9.67	34.67	-195.15	-1792.36	0.00	1202.65	494.29	11.56	30.80	4.80	-7.66	39.49
44.00	-4.23	-6.66	34.15	-150.85	-1943.46	0.00	1202.65	494.29	8.93	33.39	4.80	-7.66	39.46
46.00	-3.25	-5.00	33.55	-126.74	-2094.08	0.00	1202.65	494.29	7.51	35.98	4.80	-7.66	40.62
48.00	-2.63	-3.95	32.93	-111.66	-2245.35	0.00	1202.65	494.29	6.61	38.58	4.80	-7.66	42.33
50.00	-2.20	-3.22	32.28	-101.44	-2397.27	-0.01	1202.65	494.29	6.01	41.19	4.80	-7.66	44.33
52.00	-1.89	-2.69	31.62	-94.15	-2549.61	-0.01	1202.65	494.29	5.58	43.81	4.80	-7.66	46.52
54.00	-1.65	-2.29	30.95	-88.78	-2702.03	-0.01	1202.65	494.29	5.26	46.43	4.80	-7.66	48.82
56.00	-1.46	-1.97	30.27	-84.74	-2854.25	-0.01	1202.65	494.29	5.02	49.04	4.80	-7.66	51.20
58.00	-1.32	-1.72	29.58	-81.67	-3005.96	-0.01	1202.65	494.29	4.84	51.65	4.80	-7.66	53.62
60.00	-1.19	-1.51	28.90	-79.32	-3156.93	-0.01	1202.65	494.29	4.70	54.24	4.80	-7.66	56.08

Case 8: I60A100, f_{ck} = 40 MPa

L (m)	β (°)	W (cm)	V (cm)	M_y (KNm)	M_z (KNm)	φ (°)	P_{max} (KN)	M_{Pmax} (KNm)	σ_{my} (Mpa)	σ_{mz} (Mpa)	σ_p (Mpa)	σ_{MP} (Mpa)	σ_t (Mpa)
10.00	1.00	2.02	84.89	1.67	-115.06	0.00	1093.27	341.10	-0.10	3.04	4.82	-7.89	-0.12
12.00	1.21	2.34	82.00	2.91	-160.84	0.00	1093.27	341.10	-0.17	4.25	4.82	-7.89	1.01
14.00	1.43	2.68	79.89	4.68	-214.07	0.00	1093.27	341.10	-0.28	5.66	4.82	-7.89	2.31
16.00	1.67	3.04	78.23	7.12	-274.65	0.00	1093.27	341.10	-0.42	7.26	4.82	-7.89	3.77
18.00	1.93	3.44	76.87	10.42	-342.45	0.00	1093.27	341.10	-0.62	9.05	4.82	-7.89	5.37
20.00	2.22	3.90	75.70	14.85	-417.29	0.00	1093.27	341.10	-0.88	11.02	4.82	-7.89	7.08
22.00	2.58	4.45	74.65	20.84	-498.94	0.00	1093.27	341.10	-1.24	13.18	4.82	-7.89	8.88
24.00	3.03	5.14	73.66	29.11	-587.12	0.00	1093.27	341.10	-1.73	15.51	4.82	-7.89	10.72
26.00	3.63	6.07	72.71	40.92	-681.47	0.00	1093.27	341.10	-2.43	18.00	4.82	-7.89	12.51
28.00	4.49	7.40	71.75	58.75	-781.42	0.00	1093.27	341.10	-3.49	20.64	4.82	-7.89	14.09
30.00	5.88	9.53	70.72	88.15	-885.95	0.00	1093.27	341.10	-5.24	23.41	4.82	-7.89	15.10
32.00	8.46	13.48	69.47	144.07	-992.09	0.00	1093.27	341.10	-8.56	26.21	4.82	-7.89	14.59
34.00	14.43	22.50	67.23	275.42	-1086.01	0.00	1093.27	341.10	-16.37	28.69	4.82	-7.89	9.26
36.00	27.39	41.15	61.16	570.18	-1109.05	0.00	1093.27	341.10	-33.89	29.30	4.82	-7.89	-7.65
38.00	-46.88	-64.07	46.38	-1007.99	-939.42	0.00	1093.27	341.10	59.91	24.82	4.82	-7.89	81.66
40.00	-9.30	-13.82	65.58	-247.34	-1476.87	0.00	1093.27	341.10	14.70	39.02	4.82	-7.89	50.66
42.00	-5.86	-8.56	65.06	-172.33	-1619.82	0.00	1093.27	341.10	10.24	42.80	4.82	-7.89	49.97
44.00	-4.27	-6.12	64.16	-137.92	-1758.28	0.00	1093.27	341.10	8.20	46.45	4.82	-7.89	51.59
46.00	-3.34	-4.69	63.15	-118.01	-1897.09	0.00	1093.27	341.10	7.01	50.12	4.82	-7.89	54.07
48.00	-2.73	-3.75	62.08	-105.10	-2036.93	0.00	1093.27	341.10	6.25	53.81	4.82	-7.89	57.00
50.00	-2.30	-3.08	60.96	-96.13	-2177.76	-0.01	1093.27	341.10	5.71	57.54	4.82	-7.89	60.19
52.00	-1.99	-2.59	59.81	-89.61	-2319.31	-0.01	1093.27	341.10	5.33	61.28	4.82	-7.89	63.54
54.00	-1.74	-2.21	58.64	-84.73	-2461.30	-0.01	1093.27	341.10	5.04	65.03	4.82	-7.89	67.00
56.00	-1.55	-1.92	57.45	-81.00	-2603.40	-0.01	1093.27	341.10	4.81	68.78	4.82	-7.89	70.53
58.00	-1.39	-1.68	56.24	-78.12	-2745.34	-0.01	1093.27	341.10	4.64	72.53	4.82	-7.89	74.11
60.00	-1.26	-1.48	55.03	-75.89	-2886.87	-0.01	1093.27	341.10	4.51	76.27	4.82	-7.89	77.72

Case 8: I120A100, f_{ck} = 60 MPa

L (m)	β (°)	W (cm)	V (cm)	M_y (KNm)	M_z (KNm)	φ (°)	P_{max} (KN)	M_{Pmax} (KNm)	σ_{my} (Mpa)	σ_{mz} (Mpa)	σ_p (Mpa)	σ_{MP} (Mpa)	σ_t (Mpa)
10.00	0.63	1.65	19.26	1.39	-166.53	0.00	1640.91	999.32	-0.08	1.60	5.49	-8.90	-1.89
12.00	0.76	1.88	18.34	2.42	-229.78	0.00	1640.91	999.32	-0.14	2.20	5.49	-8.90	-1.35
14.00	0.90	2.12	17.67	3.88	-302.81	0.00	1640.91	999.32	-0.23	2.90	5.49	-8.90	-0.73
16.00	1.04	2.37	17.15	5.88	-385.46	0.00	1640.91	999.32	-0.35	3.70	5.49	-8.90	-0.06
18.00	1.20	2.65	16.73	8.55	-477.53	0.00	1640.91	999.32	-0.50	4.58	5.49	-8.90	0.67
20.00	1.37	2.95	16.37	12.07	-578.76	0.00	1640.91	999.32	-0.71	5.55	5.49	-8.90	1.43
22.00	1.57	3.30	16.06	16.70	-688.84	0.00	1640.91	999.32	-0.98	6.61	5.49	-8.90	2.21
24.00	1.80	3.71	15.78	22.86	-807.39	0.00	1640.91	999.32	-1.34	7.74	5.49	-8.90	2.99
26.00	2.10	4.22	15.51	31.18	-933.99	0.00	1640.91	999.32	-1.83	8.96	5.49	-8.90	3.71
28.00	2.48	4.90	15.26	42.76	-1068.10	0.00	1640.91	999.32	-2.52	10.24	5.49	-8.90	4.32
30.00	3.02	5.84	15.01	59.68	-1209.08	0.00	1640.91	999.32	-3.51	11.59	5.49	-8.90	4.68
32.00	3.83	7.27	14.76	86.20	-1356.02	0.00	1640.91	999.32	-5.07	13.00	5.49	-8.90	4.52
34.00	5.23	9.72	14.49	132.83	-1507.21	0.00	1640.91	999.32	-7.81	14.45	5.49	-8.90	3.23
36.00	8.18	14.88	14.17	232.45	-1656.88	0.00	1640.91	999.32	-13.67	15.89	5.49	-8.90	-1.19
38.00	16.29	28.80	13.54	510.53	-1768.68	0.00	1640.91	999.32	-30.03	16.96	5.49	-8.90	-16.48
40.00	31.38	53.00	11.96	1049.97	-1732.99	0.00	1640.91	999.32	-61.77	16.62	5.49	-8.90	-48.56
42.00	-34.55	-56.60	11.36	-1260.72	-1819.30	0.00	1640.91	999.32	74.17	17.45	5.49	-8.90	88.20
44.00	-5.71	-9.49	13.24	-242.74	-2340.76	0.00	1640.91	999.32	14.28	22.45	5.49	-8.90	33.32
46.00	-3.95	-6.40	13.01	-183.67	-2522.79	0.00	1640.91	999.32	10.80	24.19	5.49	-8.90	31.59
48.00	-3.01	-4.76	12.76	-152.61	-2703.21	0.00	1640.91	999.32	8.98	25.92	5.49	-8.90	31.49
50.00	-2.43	-3.73	12.49	-133.59	-2883.58	0.00	1640.91	999.32	7.86	27.65	5.49	-8.90	32.10
52.00	-2.03	-3.04	12.22	-120.89	-3063.98	0.00	1640.91	999.32	7.11	29.38	5.49	-8.90	33.08
54.00	-1.75	-2.53	11.95	-111.94	-3244.16	-0.01	1640.91	999.32	6.59	31.11	5.49	-8.90	34.29
56.00	-1.53	-2.15	11.67	-105.41	-3423.82	-0.01	1640.91	999.32	6.20	32.83	5.49	-8.90	35.62
58.00	-1.36	-1.85	11.40	-100.55	-3602.66	-0.01	1640.91	999.32	5.92	34.55	5.49	-8.90	37.05
60.00	-1.22	-1.61	11.12	-96.89	-3780.41	-0.01	1640.91	999.32	5.70	36.25	5.49	-8.90	38.54

Case 8: I100A100 f_{ck} = 60 MPa

L (m)	β (°)	W (cm)	V (cm)	M_y (KNm)	M_z (KNm)	φ (°)	P_{max} (KN)	M_{Pmax} (KNm)	σ_{my} (Mpa)	σ_{mz} (Mpa)	σ_p (Mpa)	σ_{MP} (Mpa)	σ_t (Mpa)
10.00	0.72	1.67	26.77	1.46	-148.58	0.00	1606.43	819.28	-0.09	1.85	5.85	-9.36	-1.75
12.00	0.87	1.91	25.61	2.54	-205.87	0.00	1606.43	819.28	-0.15	2.56	5.85	-9.36	-1.10
14.00	1.03	2.16	24.76	4.07	-272.17	0.00	1606.43	819.28	-0.24	3.39	5.85	-9.36	-0.37
16.00	1.19	2.43	24.10	6.17	-347.35	0.00	1606.43	819.28	-0.36	4.32	5.85	-9.36	0.45
18.00	1.37	2.72	23.57	8.97	-431.25	0.00	1606.43	819.28	-0.53	5.36	5.85	-9.36	1.32
20.00	1.57	3.04	23.11	12.67	-523.64	0.00	1606.43	819.28	-0.75	6.51	5.85	-9.36	2.25
22.00	1.79	3.41	22.71	17.57	-624.26	0.00	1606.43	819.28	-1.04	7.77	5.85	-9.36	3.22
24.00	2.07	3.85	22.35	24.10	-732.79	0.00	1606.43	819.28	-1.42	9.12	5.85	-9.36	4.18
26.00	2.41	4.41	22.01	32.97	-848.83	0.00	1606.43	819.28	-1.95	10.56	5.85	-9.36	5.10
28.00	2.87	5.15	21.68	45.46	-971.92	0.00	1606.43	819.28	-2.68	12.09	5.85	-9.36	5.90
30.00	3.51	6.19	21.35	63.93	-1101.42	0.00	1606.43	819.28	-3.77	13.70	5.85	-9.36	6.42
32.00	4.52	7.82	21.02	93.52	-1236.38	0.00	1606.43	819.28	-5.52	15.38	5.85	-9.36	6.35
34.00	6.32	10.72	20.65	147.38	-1374.57	0.00	1606.43	819.28	-8.70	17.10	5.85	-9.36	4.89
36.00	10.30	17.12	20.15	268.62	-1507.07	0.00	1606.43	819.28	-15.86	18.75	5.85	-9.36	-0.62
38.00	20.77	33.46	18.93	593.37	-1580.38	0.00	1606.43	819.28	-35.03	19.66	5.85	-9.36	-18.88
40.00	395.48	54.46	16.41	1076.22	-1519.17	0.00	1606.43	819.28	-63.53	18.90	5.85	-9.36	-48.14
42.00	46.68	68.13	13.80	1487.19	-1409.46	0.00	1606.43	819.28	-87.79	17.53	5.85	-9.36	-73.76
44.00	-5.63	-8.63	19.04	-220.12	-2151.86	0.00	1606.43	819.28	12.99	26.77	5.85	-9.36	36.25
46.00	-4.00	-5.99	18.73	-171.17	-2321.61	0.00	1606.43	819.28	10.10	28.88	5.85	-9.36	35.47
48.00	-3.10	-4.52	18.39	-144.19	-2490.63	0.00	1606.43	819.28	8.51	30.98	5.85	-9.36	35.98
50.00	-2.52	-3.59	18.04	-127.22	-2660.04	0.00	1606.43	819.28	7.51	33.09	5.85	-9.36	37.09
52.00	-2.12	-2.94	17.68	-115.67	-2829.85	0.00	1606.43	819.28	6.83	35.20	5.85	-9.36	38.52
54.00	-1.82	-2.46	17.31	-107.42	-2999.81	-0.01	1606.43	819.28	6.34	37.32	5.85	-9.36	40.15
56.00	-1.60	-2.10	16.94	-101.33	-3169.60	-0.01	1606.43	819.28	5.98	39.43	5.85	-9.36	41.90
58.00	-1.42	-1.81	16.56	-96.75	-3338.91	-0.01	1606.43	819.28	5.71	41.54	5.85	-9.36	43.74
60.00	-1.28	-1.58	16.18	-93.26	-3507.48	-0.01	1606.43	819.28	5.50	43.63	5.85	-9.36	45.63

Case 8: I80A100, f_{ck} = 60 MPa

L (m)	β (°)	W (cm)	V (cm)	M_y (KNm)	M_z (KNm)	φ (°)	P_{max} (KN)	M_{Pmax} (KNm)	σ_{my} (Mpa)	σ_{mz} (Mpa)	σ_p (Mpa)	σ_{MP} (Mpa)	σ_t (Mpa)
10.00	0.84	1.70	41.00	1.55	-131.43	0.00	1539.86	632.88	-0.09	2.26	6.14	-9.81	-1.50
12.00	1.01	1.96	39.41	2.69	-182.90	0.00	1539.86	632.88	-0.16	3.14	6.14	-9.81	-0.69
14.00	1.19	2.23	38.25	4.32	-242.62	0.00	1539.86	632.88	-0.26	4.17	6.14	-9.81	0.24
16.00	1.39	2.51	37.35	6.55	-310.48	0.00	1539.86	632.88	-0.39	5.33	6.14	-9.81	1.28
18.00	1.59	2.82	36.61	9.53	-386.33	0.00	1539.86	632.88	-0.56	6.64	6.14	-9.81	2.40
20.00	1.83	3.17	35.98	13.49	-470.00	0.00	1539.86	632.88	-0.80	8.08	6.14	-9.81	3.61
22.00	2.10	3.57	35.43	18.74	-561.25	0.00	1539.86	632.88	-1.11	9.64	6.14	-9.81	4.86
24.00	2.42	4.06	34.92	25.78	-659.80	0.00	1539.86	632.88	-1.53	11.34	6.14	-9.81	6.14
26.00	2.84	4.67	34.44	35.43	-765.31	0.00	1539.86	632.88	-2.10	13.15	6.14	-9.81	7.38
28.00	3.40	5.50	33.98	49.19	-877.34	0.00	1539.86	632.88	-2.91	15.08	6.14	-9.81	8.49
30.00	4.21	6.71	33.51	69.92	-995.25	0.00	1539.86	632.88	-4.14	17.10	6.14	-9.81	9.29
32.00	5.52	8.64	33.01	104.13	-1117.86	0.00	1539.86	632.88	-6.17	19.21	6.14	-9.81	9.37
34.00	7.96	12.25	32.42	169.34	-1241.92	0.00	1539.86	632.88	-10.03	21.34	6.14	-9.81	7.64
36.00	13.68	20.58	31.41	324.08	-1351.86	0.00	1539.86	632.88	-19.20	23.23	6.14	-9.81	0.36
38.00	26.41	38.33	28.71	679.41	-1378.71	0.00	1539.86	632.88	-40.24	23.69	6.14	-9.81	-20.22
40.00	-178.32	-2.04	-27.12	-49.60	1486.31	0.00	1539.86	632.88	2.94	-25.54	6.14	-9.81	-26.27
42.00	-8.78	-12.54	30.50	-284.77	-1800.85	0.00	1539.86	632.88	16.87	30.94	6.14	-9.81	44.14
44.00	-5.56	-7.79	30.21	-198.35	-1963.15	0.00	1539.86	632.88	11.75	33.73	6.14	-9.81	41.81
46.00	-4.06	-5.58	29.77	-158.56	-2120.30	0.00	1539.86	632.88	9.39	36.43	6.14	-9.81	42.15
48.00	-3.19	-4.28	29.27	-135.54	-2277.49	0.00	1539.86	632.88	8.03	39.13	6.14	-9.81	43.49
50.00	-2.61	-3.43	28.75	-120.62	-2435.47	0.00	1539.86	632.88	7.14	41.85	6.14	-9.81	45.32
52.00	-2.21	-2.83	28.22	-110.27	-2594.19	0.00	1539.86	632.88	6.53	44.58	6.14	-9.81	47.44
54.00	-1.91	-2.38	27.67	-102.75	-2753.40	-0.01	1539.86	632.88	6.09	47.31	6.14	-9.81	49.73
56.00	-1.68	-2.04	27.12	-97.13	-2912.78	-0.01	1539.86	632.88	5.75	50.05	6.14	-9.81	52.13
58.00	-1.50	-1.77	26.55	-92.84	-3072.04	-0.01	1539.86	632.88	5.50	52.79	6.14	-9.81	54.61
60.00	-1.35	-1.55	25.98	-89.53	-3230.88	-0.01	1539.86	632.88	5.30	55.52	6.14	-9.81	57.15

Case 8: I60A100, f_{ck} = 60 MPa

L (m)	β (°)	W (cm)	V (cm)	M_y (KNm)	M_z (KNm)	φ (°)	P_{max} (KN)	M_{Pmax} (KNm)	σ_{my} (Mpa)	σ_{mz} (Mpa)	σ_p (Mpa)	σ_{MP} (Mpa)	σ_t (Mpa)
10.00	1.00	1.76	74.17	1.67	-115.08	0.00	1399.82	436.74	-0.10	3.04	6.17	-10.10	-0.98
12.00	1.21	2.04	71.66	2.91	-160.88	0.00	1399.82	436.74	-0.17	4.25	6.17	-10.10	0.16
14.00	1.43	2.33	69.83	4.67	-214.16	0.00	1399.82	436.74	-0.28	5.66	6.17	-10.10	1.46
16.00	1.66	2.65	68.40	7.08	-274.83	0.00	1399.82	436.74	-0.42	7.26	6.17	-10.10	2.92
18.00	1.91	2.98	67.23	10.32	-342.77	0.00	1399.82	436.74	-0.61	9.06	6.17	-10.10	4.52
20.00	2.19	3.37	66.23	14.63	-417.81	0.00	1399.82	436.74	-0.87	11.04	6.17	-10.10	6.25
22.00	2.52	3.81	65.34	20.39	-499.77	0.00	1399.82	436.74	-1.21	13.20	6.17	-10.10	8.07
24.00	2.93	4.36	64.51	28.17	-588.41	0.00	1399.82	436.74	-1.67	15.55	6.17	-10.10	9.95
26.00	3.46	5.07	63.73	38.99	-683.39	0.00	1399.82	436.74	-2.32	18.05	6.17	-10.10	11.82
28.00	4.18	6.04	62.95	54.66	-784.28	0.00	1399.82	436.74	-3.25	20.72	6.17	-10.10	13.55
30.00	5.26	7.50	62.13	78.96	-890.34	0.00	1399.82	436.74	-4.69	23.52	6.17	-10.10	14.91
32.00	7.08	9.93	61.22	120.73	-999.90	0.00	1399.82	436.74	-7.18	26.42	6.17	-10.10	15.32
34.00	10.71	14.76	59.93	205.40	-1107.12	0.00	1399.82	436.74	-12.21	29.25	6.17	-10.10	13.12
36.00	19.22	25.84	57.03	407.96	-1183.06	0.00	1399.82	436.74	-24.25	31.26	6.17	-10.10	3.09
38.00	33.05	42.54	50.37	753.24	-1165.06	0.00	1399.82	436.74	-44.77	30.78	6.17	-10.10	-17.91
40.00	-29.42	-37.53	51.49	-751.55	-1323.29	0.00	1399.82	436.74	44.67	34.96	6.17	-10.10	75.71
42.00	-8.15	-10.53	57.25	-239.03	-1628.13	0.00	1399.82	436.74	14.21	43.01	6.17	-10.10	53.30
44.00	-5.50	-6.99	56.71	-177.32	-1774.62	0.00	1399.82	436.74	10.54	46.88	6.17	-10.10	53.50
46.00	-4.13	-5.15	55.95	-145.79	-1918.83	0.00	1399.82	436.74	8.66	50.69	6.17	-10.10	55.44
48.00	-3.29	-4.03	55.11	-126.60	-2063.73	0.00	1399.82	436.74	7.52	54.52	6.17	-10.10	58.13
50.00	-2.73	-3.26	54.22	-113.75	-2209.76	0.00	1399.82	436.74	6.76	58.38	6.17	-10.10	61.22
52.00	-2.32	-2.71	53.29	-104.62	-2356.85	-0.01	1399.82	436.74	6.22	62.27	6.17	-10.10	64.56
54.00	-2.01	-2.30	52.34	-97.88	-2504.74	-0.01	1399.82	436.74	5.82	66.17	6.17	-10.10	68.07
56.00	-1.77	-1.98	51.37	-92.75	-2653.14	-0.01	1399.82	436.74	5.51	70.09	6.17	-10.10	71.69
58.00	-1.58	-1.72	50.39	-88.79	-2801.73	-0.01	1399.82	436.74	5.28	74.02	6.17	-10.10	75.38
60.00	-1.43	-1.51	49.39	-85.70	-2950.25	-0.01	1399.82	436.74	5.09	77.94	6.17	-10.10	79.12

Case 8: I120B120, f_{ck} = 20 MPa

L (m)	β (°)	W (cm)	V (cm)	M_y (KNm)	M_z (KNm)	φ (°)	P_{max} (KN)	M_{Pmax} (KNm)	σ_{my} (Mpa)	σ_{mz} (Mpa)	σ_p (Mpa)	σ_{MP} (Mpa)	σ_t (Mpa)
10.00	0.64	1.07	21.03	2.18	-195.27	0.00	1448.85	866.41	-0.07	1.29	3.13	-4.65	-0.29
12.00	0.77	1.29	21.03	3.79	-281.18	0.00	1448.85	866.41	-0.11	1.86	3.13	-4.65	0.23
14.00	0.91	1.51	21.03	6.06	-382.71	0.00	1448.85	866.41	-0.18	2.53	3.13	-4.65	0.83
16.00	1.05	1.75	21.03	9.15	-499.84	0.00	1448.85	866.41	-0.27	3.31	3.13	-4.65	1.52
18.00	1.20	2.00	21.03	13.24	-632.58	0.00	1448.85	866.41	-0.40	4.18	3.13	-4.65	2.27
20.00	1.36	2.27	21.03	18.60	-780.92	0.00	1448.85	866.41	-0.56	5.17	3.13	-4.65	3.09
22.00	1.55	2.58	21.03	25.57	-944.83	0.00	1448.85	866.41	-0.77	6.25	3.13	-4.65	3.97
24.00	1.77	2.95	21.02	34.70	-1124.30	0.00	1448.85	866.41	-1.04	7.44	3.13	-4.65	4.88
26.00	2.03	3.39	21.02	46.85	-1319.29	0.00	1448.85	866.41	-1.40	8.73	3.13	-4.65	5.81
28.00	2.37	3.96	21.02	63.45	-1529.72	0.00	1448.85	866.41	-1.90	10.12	3.13	-4.65	6.70
30.00	2.84	4.73	21.01	87.12	-1755.40	0.00	1448.85	866.41	-2.61	11.61	3.13	-4.65	7.49
32.00	3.53	5.88	21.00	123.22	-1995.91	0.00	1448.85	866.41	-3.69	13.20	3.13	-4.65	8.00
34.00	4.68	7.80	20.96	184.38	-2249.95	0.00	1448.85	866.41	-5.52	14.88	3.13	-4.65	7.85
36.00	7.00	11.63	20.88	308.29	-2512.04	0.00	1448.85	866.41	-9.23	16.62	3.13	-4.65	5.87
38.00	13.22	21.83	20.48	644.70	-2745.22	0.00	1448.85	866.41	-19.30	18.16	3.13	-4.65	-2.66
40.00	27.72	44.41	18.62	1453.29	-2766.01	0.00	1448.85	866.41	-43.50	18.30	3.13	-4.65	-26.72
42.00	-30.91	-49.05	18.05	-1769.69	-2955.50	0.00	1448.85	866.41	52.98	19.55	3.13	-4.65	71.01
44.00	-5.53	-9.19	20.94	-364.07	-3763.14	0.00	1448.85	866.41	10.90	24.89	3.13	-4.65	34.28
46.00	-3.64	-6.07	20.99	-262.64	-4123.87	0.00	1448.85	866.41	7.86	27.28	3.13	-4.65	33.63
48.00	-2.68	-4.47	21.01	-210.53	-4494.43	0.00	1448.85	866.41	6.30	29.73	3.13	-4.65	34.52
50.00	-2.10	-3.49	21.02	-178.49	-4878.85	0.00	1448.85	866.41	5.34	32.27	3.13	-4.65	36.10
52.00	-1.70	-2.83	21.03	-156.67	-5278.17	0.00	1448.85	866.41	4.69	34.92	3.13	-4.65	38.09
54.00	-1.42	-2.36	21.03	-140.75	-5692.76	0.00	1448.85	866.41	4.21	37.66	3.13	-4.65	40.36
56.00	-1.20	-2.00	21.03	-128.56	-6122.77	0.00	1448.85	866.41	3.85	40.50	3.13	-4.65	42.84
58.00	-1.04	-1.73	21.03	-118.89	-6568.30	0.00	1448.85	866.41	3.56	43.45	3.13	-4.65	45.49
60.00	-0.90	-1.51	21.03	-110.98	-7029.37	0.00	1448.85	866.41	3.32	46.50	3.13	-4.65	48.31

Case 8: I140B120, f_{ck} = 20 MPa

L (m)	β (°)	W (cm)	V (cm)	M_y (KNm)	M_z (KNm)	φ (°)	P_{max} (KN)	M_{Pmax} (KNm)	σ_{my} (Mpa)	σ_{mz} (Mpa)	σ_p (Mpa)	σ_{MP} (Mpa)	σ_t (Mpa)
10.00	0.57	1.01	15.20	2.08	-207.93	0.00	1481.75	1026.85	-0.06	1.10	3.01	-4.46	-0.42
12.00	0.69	1.22	15.20	3.61	-299.41	0.00	1481.75	1026.85	-0.11	1.58	3.01	-4.46	0.01
14.00	0.81	1.43	15.20	5.76	-407.52	0.00	1481.75	1026.85	-0.17	2.15	3.01	-4.46	0.52
16.00	0.94	1.66	15.20	8.70	-532.26	0.00	1481.75	1026.85	-0.26	2.81	3.01	-4.46	1.09
18.00	1.07	1.89	15.19	12.57	-673.61	0.00	1481.75	1026.85	-0.38	3.55	3.01	-4.46	1.72
20.00	1.21	2.15	15.19	17.64	-831.58	0.00	1481.75	1026.85	-0.53	4.38	3.01	-4.46	2.40
22.00	1.38	2.44	15.19	24.21	-1006.14	0.00	1481.75	1026.85	-0.72	5.30	3.01	-4.46	3.12
24.00	1.57	2.77	15.19	32.77	-1197.29	0.00	1481.75	1026.85	-0.98	6.31	3.01	-4.46	3.88
26.00	1.80	3.18	15.19	44.08	-1404.99	0.00	1481.75	1026.85	-1.32	7.41	3.01	-4.46	4.63
28.00	2.09	3.69	15.19	59.38	-1629.17	0.00	1481.75	1026.85	-1.77	8.59	3.01	-4.46	5.36
30.00	2.48	4.38	15.18	80.93	-1869.72	0.00	1481.75	1026.85	-2.42	9.86	3.01	-4.46	5.98
32.00	3.05	5.39	15.18	113.11	-2126.31	0.00	1481.75	1026.85	-3.38	11.21	3.01	-4.46	6.37
34.00	3.96	7.00	15.16	165.92	-2398.06	0.00	1481.75	1026.85	-4.95	12.64	3.01	-4.46	6.23
36.00	5.69	10.05	15.12	267.26	-2681.63	0.00	1481.75	1026.85	-7.98	14.14	3.01	-4.46	4.70
38.00	10.06	17.71	14.96	524.36	-2956.52	0.00	1481.75	1026.85	-15.65	15.58	3.01	-4.46	-1.53
40.00	22.71	39.15	14.02	1284.71	-3069.00	0.00	1481.75	1026.85	-38.35	16.18	3.01	-4.46	-23.63
42.00	-178.91	-1.93	-15.19	-69.94	3667.41	0.00	1481.75	1026.85	2.09	-19.33	3.01	-4.46	-18.70
44.00	-5.83	-10.30	15.12	-409.05	-4004.90	0.00	1481.75	1026.85	12.21	21.11	3.01	-4.46	31.86
46.00	-3.68	-6.51	15.17	-282.30	-4390.96	0.00	1481.75	1026.85	8.43	23.15	3.01	-4.46	30.12
48.00	-2.65	-4.69	15.18	-221.58	-4785.83	0.00	1481.75	1026.85	6.61	25.23	3.01	-4.46	30.38
50.00	-2.05	-3.62	15.19	-185.56	-5195.20	0.00	1481.75	1026.85	5.54	27.38	3.01	-4.46	31.47
52.00	-1.65	-2.91	15.19	-161.57	-5620.40	0.00	1481.75	1026.85	4.82	29.63	3.01	-4.46	32.99
54.00	-1.36	-2.41	15.19	-144.34	-6061.83	0.00	1481.75	1026.85	4.31	31.95	3.01	-4.46	34.80
56.00	-1.15	-2.04	15.19	-131.31	-6519.70	0.00	1481.75	1026.85	3.92	34.37	3.01	-4.46	36.83
58.00	-0.99	-1.75	15.20	-121.05	-6994.08	0.00	1481.75	1026.85	3.61	36.87	3.01	-4.46	39.02
60.00	-0.86	-1.53	15.20	-112.73	-7485.02	0.00	1481.75	1026.85	3.37	39.45	3.01	-4.46	41.36

Case 8: I180B120, f_{ck} = 20 MPa

L (m)	β (°)	W (cm)	V (cm)	M_y (KNm)	M_z (KNm)	φ (°)	P_{max} (KN)	M_{Pmax} (KNm)	σ_{my} (Mpa)	σ_{mz} (Mpa)	σ_p (Mpa)	σ_{MP} (Mpa)	σ_t (Mpa)
10.00	0.47	0.93	9.13	1.92	-233.25	0.00	1514.27	1341.64	-0.06	0.85	2.74	-4.15	-0.62
12.00	0.57	1.12	9.13	3.32	-335.87	0.00	1514.27	1341.64	-0.10	1.23	2.74	-4.15	-0.29
14.00	0.67	1.31	9.13	5.31	-457.15	0.00	1514.27	1341.64	-0.16	1.67	2.74	-4.15	0.09
16.00	0.77	1.52	9.13	8.00	-597.07	0.00	1514.27	1341.64	-0.24	2.18	2.74	-4.15	0.52
18.00	0.88	1.73	9.13	11.56	-755.65	0.00	1514.27	1341.64	-0.34	2.76	2.74	-4.15	1.00
20.00	0.99	1.96	9.13	16.18	-932.87	0.00	1514.27	1341.64	-0.48	3.40	2.74	-4.15	1.51
22.00	1.12	2.22	9.13	22.15	-1128.73	0.00	1514.27	1341.64	-0.66	4.12	2.74	-4.15	2.04
24.00	1.27	2.51	9.12	29.87	-1343.21	0.00	1514.27	1341.64	-0.89	4.90	2.74	-4.15	2.60
26.00	1.45	2.87	9.12	39.96	-1576.28	0.00	1514.27	1341.64	-1.19	5.75	2.74	-4.15	3.15
28.00	1.67	3.30	9.12	53.43	-1827.92	0.00	1514.27	1341.64	-1.59	6.67	2.74	-4.15	3.67
30.00	1.97	3.88	9.12	72.00	-2098.04	0.00	1514.27	1341.64	-2.14	7.65	2.74	-4.15	4.10
32.00	2.37	4.68	9.12	98.94	-2386.46	0.00	1514.27	1341.64	-2.94	8.70	2.74	-4.15	4.35
34.00	3.00	5.92	9.11	141.13	-2692.71	0.00	1514.27	1341.64	-4.19	9.82	2.74	-4.15	4.22
36.00	4.10	8.08	9.10	216.09	-3015.23	0.00	1514.27	1341.64	-6.41	11.00	2.74	-4.15	3.17
38.00	6.53	12.86	9.07	382.84	-3346.35	0.00	1514.27	1341.64	-11.36	12.21	2.74	-4.15	-0.57
40.00	14.33	27.99	8.84	923.50	-3615.98	0.00	1514.27	1341.64	-27.41	13.19	2.74	-4.15	-15.64
42.00	30.56	57.50	7.86	2092.04	-3543.04	0.00	1514.27	1341.64	-62.10	12.92	2.74	-4.15	-50.60
44.00	180.89	-1.76	-9.13	-70.17	4515.23	0.00	1514.27	1341.64	2.08	-16.47	2.74	-4.15	-15.80
46.00	-3.78	-7.45	9.11	-325.13	-4924.91	0.00	1514.27	1341.64	9.65	17.96	2.74	-4.15	26.20
48.00	-2.60	-5.14	9.12	-244.15	-5368.60	0.00	1514.27	1341.64	7.25	19.58	2.74	-4.15	25.41
50.00	-1.96	-3.87	9.12	-199.51	-5827.91	0.00	1514.27	1341.64	5.92	21.26	2.74	-4.15	25.76
52.00	-1.55	-3.07	9.12	-171.04	-6304.84	0.00	1514.27	1341.64	5.08	23.00	2.74	-4.15	26.66
54.00	-1.27	-2.51	9.12	-151.19	-6799.98	0.00	1514.27	1341.64	4.49	24.80	2.74	-4.15	27.87
56.00	-1.07	-2.11	9.13	-136.49	-7313.54	0.00	1514.27	1341.64	4.05	26.68	2.74	-4.15	29.31
58.00	-0.91	-1.80	9.13	-125.11	-7845.63	0.00	1514.27	1341.64	3.71	28.62	2.74	-4.15	30.91
60.00	-0.79	-1.56	9.13	-116.00	-8396.31	0.00	1514.27	1341.64	3.44	30.63	2.74	-4.15	32.65

Case 8: I200B120, f_{ck} = 20 MPa

L (m)	β (°)	W (cm)	V (cm)	M_y (KNm)	M_z (KNm)	φ (°)	P_{max} (KN)	M_{Pmax} (KNm)	σ_{my} (Mpa)	σ_{mz} (Mpa)	σ_p (Mpa)	σ_{MP} (Mpa)	σ_t (Mpa)
10.00	0.43	0.90	7.42	1.86	-245.90	0.00	1523.65	1496.22	-0.05	0.77	2.61	-4.01	-0.68
12.00	0.52	1.08	7.42	3.22	-354.09	0.00	1523.65	1496.22	-0.10	1.11	2.61	-4.01	-0.39
14.00	0.61	1.27	7.42	5.14	-481.95	0.00	1523.65	1496.22	-0.15	1.51	2.61	-4.01	-0.04
16.00	0.71	1.46	7.42	7.75	-629.48	0.00	1523.65	1496.22	-0.23	1.97	2.61	-4.01	0.34
18.00	0.80	1.67	7.42	11.18	-796.67	0.00	1523.65	1496.22	-0.33	2.50	2.61	-4.01	0.76
20.00	0.91	1.89	7.42	15.64	-983.51	0.00	1523.65	1496.22	-0.46	3.08	2.61	-4.01	1.22
22.00	1.03	2.14	7.42	21.39	-1190.01	0.00	1523.65	1496.22	-0.63	3.73	2.61	-4.01	1.69
24.00	1.17	2.42	7.42	28.80	-1416.14	0.00	1523.65	1496.22	-0.85	4.44	2.61	-4.01	2.18
26.00	1.33	2.75	7.42	38.46	-1661.90	0.00	1523.65	1496.22	-1.14	5.21	2.61	-4.01	2.67
28.00	1.52	3.16	7.42	51.28	-1927.25	0.00	1523.65	1496.22	-1.52	6.04	2.61	-4.01	3.12
30.00	1.78	3.70	7.42	68.84	-2212.11	0.00	1523.65	1496.22	-2.04	6.93	2.61	-4.01	3.49
32.00	2.14	4.44	7.41	94.02	-2516.35	0.00	1523.65	1496.22	-2.78	7.88	2.61	-4.01	3.70
34.00	2.68	5.56	7.41	132.83	-2839.61	0.00	1523.65	1496.22	-3.93	8.89	2.61	-4.01	3.56
36.00	3.60	7.46	7.40	199.96	-3180.70	0.00	1523.65	1496.22	-5.92	9.96	2.61	-4.01	2.64
38.00	5.53	11.47	7.38	342.29	-3534.39	0.00	1523.65	1496.22	-10.14	11.07	2.61	-4.01	-0.47
40.00	11.49	23.70	7.27	784.04	-3855.64	0.00	1523.65	1496.22	-23.22	12.08	2.61	-4.01	-12.54
42.00	27.33	54.62	6.59	1991.80	-3853.51	0.00	1523.65	1496.22	-58.99	12.07	2.61	-4.01	-48.32
44.00	-34.59	-67.54	6.11	-2702.95	-3919.09	0.00	1523.65	1496.22	80.05	12.27	2.61	-4.01	90.92
46.00	-3.83	-7.94	7.40	-347.13	-5191.85	0.00	1523.65	1496.22	10.28	16.26	2.61	-4.01	25.14
48.00	-2.58	-5.35	7.41	-255.01	-5660.01	0.00	1523.65	1496.22	7.55	17.73	2.61	-4.01	23.88
50.00	-1.92	-3.99	7.42	-205.98	-6144.28	0.00	1523.65	1496.22	6.10	19.24	2.61	-4.01	23.94
52.00	-1.51	-3.14	7.42	-175.33	-6647.07	0.00	1523.65	1496.22	5.19	20.82	2.61	-4.01	24.61
54.00	-1.23	-2.56	7.42	-154.25	-7169.05	0.00	1523.65	1496.22	4.57	22.45	2.61	-4.01	25.62
56.00	-1.03	-2.14	7.42	-138.78	-7710.46	0.00	1523.65	1496.22	4.11	24.15	2.61	-4.01	26.86
58.00	-0.88	-1.82	7.42	-126.89	-8271.41	0.00	1523.65	1496.22	3.76	25.91	2.61	-4.01	28.26
60.00	-0.76	-1.58	7.42	-117.42	-8851.95	0.00	1523.65	1496.22	3.48	27.72	2.61	-4.01	29.80

Case 8: I120B120, f_{ck} = 40 MPa

L (m)	β (°)	W (cm)	V (cm)	M_y (KNm)	M_z (KNm)	φ (°)	P_{max} (KN)	M_{Pmax} (KNm)	σ_{my} (Mpa)	σ_{mz} (Mpa)	σ_p (Mpa)	σ_{MP} (Mpa)	σ_t (Mpa)
10.00	0.64	0.85	16.70	2.18	-195.27	0.00	2299.91	1375.35	-0.07	1.29	4.97	-7.38	-1.18
12.00	0.77	1.02	16.69	3.78	-281.18	0.00	2299.91	1375.35	-0.11	1.86	4.97	-7.38	-0.66
14.00	0.90	1.20	16.69	6.04	-382.71	0.00	2299.91	1375.35	-0.18	2.53	4.97	-7.38	-0.06
16.00	1.04	1.38	16.69	9.10	-499.85	0.00	2299.91	1375.35	-0.27	3.31	4.97	-7.38	0.63
18.00	1.19	1.57	16.69	13.12	-632.59	0.00	2299.91	1375.35	-0.39	4.18	4.97	-7.38	1.38
20.00	1.35	1.78	16.69	18.34	-780.92	0.00	2299.91	1375.35	-0.55	5.17	4.97	-7.38	2.21
22.00	1.52	2.01	16.69	25.03	-944.85	0.00	2299.91	1375.35	-0.75	6.25	4.97	-7.38	3.09
24.00	1.71	2.27	16.69	33.63	-1124.34	0.00	2299.91	1375.35	-1.01	7.44	4.97	-7.38	4.02
26.00	1.94	2.57	16.69	44.76	-1319.36	0.00	2299.91	1375.35	-1.34	8.73	4.97	-7.38	4.98
28.00	2.22	2.94	16.68	59.41	-1529.88	0.00	2299.91	1375.35	-1.78	10.12	4.97	-7.38	5.94
30.00	2.58	3.42	16.68	79.22	-1755.77	0.00	2299.91	1375.35	-2.37	11.61	4.97	-7.38	6.84
32.00	3.07	4.06	16.67	107.13	-1996.84	0.00	2299.91	1375.35	-3.21	13.21	4.97	-7.38	7.60
34.00	3.78	5.00	16.66	148.99	-2252.57	0.00	2299.91	1375.35	-4.46	14.90	4.97	-7.38	8.03
36.00	4.94	6.53	16.63	218.08	-2521.47	0.00	2299.91	1375.35	-6.53	16.68	4.97	-7.38	7.74
38.00	7.16	9.45	16.57	351.56	-2797.91	0.00	2299.91	1375.35	-10.52	18.51	4.97	-7.38	5.58
40.00	12.61	16.54	16.29	681.93	-3049.23	0.00	2299.91	1375.35	-20.41	20.17	4.97	-7.38	-2.65
42.00	25.36	32.46	15.09	1475.33	-3112.91	0.00	2299.91	1375.35	-44.16	20.59	4.97	-7.38	-25.98
44.00	-16.87	-21.99	15.98	-1097.12	-3618.02	0.00	2299.91	1375.35	32.84	23.93	4.97	-7.38	54.37
46.00	-6.88	-9.08	16.58	-494.81	-4102.49	0.00	2299.91	1375.35	14.81	27.14	4.97	-7.38	39.54
48.00	-4.39	-5.80	16.65	-344.38	-4486.16	0.00	2299.91	1375.35	10.31	29.68	4.97	-7.38	37.58
50.00	-3.19	-4.21	16.67	-271.43	-4874.56	0.00	2299.91	1375.35	8.13	32.25	4.97	-7.38	37.96
52.00	-2.47	-3.27	16.68	-227.80	-5275.58	0.00	2299.91	1375.35	6.82	34.90	4.97	-7.38	39.31
54.00	-2.00	-2.64	16.68	-198.58	-5691.03	0.00	2299.91	1375.35	5.94	37.65	4.97	-7.38	41.19
56.00	-1.66	-2.20	16.69	-177.53	-6121.55	0.00	2299.91	1375.35	5.31	40.50	4.97	-7.38	43.40
58.00	-1.41	-1.86	16.69	-161.56	-6567.39	0.00	2299.91	1375.35	4.84	43.44	4.97	-7.38	45.87
60.00	-1.21	-1.61	16.69	-148.98	-7028.67	0.00	2299.91	1375.35	4.46	46.50	4.97	-7.38	48.55

Case 8: I140B120, f_{ck} = 40 MPa

L (m)	β (°)	W (cm)	V (cm)	M_y (KNm)	M_z (KNm)	φ (°)	P_{max} (KN)	M_{Pmax} (KNm)	σ_{my} (Mpa)	σ_{mz} (Mpa)	σ_p (Mpa)	σ_{MP} (Mpa)	σ_t (Mpa)
10.00	0.57	0.80	12.06	2.08	-207.93	0.00	2352.13	1630.03	-0.06	1.10	4.77	-7.09	-1.28
12.00	0.69	0.97	12.06	3.60	-299.41	0.00	2352.13	1630.03	-0.11	1.58	4.77	-7.09	-0.84
14.00	0.81	1.13	12.06	5.75	-407.52	0.00	2352.13	1630.03	-0.17	2.15	4.77	-7.09	-0.34
16.00	0.93	1.31	12.06	8.65	-532.26	0.00	2352.13	1630.03	-0.26	2.81	4.77	-7.09	0.23
18.00	1.06	1.49	12.06	12.47	-673.61	0.00	2352.13	1630.03	-0.37	3.55	4.77	-7.09	0.87
20.00	1.20	1.68	12.06	17.40	-831.58	0.00	2352.13	1630.03	-0.52	4.38	4.77	-7.09	1.55
22.00	1.35	1.90	12.06	23.72	-1006.15	0.00	2352.13	1630.03	-0.71	5.30	4.77	-7.09	2.28
24.00	1.52	2.14	12.06	31.81	-1197.32	0.00	2352.13	1630.03	-0.95	6.31	4.77	-7.09	3.05
26.00	1.72	2.42	12.06	42.23	-1405.04	0.00	2352.13	1630.03	-1.26	7.41	4.77	-7.09	3.83
28.00	1.96	2.76	12.06	55.84	-1629.30	0.00	2352.13	1630.03	-1.67	8.59	4.77	-7.09	4.61
30.00	2.27	3.19	12.05	74.08	-1870.00	0.00	2352.13	1630.03	-2.21	9.86	4.77	-7.09	5.33
32.00	2.68	3.76	12.05	99.42	-2126.99	0.00	2352.13	1630.03	-2.97	11.21	4.77	-7.09	5.93
34.00	3.26	4.58	12.04	136.68	-2399.91	0.00	2352.13	1630.03	-4.08	12.65	4.77	-7.09	6.26
36.00	4.18	5.86	12.03	196.35	-2687.75	0.00	2352.13	1630.03	-5.86	14.17	4.77	-7.09	5.99
38.00	5.85	8.20	12.00	306.08	-2987.02	0.00	2352.13	1630.03	-9.14	15.74	4.77	-7.09	4.29
40.00	9.71	13.58	11.89	561.42	-3279.34	0.00	2352.13	1630.03	-16.76	17.29	4.77	-7.09	-1.79
42.00	20.35	27.99	11.31	1275.78	-3439.06	0.00	2352.13	1630.03	-38.08	18.13	4.77	-7.09	-22.27
44.00	711.63	-11.72	11.93	-586.24	-3982.82	0.00	2352.13	1630.03	17.50	20.99	4.77	-7.09	36.18
46.00	-7.45	-10.43	11.96	-570.31	-4362.91	0.00	2352.13	1630.03	17.02	23.00	4.77	-7.09	37.71
48.00	-4.48	-6.29	12.03	-374.38	-4776.30	0.00	2352.13	1630.03	11.18	25.18	4.77	-7.09	34.04
50.00	-3.17	-4.45	12.04	-287.69	-5190.55	0.00	2352.13	1630.03	8.59	27.36	4.77	-7.09	33.63
52.00	-2.43	-3.41	12.05	-238.00	-5617.68	0.00	2352.13	1630.03	7.10	29.61	4.77	-7.09	34.40
54.00	-1.94	-2.73	12.06	-205.56	-6060.07	0.00	2352.13	1630.03	6.14	31.94	4.77	-7.09	35.77
56.00	-1.60	-2.25	12.06	-182.60	-6518.46	0.00	2352.13	1630.03	5.45	34.36	4.77	-7.09	37.50
58.00	-1.35	-1.90	12.06	-165.41	-6993.17	0.00	2352.13	1630.03	4.94	36.86	4.77	-7.09	39.49
60.00	-1.16	-1.63	12.06	-151.99	-7484.32	0.00	2352.13	1630.03	4.54	39.45	4.77	-7.09	41.67

Case 8: I180B120, f_{ck} = 40 MPa

L (m)	β (°)	W (cm)	V (cm)	M_y (KNm)	M_z (KNm)	φ (°)	P_{max} (KN)	M_{Pmax} (KNm)	σ_{my} (Mpa)	σ_{mz} (Mpa)	σ_p (Mpa)	σ_{MP} (Mpa)	σ_t (Mpa)
10.00	0.47	0.74	7.24	1.91	-233.25	0.00	2403.75	2129.72	-0.06	0.85	4.35	-6.60	-1.45
12.00	0.57	0.89	7.24	3.32	-335.87	0.00	2403.75	2129.72	-0.10	1.23	4.35	-6.60	-1.12
14.00	0.66	1.04	7.24	5.30	-457.15	0.00	2403.75	2129.72	-0.16	1.67	4.35	-6.60	-0.74
16.00	0.76	1.20	7.24	7.96	-597.07	0.00	2403.75	2129.72	-0.24	2.18	4.35	-6.60	-0.31
18.00	0.87	1.36	7.24	11.47	-755.65	0.00	2403.75	2129.72	-0.34	2.76	4.35	-6.60	0.17
20.00	0.98	1.54	7.24	15.98	-932.88	0.00	2403.75	2129.72	-0.47	3.40	4.35	-6.60	0.68
22.00	1.10	1.73	7.24	21.75	-1128.74	0.00	2403.75	2129.72	-0.65	4.12	4.35	-6.60	1.22
24.00	1.24	1.94	7.24	29.08	-1343.22	0.00	2403.75	2129.72	-0.86	4.90	4.35	-6.60	1.79
26.00	1.40	2.19	7.24	38.45	-1576.32	0.00	2403.75	2129.72	-1.14	5.75	4.35	-6.60	2.36
28.00	1.58	2.48	7.24	50.56	-1828.00	0.00	2403.75	2129.72	-1.50	6.67	4.35	-6.60	2.92
30.00	1.82	2.85	7.24	66.55	-2098.22	0.00	2403.75	2129.72	-1.98	7.65	4.35	-6.60	3.43
32.00	2.12	3.32	7.24	88.34	-2386.88	0.00	2403.75	2129.72	-2.62	8.71	4.35	-6.60	3.84
34.00	2.54	3.98	7.24	119.45	-2693.76	0.00	2403.75	2129.72	-3.55	9.83	4.35	-6.60	4.03
36.00	3.17	4.96	7.23	167.13	-3018.34	0.00	2403.75	2129.72	-4.96	11.01	4.35	-6.60	3.80
38.00	4.24	6.63	7.22	248.81	-3358.97	0.00	2403.75	2129.72	-7.39	12.25	4.35	-6.60	2.62
40.00	6.43	10.06	7.20	418.20	-3708.54	0.00	2403.75	2129.72	-12.41	13.53	4.35	-6.60	-1.14
42.00	12.66	19.67	7.07	901.80	-4014.54	0.00	2403.75	2129.72	-26.77	14.64	4.35	-6.60	-14.38
44.00	27.20	41.04	6.44	2064.50	-4016.23	0.00	2403.75	2129.72	-61.29	14.65	4.35	-6.60	-48.88
46.00	-31.89	-47.43	6.15	-2607.73	-4190.49	0.00	2403.75	2129.72	77.41	15.28	4.35	-6.60	90.45
48.00	-4.72	-7.39	7.22	-442.18	-5355.93	0.00	2403.75	2129.72	13.13	19.54	4.35	-6.60	30.41
50.00	-3.16	-4.95	7.23	-321.61	-5822.45	0.00	2403.75	2129.72	9.55	21.24	4.35	-6.60	28.54
52.00	-2.35	-3.68	7.24	-258.40	-6301.87	0.00	2403.75	2129.72	7.67	22.99	4.35	-6.60	28.41
54.00	-1.85	-2.89	7.24	-219.18	-6798.13	0.00	2403.75	2129.72	6.51	24.80	4.35	-6.60	29.05
56.00	-1.51	-2.36	7.24	-192.34	-7312.29	0.00	2403.75	2129.72	5.71	26.67	4.35	-6.60	30.13
58.00	-1.26	-1.98	7.24	-172.72	-7844.73	0.00	2403.75	2129.72	5.13	28.61	4.35	-6.60	31.49
60.00	-1.08	-1.69	7.24	-157.68	-8395.63	0.00	2403.75	2129.72	4.68	30.62	4.35	-6.60	33.06

Case 8: I200B120, f_{ck} = 40 MPa

L (m)	β (°)	W (cm)	V (cm)	M_y (KNm)	M_z (KNm)	φ (°)	P_{max} (KN)	M_{Pmax} (KNm)	σ_{my} (Mpa)	σ_{mz} (Mpa)	σ_p (Mpa)	σ_{MP} (Mpa)	σ_t (Mpa)
10.00	0.43	0.71	5.89	1.85	-245.90	0.00	2418.64	2375.11	-0.05	0.77	4.15	-6.37	-1.51
12.00	0.52	0.86	5.89	3.21	-354.09	0.00	2418.64	2375.11	-0.10	1.11	4.15	-6.37	-1.21
14.00	0.61	1.00	5.89	5.13	-481.95	0.00	2418.64	2375.11	-0.15	1.51	4.15	-6.37	-0.86
16.00	0.70	1.16	5.89	7.71	-629.48	0.00	2418.64	2375.11	-0.23	1.97	4.15	-6.37	-0.48
18.00	0.80	1.32	5.89	11.10	-796.67	0.00	2418.64	2375.11	-0.33	2.50	4.15	-6.37	-0.06
20.00	0.90	1.48	5.89	15.46	-983.52	0.00	2418.64	2375.11	-0.46	3.08	4.15	-6.37	0.40
22.00	1.01	1.67	5.89	21.02	-1190.01	0.00	2418.64	2375.11	-0.62	3.73	4.15	-6.37	0.88
24.00	1.14	1.87	5.89	28.07	-1416.16	0.00	2418.64	2375.11	-0.83	4.44	4.15	-6.37	1.38
26.00	1.28	2.10	5.89	37.06	-1661.93	0.00	2418.64	2375.11	-1.10	5.21	4.15	-6.37	1.89
28.00	1.45	2.38	5.89	48.64	-1927.31	0.00	2418.64	2375.11	-1.44	6.04	4.15	-6.37	2.37
30.00	1.65	2.72	5.89	63.85	-2212.26	0.00	2418.64	2375.11	-1.89	6.93	4.15	-6.37	2.82
32.00	1.92	3.16	5.89	84.41	-2516.69	0.00	2418.64	2375.11	-2.50	7.88	4.15	-6.37	3.16
34.00	2.29	3.77	5.88	113.47	-2840.44	0.00	2418.64	2375.11	-3.36	8.90	4.15	-6.37	3.31
36.00	2.83	4.66	5.88	157.32	-3183.10	0.00	2418.64	2375.11	-4.66	9.97	4.15	-6.37	3.09
38.00	3.72	6.13	5.88	230.62	-3543.43	0.00	2418.64	2375.11	-6.83	11.10	4.15	-6.37	2.05
40.00	5.49	9.03	5.86	376.35	-3916.51	0.00	2418.64	2375.11	-11.15	12.27	4.15	-6.37	-1.10
42.00	10.26	16.81	5.79	772.40	-4268.52	0.00	2418.64	2375.11	-22.87	13.37	4.15	-6.37	-11.73
44.00	23.75	38.03	5.39	1917.76	-4357.46	0.00	2418.64	2375.11	-56.80	13.65	4.15	-6.37	-45.37
46.00	-28.10	-44.47	5.19	-2450.66	-4590.21	0.00	2418.64	2375.11	72.58	14.38	4.15	-6.37	84.73
48.00	-4.84	-7.97	5.87	-478.43	-5645.51	0.00	2418.64	2375.11	14.17	17.68	4.15	-6.37	29.63
50.00	-3.15	-5.19	5.88	-338.26	-6138.42	0.00	2418.64	2375.11	10.02	19.23	4.15	-6.37	27.02
52.00	-2.31	-3.81	5.88	-267.99	-6643.98	0.00	2418.64	2375.11	7.94	20.81	4.15	-6.37	26.52
54.00	-1.80	-2.97	5.89	-225.42	-7167.17	0.00	2418.64	2375.11	6.68	22.45	4.15	-6.37	26.90
56.00	-1.46	-2.41	5.89	-196.72	-7709.20	0.00	2418.64	2375.11	5.83	24.14	4.15	-6.37	27.75
58.00	-1.22	-2.01	5.89	-175.97	-8270.51	0.00	2418.64	2375.11	5.21	25.90	4.15	-6.37	28.89
60.00	-1.04	-1.71	5.89	-160.19	-8851.28	0.00	2418.64	2375.11	4.74	27.72	4.15	-6.37	30.24

Case 8: I120B120, f_{ck} = 60 MPa

L (m)	β (°)	W (cm)	V (cm)	M_y (KNm)	M_z (KNm)	φ (°)	P_{max} (KN)	M_{Pmax} (KNm)	σ_{my} (Mpa)	σ_{mz} (Mpa)	σ_p (Mpa)	σ_{MP} (Mpa)	σ_t (Mpa)
10.00	0.64	0.74	14.58	2.18	-195.27	0.00	2944.79	1760.98	-0.07	1.29	6.36	-9.44	-1.86
12.00	0.77	0.89	14.58	3.78	-281.18	0.00	2944.79	1760.98	-0.11	1.86	6.36	-9.44	-1.33
14.00	0.90	1.04	14.58	6.03	-382.71	0.00	2944.79	1760.98	-0.18	2.53	6.36	-9.44	-0.73
16.00	1.04	1.20	14.58	9.07	-499.85	0.00	2944.79	1760.98	-0.27	3.31	6.36	-9.44	-0.05
18.00	1.18	1.37	14.58	13.07	-632.59	0.00	2944.79	1760.98	-0.39	4.18	6.36	-9.44	0.71
20.00	1.34	1.54	14.58	18.21	-780.93	0.00	2944.79	1760.98	-0.55	5.17	6.36	-9.44	1.54
22.00	1.50	1.74	14.58	24.78	-944.85	0.00	2944.79	1760.98	-0.74	6.25	6.36	-9.44	2.43
24.00	1.69	1.95	14.58	33.13	-1124.35	0.00	2944.79	1760.98	-0.99	7.44	6.36	-9.44	3.36
26.00	1.90	2.20	14.58	43.81	-1319.40	0.00	2944.79	1760.98	-1.31	8.73	6.36	-9.44	4.33
28.00	2.16	2.49	14.57	57.63	-1529.95	0.00	2944.79	1760.98	-1.73	10.12	6.36	-9.44	5.31
30.00	2.47	2.86	14.57	75.87	-1755.92	0.00	2944.79	1760.98	-2.27	11.62	6.36	-9.44	6.26
32.00	2.89	3.33	14.57	100.72	-1997.18	0.00	2944.79	1760.98	-3.02	13.21	6.36	-9.44	7.11
34.00	3.46	3.99	14.56	136.22	-2253.38	0.00	2944.79	1760.98	-4.08	14.91	6.36	-9.44	7.75
36.00	4.32	4.99	14.54	190.57	-2523.70	0.00	2944.79	1760.98	-5.70	16.69	6.36	-9.44	7.91
38.00	5.77	6.65	14.51	283.36	-2805.64	0.00	2944.79	1760.98	-8.48	18.56	6.36	-9.44	7.00
40.00	8.69	10.01	14.42	472.24	-3088.66	0.00	2944.79	1760.98	-14.14	20.43	6.36	-9.44	3.21
42.00	16.05	18.30	14.02	952.23	-3310.59	0.00	2944.79	1760.98	-28.51	21.90	6.36	-9.44	-9.69
44.00	29.50	32.61	12.69	1861.99	-3290.40	0.00	2944.79	1760.98	-55.74	21.77	6.36	-9.44	-37.05
46.00	-29.59	-32.69	12.68	-2040.27	-3593.41	0.00	2944.79	1760.98	61.08	23.77	6.36	-9.44	81.77
48.00	-6.39	-7.37	14.49	-501.04	-4471.37	0.00	2944.79	1760.98	15.00	29.58	6.36	-9.44	41.50
50.00	-4.27	-4.93	14.54	-363.87	-4868.53	0.00	2944.79	1760.98	10.89	32.21	6.36	-9.44	40.02
52.00	-3.18	-3.67	14.56	-292.47	-5272.39	0.00	2944.79	1760.98	8.76	34.88	6.36	-9.44	40.55
54.00	-2.50	-2.89	14.57	-248.21	-5689.09	0.00	2944.79	1760.98	7.43	37.63	6.36	-9.44	41.98
56.00	-2.04	-2.36	14.58	-217.91	-6120.25	0.00	2944.79	1760.98	6.52	40.49	6.36	-9.44	43.93
58.00	-1.71	-1.97	14.58	-195.74	-6566.46	0.00	2944.79	1760.98	5.86	43.44	6.36	-9.44	46.22
60.00	-1.46	-1.68	14.58	-178.75	-7027.97	0.00	2944.79	1760.98	5.35	46.49	6.36	-9.44	48.76

Case 8: I140B120, f_{ck} = 60 MPa

L (m)	β (°)	W (cm)	V (cm)	M_y (KNm)	M_z (KNm)	φ (°)	P_{max} (KN)	M_{Pmax} (KNm)	σ_{my} (Mpa)	σ_{mz} (Mpa)	σ_p (Mpa)	σ_{MP} (Mpa)	σ_t (Mpa)
10.00	0.57	0.70	10.54	2.08	-207.93	0.00	3011.65	2087.07	-0.06	1.10	6.11	-9.07	-1.93
12.00	0.69	0.84	10.54	3.60	-299.41	0.00	3011.65	2087.07	-0.11	1.58	6.11	-9.07	-1.49
14.00	0.81	0.99	10.54	5.74	-407.52	0.00	3011.65	2087.07	-0.17	2.15	6.11	-9.07	-0.98
16.00	0.93	1.14	10.54	8.63	-532.26	0.00	3011.65	2087.07	-0.26	2.81	6.11	-9.07	-0.41
18.00	1.06	1.30	10.54	12.42	-673.61	0.00	3011.65	2087.07	-0.37	3.55	6.11	-9.07	0.22
20.00	1.19	1.46	10.54	17.29	-831.58	0.00	3011.65	2087.07	-0.52	4.38	6.11	-9.07	0.91
22.00	1.34	1.64	10.53	23.50	-1006.16	0.00	3011.65	2087.07	-0.70	5.30	6.11	-9.07	1.64
24.00	1.50	1.84	10.53	31.37	-1197.33	0.00	3011.65	2087.07	-0.94	6.31	6.11	-9.07	2.41
26.00	1.69	2.07	10.53	41.39	-1405.07	0.00	3011.65	2087.07	-1.24	7.41	6.11	-9.07	3.21
28.00	1.91	2.34	10.53	54.27	-1629.35	0.00	3011.65	2087.07	-1.62	8.59	6.11	-9.07	4.01
30.00	2.18	2.67	10.53	71.14	-1870.11	0.00	3011.65	2087.07	-2.12	9.86	6.11	-9.07	4.77
32.00	2.53	3.10	10.53	93.89	-2127.24	0.00	3011.65	2087.07	-2.80	11.21	6.11	-9.07	5.45
34.00	3.00	3.68	10.52	125.87	-2400.50	0.00	3011.65	2087.07	-3.76	12.65	6.11	-9.07	5.93
36.00	3.70	4.53	10.52	173.74	-2689.31	0.00	3011.65	2087.07	-5.19	14.18	6.11	-9.07	6.03
38.00	4.83	5.91	10.50	252.64	-2992.02	0.00	3011.65	2087.07	-7.54	15.77	6.11	-9.07	5.27
40.00	6.99	8.55	10.46	404.71	-3302.34	0.00	3011.65	2087.07	-12.08	17.41	6.11	-9.07	2.36
42.00	12.27	14.95	10.30	779.82	-3584.22	0.00	3011.65	2087.07	-23.28	18.89	6.11	-9.07	-7.35
44.00	24.70	29.37	9.57	1681.92	-3657.55	0.00	3011.65	2087.07	-50.21	19.28	6.11	-9.07	-33.89
46.00	-178.80	-1.47	-10.54	-92.00	4399.06	0.00	3011.65	2087.07	2.75	-23.19	6.11	-9.07	-23.40
48.00	-6.80	-8.33	10.46	-567.58	-4757.21	0.00	3011.65	2087.07	16.94	25.08	6.11	-9.07	39.06
50.00	-4.34	-5.32	10.51	-393.39	-5183.61	0.00	3011.65	2087.07	11.74	27.32	6.11	-9.07	36.10
52.00	-3.15	-3.87	10.52	-309.25	-5614.21	0.00	3011.65	2087.07	9.23	29.59	6.11	-9.07	35.86
54.00	-2.45	-3.00	10.53	-259.03	-6058.02	0.00	3011.65	2087.07	7.73	31.93	6.11	-9.07	36.70
56.00	-1.98	-2.43	10.53	-225.45	-6517.12	0.00	3011.65	2087.07	6.73	34.35	6.11	-9.07	38.12
58.00	-1.65	-2.02	10.53	-201.29	-6992.23	0.00	3011.65	2087.07	6.01	36.86	6.11	-9.07	39.90
60.00	-1.40	-1.72	10.53	-183.00	-7483.63	0.00	3011.65	2087.07	5.46	39.45	6.11	-9.07	41.95

Case 8: I180B120, f_{ck} = 60 MPa

L (m)	β (°)	W (cm)	V (cm)	M_y (KNm)	M_z (KNm)	φ (°)	P_{max} (KN)	M_{Pmax} (KNm)	σ_{my} (Mpa)	σ_{mz} (Mpa)	σ_p (Mpa)	σ_{MP} (Mpa)	σ_t (Mpa)
10.00	0.47	0.64	6.33	1.91	-233.25	0.00	3077.74	2726.87	-0.06	0.85	5.57	-8.44	-2.08
12.00	0.57	0.77	6.33	3.32	-335.87	0.00	3077.74	2726.87	-0.10	1.23	5.57	-8.44	-1.75
14.00	0.66	0.91	6.33	5.29	-457.15	0.00	3077.74	2726.87	-0.16	1.67	5.57	-8.44	-1.37
16.00	0.76	1.04	6.33	7.95	-597.07	0.00	3077.74	2726.87	-0.24	2.18	5.57	-8.44	-0.94
18.00	0.87	1.19	6.33	11.43	-755.65	0.00	3077.74	2726.87	-0.34	2.76	5.57	-8.44	-0.46
20.00	0.98	1.34	6.33	15.89	-932.88	0.00	3077.74	2726.87	-0.47	3.40	5.57	-8.44	0.05
22.00	1.09	1.50	6.33	21.56	-1128.74	0.00	3077.74	2726.87	-0.64	4.12	5.57	-8.44	0.60
24.00	1.22	1.68	6.33	28.71	-1343.23	0.00	3077.74	2726.87	-0.85	4.90	5.57	-8.44	1.17
26.00	1.37	1.88	6.33	37.75	-1576.34	0.00	3077.74	2726.87	-1.12	5.75	5.57	-8.44	1.75
28.00	1.54	2.11	6.33	49.27	-1828.04	0.00	3077.74	2726.87	-1.46	6.67	5.57	-8.44	2.33
30.00	1.75	2.40	6.32	64.19	-2098.30	0.00	3077.74	2726.87	-1.91	7.65	5.57	-8.44	2.87
32.00	2.01	2.76	6.32	83.96	-2387.03	0.00	3077.74	2726.87	-2.49	8.71	5.57	-8.44	3.34
34.00	2.36	3.23	6.32	111.14	-2694.11	0.00	3077.74	2726.87	-3.30	9.83	5.57	-8.44	3.65
36.00	2.85	3.90	6.32	150.48	-3019.21	0.00	3077.74	2726.87	-4.47	11.01	5.57	-8.44	3.67
38.00	3.61	4.94	6.32	212.14	-3361.49	0.00	3077.74	2726.87	-6.30	12.26	5.57	-8.44	3.09
40.00	4.94	6.76	6.30	321.67	-3718.16	0.00	3077.74	2726.87	-9.55	13.56	5.57	-8.44	1.14
42.00	7.87	10.73	6.27	563.15	-4075.86	0.00	3077.74	2726.87	-16.72	14.87	5.57	-8.44	-4.73
44.00	16.29	22.00	6.07	1266.61	-4334.51	0.00	3077.74	2726.87	-37.60	15.81	5.57	-8.44	-24.67
46.00	30.84	40.20	5.43	2529.86	-4237.96	0.00	3077.74	2726.87	-75.10	15.46	5.57	-8.44	-62.52
48.00	-35.33	-45.35	5.16	-3107.80	-4384.41	0.00	3077.74	2726.87	92.26	15.99	5.57	-8.44	105.37
50.00	-4.51	-6.17	6.31	-458.90	-5813.24	0.00	3077.74	2726.87	13.62	21.20	5.57	-8.44	31.95
52.00	-3.13	-4.28	6.32	-343.99	-6297.77	0.00	3077.74	2726.87	10.21	22.97	5.57	-8.44	30.30
54.00	-2.36	-3.24	6.32	-280.60	-6795.87	0.00	3077.74	2726.87	8.33	24.79	5.57	-8.44	30.24
56.00	-1.88	-2.57	6.33	-240.15	-7310.87	0.00	3077.74	2726.87	7.13	26.67	5.57	-8.44	30.92
58.00	-1.55	-2.12	6.33	-211.95	-7843.77	0.00	3077.74	2726.87	6.29	28.61	5.57	-8.44	32.02
60.00	-1.30	-1.78	6.33	-191.08	-8394.93	0.00	3077.74	2726.87	5.67	30.62	5.57	-8.44	33.41

Case 8: I200B120, f_{ck} = 60 MPa

L (m)	β (°)	W (cm)	V (cm)	M_y (KNm)	M_z (KNm)	φ (°)	P_{max} (KN)	M_{Pmax} (KNm)	σ_{my} (Mpa)	σ_{mz} (Mpa)	σ_p (Mpa)	σ_{MP} (Mpa)	σ_t (Mpa)
10.00	0.43	0.62	5.14	1.85	-245.90	0.00	3096.81	3041.06	-0.05	0.77	5.31	-8.16	-2.13
12.00	0.52	0.75	5.14	3.21	-354.09	0.00	3096.81	3041.06	-0.10	1.11	5.31	-8.16	-1.83
14.00	0.61	0.88	5.14	5.12	-481.95	0.00	3096.81	3041.06	-0.15	1.51	5.31	-8.16	-1.49
16.00	0.70	1.01	5.14	7.69	-629.48	0.00	3096.81	3041.06	-0.23	1.97	5.31	-8.16	-1.10
18.00	0.80	1.14	5.14	11.06	-796.67	0.00	3096.81	3041.06	-0.33	2.50	5.31	-8.16	-0.68
20.00	0.90	1.29	5.14	15.37	-983.52	0.00	3096.81	3041.06	-0.46	3.08	5.31	-8.16	-0.22
22.00	1.00	1.44	5.14	20.84	-1190.02	0.00	3096.81	3041.06	-0.62	3.73	5.31	-8.16	0.26
24.00	1.12	1.61	5.14	27.73	-1416.17	0.00	3096.81	3041.06	-0.82	4.44	5.31	-8.16	0.77
26.00	1.26	1.81	5.14	36.41	-1661.95	0.00	3096.81	3041.06	-1.08	5.21	5.31	-8.16	1.28
28.00	1.41	2.03	5.14	47.45	-1927.34	0.00	3096.81	3041.06	-1.41	6.04	5.31	-8.16	1.79
30.00	1.60	2.30	5.14	61.67	-2212.32	0.00	3096.81	3041.06	-1.83	6.93	5.31	-8.16	2.26
32.00	1.83	2.63	5.14	80.41	-2516.83	0.00	3096.81	3041.06	-2.38	7.88	5.31	-8.16	2.66
34.00	2.14	3.07	5.14	105.96	-2840.73	0.00	3096.81	3041.06	-3.14	8.90	5.31	-8.16	2.91
36.00	2.56	3.69	5.14	142.51	-3183.80	0.00	3096.81	3041.06	-4.22	9.97	5.31	-8.16	2.91
38.00	3.21	4.62	5.14	198.77	-3545.36	0.00	3096.81	3041.06	-5.89	11.10	5.31	-8.16	2.37
40.00	4.31	6.20	5.13	295.92	-3923.40	0.00	3096.81	3041.06	-8.76	12.29	5.31	-8.16	0.68
42.00	6.62	9.51	5.11	500.21	-4308.90	0.00	3096.81	3041.06	-14.81	13.50	5.31	-8.16	-4.16
44.00	13.23	18.88	5.01	1089.57	-4634.44	0.00	3096.81	3041.06	-32.27	14.51	5.31	-8.16	-20.60
46.00	27.66	38.28	4.56	2415.19	-4608.97	0.00	3096.81	3041.06	-71.53	14.44	5.31	-8.16	-59.94
48.00	-32.26	-44.02	4.35	-3023.96	-4791.28	0.00	3096.81	3041.06	89.56	15.01	5.31	-8.16	101.72
50.00	-4.60	-6.62	5.13	-493.24	-6127.91	0.00	3096.81	3041.06	14.61	19.19	5.31	-8.16	30.95
52.00	-3.11	-4.48	5.14	-360.93	-6639.58	0.00	3096.81	3041.06	10.69	20.79	5.31	-8.16	28.64
54.00	-2.32	-3.34	5.14	-290.71	-7164.82	0.00	3096.81	3041.06	8.61	22.44	5.31	-8.16	28.20
56.00	-1.83	-2.64	5.14	-246.87	-7707.76	0.00	3096.81	3041.06	7.31	24.14	5.31	-8.16	28.61
58.00	-1.50	-2.16	5.14	-216.74	-8269.55	0.00	3096.81	3041.06	6.42	25.90	5.31	-8.16	29.47
60.00	-1.26	-1.81	5.14	-194.67	-8850.59	0.00	3096.81	3041.06	5.77	27.72	5.31	-8.16	30.64

Case 8: I95C150, f_{ck} = 20 MPa

L (m)	β (°)	W (cm)	V (cm)	M_y (KNm)	M_z (KNm)	φ (°)	P_{max} (KN)	M_{Pmax} (KNm)	σ_{my} (Mpa)	σ_{mz} (Mpa)	σ_p (Mpa)	σ_{MP} (Mpa)	σ_t (Mpa)
10.00	0.74	0.55	32.65	2.79	-217.67	0.00	1568.71	774.94	-0.04	1.52	3.04	-4.97	-0.45
12.00	0.88	0.66	32.65	4.84	-313.43	0.00	1568.71	774.94	-0.07	2.19	3.04	-4.97	0.19
14.00	1.04	0.77	32.65	7.71	-426.59	0.00	1568.71	774.94	-0.12	2.98	3.04	-4.97	0.93
16.00	1.19	0.89	32.65	11.58	-557.16	0.00	1568.71	774.94	-0.17	3.89	3.04	-4.97	1.79
18.00	1.35	1.01	32.65	16.62	-705.11	0.00	1568.71	774.94	-0.25	4.92	3.04	-4.97	2.74
20.00	1.52	1.13	32.64	23.06	-870.44	0.00	1568.71	774.94	-0.35	6.08	3.04	-4.97	3.80
22.00	1.70	1.27	32.64	31.19	-1053.14	0.00	1568.71	774.94	-0.47	7.35	3.04	-4.97	4.95
24.00	1.89	1.41	32.64	41.37	-1253.19	0.00	1568.71	774.94	-0.62	8.75	3.04	-4.97	6.20
26.00	2.11	1.57	32.63	54.11	-1470.56	0.00	1568.71	774.94	-0.81	10.26	3.04	-4.97	7.52
28.00	2.35	1.76	32.63	70.10	-1705.22	0.00	1568.71	774.94	-1.05	11.90	3.04	-4.97	8.92
30.00	2.64	1.97	32.62	90.40	-1957.09	0.00	1568.71	774.94	-1.36	13.66	3.04	-4.97	10.37
32.00	3.00	2.24	32.61	116.62	-2226.05	0.00	1568.71	774.94	-1.75	15.54	3.04	-4.97	11.85
34.00	3.45	2.57	32.60	151.35	-2511.89	0.00	1568.71	774.94	-2.27	17.53	3.04	-4.97	13.33
36.00	4.05	3.02	32.57	199.09	-2814.18	0.00	1568.71	774.94	-2.99	19.64	3.04	-4.97	14.72
38.00	4.90	3.65	32.54	268.27	-3131.92	0.00	1568.71	774.94	-4.03	21.86	3.04	-4.97	15.90
40.00	6.21	4.62	32.46	376.60	-3462.56	0.00	1568.71	774.94	-5.66	24.17	3.04	-4.97	16.58
42.00	8.49	6.31	32.30	566.96	-3797.89	0.00	1568.71	774.94	-8.52	26.51	3.04	-4.97	16.06
44.00	13.14	9.72	31.80	958.15	-4104.04	0.00	1568.71	774.94	-14.40	28.64	3.04	-4.97	12.32
46.00	22.65	16.46	30.14	1773.98	-4250.93	0.00	1568.71	774.94	-26.65	29.67	3.04	-4.97	1.09
48.00	181.67	-1.25	-32.64	-146.57	5013.34	0.00	1568.71	774.94	2.20	-34.99	3.04	-4.97	-34.72
50.00	-31.89	-22.58	27.73	-2875.20	-4620.63	0.00	1568.71	774.94	43.20	32.25	3.04	-4.97	73.52
52.00	-7.49	-5.57	32.38	-767.11	-5836.03	0.00	1568.71	774.94	11.53	40.73	3.04	-4.97	50.33
54.00	-5.20	-3.87	32.52	-575.29	-6321.60	0.00	1568.71	774.94	8.64	44.12	3.04	-4.97	50.83
56.00	-3.95	-2.94	32.58	-470.07	-6810.43	0.00	1568.71	774.94	7.06	47.53	3.04	-4.97	52.67
58.00	-3.15	-2.35	32.61	-402.81	-7311.87	0.00	1568.71	774.94	6.05	51.03	3.04	-4.97	55.15
60.00	-2.60	-1.94	32.62	-355.81	-7828.61	0.00	1568.71	774.94	5.35	54.64	3.04	-4.97	58.05

Case 8: I135C150, f_{ck} = 20 MPa

L (m)	β (°)	W (cm)	V (cm)	M_y (KNm)	M_z (KNm)	φ (°)	P_{max} (KN)	M_{Pmax} (KNm)	σ_{my} (Mpa)	σ_{mz} (Mpa)	σ_p (Mpa)	σ_{MP} (Mpa)	σ_t (Mpa)
10.00	0.57	0.48	15.55	2.47	-248.05	0.00	1727.08	1202.05	-0.04	1.04	2.94	-4.77	-0.84
12.00	0.68	0.58	15.55	4.27	-357.18	0.00	1727.08	1202.05	-0.06	1.49	2.94	-4.77	-0.41
14.00	0.80	0.68	15.55	6.80	-486.15	0.00	1727.08	1202.05	-0.10	2.03	2.94	-4.77	0.10
16.00	0.92	0.78	15.54	10.20	-634.95	0.00	1727.08	1202.05	-0.15	2.65	2.94	-4.77	0.67
18.00	1.04	0.88	15.54	14.63	-803.58	0.00	1727.08	1202.05	-0.22	3.36	2.94	-4.77	1.31
20.00	1.17	0.99	15.54	20.28	-992.04	0.00	1727.08	1202.05	-0.30	4.15	2.94	-4.77	2.01
22.00	1.31	1.11	15.54	27.37	-1200.30	0.00	1727.08	1202.05	-0.41	5.02	2.94	-4.77	2.77
24.00	1.45	1.23	15.54	36.20	-1428.37	0.00	1727.08	1202.05	-0.54	5.97	2.94	-4.77	3.60
26.00	1.61	1.36	15.54	47.17	-1676.23	0.00	1727.08	1202.05	-0.71	7.01	2.94	-4.77	4.47
28.00	1.79	1.52	15.54	60.82	-1943.84	0.00	1727.08	1202.05	-0.91	8.13	2.94	-4.77	5.38
30.00	2.00	1.69	15.54	77.93	-2231.19	0.00	1727.08	1202.05	-1.17	9.33	2.94	-4.77	6.33
32.00	2.25	1.90	15.53	99.66	-2538.19	0.00	1727.08	1202.05	-1.49	10.61	2.94	-4.77	7.29
34.00	2.55	2.16	15.53	127.81	-2864.73	0.00	1727.08	1202.05	-1.91	11.98	2.94	-4.77	8.23
36.00	2.95	2.50	15.53	165.35	-3210.61	0.00	1727.08	1202.05	-2.47	13.42	2.94	-4.77	9.11
38.00	3.48	2.95	15.52	217.51	-3575.39	0.00	1727.08	1202.05	-3.26	14.95	2.94	-4.77	9.86
40.00	4.25	3.60	15.50	294.41	-3958.04	0.00	1727.08	1202.05	-4.41	16.55	2.94	-4.77	10.31
42.00	5.48	4.64	15.48	418.19	-4355.76	0.00	1727.08	1202.05	-6.26	18.21	2.94	-4.77	10.12
44.00	7.74	6.53	15.41	646.46	-4758.75	0.00	1727.08	1202.05	-9.68	19.90	2.94	-4.77	8.39
46.00	12.73	10.69	15.16	1157.03	-5119.86	0.00	1727.08	1202.05	-17.32	21.41	2.94	-4.77	2.26
48.00	23.42	19.29	14.27	2272.09	-5244.28	0.00	1727.08	1202.05	-34.01	21.93	2.94	-4.77	-13.91
50.00	901.33	-1.12	-15.54	-143.59	6199.86	0.00	1727.08	1202.05	2.15	-25.92	2.94	-4.77	-25.61
52.00	-36.88	-29.11	12.44	-4025.29	-5365.49	0.00	1727.08	1202.05	60.24	22.43	2.94	-4.77	80.84
54.00	-5.60	-4.73	15.47	-705.82	-7198.93	0.00	1727.08	1202.05	10.56	30.10	2.94	-4.77	38.83
56.00	-4.01	-3.39	15.51	-543.85	-7760.15	0.00	1727.08	1202.05	8.14	32.45	2.94	-4.77	38.75
58.00	-3.09	-2.62	15.52	-450.23	-8332.61	0.00	1727.08	1202.05	6.74	34.84	2.94	-4.77	39.74
60.00	-2.50	-2.11	15.53	-388.76	-8921.72	0.00	1727.08	1202.05	5.82	37.30	2.94	-4.77	41.29

Case 8: I175C150, f_{ck} = 20 MPa

L (m)	β (°)	W (cm)	V (cm)	M_y (KNm)	M_z (KNm)	φ (°)	P_{max} (KN)	M_{Pmax} (KNm)	σ_{my} (Mpa)	σ_{mz} (Mpa)	σ_p (Mpa)	σ_{MP} (Mpa)	σ_t (Mpa)
10.00	0.47	0.44	9.27	2.26	-278.43	0.00	1787.68	1603.55	-0.03	0.81	2.71	-4.48	-0.99
12.00	0.56	0.53	9.27	3.91	-400.93	0.00	1787.68	1603.55	-0.06	1.16	2.71	-4.48	-0.66
14.00	0.65	0.62	9.27	6.23	-545.70	0.00	1787.68	1603.55	-0.09	1.58	2.71	-4.48	-0.28
16.00	0.75	0.71	9.27	9.34	-712.73	0.00	1787.68	1603.55	-0.14	2.06	2.71	-4.48	0.16
18.00	0.85	0.81	9.27	13.39	-902.03	0.00	1787.68	1603.55	-0.20	2.61	2.71	-4.48	0.65
20.00	0.95	0.90	9.27	18.54	-1113.59	0.00	1787.68	1603.55	-0.28	3.23	2.71	-4.48	1.18
22.00	1.06	1.01	9.27	25.00	-1347.40	0.00	1787.68	1603.55	-0.37	3.90	2.71	-4.48	1.76
24.00	1.18	1.12	9.27	33.01	-1603.45	0.00	1787.68	1603.55	-0.49	4.64	2.71	-4.48	2.38
26.00	1.31	1.24	9.27	42.92	-1881.73	0.00	1787.68	1603.55	-0.64	5.45	2.71	-4.48	3.04
28.00	1.45	1.37	9.27	55.17	-2182.24	0.00	1787.68	1603.55	-0.82	6.32	2.71	-4.48	3.73
30.00	1.61	1.52	9.27	70.40	-2504.93	0.00	1787.68	1603.55	-1.05	7.25	2.71	-4.48	4.44
32.00	1.80	1.70	9.26	89.56	-2849.77	0.00	1787.68	1603.55	-1.34	8.25	2.71	-4.48	5.15
34.00	2.03	1.92	9.26	114.03	-3216.69	0.00	1787.68	1603.55	-1.70	9.32	2.71	-4.48	5.85
36.00	2.32	2.20	9.26	146.09	-3605.57	0.00	1787.68	1603.55	-2.18	10.44	2.71	-4.48	6.50
38.00	2.70	2.56	9.26	189.54	-4016.14	0.00	1787.68	1603.55	-2.83	11.63	2.71	-4.48	7.04
40.00	3.23	3.06	9.26	251.39	-4447.87	0.00	1787.68	1603.55	-3.75	12.88	2.71	-4.48	7.37
42.00	4.04	3.82	9.25	345.93	-4899.41	0.00	1787.68	1603.55	-5.16	14.19	2.71	-4.48	7.27
44.00	5.40	5.10	9.23	507.14	-5366.60	0.00	1787.68	1603.55	-7.56	15.54	2.71	-4.48	6.22
46.00	8.15	7.69	9.18	835.02	-5832.22	0.00	1787.68	1603.55	-12.45	16.89	2.71	-4.48	2.68
48.00	15.06	14.09	8.95	1666.87	-6194.82	0.00	1787.68	1603.55	-24.85	17.94	2.71	-4.48	-8.68
50.00	27.76	25.26	8.20	3241.63	-6160.01	0.00	1787.68	1603.55	-48.33	17.84	2.71	-4.48	-32.25
52.00	-27.71	-25.23	8.21	-3501.23	-6665.26	0.00	1787.68	1603.55	52.20	19.30	2.71	-4.48	69.74
54.00	-6.08	-5.74	9.22	-859.45	-8073.56	0.00	1787.68	1603.55	12.81	23.38	2.71	-4.48	34.43
56.00	-4.07	-3.85	9.25	-620.37	-8709.67	0.00	1787.68	1603.55	9.25	25.23	2.71	-4.48	32.71
58.00	-3.04	-2.87	9.26	-496.21	-9353.42	0.00	1787.68	1603.55	7.40	27.09	2.71	-4.48	32.72
60.00	-2.40	-2.27	9.26	-419.41	-10014.90	0.00	1787.68	1603.55	6.25	29.01	2.71	-4.48	33.49

Case 8: I215C150, f_{ck} = 20 MPa

L (m)	β (°)	W (cm)	V (cm)	M_y (KNm)	M_z (KNm)	φ (°)	P_{max} (KN)	M_{Pmax} (KNm)	σ_{my} (Mpa)	σ_{mz} (Mpa)	σ_p (Mpa)	σ_{MP} (Mpa)	σ_t (Mpa)
10.00	0.39	0.41	6.24	2.12	-308.80	0.00	1818.50	1996.72	-0.03	0.67	2.48	-4.21	-1.09
12.00	0.47	0.49	6.24	3.67	-444.67	0.00	1818.50	1996.72	-0.05	0.96	2.48	-4.21	-0.81
14.00	0.55	0.58	6.24	5.84	-605.24	0.00	1818.50	1996.72	-0.09	1.31	2.48	-4.21	-0.50
16.00	0.63	0.66	6.24	8.75	-790.51	0.00	1818.50	1996.72	-0.13	1.71	2.48	-4.21	-0.14
18.00	0.72	0.75	6.24	12.54	-1000.47	0.00	1818.50	1996.72	-0.19	2.17	2.48	-4.21	0.26
20.00	0.80	0.84	6.24	17.35	-1235.12	0.00	1818.50	1996.72	-0.26	2.68	2.48	-4.21	0.70
22.00	0.90	0.94	6.24	23.37	-1494.46	0.00	1818.50	1996.72	-0.35	3.24	2.48	-4.21	1.17
24.00	0.99	1.04	6.24	30.82	-1778.48	0.00	1818.50	1996.72	-0.46	3.85	2.48	-4.21	1.67
26.00	1.10	1.15	6.24	40.01	-2087.17	0.00	1818.50	1996.72	-0.59	4.52	2.48	-4.21	2.21
28.00	1.21	1.27	6.24	51.33	-2420.53	0.00	1818.50	1996.72	-0.76	5.25	2.48	-4.21	2.76
30.00	1.35	1.41	6.24	65.33	-2778.52	0.00	1818.50	1996.72	-0.97	6.02	2.48	-4.21	3.33
32.00	1.50	1.57	6.24	82.80	-3161.13	0.00	1818.50	1996.72	-1.23	6.85	2.48	-4.21	3.90
34.00	1.68	1.76	6.24	104.92	-3568.30	0.00	1818.50	1996.72	-1.56	7.73	2.48	-4.21	4.45
36.00	1.91	2.00	6.24	133.54	-3999.95	0.00	1818.50	1996.72	-1.98	8.67	2.48	-4.21	4.96
38.00	2.21	2.31	6.23	171.70	-4455.91	0.00	1818.50	1996.72	-2.55	9.66	2.48	-4.21	5.38
40.00	2.61	2.73	6.23	224.78	-4935.85	0.00	1818.50	1996.72	-3.34	10.70	2.48	-4.21	5.63
42.00	3.19	3.34	6.23	303.24	-5438.97	0.00	1818.50	1996.72	-4.50	11.79	2.48	-4.21	5.56
44.00	4.13	4.31	6.22	430.39	-5963.06	0.00	1818.50	1996.72	-6.39	12.92	2.48	-4.21	4.81
46.00	5.88	6.14	6.21	669.21	-6500.07	0.00	1818.50	1996.72	-9.94	14.09	2.48	-4.21	2.42
48.00	10.05	10.46	6.14	1241.39	-7005.86	0.00	1818.50	1996.72	-18.44	15.18	2.48	-4.21	-4.98
50.00	20.85	21.33	5.83	2748.12	-7214.58	0.00	1818.50	1996.72	-40.81	15.63	2.48	-4.21	-26.90
52.00	540.95	-1.00	-6.24	-138.99	8349.07	0.00	1818.50	1996.72	2.06	-18.09	2.48	-4.21	-17.75
54.00	43.50	41.26	4.52	6199.06	-6531.46	0.00	1818.50	1996.72	-92.06	14.15	2.48	-4.21	-79.63
56.00	-4.15	-4.34	6.22	-700.97	-9658.89	0.00	1818.50	1996.72	10.41	20.93	2.48	-4.21	29.62
58.00	-2.99	-3.12	6.23	-541.48	-10374.26	0.00	1818.50	1996.72	8.04	22.48	2.48	-4.21	28.80
60.00	-2.31	-2.42	6.23	-448.42	-11108.12	0.00	1818.50	1996.72	6.66	24.07	2.48	-4.21	29.01

Case 8: I95C150, f_{ck} = 40 MPa

L (m)	β (°)	W (cm)	V (cm)	M_y (KNm)	M_z (KNm)	φ (°)	P_{max} (KN)	M_{Pmax} (KNm)	σ_{my} (Mpa)	σ_{mz} (Mpa)	σ_p (Mpa)	σ_{MP} (Mpa)	σ_t (Mpa)
10.00	0.74	0.44	25.92	2.79	-217.67	0.00	2490.18	1230.15	-0.04	1.52	4.83	-7.89	-1.59
12.00	0.88	0.52	25.92	4.83	-313.43	0.00	2490.18	1230.15	-0.07	2.19	4.83	-7.89	-0.95
14.00	1.03	0.61	25.92	7.70	-426.60	0.00	2490.18	1230.15	-0.12	2.98	4.83	-7.89	-0.20
16.00	1.19	0.70	25.91	11.54	-557.16	0.00	2490.18	1230.15	-0.17	3.89	4.83	-7.89	0.65
18.00	1.34	0.80	25.91	16.54	-705.11	0.00	2490.18	1230.15	-0.25	4.92	4.83	-7.89	1.61
20.00	1.51	0.89	25.91	22.90	-870.44	0.00	2490.18	1230.15	-0.34	6.08	4.83	-7.89	2.67
22.00	1.68	0.99	25.91	30.87	-1053.15	0.00	2490.18	1230.15	-0.46	7.35	4.83	-7.89	3.82
24.00	1.86	1.10	25.91	40.75	-1253.21	0.00	2490.18	1230.15	-0.61	8.75	4.83	-7.89	5.07
26.00	2.06	1.22	25.90	52.96	-1470.60	0.00	2490.18	1230.15	-0.80	10.26	4.83	-7.89	6.41
28.00	2.29	1.35	25.90	68.05	-1705.30	0.00	2490.18	1230.15	-1.02	11.90	4.83	-7.89	7.82
30.00	2.54	1.50	25.89	86.79	-1957.25	0.00	2490.18	1230.15	-1.30	13.66	4.83	-7.89	9.29
32.00	2.84	1.68	25.89	110.31	-2226.37	0.00	2490.18	1230.15	-1.66	15.54	4.83	-7.89	10.82
34.00	3.20	1.89	25.88	140.29	-2512.54	0.00	2490.18	1230.15	-2.11	17.54	4.83	-7.89	12.36
36.00	3.65	2.16	25.87	179.44	-2815.50	0.00	2490.18	1230.15	-2.70	19.65	4.83	-7.89	13.89
38.00	4.24	2.51	25.85	232.24	-3134.79	0.00	2490.18	1230.15	-3.49	21.88	4.83	-7.89	15.33
40.00	5.05	2.99	25.82	306.81	-3469.44	0.00	2490.18	1230.15	-4.61	24.21	4.83	-7.89	16.54
42.00	6.27	3.70	25.76	419.26	-3817.02	0.00	2490.18	1230.15	-6.30	26.64	4.83	-7.89	17.28
44.00	8.26	4.87	25.65	605.60	-4170.66	0.00	2490.18	1230.15	-9.10	29.11	4.83	-7.89	16.95
46.00	11.99	7.05	25.35	956.69	-4505.79	0.00	2490.18	1230.15	-14.37	31.45	4.83	-7.89	14.01
48.00	19.44	11.29	24.44	1669.06	-4729.62	0.00	2490.18	1230.15	-25.08	33.01	4.83	-7.89	4.87
50.00	30.28	17.11	22.38	2744.34	-4699.53	0.00	2490.18	1230.15	-41.23	32.80	4.83	-7.89	-11.50
52.00	-178.27	-1.02	-25.91	-177.66	5883.55	0.00	2490.18	1230.15	2.67	-41.06	4.83	-7.89	-41.46
54.00	-10.31	-6.07	25.50	-1136.60	-6245.14	0.00	2490.18	1230.15	17.08	43.59	4.83	-7.89	57.60
56.00	-6.69	-3.95	25.74	-795.56	-6780.12	0.00	2490.18	1230.15	11.95	47.32	4.83	-7.89	56.21
58.00	-4.94	-2.92	25.82	-630.30	-7295.78	0.00	2490.18	1230.15	9.47	50.92	4.83	-7.89	57.33
60.00	-3.88	-2.30	25.86	-530.31	-7818.73	0.00	2490.18	1230.15	7.97	54.57	4.83	-7.89	59.47

Case 8: I135C150, f_{ck} = 40 MPa

L (m)	β (°)	W (cm)	V (cm)	M_y (KNm)	M_z (KNm)	φ (°)	P_{max} (KN)	M_{Pmax} (KNm)	σ_{my} (Mpa)	σ_{mz} (Mpa)	σ_p (Mpa)	σ_{MP} (Mpa)	σ_t (Mpa)
10.00	0.57	0.38	12.34	2.46	-248.05	0.00	2741.57	1908.13	-0.04	1.04	4.66	-7.58	-1.91
12.00	0.68	0.46	12.34	4.26	-357.18	0.00	2741.57	1908.13	-0.06	1.49	4.66	-7.58	-1.48
14.00	0.80	0.54	12.34	6.79	-486.15	0.00	2741.57	1908.13	-0.10	2.03	4.66	-7.58	-0.98
16.00	0.92	0.62	12.34	10.18	-634.95	0.00	2741.57	1908.13	-0.15	2.65	4.66	-7.58	-0.41
18.00	1.04	0.70	12.34	14.57	-803.58	0.00	2741.57	1908.13	-0.22	3.36	4.66	-7.58	0.23
20.00	1.16	0.78	12.34	20.15	-992.04	0.00	2741.57	1908.13	-0.30	4.15	4.66	-7.58	0.93
22.00	1.29	0.87	12.34	27.12	-1200.31	0.00	2741.57	1908.13	-0.41	5.02	4.66	-7.58	1.70
24.00	1.43	0.96	12.34	35.73	-1428.38	0.00	2741.57	1908.13	-0.53	5.97	4.66	-7.58	2.52
26.00	1.58	1.06	12.33	46.30	-1676.25	0.00	2741.57	1908.13	-0.69	7.01	4.66	-7.58	3.40
28.00	1.75	1.17	12.33	59.28	-1943.89	0.00	2741.57	1908.13	-0.89	8.13	4.66	-7.58	4.33
30.00	1.93	1.30	12.33	75.24	-2231.28	0.00	2741.57	1908.13	-1.13	9.33	4.66	-7.58	5.29
32.00	2.14	1.44	12.33	95.02	-2538.36	0.00	2741.57	1908.13	-1.42	10.61	4.66	-7.58	6.28
34.00	2.40	1.61	12.33	119.85	-2865.08	0.00	2741.57	1908.13	-1.79	11.98	4.66	-7.58	7.27
36.00	2.70	1.82	12.33	151.57	-3211.29	0.00	2741.57	1908.13	-2.27	13.43	4.66	-7.58	8.25
38.00	3.09	2.08	12.32	193.17	-3576.78	0.00	2741.57	1908.13	-2.89	14.96	4.66	-7.58	9.15
40.00	3.61	2.42	12.31	249.72	-3961.11	0.00	2741.57	1908.13	-3.74	16.56	4.66	-7.58	9.91
42.00	4.33	2.91	12.30	330.56	-4363.29	0.00	2741.57	1908.13	-4.95	18.24	4.66	-7.58	10.38
44.00	5.43	3.65	12.28	454.83	-4780.87	0.00	2741.57	1908.13	-6.81	19.99	4.66	-7.58	10.27
46.00	7.31	4.90	12.24	667.62	-5206.33	0.00	2741.57	1908.13	-9.99	21.77	4.66	-7.58	8.86
48.00	11.03	7.37	12.11	1093.44	-5609.75	0.00	2741.57	1908.13	-16.37	23.46	4.66	-7.58	4.18
50.00	19.09	12.59	11.66	2027.91	-5860.58	0.00	2741.57	1908.13	-30.35	24.50	4.66	-7.58	-8.76
52.00	30.60	19.60	10.62	3414.51	-5773.43	0.00	2741.57	1908.13	-51.10	24.14	4.66	-7.58	-29.88
54.00	-25.69	-16.69	11.12	-3135.57	-6518.52	0.00	2741.57	1908.13	46.93	27.26	4.66	-7.58	71.27
56.00	-7.65	-5.13	12.23	-1035.42	-7709.97	0.00	2741.57	1908.13	15.50	32.24	4.66	-7.58	44.82
58.00	-5.18	-3.48	12.29	-753.52	-8310.67	0.00	2741.57	1908.13	11.28	34.75	4.66	-7.58	43.11
60.00	-3.89	-2.61	12.31	-605.85	-8909.61	0.00	2741.57	1908.13	9.07	37.25	4.66	-7.58	43.41

Case 8: I175C150, f_{ck} = 40 MPa

L (m)	β (°)	W (cm)	V (cm)	M_y (KNm)	M_z (KNm)	φ (°)	P_{max} (KN)	M_{Pmax} (KNm)	σ_{my} (Mpa)	σ_{mz} (Mpa)	σ_p (Mpa)	σ_{MP} (Mpa)	σ_t (Mpa)
10.00	0.46	0.35	7.36	2.26	-278.43	0.00	2837.76	2545.47	-0.03	0.81	4.30	-7.10	-2.03
12.00	0.56	0.42	7.36	3.91	-400.93	0.00	2837.76	2545.47	-0.06	1.16	4.30	-7.10	-1.70
14.00	0.65	0.49	7.36	6.22	-545.70	0.00	2837.76	2545.47	-0.09	1.58	4.30	-7.10	-1.32
16.00	0.75	0.56	7.36	9.32	-712.73	0.00	2837.76	2545.47	-0.14	2.06	4.30	-7.10	-0.88
18.00	0.85	0.64	7.36	13.34	-902.03	0.00	2837.76	2545.47	-0.20	2.61	4.30	-7.10	-0.39
20.00	0.95	0.71	7.36	18.44	-1113.59	0.00	2837.76	2545.47	-0.27	3.23	4.30	-7.10	0.15
22.00	1.05	0.79	7.36	24.79	-1347.40	0.00	2837.76	2545.47	-0.37	3.90	4.30	-7.10	0.73
24.00	1.17	0.88	7.36	32.62	-1603.46	0.00	2837.76	2545.47	-0.49	4.64	4.30	-7.10	1.35
26.00	1.28	0.97	7.36	42.20	-1881.75	0.00	2837.76	2545.47	-0.63	5.45	4.30	-7.10	2.02
28.00	1.41	1.06	7.35	53.90	-2182.27	0.00	2837.76	2545.47	-0.80	6.32	4.30	-7.10	2.71
30.00	1.56	1.17	7.35	68.21	-2504.99	0.00	2837.76	2545.47	-1.02	7.25	4.30	-7.10	3.43
32.00	1.72	1.30	7.35	85.81	-2849.89	0.00	2837.76	2545.47	-1.28	8.25	4.30	-7.10	4.17
34.00	1.92	1.44	7.35	107.67	-3216.91	0.00	2837.76	2545.47	-1.61	9.32	4.30	-7.10	4.91
36.00	2.15	1.61	7.35	135.26	-3605.99	0.00	2837.76	2545.47	-2.02	10.44	4.30	-7.10	5.62
38.00	2.44	1.83	7.35	170.82	-4016.98	0.00	2837.76	2545.47	-2.55	11.63	4.30	-7.10	6.28
40.00	2.81	2.11	7.35	218.08	-4449.63	0.00	2837.76	2545.47	-3.25	12.89	4.30	-7.10	6.83
42.00	3.31	2.49	7.34	283.54	-4903.41	0.00	2837.76	2545.47	-4.23	14.20	4.30	-7.10	7.17
44.00	4.04	3.03	7.34	379.79	-5377.12	0.00	2837.76	2545.47	-5.66	15.57	4.30	-7.10	7.11
46.00	5.20	3.90	7.33	534.21	-5867.43	0.00	2837.76	2545.47	-7.96	16.99	4.30	-7.10	6.22
48.00	7.32	5.49	7.30	817.79	-6362.82	0.00	2837.76	2545.47	-12.19	18.43	4.30	-7.10	3.43
50.00	12.02	8.96	7.20	1449.43	-6808.31	0.00	2837.76	2545.47	-21.61	19.72	4.30	-7.10	-4.70
52.00	22.19	16.26	6.81	2843.82	-6971.15	0.00	2837.76	2545.47	-42.40	20.19	4.30	-7.10	-25.01
54.00	181.18	-0.89	-7.36	-167.06	8117.46	0.00	2837.76	2545.47	2.49	-23.51	4.30	-7.10	-23.82
56.00	-35.21	-24.82	6.01	-5034.49	-7134.23	0.00	2837.76	2545.47	75.06	20.66	4.30	-7.10	92.92
58.00	-5.46	-4.09	7.32	-890.42	-9324.15	0.00	2837.76	2545.47	13.28	27.00	4.30	-7.10	37.48
60.00	-3.90	-2.93	7.34	-682.25	-10000.43	0.00	2837.76	2545.47	10.17	28.96	4.30	-7.10	36.33

Case 8: I215C150, f_{ck} = 40 MPa

L (m)	β (°)	W (cm)	V (cm)	M_y (KNm)	M_z (KNm)	φ (°)	P_{max} (KN)	M_{Pmax} (KNm)	σ_{my} (Mpa)	σ_{mz} (Mpa)	σ_p (Mpa)	σ_{MP} (Mpa)	σ_t (Mpa)
10.00	0.39	0.33	4.95	2.12	-308.80	0.00	2886.69	3169.59	-0.03	0.67	3.94	-6.68	-2.10
12.00	0.47	0.39	4.95	3.66	-444.67	0.00	2886.69	3169.59	-0.05	0.96	3.94	-6.68	-1.83
14.00	0.55	0.46	4.95	5.83	-605.24	0.00	2886.69	3169.59	-0.09	1.31	3.94	-6.68	-1.51
16.00	0.63	0.53	4.95	8.73	-790.51	0.00	2886.69	3169.59	-0.13	1.71	3.94	-6.68	-1.15
18.00	0.72	0.59	4.95	12.49	-1000.47	0.00	2886.69	3169.59	-0.19	2.17	3.94	-6.68	-0.75
20.00	0.80	0.66	4.95	17.26	-1235.12	0.00	2886.69	3169.59	-0.26	2.68	3.94	-6.68	-0.32
22.00	0.89	0.74	4.95	23.19	-1494.46	0.00	2886.69	3169.59	-0.34	3.24	3.94	-6.68	0.16
24.00	0.98	0.82	4.95	30.48	-1778.49	0.00	2886.69	3169.59	-0.45	3.85	3.94	-6.68	0.67
26.00	1.08	0.90	4.95	39.39	-2087.19	0.00	2886.69	3169.59	-0.58	4.52	3.94	-6.68	1.20
28.00	1.19	0.99	4.95	50.23	-2420.55	0.00	2886.69	3169.59	-0.75	5.25	3.94	-6.68	1.76
30.00	1.31	1.09	4.95	63.44	-2778.57	0.00	2886.69	3169.59	-0.94	6.02	3.94	-6.68	2.34
32.00	1.44	1.20	4.95	79.59	-3161.22	0.00	2886.69	3169.59	-1.18	6.85	3.94	-6.68	2.93
34.00	1.60	1.33	4.95	99.53	-3568.46	0.00	2886.69	3169.59	-1.48	7.73	3.94	-6.68	3.52
36.00	1.78	1.48	4.95	124.46	-4000.25	0.00	2886.69	3169.59	-1.85	8.67	3.94	-6.68	4.08
38.00	2.01	1.67	4.95	156.24	-4456.48	0.00	2886.69	3169.59	-2.32	9.66	3.94	-6.68	4.60
40.00	2.29	1.90	4.95	197.82	-4937.00	0.00	2886.69	3169.59	-2.94	10.70	3.94	-6.68	5.03
42.00	2.68	2.22	4.95	254.25	-5441.48	0.00	2886.69	3169.59	-3.78	11.79	3.94	-6.68	5.28
44.00	3.21	2.66	4.94	334.83	-5969.18	0.00	2886.69	3169.59	-4.97	12.94	3.94	-6.68	5.23
46.00	4.03	3.34	4.94	458.74	-6518.30	0.00	2886.69	3169.59	-6.81	14.13	3.94	-6.68	4.58
48.00	5.42	4.49	4.93	672.14	-7083.17	0.00	2886.69	3169.59	-9.98	15.35	3.94	-6.68	2.63
50.00	8.29	6.86	4.90	1112.72	-7639.65	0.00	2886.69	3169.59	-16.53	16.56	3.94	-6.68	-2.71
52.00	15.48	12.70	4.77	2229.33	-8047.14	0.00	2886.69	3169.59	-33.11	17.44	3.94	-6.68	-18.41
54.00	27.83	22.21	4.38	4204.55	-7963.05	0.00	2886.69	3169.59	-62.44	17.26	3.94	-6.68	-47.92
56.00	-28.26	-22.52	4.36	-4585.02	-8530.13	0.00	2886.69	3169.59	68.09	18.49	3.94	-6.68	83.84
58.00	-5.78	-4.79	4.93	-1045.96	-10335.59	0.00	2886.69	3169.59	15.53	22.40	3.94	-6.68	35.20
60.00	-3.92	-3.25	4.94	-760.67	-11091.12	0.00	2886.69	3169.59	11.30	24.04	3.94	-6.68	32.60

Case 8: I95C150, f_{ck} = 60 MPa

L (m)	β (°)	W (cm)	V (cm)	M_y (KNm)	M_z (KNm)	φ (°)	P_{max} (KN)	M_{Pmax} (KNm)	$σ_{my}$ (Mpa)	$σ_{mz}$ (Mpa)	$σ_p$ (Mpa)	$σ_{MP}$ (Mpa)	$σ_t$ (Mpa)
10.00	0.73	0.38	22.64	2.79	-217.67	0.00	3188.40	1575.07	-0.04	1.52	6.18	-10.10	-2.44
12.00	0.88	0.46	22.64	4.83	-313.43	0.00	3188.40	1575.07	-0.07	2.19	6.18	-10.10	-1.81
14.00	1.03	0.53	22.64	7.69	-426.60	0.00	3188.40	1575.07	-0.12	2.98	6.18	-10.10	-1.06
16.00	1.19	0.61	22.64	11.53	-557.16	0.00	3188.40	1575.07	-0.17	3.89	6.18	-10.10	-0.21
18.00	1.34	0.69	22.64	16.51	-705.11	0.00	3188.40	1575.07	-0.25	4.92	6.18	-10.10	0.75
20.00	1.50	0.78	22.63	22.82	-870.44	0.00	3188.40	1575.07	-0.34	6.08	6.18	-10.10	1.81
22.00	1.67	0.86	22.63	30.71	-1053.15	0.00	3188.40	1575.07	-0.46	7.35	6.18	-10.10	2.97
24.00	1.85	0.96	22.63	40.46	-1253.22	0.00	3188.40	1575.07	-0.61	8.75	6.18	-10.10	4.22
26.00	2.04	1.06	22.63	52.42	-1470.62	0.00	3188.40	1575.07	-0.79	10.26	6.18	-10.10	5.55
28.00	2.25	1.17	22.63	67.10	-1705.34	0.00	3188.40	1575.07	-1.01	11.90	6.18	-10.10	6.97
30.00	2.49	1.29	22.62	85.14	-1957.32	0.00	3188.40	1575.07	-1.28	13.66	6.18	-10.10	8.46
32.00	2.76	1.43	22.62	107.48	-2226.51	0.00	3188.40	1575.07	-1.61	15.54	6.18	-10.10	10.00
34.00	3.09	1.60	22.61	135.48	-2512.80	0.00	3188.40	1575.07	-2.04	17.54	6.18	-10.10	11.58
36.00	3.48	1.80	22.60	171.21	-2816.01	0.00	3188.40	1575.07	-2.57	19.65	6.18	-10.10	13.16
38.00	3.98	2.05	22.59	217.96	-3135.82	0.00	3188.40	1575.07	-3.27	21.89	6.18	-10.10	14.69
40.00	4.63	2.39	22.57	281.30	-3471.60	0.00	3188.40	1575.07	-4.23	24.23	6.18	-10.10	16.08
42.00	5.55	2.87	22.54	371.34	-3821.98	0.00	3188.40	1575.07	-5.58	26.67	6.18	-10.10	17.17
44.00	6.93	3.57	22.48	508.34	-4183.63	0.00	3188.40	1575.07	-7.64	29.20	6.18	-10.10	17.64
46.00	9.22	4.75	22.35	737.79	-4546.76	0.00	3188.40	1575.07	-11.09	31.73	6.18	-10.10	16.73
48.00	13.50	6.92	22.02	1170.60	-4876.96	0.00	3188.40	1575.07	-17.59	34.04	6.18	-10.10	12.53
50.00	21.54	10.88	21.06	1998.25	-5062.01	0.00	3188.40	1575.07	-30.02	35.33	6.18	-10.10	1.38
52.00	32.01	15.71	19.20	3120.17	-4991.21	0.00	3188.40	1575.07	-46.88	34.84	6.18	-10.10	-15.97
54.00	-26.60	-13.27	20.25	-2841.85	-5676.05	0.00	3188.40	1575.07	42.70	39.61	6.18	-10.10	78.39
56.00	-10.31	-5.30	22.28	-1221.56	-6716.45	0.00	3188.40	1575.07	18.35	46.88	6.18	-10.10	61.31
58.00	-6.84	-3.53	22.48	-872.30	-7270.82	0.00	3188.40	1575.07	13.11	50.75	6.18	-10.10	59.93
60.00	-5.10	-2.64	22.55	-697.30	-7805.61	0.00	3188.40	1575.07	10.48	54.48	6.18	-10.10	61.03

Case 8: I135C150, f_{ck} = 60 MPa

L (m)	β (°)	W (cm)	V (cm)	M_y (KNm)	M_z (KNm)	φ (°)	P_{max} (KN)	M_{Pmax} (KNm)	σ_{my} (Mpa)	σ_{mz} (Mpa)	σ_p (Mpa)	σ_{MP} (Mpa)	σ_t (Mpa)
10.00	0.57	0.33	10.78	2.46	-248.05	0.00	3510.28	2443.15	-0.04	1.04	5.97	-9.70	-2.73
12.00	0.68	0.40	10.78	4.26	-357.18	0.00	3510.28	2443.15	-0.06	1.49	5.97	-9.70	-2.30
14.00	0.80	0.47	10.78	6.79	-486.15	0.00	3510.28	2443.15	-0.10	2.03	5.97	-9.70	-1.80
16.00	0.92	0.54	10.78	10.16	-634.95	0.00	3510.28	2443.15	-0.15	2.65	5.97	-9.70	-1.23
18.00	1.04	0.61	10.78	14.54	-803.59	0.00	3510.28	2443.15	-0.22	3.36	5.97	-9.70	-0.59
20.00	1.16	0.68	10.78	20.09	-992.04	0.00	3510.28	2443.15	-0.30	4.15	5.97	-9.70	0.12
22.00	1.29	0.76	10.78	27.00	-1200.31	0.00	3510.28	2443.15	-0.40	5.02	5.97	-9.70	0.88
24.00	1.42	0.84	10.78	35.50	-1428.39	0.00	3510.28	2443.15	-0.53	5.97	5.97	-9.70	1.71
26.00	1.57	0.92	10.78	45.89	-1676.26	0.00	3510.28	2443.15	-0.69	7.01	5.97	-9.70	2.59
28.00	1.73	1.01	10.78	58.56	-1943.91	0.00	3510.28	2443.15	-0.88	8.13	5.97	-9.70	3.52
30.00	1.90	1.11	10.77	74.00	-2231.32	0.00	3510.28	2443.15	-1.11	9.33	5.97	-9.70	4.49
32.00	2.10	1.23	10.77	92.92	-2538.44	0.00	3510.28	2443.15	-1.39	10.61	5.97	-9.70	5.49
34.00	2.32	1.36	10.77	116.32	-2865.22	0.00	3510.28	2443.15	-1.74	11.98	5.97	-9.70	6.51
36.00	2.60	1.52	10.77	145.67	-3211.57	0.00	3510.28	2443.15	-2.18	13.43	5.97	-9.70	7.52
38.00	2.93	1.72	10.77	183.19	-3577.31	0.00	3510.28	2443.15	-2.74	14.96	5.97	-9.70	8.49
40.00	3.36	1.97	10.76	232.52	-3962.16	0.00	3510.28	2443.15	-3.48	16.57	5.97	-9.70	9.36
42.00	3.93	2.30	10.75	299.83	-4365.51	0.00	3510.28	2443.15	-4.49	18.25	5.97	-9.70	10.04
44.00	4.74	2.78	10.74	396.62	-4786.05	0.00	3510.28	2443.15	-5.94	20.01	5.97	-9.70	10.35
46.00	5.98	3.50	10.72	546.68	-5220.42	0.00	3510.28	2443.15	-8.18	21.83	5.97	-9.70	9.92
48.00	8.11	4.75	10.67	806.35	-5658.15	0.00	3510.28	2443.15	-12.07	23.66	5.97	-9.70	7.86
50.00	12.36	7.20	10.53	1326.94	-6057.89	0.00	3510.28	2443.15	-19.86	25.33	5.97	-9.70	1.74
52.00	20.94	12.02	10.07	2397.41	-6264.49	0.00	3510.28	2443.15	-35.88	26.19	5.97	-9.70	-13.42
54.00	31.95	17.80	9.15	3828.14	-6137.44	0.00	3510.28	2443.15	-57.29	25.66	5.97	-9.70	-35.36
56.00	-27.23	-15.39	9.59	-3559.40	-6917.11	0.00	3510.28	2443.15	53.27	28.92	5.97	-9.70	78.46
58.00	-7.79	-4.56	10.68	-1131.09	-8267.75	0.00	3510.28	2443.15	16.93	34.57	5.97	-9.70	47.77
60.00	-5.36	-3.14	10.73	-833.59	-8891.20	0.00	3510.28	2443.15	12.48	37.18	5.97	-9.70	45.92

Case 8: I175C150, f_{ck} = 60 MPa

L (m)	β (°)	W (cm)	V (cm)	M_y (KNm)	M_z (KNm)	φ (°)	P_{max} (KN)	M_{Pmax} (KNm)	σ_{my} (Mpa)	σ_{mz} (Mpa)	σ_p (Mpa)	σ_{MP} (Mpa)	σ_t (Mpa)
10.00	0.46	0.31	6.43	2.26	-278.43	0.00	3633.45	3259.20	-0.03	0.81	5.51	-9.10	-2.82
12.00	0.56	0.37	6.43	3.91	-400.93	0.00	3633.45	3259.20	-0.06	1.16	5.51	-9.10	-2.49
14.00	0.65	0.43	6.43	6.22	-545.70	0.00	3633.45	3259.20	-0.09	1.58	5.51	-9.10	-2.10
16.00	0.75	0.49	6.43	9.31	-712.73	0.00	3633.45	3259.20	-0.14	2.06	5.51	-9.10	-1.67
18.00	0.85	0.56	6.43	13.32	-902.03	0.00	3633.45	3259.20	-0.20	2.61	5.51	-9.10	-1.18
20.00	0.95	0.62	6.43	18.39	-1113.59	0.00	3633.45	3259.20	-0.27	3.23	5.51	-9.10	-0.64
22.00	1.05	0.69	6.43	24.69	-1347.40	0.00	3633.45	3259.20	-0.37	3.90	5.51	-9.10	-0.06
24.00	1.16	0.76	6.43	32.43	-1603.46	0.00	3633.45	3259.20	-0.48	4.64	5.51	-9.10	0.57
26.00	1.27	0.84	6.43	41.86	-1881.76	0.00	3633.45	3259.20	-0.62	5.45	5.51	-9.10	1.23
28.00	1.40	0.92	6.43	53.30	-2182.28	0.00	3633.45	3259.20	-0.79	6.32	5.51	-9.10	1.93
30.00	1.54	1.01	6.42	67.19	-2505.02	0.00	3633.45	3259.20	-1.00	7.26	5.51	-9.10	2.66
32.00	1.69	1.11	6.42	84.10	-2849.94	0.00	3633.45	3259.20	-1.25	8.25	5.51	-9.10	3.41
34.00	1.87	1.22	6.42	104.83	-3217.01	0.00	3633.45	3259.20	-1.56	9.32	5.51	-9.10	4.16
36.00	2.07	1.36	6.42	130.55	-3606.16	0.00	3633.45	3259.20	-1.95	10.44	5.51	-9.10	4.91
38.00	2.32	1.52	6.42	162.99	-4017.30	0.00	3633.45	3259.20	-2.43	11.63	5.51	-9.10	5.61
40.00	2.64	1.73	6.42	204.86	-4450.26	0.00	3633.45	3259.20	-3.05	12.89	5.51	-9.10	6.24
42.00	3.04	2.00	6.42	260.62	-4904.68	0.00	3633.45	3259.20	-3.89	14.20	5.51	-9.10	6.73
44.00	3.60	2.36	6.41	338.19	-5379.89	0.00	3633.45	3259.20	-5.04	15.58	5.51	-9.10	6.95
46.00	4.41	2.89	6.41	452.90	-5874.26	0.00	3633.45	3259.20	-6.75	17.01	5.51	-9.10	6.67
48.00	5.71	3.74	6.39	638.53	-6383.30	0.00	3633.45	3259.20	-9.52	18.49	5.51	-9.10	5.38
50.00	8.12	5.31	6.36	982.86	-6891.15	0.00	3633.45	3259.20	-14.65	19.96	5.51	-9.10	1.71
52.00	13.39	8.71	6.25	1743.73	-7324.18	0.00	3633.45	3259.20	-26.00	21.21	5.51	-9.10	-8.38
54.00	23.75	15.15	5.88	3270.02	-7431.56	0.00	3633.45	3259.20	-48.75	21.52	5.51	-9.10	-30.82
56.00	541.22	-0.80	-6.43	-185.30	8729.77	0.00	3633.45	3259.20	2.76	-25.28	5.51	-9.10	-26.11
58.00	-35.51	-21.85	5.23	-5440.88	-7624.27	0.00	3633.45	3259.20	81.12	22.08	5.51	-9.10	99.61
60.00	-5.64	-3.70	6.40	-985.02	-9975.16	0.00	3633.45	3259.20	14.69	28.89	5.51	-9.10	39.98

Case 8: I215C150, f_{ck} = 60 MPa

L (m)	β (°)	W (cm)	V (cm)	M_y (KNm)	M_z (KNm)	φ (°)	P_{max} (KN)	M_{Pmax} (KNm)	σ_{my} (Mpa)	σ_{mz} (Mpa)	σ_p (Mpa)	σ_{MP} (Mpa)	σ_t (Mpa)
10.00	0.39	0.28	4.33	2.12	-308.80	0.00	3696.09	4058.31	-0.03	0.67	5.05	-8.55	-2.87
12.00	0.47	0.34	4.33	3.66	-444.67	0.00	3696.09	4058.31	-0.05	0.96	5.05	-8.55	-2.59
14.00	0.55	0.40	4.32	5.83	-605.24	0.00	3696.09	4058.31	-0.09	1.31	5.05	-8.55	-2.28
16.00	0.63	0.46	4.33	8.72	-790.51	0.00	3696.09	4058.31	-0.13	1.71	5.05	-8.55	-1.92
18.00	0.71	0.52	4.33	12.47	-1000.47	0.00	3696.09	4058.31	-0.19	2.17	5.05	-8.55	-1.52
20.00	0.80	0.58	4.33	17.21	-1235.12	0.00	3696.09	4058.31	-0.26	2.68	5.05	-8.55	-1.08
22.00	0.89	0.64	4.32	23.10	-1494.46	0.00	3696.09	4058.31	-0.34	3.24	5.05	-8.55	-0.61
24.00	0.98	0.71	4.32	30.32	-1778.49	0.00	3696.09	4058.31	-0.45	3.85	5.05	-8.55	-0.10
26.00	1.07	0.78	4.32	39.09	-2087.19	0.00	3696.09	4058.31	-0.58	4.52	5.05	-8.55	0.44
28.00	1.18	0.85	4.32	49.71	-2420.56	0.00	3696.09	4058.31	-0.74	5.25	5.05	-8.55	1.00
30.00	1.29	0.94	4.32	62.56	-2778.59	0.00	3696.09	4058.31	-0.93	6.02	5.05	-8.55	1.59
32.00	1.42	1.03	4.32	78.12	-3161.25	0.00	3696.09	4058.31	-1.16	6.85	5.05	-8.55	2.19
34.00	1.56	1.13	4.32	97.10	-3568.53	0.00	3696.09	4058.31	-1.44	7.73	5.05	-8.55	2.79
36.00	1.72	1.25	4.32	120.47	-4000.37	0.00	3696.09	4058.31	-1.79	8.67	5.05	-8.55	3.38
38.00	1.92	1.39	4.32	149.68	-4456.71	0.00	3696.09	4058.31	-2.22	9.66	5.05	-8.55	3.93
40.00	2.17	1.57	4.32	186.91	-4937.43	0.00	3696.09	4058.31	-2.78	10.70	5.05	-8.55	4.42
42.00	2.48	1.80	4.32	235.70	-5442.31	0.00	3696.09	4058.31	-3.50	11.79	5.05	-8.55	4.79
44.00	2.90	2.10	4.32	302.09	-5970.93	0.00	3696.09	4058.31	-4.49	12.94	5.05	-8.55	4.95
46.00	3.49	2.53	4.32	397.30	-6522.34	0.00	3696.09	4058.31	-5.90	14.13	5.05	-8.55	4.73
48.00	4.39	3.18	4.31	544.65	-7094.11	0.00	3696.09	4058.31	-8.09	15.37	5.05	-8.55	3.78
50.00	5.95	4.31	4.30	800.67	-7678.63	0.00	3696.09	4058.31	-11.89	16.64	5.05	-8.55	1.25
52.00	9.19	6.63	4.27	1333.23	-8243.11	0.00	3696.09	4058.31	-19.80	17.86	5.05	-8.55	-5.44
54.00	16.96	12.12	4.14	2626.68	-8613.30	0.00	3696.09	4058.31	-39.01	18.67	5.05	-8.55	-23.85
56.00	28.87	20.06	3.79	4676.32	-8480.42	0.00	3696.09	4058.31	-69.45	18.38	5.05	-8.55	-54.57
58.00	-28.69	-19.95	3.79	-4986.58	-9113.31	0.00	3696.09	4058.31	74.06	19.75	5.05	-8.55	90.30
60.00	-5.97	-4.32	4.30	-1157.12	-11056.79	0.00	3696.09	4058.31	17.18	23.96	5.05	-8.55	37.64

Case 8: I125D200, f_{ck} = 20 MPa

L (m)	β (°)	W (cm)	V (cm)	M_y (KNm)	M_z (KNm)	φ (°)	P_{max} (KN)	M_{Pmax} (KNm)	σ_{my} (Mpa)	σ_{mz} (Mpa)	σ_p (Mpa)	σ_{MP} (Mpa)	σ_t (Mpa)
10.00	0.61	0.36	17.97	3.07	-286.77	0.00	2120.04	1339.86	-0.04	1.13	3.12	-4.77	-0.56
12.00	0.74	0.43	17.97	5.31	-412.94	0.00	2120.04	1339.86	-0.06	1.63	3.12	-4.77	-0.08
14.00	0.86	0.51	17.97	8.45	-562.04	0.00	2120.04	1339.86	-0.10	2.22	3.12	-4.77	0.47
16.00	0.99	0.58	17.97	12.66	-734.07	0.00	2120.04	1339.86	-0.15	2.90	3.12	-4.77	1.10
18.00	1.12	0.66	17.97	18.13	-929.02	0.00	2120.04	1339.86	-0.22	3.67	3.12	-4.77	1.80
20.00	1.25	0.74	17.97	25.05	-1146.88	0.00	2120.04	1339.86	-0.30	4.53	3.12	-4.77	2.58
22.00	1.39	0.82	17.97	33.69	-1387.65	0.00	2120.04	1339.86	-0.40	5.48	3.12	-4.77	3.43
24.00	1.54	0.90	17.97	44.35	-1651.31	0.00	2120.04	1339.86	-0.53	6.52	3.12	-4.77	4.34
26.00	1.70	1.00	17.97	57.41	-1937.84	0.00	2120.04	1339.86	-0.69	7.66	3.12	-4.77	5.32
28.00	1.87	1.10	17.97	73.38	-2247.22	0.00	2120.04	1339.86	-0.88	8.88	3.12	-4.77	6.35
30.00	2.06	1.21	17.96	92.95	-2579.42	0.00	2120.04	1339.86	-1.11	10.19	3.12	-4.77	7.43
32.00	2.28	1.34	17.96	117.07	-2934.38	0.00	2120.04	1339.86	-1.40	11.59	3.12	-4.77	8.54
34.00	2.54	1.49	17.96	147.12	-3312.01	0.00	2120.04	1339.86	-1.76	13.09	3.12	-4.77	9.67
36.00	2.86	1.68	17.95	185.19	-3712.16	0.00	2120.04	1339.86	-2.22	14.67	3.12	-4.77	10.80
38.00	3.25	1.91	17.95	234.51	-4134.58	0.00	2120.04	1339.86	-2.81	16.34	3.12	-4.77	11.88
40.00	3.75	2.20	17.94	300.46	-4578.77	0.00	2120.04	1339.86	-3.60	18.09	3.12	-4.77	12.84
42.00	4.45	2.61	17.92	392.61	-5043.69	0.00	2120.04	1339.86	-4.70	19.93	3.12	-4.77	13.57
44.00	5.47	3.21	17.89	529.57	-5526.91	0.00	2120.04	1339.86	-6.34	21.84	3.12	-4.77	13.84
46.00	7.12	4.17	17.84	752.22	-6021.65	0.00	2120.04	1339.86	-9.01	23.79	3.12	-4.77	13.13
48.00	10.15	5.93	17.69	1163.89	-6504.30	0.00	2120.04	1339.86	-13.94	25.70	3.12	-4.77	10.11
50.00	16.41	9.51	17.24	2024.94	-6877.82	0.00	2120.04	1339.86	-24.25	27.18	3.12	-4.77	1.27
52.00	26.88	15.22	16.03	3505.98	-6916.97	0.00	2120.04	1339.86	-41.98	27.33	3.12	-4.77	-16.31
54.00	-375.09	-8.76	17.35	-2177.53	-8074.28	0.00	2120.04	1339.86	26.08	31.90	3.12	-4.77	56.33
56.00	-36.36	-19.95	14.48	-5332.02	-7242.65	0.00	2120.04	1339.86	63.85	28.62	3.12	-4.77	90.81
58.00	-6.61	-3.87	17.86	-1110.51	-9583.44	0.00	2120.04	1339.86	13.30	37.87	3.12	-4.77	49.51
60.00	-4.80	-2.82	17.91	-864.13	-10288.16	-0.01	2120.04	1339.86	10.35	40.65	3.12	-4.77	49.35

Case 8: I165D200, f_{ck} = 20 MPa

L (m)	β (°)	W (cm)	V (cm)	M_y (KNm)	M_z (KNm)	φ (°)	P_{max} (KN)	M_{Pmax} (KNm)	σ_{my} (Mpa)	σ_{mz} (Mpa)	σ_p (Mpa)	σ_{MP} (Mpa)	σ_t (Mpa)
10.00	0.50	0.32	10.22	2.77	-320.53	0.00	2220.30	1840.63	-0.03	0.86	2.92	-4.51	-0.77
12.00	0.60	0.39	10.22	4.80	-461.55	0.00	2220.30	1840.63	-0.06	1.23	2.92	-4.51	-0.42
14.00	0.70	0.46	10.22	7.63	-628.21	0.00	2220.30	1840.63	-0.09	1.68	2.92	-4.51	0.00
16.00	0.80	0.52	10.22	11.43	-820.50	0.00	2220.30	1840.63	-0.14	2.19	2.92	-4.51	0.46
18.00	0.90	0.59	10.22	16.36	-1038.42	0.00	2220.30	1840.63	-0.20	2.77	2.92	-4.51	0.99
20.00	1.01	0.66	10.22	22.59	-1281.95	0.00	2220.30	1840.63	-0.27	3.42	2.92	-4.51	1.56
22.00	1.12	0.73	10.22	30.35	-1551.11	0.00	2220.30	1840.63	-0.36	4.14	2.92	-4.51	2.19
24.00	1.24	0.81	10.22	39.90	-1845.87	0.00	2220.30	1840.63	-0.48	4.93	2.92	-4.51	2.86
26.00	1.36	0.89	10.22	51.55	-2166.23	0.00	2220.30	1840.63	-0.62	5.78	2.92	-4.51	3.58
28.00	1.50	0.98	10.22	65.73	-2512.16	0.00	2220.30	1840.63	-0.78	6.71	2.92	-4.51	4.33
30.00	1.65	1.08	10.22	82.99	-2883.65	0.00	2220.30	1840.63	-0.99	7.70	2.92	-4.51	5.12
32.00	1.82	1.19	10.21	104.11	-3280.66	0.00	2220.30	1840.63	-1.24	8.76	2.92	-4.51	5.93
34.00	2.01	1.32	10.21	130.14	-3703.14	0.00	2220.30	1840.63	-1.55	9.89	2.92	-4.51	6.74
36.00	2.24	1.47	10.21	162.66	-4150.99	0.00	2220.30	1840.63	-1.94	11.08	2.92	-4.51	7.55
38.00	2.53	1.65	10.21	204.07	-4624.07	0.00	2220.30	1840.63	-2.44	12.35	2.92	-4.51	8.32
40.00	2.89	1.89	10.21	258.17	-5122.11	0.00	2220.30	1840.63	-3.08	13.67	2.92	-4.51	9.00
42.00	3.36	2.20	10.20	331.40	-5644.58	0.00	2220.30	1840.63	-3.96	15.07	2.92	-4.51	9.52
44.00	4.02	2.63	10.20	435.58	-6190.32	0.00	2220.30	1840.63	-5.20	16.53	2.92	-4.51	9.74
46.00	5.03	3.29	10.18	594.71	-6756.47	0.00	2220.30	1840.63	-7.10	18.04	2.92	-4.51	9.35
48.00	6.73	4.39	10.15	864.89	-7334.38	0.00	2220.30	1840.63	-10.32	19.58	2.92	-4.51	7.67
50.00	10.07	6.56	10.06	1401.41	-7889.97	0.00	2220.30	1840.63	-16.73	21.06	2.92	-4.51	2.75
52.00	17.51	11.28	9.75	2607.28	-8265.90	0.00	2220.30	1840.63	-31.12	22.07	2.92	-4.51	-10.65
54.00	28.90	18.12	8.95	4517.66	-8182.62	0.00	2220.30	1840.63	-53.93	21.85	2.92	-4.51	-33.67
56.00	-22.78	-14.52	9.42	-3891.38	-9268.31	0.00	2220.30	1840.63	46.45	24.74	2.92	-4.51	69.60
58.00	-7.51	-4.90	10.13	-1410.09	-10690.31	0.00	2220.30	1840.63	16.83	28.54	2.92	-4.51	43.78
60.00	-5.04	-3.29	10.18	-1013.63	-11494.78	0.00	2220.30	1840.63	12.10	30.69	2.92	-4.51	41.20

Case 8: I205D200, f_{ck} = 20 MPa

L (m)	β (°)	W (cm)	V (cm)	M_y (KNm)	M_z (KNm)	φ (°)	P_{max} (KN)	M_{Pmax} (KNm)	σ_{my} (Mpa)	σ_{mz} (Mpa)	σ_p (Mpa)	σ_{MP} (Mpa)	σ_t (Mpa)
10.00	0.42	0.30	6.69	2.57	-354.28	0.00	2261.58	2320.38	-0.03	0.70	2.69	-4.25	-0.89
12.00	0.50	0.36	6.69	4.45	-510.16	0.00	2261.58	2320.38	-0.05	1.01	2.69	-4.25	-0.60
14.00	0.58	0.42	6.69	7.08	-694.37	0.00	2261.58	2320.38	-0.08	1.37	2.69	-4.25	-0.27
16.00	0.67	0.48	6.69	10.60	-906.92	0.00	2261.58	2320.38	-0.13	1.79	2.69	-4.25	0.11
18.00	0.76	0.55	6.69	15.16	-1147.79	0.00	2261.58	2320.38	-0.18	2.26	2.69	-4.25	0.53
20.00	0.85	0.61	6.69	20.93	-1417.00	0.00	2261.58	2320.38	-0.25	2.79	2.69	-4.25	0.99
22.00	0.94	0.68	6.69	28.10	-1714.52	0.00	2261.58	2320.38	-0.33	3.38	2.69	-4.25	1.49
24.00	1.04	0.75	6.69	36.90	-2040.37	0.00	2261.58	2320.38	-0.44	4.02	2.69	-4.25	2.03
26.00	1.14	0.82	6.69	47.61	-2394.51	0.00	2261.58	2320.38	-0.57	4.72	2.69	-4.25	2.60
28.00	1.25	0.90	6.69	60.61	-2776.96	0.00	2261.58	2320.38	-0.72	5.47	2.69	-4.25	3.20
30.00	1.37	0.99	6.69	76.37	-3187.68	0.00	2261.58	2320.38	-0.91	6.28	2.69	-4.25	3.82
32.00	1.51	1.09	6.69	95.53	-3626.65	0.00	2261.58	2320.38	-1.14	7.15	2.69	-4.25	4.46
34.00	1.66	1.20	6.69	119.00	-4093.84	0.00	2261.58	2320.38	-1.42	8.07	2.69	-4.25	5.10
36.00	1.85	1.33	6.69	148.05	-4589.19	0.00	2261.58	2320.38	-1.76	9.05	2.69	-4.25	5.73
38.00	2.07	1.49	6.68	184.61	-5112.59	0.00	2261.58	2320.38	-2.20	10.08	2.69	-4.25	6.33
40.00	2.34	1.69	6.68	231.65	-5663.87	0.00	2261.58	2320.38	-2.76	11.17	2.69	-4.25	6.85
42.00	2.70	1.94	6.68	294.05	-6242.72	0.00	2261.58	2320.38	-3.50	12.31	2.69	-4.25	7.25
44.00	3.18	2.29	6.68	380.37	-6848.46	0.00	2261.58	2320.38	-4.53	13.50	2.69	-4.25	7.42
46.00	3.88	2.79	6.67	507.09	-7479.57	0.00	2261.58	2320.38	-6.03	14.75	2.69	-4.25	7.16
48.00	4.99	3.59	6.66	710.08	-8131.85	0.00	2261.58	2320.38	-8.45	16.03	2.69	-4.25	6.03
50.00	7.02	5.05	6.64	1082.12	-8790.85	0.00	2261.58	2320.38	-12.88	17.33	2.69	-4.25	2.90
52.00	11.51	8.24	6.55	1911.48	-9387.32	0.00	2261.58	2320.38	-22.74	18.51	2.69	-4.25	-5.79
54.00	21.43	15.09	6.23	3774.06	-9617.01	0.00	2261.58	2320.38	-44.91	18.96	2.69	-4.25	-27.50
56.00	181.10	-0.79	-6.69	-212.92	11108.43	0.00	2261.58	2320.38	2.53	-21.90	2.69	-4.25	-20.92
58.00	-34.45	-23.37	5.52	-6742.47	-9827.71	0.00	2261.58	2320.38	80.23	19.38	2.69	-4.25	98.05
60.00	-5.31	-3.83	6.66	-1181.37	-12699.54	0.00	2261.58	2320.38	14.06	25.04	2.69	-4.25	37.54

Case 8: I245D200, f_{ck} = 20 MPa

L (m)	β (°)	W (cm)	V (cm)	M_y (KNm)	M_z (KNm)	φ (°)	P_{max} (KN)	M_{Pmax} (KNm)	σ_{my} (Mpa)	σ_{mz} (Mpa)	σ_p (Mpa)	σ_{MP} (Mpa)	σ_t (Mpa)
10.00	0.36	0.28	4.77	2.42	-388.03	0.00	2285.24	2797.13	-0.03	0.60	2.48	-4.03	-0.97
12.00	0.43	0.34	4.77	4.19	-558.76	0.00	2285.24	2797.13	-0.05	0.86	2.48	-4.03	-0.73
14.00	0.50	0.40	4.77	6.67	-760.52	0.00	2285.24	2797.13	-0.08	1.17	2.48	-4.03	-0.45
16.00	0.58	0.45	4.77	9.99	-993.33	0.00	2285.24	2797.13	-0.12	1.53	2.48	-4.03	-0.13
18.00	0.65	0.51	4.77	14.29	-1257.16	0.00	2285.24	2797.13	-0.17	1.93	2.48	-4.03	0.22
20.00	0.73	0.57	4.77	19.71	-1552.03	0.00	2285.24	2797.13	-0.23	2.38	2.48	-4.03	0.61
22.00	0.81	0.64	4.77	26.45	-1877.92	0.00	2285.24	2797.13	-0.31	2.88	2.48	-4.03	1.03
24.00	0.89	0.70	4.77	34.71	-2234.83	0.00	2285.24	2797.13	-0.41	3.43	2.48	-4.03	1.48
26.00	0.98	0.77	4.77	44.75	-2622.75	0.00	2285.24	2797.13	-0.53	4.03	2.48	-4.03	1.96
28.00	1.07	0.84	4.77	56.90	-3041.68	0.00	2285.24	2797.13	-0.67	4.67	2.48	-4.03	2.45
30.00	1.17	0.92	4.77	71.58	-3491.61	0.00	2285.24	2797.13	-0.85	5.36	2.48	-4.03	2.97
32.00	1.29	1.01	4.77	89.37	-3972.50	0.00	2285.24	2797.13	-1.06	6.10	2.48	-4.03	3.50
34.00	1.42	1.12	4.77	111.03	-4484.34	0.00	2285.24	2797.13	-1.32	6.89	2.48	-4.03	4.03
36.00	1.57	1.23	4.76	137.68	-5027.09	0.00	2285.24	2797.13	-1.63	7.72	2.48	-4.03	4.55
38.00	1.75	1.38	4.76	170.94	-5600.66	0.00	2285.24	2797.13	-2.03	8.60	2.48	-4.03	5.03
40.00	1.97	1.55	4.76	213.26	-6204.94	0.00	2285.24	2797.13	-2.53	9.53	2.48	-4.03	5.46
42.00	2.25	1.77	4.76	268.60	-6839.72	0.00	2285.24	2797.13	-3.19	10.50	2.48	-4.03	5.78
44.00	2.62	2.06	4.76	343.69	-7504.55	0.00	2285.24	2797.13	-4.08	11.52	2.48	-4.03	5.91
46.00	3.15	2.48	4.76	450.94	-8198.49	0.00	2285.24	2797.13	-5.35	12.59	2.48	-4.03	5.70
48.00	3.95	3.11	4.76	615.99	-8919.15	0.00	2285.24	2797.13	-7.31	13.70	2.48	-4.03	4.85
50.00	5.33	4.19	4.75	900.67	-9659.05	0.00	2285.24	2797.13	-10.68	14.83	2.48	-4.03	2.61
52.00	8.16	6.41	4.72	1490.04	-10386.21	0.00	2285.24	2797.13	-17.67	15.95	2.48	-4.03	-3.27
54.00	15.30	11.90	4.60	2986.33	-10913.99	0.00	2285.24	2797.13	-35.42	16.76	2.48	-4.03	-20.20
56.00	27.48	20.81	4.23	5614.58	-10796.20	0.00	2285.24	2797.13	-66.60	16.58	2.48	-4.03	-51.56
58.00	-28.02	-21.19	4.21	-6131.56	-11523.90	0.00	2285.24	2797.13	72.73	17.69	2.48	-4.03	88.88
60.00	-5.65	-4.44	4.74	-1374.49	-13901.58	0.00	2285.24	2797.13	16.30	21.35	2.48	-4.03	36.11

Case 8: I125D200, f_{ck} = 40 MPa

L (m)	β (°)	W (cm)	V (cm)	M_y (KNm)	M_z (KNm)	φ (°)	P_{max} (KN)	M_{Pmax} (KNm)	σ_{my} (Mpa)	σ_{mz} (Mpa)	σ_p (Mpa)	σ_{MP} (Mpa)	σ_t (Mpa)
10.00	0.61	0.29	14.27	3.07	-286.77	0.00	3365.35	2126.90	-0.04	1.13	4.95	-7.57	-1.53
12.00	0.74	0.34	14.27	5.31	-412.94	0.00	3365.35	2126.90	-0.06	1.63	4.95	-7.57	-1.06
14.00	0.86	0.40	14.27	8.44	-562.04	0.00	3365.35	2126.90	-0.10	2.22	4.95	-7.57	-0.50
16.00	0.99	0.46	14.26	12.64	-734.07	0.00	3365.35	2126.90	-0.15	2.90	4.95	-7.57	0.13
18.00	1.11	0.52	14.26	18.07	-929.02	0.00	3365.35	2126.90	-0.22	3.67	4.95	-7.57	0.83
20.00	1.25	0.58	14.26	24.94	-1146.88	0.00	3365.35	2126.90	-0.30	4.53	4.95	-7.57	1.61
22.00	1.38	0.64	14.26	33.46	-1387.65	0.00	3365.35	2126.90	-0.40	5.48	4.95	-7.57	2.46
24.00	1.52	0.71	14.26	43.92	-1651.32	0.00	3365.35	2126.90	-0.53	6.52	4.95	-7.57	3.37
26.00	1.67	0.78	14.26	56.63	-1937.86	0.00	3365.35	2126.90	-0.68	7.66	4.95	-7.57	4.35
28.00	1.84	0.86	14.26	72.02	-2247.27	0.00	3365.35	2126.90	-0.86	8.88	4.95	-7.57	5.39
30.00	2.01	0.94	14.26	90.63	-2579.51	0.00	3365.35	2126.90	-1.09	10.19	4.95	-7.57	6.48
32.00	2.21	1.03	14.26	113.18	-2934.53	0.00	3365.35	2126.90	-1.36	11.60	4.95	-7.57	7.62
34.00	2.43	1.13	14.25	140.67	-3312.29	0.00	3365.35	2126.90	-1.68	13.09	4.95	-7.57	8.78
36.00	2.69	1.25	14.25	174.52	-3712.68	0.00	3365.35	2126.90	-2.09	14.67	4.95	-7.57	9.96
38.00	3.00	1.40	14.25	216.82	-4135.55	0.00	3365.35	2126.90	-2.60	16.34	4.95	-7.57	11.12
40.00	3.38	1.58	14.24	270.72	-4580.62	0.00	3365.35	2126.90	-3.24	18.10	4.95	-7.57	12.23
42.00	3.87	1.80	14.23	341.31	-5047.42	0.00	3365.35	2126.90	-4.09	19.94	4.95	-7.57	13.23
44.00	4.52	2.10	14.22	437.22	-5534.99	0.00	3365.35	2126.90	-5.24	21.87	4.95	-7.57	14.01
46.00	5.43	2.53	14.20	574.28	-6041.21	0.00	3365.35	2126.90	-6.88	23.87	4.95	-7.57	14.37
48.00	6.82	3.17	14.17	784.57	-6560.86	0.00	3365.35	2126.90	-9.40	25.92	4.95	-7.57	13.90
50.00	9.16	4.25	14.08	1141.07	-7078.33	0.00	3365.35	2126.90	-13.66	27.97	4.95	-7.57	11.68
52.00	13.59	6.28	13.87	1821.75	-7537.74	0.00	3365.35	2126.90	-21.82	29.78	4.95	-7.57	5.34
54.00	21.78	9.91	13.25	3103.19	-7765.69	0.00	3365.35	2126.90	-37.16	30.68	4.95	-7.57	-9.10
56.00	31.96	14.14	12.10	4761.03	-7630.14	0.00	3365.35	2126.90	-57.01	30.15	4.95	-7.57	-29.49
58.00	-28.43	-12.72	12.55	-4592.83	-8484.19	0.00	3365.35	2126.90	55.00	33.52	4.95	-7.57	85.90
60.00	-9.44	-4.38	14.07	-1694.22	-10184.43	0.00	3365.35	2126.90	20.29	40.24	4.95	-7.57	57.91

Case 8: I165D200, f_{ck} = 40 MPa

L (m)	β (°)	W (cm)	V (cm)	M_y (KNm)	M_z (KNm)	φ (°)	P_{max} (KN)	M_{Pmax} (KNm)	σ_{my} (Mpa)	σ_{mz} (Mpa)	σ_p (Mpa)	σ_{MP} (Mpa)	σ_t (Mpa)
10.00	0.50	0.26	8.11	2.77	-320.53	0.00	3524.51	2921.82	-0.03	0.86	4.64	-7.16	-1.70
12.00	0.60	0.31	8.11	4.79	-461.55	0.00	3524.51	2921.82	-0.06	1.23	4.64	-7.16	-1.35
14.00	0.70	0.36	8.11	7.63	-628.21	0.00	3524.51	2921.82	-0.09	1.68	4.64	-7.16	-0.94
16.00	0.80	0.41	8.11	11.41	-820.50	0.00	3524.51	2921.82	-0.14	2.19	4.64	-7.16	-0.47
18.00	0.90	0.47	8.11	16.31	-1038.42	0.00	3524.51	2921.82	-0.19	2.77	4.64	-7.16	0.05
20.00	1.01	0.52	8.11	22.50	-1281.96	0.00	3524.51	2921.82	-0.27	3.42	4.64	-7.16	0.63
22.00	1.11	0.58	8.11	30.17	-1551.11	0.00	3524.51	2921.82	-0.36	4.14	4.64	-7.16	1.26
24.00	1.23	0.64	8.11	39.55	-1845.88	0.00	3524.51	2921.82	-0.47	4.93	4.64	-7.16	1.93
26.00	1.35	0.70	8.11	50.92	-2166.24	0.00	3524.51	2921.82	-0.61	5.78	4.64	-7.16	2.65
28.00	1.47	0.77	8.11	64.64	-2512.19	0.00	3524.51	2921.82	-0.77	6.71	4.64	-7.16	3.41
30.00	1.61	0.84	8.11	81.14	-2883.70	0.00	3524.51	2921.82	-0.97	7.70	4.64	-7.16	4.20
32.00	1.76	0.92	8.11	101.02	-3280.76	0.00	3524.51	2921.82	-1.21	8.76	4.64	-7.16	5.03
34.00	1.93	1.00	8.11	125.07	-3703.31	0.00	3524.51	2921.82	-1.49	9.89	4.64	-7.16	5.87
36.00	2.13	1.11	8.11	154.39	-4151.31	0.00	3524.51	2921.82	-1.84	11.08	4.64	-7.16	6.71
38.00	2.36	1.23	8.11	190.56	-4624.65	0.00	3524.51	2921.82	-2.27	12.35	4.64	-7.16	7.55
40.00	2.64	1.37	8.10	235.92	-5123.18	0.00	3524.51	2921.82	-2.82	13.68	4.64	-7.16	8.34
42.00	2.98	1.55	8.10	294.07	-5646.64	0.00	3524.51	2921.82	-3.51	15.08	4.64	-7.16	9.04
44.00	3.43	1.78	8.10	370.91	-6194.53	0.00	3524.51	2921.82	-4.43	16.54	4.64	-7.16	9.59
46.00	4.03	2.09	8.09	476.67	-6765.82	0.00	3524.51	2921.82	-5.69	18.06	4.64	-7.16	9.85
48.00	4.90	2.54	8.08	630.76	-7358.22	0.00	3524.51	2921.82	-7.53	19.64	4.64	-7.16	9.59
50.00	6.26	3.25	8.06	874.24	-7965.63	0.00	3524.51	2921.82	-10.44	21.27	4.64	-7.16	8.31
52.00	8.67	4.49	8.02	1307.18	-8568.22	0.00	3524.51	2921.82	-15.60	22.88	4.64	-7.16	4.75
54.00	13.58	6.99	7.88	2194.14	-9085.72	0.00	3524.51	2921.82	-26.19	24.26	4.64	-7.16	-4.46
56.00	22.81	11.54	7.48	3896.25	-9266.26	0.00	3524.51	2921.82	-46.51	24.74	4.64	-7.16	-24.29
58.00	181.36	-0.71	-8.11	-256.66	10779.86	0.00	3524.51	2921.82	3.06	-28.78	4.64	-7.16	-28.24
60.00	-30.76	-15.22	6.97	-5902.58	-9915.49	0.00	3524.51	2921.82	70.46	26.47	4.64	-7.16	94.40

Case 8: I205D500, f_{ck} = 40 MPa

L (m)	β (°)	W (cm)	V (cm)	M_y (KNm)	M_z (KNm)	φ (°)	P_{max} (KN)	M_{Pmax} (KNm)	σ_{my} (Mpa)	σ_{mz} (Mpa)	σ_p (Mpa)	σ_{MP} (Mpa)	σ_t (Mpa)
10.00	0.42	0.24	5.31	2.57	-354.28	0.00	3590.04	3683.38	-0.03	0.70	4.27	-6.74	-1.80
12.00	0.50	0.29	5.31	4.45	-510.16	0.00	3590.04	3683.38	-0.05	1.01	4.27	-6.74	-1.52
14.00	0.58	0.33	5.31	7.07	-694.37	0.00	3590.04	3683.38	-0.08	1.37	4.27	-6.74	-1.18
16.00	0.67	0.38	5.31	10.58	-906.92	0.00	3590.04	3683.38	-0.13	1.79	4.27	-6.74	-0.81
18.00	0.75	0.43	5.31	15.12	-1147.79	0.00	3590.04	3683.38	-0.18	2.26	4.27	-6.74	-0.39
20.00	0.84	0.48	5.31	20.85	-1417.00	0.00	3590.04	3683.38	-0.25	2.79	4.27	-6.74	0.08
22.00	0.93	0.53	5.31	27.94	-1714.53	0.00	3590.04	3683.38	-0.33	3.38	4.27	-6.74	0.58
24.00	1.03	0.59	5.31	36.60	-2040.37	0.00	3590.04	3683.38	-0.44	4.02	4.27	-6.74	1.12
26.00	1.13	0.64	5.31	47.08	-2394.52	0.00	3590.04	3683.38	-0.56	4.72	4.27	-6.74	1.69
28.00	1.23	0.70	5.31	59.69	-2776.98	0.00	3590.04	3683.38	-0.71	5.47	4.27	-6.74	2.30
30.00	1.34	0.77	5.31	74.80	-3187.72	0.00	3590.04	3683.38	-0.89	6.28	4.27	-6.74	2.93
32.00	1.47	0.84	5.31	92.94	-3626.72	0.00	3590.04	3683.38	-1.11	7.15	4.27	-6.74	3.58
34.00	1.61	0.92	5.31	114.76	-4093.96	0.00	3590.04	3683.38	-1.37	8.07	4.27	-6.74	4.24
36.00	1.76	1.01	5.31	141.18	-4589.40	0.00	3590.04	3683.38	-1.68	9.05	4.27	-6.74	4.90
38.00	1.94	1.11	5.31	173.51	-5112.98	0.00	3590.04	3683.38	-2.06	10.08	4.27	-6.74	5.55
40.00	2.16	1.24	5.31	213.61	-5664.58	0.00	3590.04	3683.38	-2.54	11.17	4.27	-6.74	6.16
42.00	2.42	1.39	5.30	264.32	-6244.05	0.00	3590.04	3683.38	-3.15	12.31	4.27	-6.74	6.70
44.00	2.76	1.58	5.30	330.12	-6851.07	0.00	3590.04	3683.38	-3.93	13.51	4.27	-6.74	7.11
46.00	3.20	1.83	5.30	418.54	-7485.04	0.00	3590.04	3683.38	-4.98	14.76	4.27	-6.74	7.31
48.00	3.82	2.18	5.30	543.13	-8144.71	0.00	3590.04	3683.38	-6.46	16.06	4.27	-6.74	7.13
50.00	4.73	2.71	5.29	731.01	-8826.99	0.00	3590.04	3683.38	-8.70	17.40	4.27	-6.74	6.24
52.00	6.26	3.57	5.28	1043.95	-9522.90	0.00	3590.04	3683.38	-12.42	18.77	4.27	-6.74	3.88
54.00	9.18	5.23	5.24	1648.19	-10198.72	0.00	3590.04	3683.38	-19.61	20.11	4.27	-6.74	-1.97
56.00	15.63	8.84	5.11	2994.13	-10699.43	0.00	3590.04	3683.38	-35.63	21.09	4.27	-6.74	-17.00
58.00	26.38	14.57	4.76	5294.67	-10677.60	0.00	3590.04	3683.38	-63.00	21.05	4.27	-6.74	-44.42
60.00	-178.85	-0.66	-5.31	-255.67	12751.81	0.00	3590.04	3683.38	3.04	-25.14	4.27	-6.74	-24.57

Case 8: I245D200, f_{ck} = 40 MPa

L (m)	β (°)	W (cm)	V (cm)	M_y (KNm)	M_z (KNm)	φ (°)	P_{max} (KN)	M_{Pmax} (KNm)	σ_{my} (Mpa)	σ_{mz} (Mpa)	σ_p (Mpa)	σ_{MP} (Mpa)	σ_t (Mpa)
10.00	0.36	0.22	3.78	2.42	-388.03	0.00	3627.59	4440.17	-0.03	0.60	3.94	-6.39	-1.88
12.00	0.43	0.27	3.78	4.19	-558.76	0.00	3627.59	4440.17	-0.05	0.86	3.94	-6.39	-1.64
14.00	0.50	0.31	3.78	6.67	-760.52	0.00	3627.59	4440.17	-0.08	1.17	3.94	-6.39	-1.36
16.00	0.58	0.36	3.78	9.98	-993.33	0.00	3627.59	4440.17	-0.12	1.53	3.94	-6.39	-1.04
18.00	0.65	0.41	3.78	14.25	-1257.16	0.00	3627.59	4440.17	-0.17	1.93	3.94	-6.39	-0.68
20.00	0.73	0.45	3.78	19.64	-1552.03	0.00	3627.59	4440.17	-0.23	2.38	3.94	-6.39	-0.30
22.00	0.80	0.50	3.78	26.31	-1877.92	0.00	3627.59	4440.17	-0.31	2.88	3.94	-6.39	0.13
24.00	0.88	0.55	3.78	34.45	-2234.83	0.00	3627.59	4440.17	-0.41	3.43	3.94	-6.39	0.58
26.00	0.97	0.60	3.78	44.28	-2622.76	0.00	3627.59	4440.17	-0.53	4.03	3.94	-6.39	1.06
28.00	1.06	0.66	3.78	56.09	-3041.70	0.00	3627.59	4440.17	-0.67	4.67	3.94	-6.39	1.56
30.00	1.15	0.72	3.78	70.21	-3491.63	0.00	3627.59	4440.17	-0.83	5.36	3.94	-6.39	2.08
32.00	1.26	0.78	3.78	87.10	-3972.55	0.00	3627.59	4440.17	-1.03	6.10	3.94	-6.39	2.62
34.00	1.37	0.86	3.78	107.34	-4484.43	0.00	3627.59	4440.17	-1.27	6.89	3.94	-6.39	3.17
36.00	1.50	0.94	3.78	131.74	-5027.24	0.00	3627.59	4440.17	-1.56	7.72	3.94	-6.39	3.71
38.00	1.65	1.03	3.78	161.40	-5600.94	0.00	3627.59	4440.17	-1.91	8.60	3.94	-6.39	4.24
40.00	1.83	1.14	3.78	197.91	-6205.45	0.00	3627.59	4440.17	-2.35	9.53	3.94	-6.39	4.74
42.00	2.04	1.27	3.78	243.63	-6840.65	0.00	3627.59	4440.17	-2.89	10.50	3.94	-6.39	5.17
44.00	2.31	1.44	3.78	302.20	-7506.33	0.00	3627.59	4440.17	-3.58	11.53	3.94	-6.39	5.50
46.00	2.65	1.66	3.78	379.57	-8202.10	0.00	3627.59	4440.17	-4.50	12.59	3.94	-6.39	5.65
48.00	3.12	1.95	3.78	486.12	-8927.17	0.00	3627.59	4440.17	-5.77	13.71	3.94	-6.39	5.50
50.00	3.79	2.37	3.78	641.66	-9679.70	0.00	3627.59	4440.17	-7.61	14.86	3.94	-6.39	4.81
52.00	4.86	3.03	3.77	888.79	-10454.83	0.00	3627.59	4440.17	-10.54	16.05	3.94	-6.39	3.07
54.00	6.78	4.23	3.76	1335.77	-11236.06	0.00	3627.59	4440.17	-15.84	17.25	3.94	-6.39	-1.04
56.00	10.95	6.80	3.71	2311.12	-11947.39	0.00	3627.59	4440.17	-27.41	18.35	3.94	-6.39	-11.51
58.00	20.16	12.34	3.55	4499.15	-12253.73	0.00	3627.59	4440.17	-53.37	18.82	3.94	-6.39	-37.00
60.00	31.40	18.65	3.23	7278.15	-11923.57	0.00	3627.59	4440.17	-86.33	18.31	3.94	-6.39	-70.47

Case 8: I125D200, f_{ck} = 60 MPa

L (m)	β (°)	W (cm)	V (cm)	M_y (KNm)	M_z (KNm)	φ (°)	P_{max} (KN)	M_{Pmax} (KNm)	σ_{my} (Mpa)	σ_{mz} (Mpa)	σ_p (Mpa)	σ_{MP} (Mpa)	σ_t (Mpa)
10.00	0.61	0.25	12.46	3.07	-286.77	0.00	4308.96	2723.26	-0.04	1.13	6.34	-9.70	-2.26
12.00	0.74	0.30	12.46	5.30	-412.94	0.00	4308.96	2723.26	-0.06	1.63	6.34	-9.70	-1.79
14.00	0.86	0.35	12.46	8.44	-562.04	0.00	4308.96	2723.26	-0.10	2.22	6.34	-9.70	-1.24
16.00	0.99	0.40	12.46	12.63	-734.07	0.00	4308.96	2723.26	-0.15	2.90	6.34	-9.70	-0.61
18.00	1.11	0.45	12.46	18.05	-929.02	0.00	4308.96	2723.26	-0.22	3.67	6.34	-9.70	0.10
20.00	1.24	0.51	12.46	24.88	-1146.88	0.00	4308.96	2723.26	-0.30	4.53	6.34	-9.70	0.87
22.00	1.38	0.56	12.46	33.36	-1387.66	0.00	4308.96	2723.26	-0.40	5.48	6.34	-9.70	1.72
24.00	1.52	0.62	12.46	43.71	-1651.32	0.00	4308.96	2723.26	-0.52	6.52	6.34	-9.70	2.64
26.00	1.66	0.68	12.46	56.26	-1937.87	0.00	4308.96	2723.26	-0.67	7.66	6.34	-9.70	3.62
28.00	1.82	0.74	12.46	71.38	-2247.29	0.00	4308.96	2723.26	-0.85	8.88	6.34	-9.70	4.67
30.00	1.99	0.81	12.46	89.54	-2579.54	0.00	4308.96	2723.26	-1.07	10.19	6.34	-9.70	5.76
32.00	2.17	0.89	12.45	111.38	-2934.60	0.00	4308.96	2723.26	-1.33	11.60	6.34	-9.70	6.90
34.00	2.38	0.97	12.45	137.73	-3312.41	0.00	4308.96	2723.26	-1.65	13.09	6.34	-9.70	8.08
36.00	2.62	1.07	12.45	169.77	-3712.90	0.00	4308.96	2723.26	-2.03	14.67	6.34	-9.70	9.28
38.00	2.89	1.18	12.45	209.14	-4135.94	0.00	4308.96	2723.26	-2.50	16.34	6.34	-9.70	10.48
40.00	3.23	1.31	12.44	258.27	-4581.34	0.00	4308.96	2723.26	-3.09	18.10	6.34	-9.70	11.65
42.00	3.64	1.48	12.44	320.87	-5048.76	0.00	4308.96	2723.26	-3.84	19.95	6.34	-9.70	12.75
44.00	4.16	1.69	12.43	402.88	-5537.59	0.00	4308.96	2723.26	-4.82	21.88	6.34	-9.70	13.70
46.00	4.86	1.98	12.42	514.41	-6046.60	0.00	4308.96	2723.26	-6.16	23.89	6.34	-9.70	14.37
48.00	5.85	2.38	12.40	674.02	-6573.14	0.00	4308.96	2723.26	-8.07	25.97	6.34	-9.70	14.54
50.00	7.37	2.99	12.36	919.17	-7110.55	0.00	4308.96	2723.26	-11.01	28.10	6.34	-9.70	13.73
52.00	9.90	4.01	12.28	1333.85	-7639.19	0.00	4308.96	2723.26	-15.97	30.18	6.34	-9.70	10.85
54.00	14.62	5.89	12.06	2111.05	-8091.92	0.00	4308.96	2723.26	-25.28	31.97	6.34	-9.70	3.33
56.00	22.84	9.06	11.49	3491.19	-8288.43	0.00	4308.96	2723.26	-41.81	32.75	6.34	-9.70	-12.42
58.00	32.55	12.56	10.50	5191.39	-8131.73	0.00	4308.96	2723.26	-62.17	32.13	6.34	-9.70	-33.40
60.00	181.66	-0.68	-12.46	-299.20	10320.05	0.00	4308.96	2723.26	3.58	-40.78	6.34	-9.70	-40.55

Case 8: I165D200, f_{ck} = 60 MPa

L (m)	β (°)	W (cm)	V (cm)	M_y (KNm)	M_z (KNm)	φ (°)	P_{max} (KN)	M_{Pmax} (KNm)	σ_{my} (Mpa)	σ_{mz} (Mpa)	σ_p (Mpa)	σ_{MP} (Mpa)	σ_t (Mpa)
10.00	0.50	0.22	7.09	2.77	-320.53	0.00	4512.74	3741.07	-0.03	0.86	5.94	-9.17	-2.41
12.00	0.59	0.27	7.09	4.79	-461.55	0.00	4512.74	3741.07	-0.06	1.23	5.94	-9.17	-2.06
14.00	0.70	0.32	7.09	7.62	-628.21	0.00	4512.74	3741.07	-0.09	1.68	5.94	-9.17	-1.65
16.00	0.80	0.36	7.09	11.40	-820.50	0.00	4512.74	3741.07	-0.14	2.19	5.94	-9.17	-1.18
18.00	0.90	0.41	7.08	16.29	-1038.42	0.00	4512.74	3741.07	-0.19	2.77	5.94	-9.17	-0.66
20.00	1.00	0.46	7.08	22.45	-1281.96	0.00	4512.74	3741.07	-0.27	3.42	5.94	-9.17	-0.08
22.00	1.11	0.50	7.08	30.08	-1551.11	0.00	4512.74	3741.07	-0.36	4.14	5.94	-9.17	0.55
24.00	1.22	0.55	7.08	39.38	-1845.88	0.00	4512.74	3741.07	-0.47	4.93	5.94	-9.17	1.22
26.00	1.34	0.61	7.08	50.63	-2166.25	0.00	4512.74	3741.07	-0.60	5.78	5.94	-9.17	1.95
28.00	1.46	0.66	7.08	64.12	-2512.20	0.00	4512.74	3741.07	-0.77	6.71	5.94	-9.17	2.71
30.00	1.59	0.72	7.08	80.27	-2883.73	0.00	4512.74	3741.07	-0.96	7.70	5.94	-9.17	3.51
32.00	1.74	0.79	7.08	99.59	-3280.80	0.00	4512.74	3741.07	-1.19	8.76	5.94	-9.17	4.34
34.00	1.90	0.86	7.08	122.75	-3703.39	0.00	4512.74	3741.07	-1.47	9.89	5.94	-9.17	5.19
36.00	2.08	0.94	7.08	150.67	-4151.44	0.00	4512.74	3741.07	-1.80	11.08	5.94	-9.17	6.05
38.00	2.29	1.04	7.08	184.62	-4624.89	0.00	4512.74	3741.07	-2.20	12.35	5.94	-9.17	6.91
40.00	2.53	1.15	7.08	226.42	-5123.61	0.00	4512.74	3741.07	-2.70	13.68	5.94	-9.17	7.74
42.00	2.83	1.28	7.08	278.78	-5647.42	0.00	4512.74	3741.07	-3.33	15.08	5.94	-9.17	8.52
44.00	3.20	1.45	7.08	345.88	-6195.98	0.00	4512.74	3741.07	-4.13	16.54	5.94	-9.17	9.18
46.00	3.67	1.67	7.07	434.53	-6768.66	0.00	4512.74	3741.07	-5.19	18.07	5.94	-9.17	9.65
48.00	4.32	1.96	7.07	556.59	-7364.20	0.00	4512.74	3741.07	-6.64	19.66	5.94	-9.17	9.78
50.00	5.26	2.38	7.06	734.45	-7979.73	0.00	4512.74	3741.07	-8.77	21.30	5.94	-9.17	9.30
52.00	6.73	3.05	7.04	1015.38	-8607.68	0.00	4512.74	3741.07	-12.12	22.98	5.94	-9.17	7.63
54.00	9.31	4.21	6.99	1512.56	-9223.70	0.00	4512.74	3741.07	-18.06	24.63	5.94	-9.17	3.34
56.00	14.44	6.48	6.86	2506.72	-9734.51	0.00	4512.74	3741.07	-29.92	25.99	5.94	-9.17	-7.17
58.00	23.52	10.37	6.50	4302.57	-9887.32	0.00	4512.74	3741.07	-51.36	26.40	5.94	-9.17	-28.19
60.00	181.41	-0.64	-7.08	-284.06	11535.88	0.00	4512.74	3741.07	3.39	-30.80	5.94	-9.17	-30.64

Case 8: I205D200, f_{ck} = 60 MPa

L (m)	β (°)	W (cm)	V (cm)	M_y (KNm)	M_z (KNm)	φ (°)	P_{max} (KN)	M_{Pmax} (KNm)	σ_{my} (Mpa)	σ_{mz} (Mpa)	σ_p (Mpa)	σ_{MP} (Mpa)	σ_t (Mpa)
10.00	0.42	0.21	4.64	2.57	-354.28	0.00	4596.65	4716.16	-0.03	0.70	5.47	-8.64	-2.49
12.00	0.50	0.25	4.64	4.45	-510.16	0.00	4596.65	4716.16	-0.05	1.01	5.47	-8.64	-2.21
14.00	0.58	0.29	4.64	7.07	-694.37	0.00	4596.65	4716.16	-0.08	1.37	5.47	-8.64	-1.88
16.00	0.67	0.33	4.64	10.58	-906.92	0.00	4596.65	4716.16	-0.13	1.79	5.47	-8.64	-1.50
18.00	0.75	0.38	4.64	15.10	-1147.79	0.00	4596.65	4716.16	-0.18	2.26	5.47	-8.64	-1.08
20.00	0.84	0.42	4.64	20.81	-1417.00	0.00	4596.65	4716.16	-0.25	2.79	5.47	-8.64	-0.62
22.00	0.93	0.47	4.64	27.86	-1714.53	0.00	4596.65	4716.16	-0.33	3.38	5.47	-8.64	-0.11
24.00	1.02	0.51	4.64	36.46	-2040.37	0.00	4596.65	4716.16	-0.43	4.02	5.47	-8.64	0.43
26.00	1.12	0.56	4.64	46.83	-2394.53	0.00	4596.65	4716.16	-0.56	4.72	5.47	-8.64	1.00
28.00	1.22	0.61	4.64	59.25	-2776.99	0.00	4596.65	4716.16	-0.70	5.47	5.47	-8.64	1.61
30.00	1.33	0.67	4.64	74.07	-3187.73	0.00	4596.65	4716.16	-0.88	6.28	5.47	-8.64	2.24
32.00	1.45	0.72	4.64	91.73	-3626.75	0.00	4596.65	4716.16	-1.09	7.15	5.47	-8.64	2.90
34.00	1.58	0.79	4.64	112.80	-4094.02	0.00	4596.65	4716.16	-1.34	8.07	5.47	-8.64	3.57
36.00	1.72	0.86	4.64	138.07	-4589.50	0.00	4596.65	4716.16	-1.64	9.05	5.47	-8.64	4.24
38.00	1.89	0.94	4.64	168.58	-5113.14	0.00	4596.65	4716.16	-2.01	10.08	5.47	-8.64	4.91
40.00	2.08	1.04	4.63	205.81	-5664.87	0.00	4596.65	4716.16	-2.45	11.17	5.47	-8.64	5.56
42.00	2.31	1.15	4.63	251.92	-6244.56	0.00	4596.65	4716.16	-3.00	12.31	5.47	-8.64	6.15
44.00	2.59	1.30	4.63	310.17	-6852.00	0.00	4596.65	4716.16	-3.69	13.51	5.47	-8.64	6.66
46.00	2.95	1.47	4.63	385.70	-7486.81	0.00	4596.65	4716.16	-4.59	14.76	5.47	-8.64	7.01
48.00	3.42	1.71	4.63	487.12	-8148.25	0.00	4596.65	4716.16	-5.80	16.06	5.47	-8.64	7.11
50.00	4.08	2.04	4.63	629.98	-8834.77	0.00	4596.65	4716.16	-7.50	17.42	5.47	-8.64	6.76
52.00	5.06	2.53	4.62	845.18	-9542.59	0.00	4596.65	4716.16	-10.06	18.81	5.47	-8.64	5.60
54.00	6.69	3.33	4.61	1202.67	-10260.80	0.00	4596.65	4716.16	-14.31	20.23	5.47	-8.64	2.76
56.00	9.77	4.86	4.57	1885.89	-10949.25	0.00	4596.65	4716.16	-22.44	21.59	5.47	-8.64	-4.01
58.00	16.32	8.05	4.45	3349.85	-11437.80	0.00	4596.65	4716.16	-39.86	22.55	5.47	-8.64	-20.47
60.00	26.66	12.85	4.14	5722.60	-11398.50	0.00	4596.65	4716.16	-68.09	22.47	5.47	-8.64	-48.78

Case 8: I245D200, f_{ck} = 60 MPa

L (m)	β (°)	W (cm)	V (cm)	M_y (KNm)	M_z (KNm)	φ (°)	P_{max} (KN)	M_{Pmax} (KNm)	σ_{my} (Mpa)	σ_{mz} (Mpa)	σ_p (Mpa)	σ_{MP} (Mpa)	σ_t (Mpa)
10.00	0.36	0.20	3.31	2.42	-388.03	0.00	4644.73	5685.16	-0.03	0.60	5.05	-8.18	-2.56
12.00	0.43	0.23	3.31	4.19	-558.76	0.00	4644.73	5685.16	-0.05	0.86	5.05	-8.18	-2.32
14.00	0.50	0.27	3.31	6.67	-760.53	0.00	4644.73	5685.16	-0.08	1.17	5.05	-8.18	-2.04
16.00	0.58	0.31	3.31	9.97	-993.33	0.00	4644.73	5685.16	-0.12	1.53	5.05	-8.18	-1.72
18.00	0.65	0.35	3.30	14.24	-1257.16	0.00	4644.73	5685.16	-0.17	1.93	5.05	-8.18	-1.37
20.00	0.72	0.40	3.31	19.61	-1552.03	0.00	4644.73	5685.16	-0.23	2.38	5.05	-8.18	-0.98
22.00	0.80	0.44	3.31	26.24	-1877.92	0.00	4644.73	5685.16	-0.31	2.88	5.05	-8.18	-0.56
24.00	0.88	0.48	3.30	34.32	-2234.83	0.00	4644.73	5685.16	-0.41	3.43	5.05	-8.18	-0.11
26.00	0.96	0.53	3.31	44.06	-2622.77	0.00	4644.73	5685.16	-0.52	4.03	5.05	-8.18	0.37
28.00	1.05	0.57	3.30	55.70	-3041.71	0.00	4644.73	5685.16	-0.66	4.67	5.05	-8.18	0.88
30.00	1.14	0.62	3.30	69.56	-3491.65	0.00	4644.73	5685.16	-0.83	5.36	5.05	-8.18	1.40
32.00	1.24	0.68	3.30	86.04	-3972.58	0.00	4644.73	5685.16	-1.02	6.10	5.05	-8.18	1.95
34.00	1.35	0.74	3.30	105.64	-4484.47	0.00	4644.73	5685.16	-1.25	6.89	5.05	-8.18	2.50
36.00	1.47	0.80	3.30	129.03	-5027.32	0.00	4644.73	5685.16	-1.53	7.72	5.05	-8.18	3.06
38.00	1.61	0.88	3.30	157.14	-5601.06	0.00	4644.73	5685.16	-1.86	8.60	5.05	-8.18	3.61
40.00	1.76	0.96	3.30	191.22	-6205.66	0.00	4644.73	5685.16	-2.27	9.53	5.05	-8.18	4.13
42.00	1.95	1.06	3.30	233.08	-6841.02	0.00	4644.73	5685.16	-2.76	10.50	5.05	-8.18	4.61
44.00	2.18	1.19	3.30	285.43	-7506.99	0.00	4644.73	5685.16	-3.39	11.53	5.05	-8.18	5.01
46.00	2.46	1.34	3.30	352.40	-8203.32	0.00	4644.73	5685.16	-4.18	12.60	5.05	-8.18	5.28
48.00	2.83	1.54	3.30	440.78	-8929.52	0.00	4644.73	5685.16	-5.23	13.71	5.05	-8.18	5.35
50.00	3.32	1.81	3.30	562.36	-9684.63	0.00	4644.73	5685.16	-6.67	14.87	5.05	-8.18	5.07
52.00	4.04	2.20	3.30	739.56	-10466.45	0.00	4644.73	5685.16	-8.77	16.07	5.05	-8.18	4.17
54.00	5.17	2.82	3.29	1020.37	-11269.08	0.00	4644.73	5685.16	-12.10	17.30	5.05	-8.18	2.07
56.00	7.20	3.92	3.28	1524.88	-12072.95	0.00	4644.73	5685.16	-18.09	18.54	5.05	-8.18	-2.68
58.00	11.50	6.23	3.24	2601.90	-12791.65	0.00	4644.73	5685.16	-30.86	19.64	5.05	-8.18	-14.35
60.00	20.50	10.95	3.10	4892.24	-13084.69	0.00	4644.73	5685.16	-58.03	20.09	5.05	-8.18	-41.07

Case 9: I200B120, f_{ck} = 35 MPa

L (m)	β (°)	W (cm)	V (cm)	M_y (KNm)	M_z (KNm)	φ (°)	P_{max} (KN)	M_{Pmax} (KNm)	σ_{my} (Mpa)	σ_{mz} (Mpa)	σ_p (Mpa)	σ_{MP} (Mpa)	σ_t (Mpa)
10,00	1,23	2,80	8,12	3,17	-147,48	0,00	2948,40	1480,10	-0,09	0,46	5,06	-4,47	0,95
12,00	1,45	3,30	8,12	5,98	-235,96	0,00	2948,40	1480,10	-0,18	0,74	5,06	-4,47	1,15
14,00	1,62	3,68	8,12	9,72	-344,10	0,00	2948,40	1480,10	-0,29	1,08	5,06	-4,47	1,38
16,00	1,75	3,98	8,12	14,41	-471,88	0,00	2948,40	1480,10	-0,43	1,48	5,06	-4,47	1,64
18,00	1,86	4,23	8,12	20,11	-619,32	0,00	2948,40	1480,10	-0,60	1,94	5,06	-4,47	1,93
20,00	1,96	4,45	8,12	26,90	-786,40	0,00	2948,40	1480,10	-0,80	2,46	5,06	-4,47	2,25
22,00	2,05	4,67	8,12	34,90	-973,13	0,00	2948,40	1480,10	-1,03	3,05	5,06	-4,47	2,60
24,00	2,15	4,89	8,12	44,30	-1179,49	0,00	2948,40	1480,10	-1,31	3,69	5,06	-4,47	2,97
26,00	2,26	5,13	8,12	55,40	-1405,46	0,00	2948,40	1480,10	-1,64	4,40	5,06	-4,47	3,35
28,00	2,38	5,41	8,12	68,62	-1651,04	0,00	2948,40	1480,10	-2,03	5,17	5,06	-4,47	3,73
30,00	2,53	5,75	8,12	84,62	-1916,18	0,00	2948,40	1480,10	-2,51	6,00	5,06	-4,47	4,08
32,00	2,72	6,18	8,11	104,47	-2200,82	0,00	2948,40	1480,10	-3,09	6,89	5,06	-4,47	4,39
34,00	2,97	6,75	8,11	129,88	-2504,87	0,00	2948,40	1480,10	-3,85	7,85	5,06	-4,47	4,59
36,00	3,32	7,53	8,11	163,85	-2828,09	0,00	2948,40	1480,10	-4,85	8,86	5,06	-4,47	4,59
38,00	3,83	8,70	8,11	212,12	-3170,02	0,00	2948,40	1480,10	-6,28	9,93	5,06	-4,47	4,23
40,00	4,65	10,55	8,10	286,89	-3529,41	0,00	2948,40	1480,10	-8,50	11,05	5,06	-4,47	3,14
42,00	6,13	13,92	8,08	419,31	-3902,21	0,00	2948,40	1480,10	-12,42	12,22	5,06	-4,47	0,39
44,00	9,46	21,41	8,01	711,28	-4269,12	0,00	2948,40	1480,10	-21,06	13,37	5,06	-4,47	-7,11
46,00	18,56	41,46	7,70	1512,12	-4503,87	0,00	2948,40	1480,10	-44,78	14,11	5,06	-4,47	-30,09
48,00	181,11	-2,53	-8,12	-100,87	5192,59	0,00	2948,40	1480,10	2,99	-16,26	5,06	-4,47	-12,69
50,00	-178,98	-2,31	-8,12	-100,51	5654,99	0,00	2948,40	1480,10	2,98	-17,71	5,06	-4,47	-14,15
52,00	-4,30	-9,76	8,10	-459,95	-6120,61	0,00	2948,40	1480,10	13,62	19,17	5,06	-4,47	33,38
54,00	-2,90	-6,60	8,11	-336,20	-6631,01	0,00	2948,40	1480,10	9,96	20,77	5,06	-4,47	31,31
56,00	-2,13	-4,85	8,12	-266,49	-7155,90	0,00	2948,40	1480,10	7,89	22,41	5,06	-4,47	30,89
58,00	-1,65	-3,74	8,12	-221,41	-7698,68	0,00	2948,40	1480,10	6,56	24,11	5,06	-4,47	31,26
60,00	-1,32	-2,99	8,12	-189,69	-8260,36	0,00	2948,40	1480,10	5,62	25,87	5,06	-4,47	32,08

Case 9: I200B120, f_{ck} = 35 MPa (without safety factors)

L (m)	β (°)	W (cm)	V (cm)	M_y (KNm)	M_z (KNm)	φ (°)	P_{max} (KN)	M_{Pmax} (KNm)	σ_{my} (Mpa)	σ_{mz} (Mpa)	σ_p (Mpa)	σ_{MP} (Mpa)	σ_t (Mpa)
10,00	1,23	2,80	8,12	2,35	-109,25	0,00	2948,40	1480,10	-0,07	0,34	5,06	-4,47	0,86
12,00	1,45	3,30	8,12	4,43	-174,79	0,00	2948,40	1480,10	-0,13	0,55	5,06	-4,47	1,00
14,00	1,62	3,67	8,12	7,19	-254,89	0,00	2948,40	1480,10	-0,21	0,80	5,06	-4,47	1,17
16,00	1,75	3,97	8,12	10,65	-349,54	0,00	2948,40	1480,10	-0,32	1,09	5,06	-4,47	1,37
18,00	1,85	4,21	8,12	14,84	-458,76	0,00	2948,40	1480,10	-0,44	1,44	5,06	-4,47	1,58
20,00	1,95	4,42	8,12	19,80	-582,53	0,00	2948,40	1480,10	-0,59	1,82	5,06	-4,47	1,82
22,00	2,03	4,62	8,12	25,60	-720,85	0,00	2948,40	1480,10	-0,76	2,26	5,06	-4,47	2,09
24,00	2,12	4,82	8,12	32,33	-873,71	0,00	2948,40	1480,10	-0,96	2,74	5,06	-4,47	2,37
26,00	2,21	5,02	8,12	40,15	-1041,12	0,00	2948,40	1480,10	-1,19	3,26	5,06	-4,47	2,66
28,00	2,31	5,24	8,12	49,27	-1223,05	0,00	2948,40	1480,10	-1,46	3,83	5,06	-4,47	2,96
30,00	2,42	5,50	8,12	60,01	-1419,51	0,00	2948,40	1480,10	-1,78	4,45	5,06	-4,47	3,26
32,00	2,56	5,81	8,12	72,82	-1630,45	0,00	2948,40	1480,10	-2,16	5,11	5,06	-4,47	3,54
34,00	2,73	6,20	8,12	88,44	-1855,84	0,00	2948,40	1480,10	-2,62	5,81	5,06	-4,47	3,78
36,00	2,95	6,70	8,11	107,97	-2095,61	0,00	2948,40	1480,10	-3,20	6,56	5,06	-4,47	3,95
38,00	3,25	7,38	8,11	133,31	-2349,63	0,00	2948,40	1480,10	-3,95	7,36	5,06	-4,47	4,00
40,00	3,67	8,33	8,11	167,75	-2617,63	0,00	2948,40	1480,10	-4,97	8,20	5,06	-4,47	3,82
42,00	4,30	9,76	8,10	217,79	-2899,00	0,00	2948,40	1480,10	-6,45	9,08	5,06	-4,47	3,22
44,00	5,33	12,10	8,09	297,73	-3192,05	0,00	2948,40	1480,10	-8,82	10,00	5,06	-4,47	1,77
46,00	7,28	16,50	8,06	445,85	-3490,85	0,00	2948,40	1480,10	-13,20	10,93	5,06	-4,47	-1,68
48,00	11,84	26,74	7,95	789,59	-3765,19	0,00	2948,40	1480,10	-23,38	11,79	5,06	-4,47	-11,01
50,00	22,66	50,19	7,50	1614,20	-3866,09	0,00	2948,40	1480,10	-47,80	12,11	5,06	-4,47	-35,11
52,00	-754,47	-73,73	6,70	-2573,23	-3748,31	0,00	2948,40	1480,10	76,21	11,74	5,06	-4,47	88,53
54,00	-6,97	-15,81	8,06	-596,79	-4881,83	0,00	2948,40	1480,10	17,67	15,29	5,06	-4,47	33,55
56,00	-4,20	-9,55	8,10	-388,67	-5290,08	0,00	2948,40	1480,10	11,51	16,57	5,06	-4,47	28,67
58,00	-2,93	-6,66	8,11	-291,62	-5697,62	0,00	2948,40	1480,10	8,64	17,84	5,06	-4,47	27,07
60,00	-2,20	-4,99	8,12	-234,54	-6115,90	0,00	2948,40	1480,10	6,95	19,15	5,06	-4,47	26,69